

Epigenetic Reprogramming of Sweet Taste by Diet

by

Anoumid Vaziri

A dissertation submitted in partial fulfillment
of the requirements for the degree of
Doctor of Philosophy
(Molecular, Cellular, and Developmental Biology)
in the University of Michigan
2021

Doctoral Committee:

Assistant Professor Monica Dus, Chair
Assistant Professor E. Josie Clowney
Assistant Professor Adelheid Lempradl
Professor Randy Seeley
Professor Andrzej T. Wierzbicki

Anoumid Vaziri

avaziri@umich.edu

ORCID iD: 0000-0002-3406-0656

© Anoumid Vaziri 2021

Dedication

This dissertation is dedicated to my mother, father, and brother.

”در من بدمی من زنده شوم

یک جان چه بود، صد جان منی“

- مولانا

Acknowledgements

I would like to express my sincere gratitude to Dr. Monica Dus for her guidance, mentorship, and confidence as well as the unwavering support she has given me to pursue my scientific curiosities and goals. I also thank my committee members Drs. Josie Clowney, Heidi Lempradl, Randy Seely, and Andrzej Wierzbicki for their mentorship, feedback, and support throughout the development of this dissertation. I also thank Dr. Peter Freddolino for his invaluable guidance and expertise. I am thankful to members of the Dus lab, past and present. Specifically, Daniel Wilinski, Manaswini Sarangi, Christina May, Hayeon Sung and Ewelina Nowak. The wonderful undergraduate students that I worked with Brendan Genaw and Amishi Taneja. I also thank my MCDB 2016 cohort for their camaraderie, because graduate school is so much better when you are surrounded with amazing people. I am also grateful for the incredible friendship of Donya Shodja.

Thank you, Thibaut Pardo García, for your companionship, and friendship, and for helping me build a home away from home.

Finally, thank you to my parents and brother for their unshakable love, support, and words of encouragement.

Each chapter in this dissertation was generated with the input of many collaborators: For chapter 2 we thank Josie Clowney, Marco Gallio, Leslie VossHall, and Randy Seeley for comments and suggestions on the manuscript. We also thank all the researchers that shared protocols and fly lines with us. We thank Caleb Vogt and Katty Wu for their help with some TAGs experiments and Jenna Persons for collecting samples for metabolomics. Katherine

Hoffman wrote the FLIC meal patterns code. Julia Kuhn designed the graphical abstract and some of the graphics for the manuscript.

For chapter 3 we thank Sundeep Kalantry, Josie Clowney, and Giacomo Cavalli for comments and discussions. We also thank the University of Indiana at Bloomington, the VDRC, the FLYORF stock collections, and all the investigators who shared fly lines with us. We also thank Daniel Wilinski for help with data analysis, D. Dickman and X. Chen for comments on riboTRAP, and M. Brovkina (J Clowney laboratory) for discussions on TaDa analysis. M. Burkhard assisted with analysis of expression changes for different GO terms. J. Kuhn designed some of the graphics for the manuscript.

Author contributions are as follows: For chapter 2 author contributions are as follows: C.E.M. performed FLIC, TAGs, Nile red, taste sensitivity, and calcium imaging experiments. A.V. performed PER, qPCR, and the OGT RNA-seq experiments. M.D. performed PER experiments. O.G. quantified taste cells in the proboscis and collected the RNA-seq data from control and sugar diet probosces. P.L.F. and M.K. analyzed the RNA-seq data. Y.Q.L. and Q.-P.W. performed the sensilla recordings. C.E.M., K.J.H., and S.D.P. developed the optoFLIC. C.E.M., A.V., and M.D. designed the experiments, wrote the manuscript, and prepared the figures with input from the other authors. M.D. supervised the project.

For chapter 3 author contributions are as follows: A.V. performed all experiments and analyzed RNA-seq, TaDa, and CATaDa datasets, with the exception of in vivo calcium imaging. B.T.G. helped with PER and triglyceride measurements. C.E.M. performed in vivo calcium imaging. M.K. and P.L.F. developed the PREdictor, calculated regulatory targets of transcription factors, analyzed GO term enrichment analysis, provided statistical consultation, and tested for

practical significance. M.D. oversaw the project and secured funding. A.V. and M.D. designed the experiments, wrote the manuscript, and prepared the figures with input from all authors.

For chapter 4 author contributions are as follows: AV performed all experiments and analyzed RNA-seq, TaDa, and CATaDa datasets. PLF ran and analyzed GO term enrichment analysis, provided statistical consultation, and tested for practical significance. MD oversaw the project and secured funding. AV and MD designed the experiments, wrote the manuscript, and prepared the figures with input from all authors.

The work in this dissertation was made possible through funding from NIH R00 DK-97141 (MD), NIH 1DP2DK-113750 (MD), the NARSAD Young Investigator Award (MD), the Klingenstein-Simons Fellowship in the Neurosciences (MD), the Rita Allen Foundation (MD), and the Rackham Predoctoral Fellowship (AV).

Table of Contents

Dedication.....	ii
Acknowledgements.....	iii
List of Figures.....	ix
Abstract.....	xii
Chapter 1 Introduction.....	1
1.1 The relationship between diet and eating behavior.....	1
1.2 The influence of diet on gene expression.....	3
1.2.1 DNA and Histone Methylation.....	4
1.2.2 Histone Acetylation.....	5
1.2.3 O-GlcNAcylation.....	5
1.3 The influence of diet on feeding behavior.....	8
1.4 The gustatory system links diet to feeding behavior.....	12
1.5 The mechanisms of diet-induced taste dysfunction.....	15
1.6 <i>Drosophila melanogaster</i> as a model for diet induced obesity.....	15
1.7 Epigenetic reprogramming of sweet taste.....	17
1.8 References.....	20
Chapter 2 High Dietary Sugar Reshapes Sweet Taste to Promote Feeding Behavior in <i>Drosophila melanogaster</i>	30
2.1 Abstract.....	30
2.2 Introduction.....	31
2.3 Results.....	32
2.4 Discussion.....	52
2.5 Method Details.....	54

2.6 Statistical Analysis	65
2.7 Data and Software Availability	70
2.8 Supplemental Figures	71
2.9 References	78
Chapter 3 Persistent Epigenetic Reprogramming of Sweet Taste by Diet	86
3.1 Abstract	86
3.2 Introduction	87
3.3 Results	88
3.4 Discussion	114
3.5 Materials and Methods	120
3.6 Data Analysis and Statistics	129
3.7 Supplemental Figures	131
3.8 References	144
Chapter 4 A Nutrient Information Pathway Links Diet to Taste	154
4.1 Abstract	154
4.2 Introduction	155
4.3 Results	156
4.4 Discussion	174
4.5 Methods	179
4.6 Supplemental Figures	186
4.7 References	192
Chapter 5 Discussion	200
5.1 Mechanisms of diet induced obesity	201
5.2 Mechanisms of diet induced taste defects	202
5.3 Alterations in taste and increased food intake	206

5.4 Concluding remarks and future directions 206

5.5 References 208

List of Figures

Figure 1.1 The influence of diets on metabolites and the epigenetic machinery.....	7
Figure 1.2 A Model for the Role of Chemosensory Plasticity in Nutrition and Metabolic Disease.	14
Figure 2.1 High sugar diet decreases sweet taste sensation.....	36
Figure 2.2 A sugar diet decreases taste sensation independently of obesity	37
Figure 2.3 A sugar diet decreases synaptic responses to a sugar stimulus in the sweet taste neurons.....	39
Figure 2.4 Flies fed a high sugar diet show increased feeding behavior, meal size, and duration	42
Figure 2.5 Sugar diet promotes increased feeding behaviors independently of fat accumulation	44
Figure 2.6 Restoring sweet taste sensation and optogenetic activation of the Gr64f+ neurons protects animals from diet-induced obesity	47
Figure 2.7 OGT mediates the effects of sugar diet on sweet taste, feeding behavior, and obesity	51
Figure 2.8 Changes in sweet taste sensation and obesity with different diets. Related to Figure 1	71
Figure 2.9 The mRNA levels of Drosophila insulin-like peptides Dilp2 and Dilp5 are unchanged in control and plin2 mutant flies on a sugar diet. Related to Figure 2.....	72
Figure 2.10 A sugar diet has no effect on the number of sweet taste cells in the proboscis. Related to Figure 3.....	73
Figure 2.11 A 20% sucrose diet leads to a diminished sweet taste responses and obesity. Related to Figure 4.....	74
Figure 2.12 Control flies for bmm, plin2 mutant, NaChBac and csChrimson FLIC experiments. Related to Figures 5 and 6.	75
Figure 2.13 The HBP mediates changes in sweet taste sensation. Related to Figure 7.....	76
Figure 2.14 . iPAGE profile of differential gene expression changes in the labella of flies fed a sugar diet with or without OGT knockdown. Related to Figure 7.....	77

Figure 3.1 PRC2.1 modulates sweet taste in response to diet	92
Figure 3.2 Pcl mutant animals have the same neural responses to sucrose, regardless of diet.....	95
Figure 3.3 Pcl chromatin occupancy is redistributed in the high sugar environment.....	99
Figure 3.4 PRC2.1 sculpts the transcriptional responses of the Gr5a+neurons in response to diet.	103
Figure 3.5 PRC2.1 represses a transcriptional program required for sweet taste.	110
Figure 3.6 The persistent phenotypic memory of the food environment is dependent on PRC2.1.	113
Figure 3.7 The PRC1 and PhoRC complex are not required for sugar diet mediated sweet taste defects	131
Figure 3.8 The effects of Pcl on sweet taste are independent of changes in cell number or development.....	132
Figure 3.9 Chromatin occupancy and accessibility analysis of Pcl in the Gr5a+ neurons.	134
Figure 3.10 Pathway enrichment analysis of Pcl chromatin targets in the Gr5a+ neurons	135
Figure 3.11 PRC2.1 mediates the transcriptional responses of the Gr5a+ neurons to diet.....	136
Figure 3.12 Pathway enrichment analysis of the Gr5a+ neurons in flies fed a sugar diet for 3 days.	138
Figure 3.13 . Pathway enrichment analysis of the Gr5a+ neurons in flies fed a high sugar diet for 7 days.	139
Figure 3.14 Pathway enrichment analysis of the Gr5a+ neurons in Pcl ^{c429} mutant flies fed a high sugar diet for 7 days.....	140
Figure 3.15 Identification of a transcriptional program mediated by PRC2.1 on a sugar diet. ..	141
Figure 3.16 . PRC2.1 modulates the synaptic and neural properties of the Gr5a+ neurons.	142
Figure 4.1 OGT modulates sweet taste in response to diet.....	160
Figure 4.2 OGT modulates sweet taste through the PRC2.1 complex	162
Figure 4.3 The diet dependent chromatin redistribution of Pcl is dependent on OGT	165
Figure 4.4 OGT specifies the chromatin targeting of Pcl in response to diet.....	169
Figure 4.5 OGT and Pcl control a transcriptional program required for sweet taste.....	173

Figure 4.6 OGT modulates sweet taste in response to diet.....	186
Figure 4.7 The diet mediated Pcl chromatin redistribution is dependent on OGT	187
Figure 4.8 OGT specifies the chromatin targeting of Pcl in response to diet.....	188
Figure 4.9 Pathway enrichment analysis on OGT chromatin targets in the Gr5a+ neurons	189
Figure 4.10 Pathway enrichment analysis on OGT and Pcl chromatin targets in the Gr5a+ neurons.....	190
Figure 4.11 OGT and Pcl control a transcriptional program required for sweet taste.....	191

Abstract

Diets rich in sugar, salt, and fat alter taste perception and food preference, contributing to obesity and metabolic disorders, but the molecular mechanisms through which this occurs are unknown. Here, we show that in response to a high sugar diet, the epigenetic regulator Polycomb Repressive Complex 2.1 (PRC2.1) persistently reprograms the sensory neurons of *Drosophila melanogaster* flies to reduce sweet sensation and promote obesity. In animals fed high sugar, the binding of PRC2.1 to the chromatin of the sweet gustatory neurons is redistributed to repress a developmental transcriptional network that modulates the responsiveness of these cells to sweet stimuli, reducing sweet sensation. The specificity of this redistribution depends on the activity of the metabolic enzyme O-GlcNAc Transferase, which is also present at a subset of PRC2-bound genes. Half of these transcriptional changes persist despite returning the animals to a control diet, causing a permanent decrease in sweet taste. Our results uncover a new epigenetic mechanism that, in response to the dietary environment, informs a nutrient information pathway that regulates neural plasticity and feeding behavior to promote weight gain and obesity.

Chapter 1 Introduction

“Let food be thy medicine and medicine be thy food”

-Hippocrates

1.1 The relationship between diet and eating behavior

The connection between nutrition and health is ancient: philosophers like Hippocrates, Plutarch, Confucius, and Muhammad ibn Zakariya Razi wrote about it in books and religious texts, and oral traditions worldwide contain extensive references to diet, wellbeing, and disease. Philosophers and sages were not the only ones interested in this topic: the first printed gastronomy book, *De honesta voluptate et valetudine*, – authored in Latin by humanist Bartolomeo Platina in ~1465– was so successful that it was quickly translated into Italian, French, and German (1). In this light, today’s public interest, and often obsession, with diet, lifestyle, and wellbeing is not surprising.

It is well established that the dietary environment influences health, life expectancy, and the risk for diseases such as diabetes, cancer, and neurodegeneration (2, 3). The dietary environment also plays an important role in the amount of food we consume and the complications that arise from it such as obesity, which is excess body fat defined by a Body Mass Index > 30 (BMI > 30) (4). The modern dietary environment has an abundance of high calorie foods that are rich in salt, fat, and sugar. These foods are often cheaper, highly advertised, and readily available (5). Consistent with the change in the dietary environment to highly caloric foods, the amount of food consumed per day for all ages and genders has increased by 23% since

the 1970s. About half of these calories come from just two food groups: flours and grains (23.4%) and fats and oils (23.2%) (6). These foods are mostly consumed in the forms of breads, pastries and other baked goods which are often combined with high amounts of added sugars. Added sugars are added to foods or beverages when they are processed or prepared. Added sugars have many different names. Examples of added sugars include cane juice, corn syrup, dextrose, fructose, fruit nectars, glucose, high-fructose corn syrup, honey, lactose, malt syrup, maltose, maple syrup, molasses, raw sugar, and sucrose (7). Naturally occurring sugars such as those in fruit are not added sugars. These naturally occurring sugars increase the nutritional value of food and provide pleasant sensory qualities (8). The lack of recognized standards for sugar content in food, together with the fact that flavor is the primary driver of eating choices, has led to high levels of added sugar in food. In the USA, ~80% of grocery store foods contain added sugar (9) and food deserts in rural and urban areas make access to unprocessed food challenging (10, 11). Worldwide, added sugar consumption is higher than that recommended for both adults and children (12, 13), and even countries with food insecurity face the double burden of malnutrition, as many of the foods available are processed, nutrient poor, and high in added sugar and fat (14, 15).

The addition of sugar to foods is associated with higher caloric intake (12, 16–18), weight gain, obesity (19, 20), as well as a whole host of metabolic-related diseases, from diabetes and heart diseases to cancer and neurodegeneration (12, 21). As a result of this shift in the dietary environment and eating habits more than 70% of Americans are reported to have overweight or obesity, and the prevalence of severe obesity has increased over the past 2 decades. Obesity is not only a risk factor for heart disease, stroke, diabetes, and some types of cancer which are some of the leading causes of death in the U.S, but it is also costly. The average Obese persons require

more costly medical care placing a huge financial burden on families and the medical care system (5).

The availability of highly processed foods and an increase in food intake raises the question of whether processed foods high in salt, fat, and sugar promote food intake. Research over the past decade suggests that consumption of high fat and sugar diets have been associated with disrupted feeding behavior and weight gain, which raises the question of why we eat more in the presence of such foods. Studies in animal models and humans shows that intake of high fat and high sugar foods alters preference in a way that promotes increased intake of these high calorie foods that then promote weight gain, obesity, and the complications that arise with it (22–27). In addition to alterations in food preference, changes in the responsiveness of the gustatory system are shown to play a role in overeating and obesity. The gustatory system’s sensory signals function as cues to predict satiation (28–30) before nutrient signals determine satiation (31). This phenomenon is known as sensory-enhanced satiety (28). Interestingly, the intensity of sensory signals such as taste and smell are positively correlated with the satiation power of food (29, 32). The satiation power of food depends on the correct sensory cue (taste) paired with the correct caloric value of food. Because of this any variation from the expected sensory signals could lead to disrupted sensory enhanced satiety signals and food intake.

1.2 The influence of diet on gene expression

The idea that disruptions in the gustatory system in response to diet can be attributed to changes in gene expression is supported by the last decade of research in the field of nutrigenetics and nutriepigenetics which has illuminated the cellular networks connecting diet with cell function, as well as shedding light on how individual genetic variation interacts with dietary nutrients to promote or protect from disease susceptibility (33). In addition to identifying

how metabolic pathways sense and respond to variations in the nutrient environment to acutely regulate cell physiology (34), these studies have also revealed that nutrients can produce long-lasting epigenetic effects (35–37).

The sensitivity of the epigenome to diet arises from the ability of nutrients and metabolites to function as substrates and cofactors for enzymes that covalently modify DNA, RNA, and histone proteins (38, 39). By changing the activity of metabolic enzymes or the flux of metabolic pathways, diet composition alters the availability of the cofactors for these modifications, as well as regulates the binding of gene-regulatory complexes to their substrates (36, 39). This discovery that diet-derived metabolites fuel the epigenetic machinery has reshaped our understanding of the interplay between nutrition, health, and disease and led to new avenues of investigation and treatment, especially for cancer and metabolic disease (40–43). Below is a summary of how nutrients fuel the epigenetic machinery (Fig. 1):

1.2.1 DNA and Histone Methylation

Covalent methylation of DNA and histones leads to alterations in chromatin accessibility, transcription factor binding, and gene expression (44). Methylation is regulated by the abundance of S-Adenosylmethionine (SAM), the universal methyl donor for enzymes that methylate not just DNA and proteins, but also RNA and lipids. SAM is synthesized from methionine and ATP, depending on the availability of substrates and cofactors for 1-carbon metabolism, such as methionine, threonine, serine, glycine, choline, histidine, glucose, and folate (45). The transfer of a methyl group from SAM to its substrate, produces S-adenosylhomocysteine (SAH), which negatively regulates this process by robustly inhibiting methyltransferases (46). Because of this, the intracellular SAM:SAH ratio, as well as other 1-carbon cycle metabolites, dynamically regulates the activity of methyltransferases (47, 48). Consumption of foods that are rich in

methyl-donors (SAM, folic acid and vitamin B) increases these metabolites and can promote DNA and histone methylation and influence gene expression (44). Enzymes that remove the methyl group from DNA and histones are also sensitive to metabolic cofactors. Specifically, both Jumonji-domain containing histone demethylases and Ten-Eleven Translocation proteins (TET), which catalyze the creation of 5-hydroxymethylation, an intermediate in the removal of cytosine methylation– use the TCA cycle intermediate α -Ketoglutarate (α -KG). High α -KG levels – maintained by glucose and glutamine catabolism– promote the demethylation of histones and DNA, while high levels of fumarate and succinate inhibit their removal (49).

1.2.2 Histone Acetylation

Histone acetylation is a dynamic and reversible process primarily regulated by the activity of histone acetyltransferases (HATs) and histone deacetylases (HDACs). HATs acetylate conserved lysine residues on histone tails by transferring an acetyl group from acetyl-Coenzyme A. Acetyl-CoA is produced from acetate, citrate and pyruvate by Acetyl-CoA Synthetase Short-chain family member (ACSS), ATP citrate synthase (ACLY), and the pyruvate dehydrogenase complex (PDC); it can also be generated from fatty acid β -oxidation and amino acids and ketone bodies (50). The levels of acetyl-CoA are affected by the catabolic/anabolic state of the cell and affect global histone acetylation levels by serving as a cofactor for HATs (50). HDACs are sensitive to metabolites that are increased by catabolism. The Sirtuin 1 and 2 deacetylases (SIRT1 and SIRT2) require oxidized Nicotinamide adenine dinucleotide (NAD⁺) for their activity: high levels of NAD⁺ activate these enzymes while nicotinamide (NAM), a precursor of NAD⁺, inhibits them (51). Class I histone deacetylases (HDACs) are inhibited by the major ketone body β -hydroxybutyrate (BHB), a byproduct of fatty acid breakdown during fasting (52).

1.2.3 O-GlcNAcylation

O-GlcNAcylation (short for O-linked β -N-acetylglucosamine) is a type of glycosylation that involves the attachment of a single O-GlcNAc moiety to serine and threonine residues of cytoplasmic, nuclear, and mitochondrial proteins (53). The output of glucose, amino acid, fatty acid, and nucleotide metabolisms generate uridine diphosphate GlcNAc (UDP-GlcNAc), the donor substrate for O-GlcNAcylation (54). A single pair of enzymes, O-GlcNAc transferase (OGT) and O-GlcNAcase (OGA), add and remove O-GlcNAc groups to and from proteins, controlling the dynamic cycling of this post-translational protein modification in a nutrient-responsive and stress-responsive manner (53, 55). O-GlcNAcylation is also targeted to other epigenetic regulators besides histones, such as TET proteins, Polycomb Group Proteins, and transcription factors such as cyclic AMP response-element binding protein (CREB) (40, 53, 56).

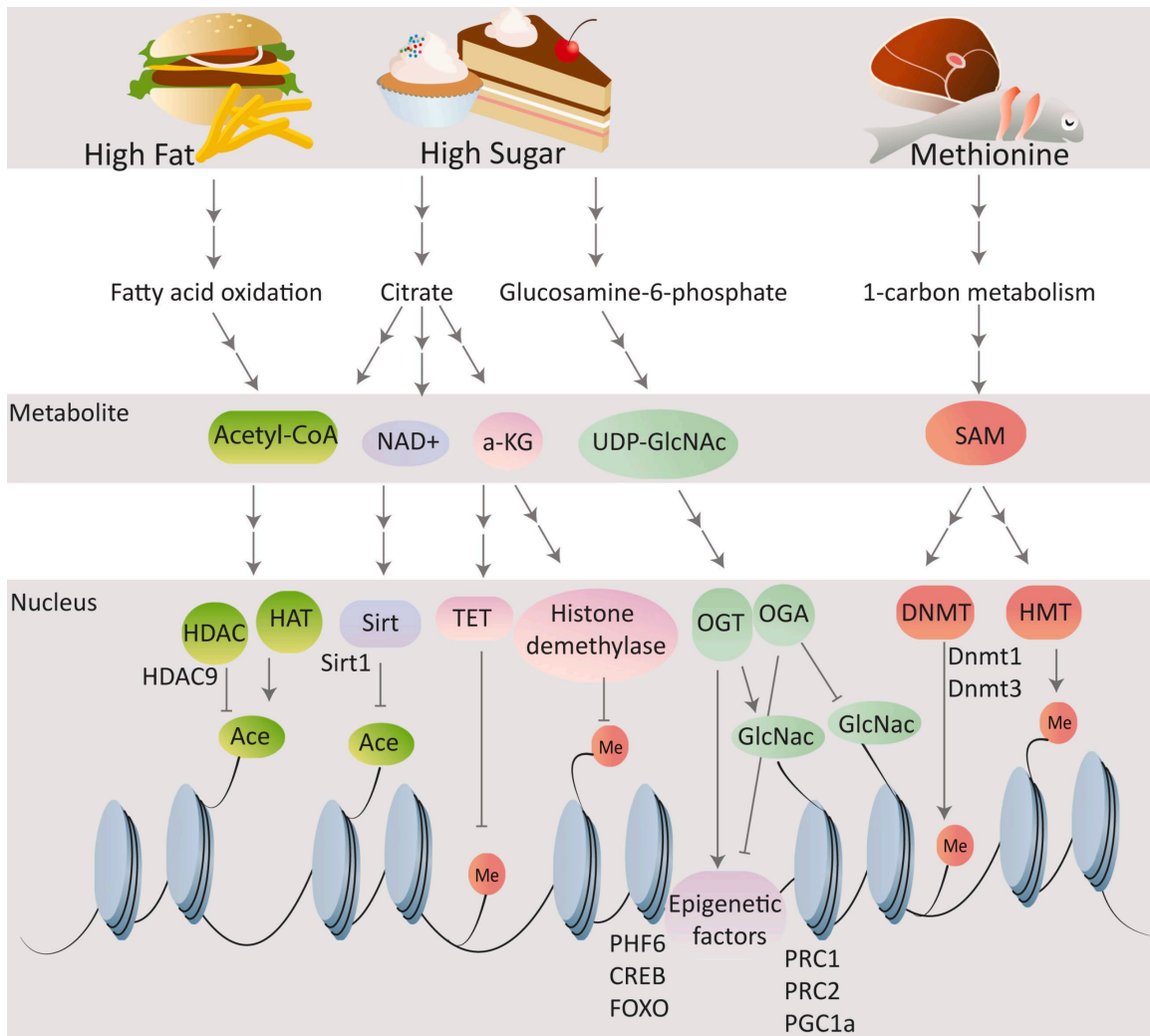


Figure 1.1 The influence of diets on metabolites and the epigenetic machinery

1.3 The influence of diet on feeding behavior

Consumption of high fat and sugar diets are associated with disrupted feeding behavior and weight gain, as well as changes in gene expression, raising the possibility that epigenetic processes may mediate these effects. This question has been addressed by examining the mRNA levels and DNA methylation status of genes important for feeding behavior in the hypothalamus, which controls energy balance and food intake via dedicated circuits (57). In the arcuate nucleus (ARC) of the hypothalamus an increase in the DNA methylation at the promoter of the Proopiomelanocortin (POMC) gene, an anorexigenic neuropeptide, was found in male rats fed a high fat diet for shorter (post weaning to 90 days) (58, 59), longer (21 weeks) exposures (60), and during neonatal development (61); interestingly, a positive correlation between POMC promoter hypermethylation and BMI has also been established in humans (62). However, higher POMC promoter methylation corresponded to a decrease in mRNA abundance only in (60, 61), but not in (58). Further, the mRNA and DNA methylation levels of other obesity-related ARC genes, such as Neuropeptide Y gene (NPY, orexigenic) was changed, but not that of the Agouti Related Peptide (AgRP, orexigenic) in male rats fed the high fat diet (60), although a recent study using single cell sequencing of the ARC in male mice fed a high fat diet for 10 weeks found that both POMC and AgRP mRNAs were lower (63). Expression of both NPY (in other hypothalamic nuclei) and POMC (in the ARC) however, was higher in female rats fed a western type cafeteria diet for 20 weeks, with a corresponding decrease in DNA methylation (64); in these animals the levels of steroid hormone receptors thought to play a role in obesity were also altered, suggesting that there may be sex specific differences in the regulation of these neuropeptide genes by diet. More recently, the single-cell transcriptome of the Lateral Hypothalamic Area, and especially of glutamatergic neurons in this region, was found to be

changed by a high fat diet in mice, but how these alterations in expression were connected to deficits in the responses of glutamatergic neurons to satiety in the diet-induced obesity animals was not investigated (65). Importantly, connections between SAM, SAH, and α -KG levels in relation to changes in DNA methylation were not investigated in any of these studies.

In addition to the hypothalamus, dopamine and opioid-receptor expressing neurons in the Ventral Tegmental Area (VTA) and the Nucleus Accumbens (NAcc) also play a critical role in food intake and weight gain (66, 67). Indeed, dysfunctions in dopaminergic signaling and transduction have been described with a high fat diet (68) and are thought to deregulate energy intake (30, 66, 69). Studies in male mice fed a high fat diet for 20 weeks showed a decrease in expression and an increase in DNA methylation at the promoters of genes critical for dopaminergic transmission, such as the Tyrosine Hydroxylase and Dopamine Transporter (DAT) genes in the VTA, as well as an increase in food intake, meal number, and meal size (70). The same group also identified lower expression of the μ -opioid receptor in the VTA, NAcc, and prefrontal cortex with diet-induced obesity. They also uncovered higher 5mC, histone 3 lysine 9 methylation, and Methyl CpG Binding Protein 2 binding, and lower H3 K4 acetylation in the μ -opioid receptor promoter region (71). An association between changes in DNA methylation at genes involved in DA transmission and BMI have been observed in a study that measured the methylation patterns of white blood cells among ~400 adults in the Methyl Epigenome Network association (72). Of note, *SLC18A1* (*VMAT1*) and *SLC6A3* (*DAT*) DNA methylation signatures were also correlated with total energy and carbohydrate intakes (72); some alleles of the *SLC6A3* gene have been previously associated with obesity risk (73) suggesting that gene x environment effects could converge on this gene. Together, these findings in the midbrain and those in the hypothalamus suggest that calorically dense diets may enhance gene repression to promote

feeding behavior and metabolic disease, but direct links between metabolite levels and these epigenetic modifications were not established.

Nonetheless, the notion that some diets may enhance gene repression is interesting in the light of research that used transgenic animals to address the role of epigenetic modifiers in diet-induced obesity. One study showed that pan-neuronal knockout of the DNA methyltransferase 1 (*DNMT1*) reduced obesity, food intake, and attenuated changes in gene expression in the ventromedial hypothalamus in mice fed a high fat diet (74). However, in the paraventricular nucleus of the hypothalamus—which is sensitive to anorexigenic signals—(75) showed that the expression of the de novo methyltransferase *Dnmt3a* was reduced with high fat diet treatment for 6 weeks, and that knockout of this gene led to hyperphagia and higher body weight and fat mass. Notably, knockout of *MeCP2* in the same neurons also induced hyperphagia and obesity via upregulation of NPY levels. Interestingly, knockout of *Sirt1* in the AgRP neurons promoted lower food intake and body weight (76); in the same light, loss of the transcriptional repressor PHD finger protein 6 (PHF6) from the orexigenic AgRP neurons protected mice from weight gain and obesity when they ate a high fat yo-yo diet (77). Specifically, the authors showed that binding of PHF6 at the promoters of immediate early genes— such as transcriptional regulators, signaling, and channels— shifted upon refeeding to alter the firing properties of the AgRP neurons and the levels of the AgRP neuropeptide (77). Together, these studies suggest that alterations in the DNA methylation patterns at the promoters of feeding and energy homeostasis genes in the hypothalamus and striatum, and more broadly an increase in repressive drive, may play an important role in the regulation of food intake and energy homeostasis. However, the exact mechanisms via which this epigenetic mark is altered by diet are still unknown; further, whether these effects are due to the direct action of metabolites on epigenetic modifiers or are

instead a consequence of overall higher caloric intake or weight gain, was not addressed in these studies.

The hexosamine biosynthesis pathway (HBP) is a cellular nutrient sensor and its activity has been implicated in a wide range of diet related phenotypes (55, 78, 79). This pathway is regulated by the two enzymes OGT and OGA. OGT also regulates the activity of the other important transcription factors involved in synaptic plasticity and neural physiology. Indeed, O-glcNAcylation of cAMP response element-binding protein (CREB) inhibits transcriptional activation by blocking its association with the cofactor CRTC, and preventing long term memory formation (80). In hippocampal mouse tissue, CREB phosphorylation (81) and CREB-mediated activation of Brain-derived neurotrophic factor (BDNF) (82) were decreased in mice fed a high fat diet; the chemosensory plasticity of the sensory neurons of flies on a high sugar diet was also dependent on CREB signaling (83). A recent study also found that the activity of OGT changes during memory consolidation to influence the binding of PRC2 and remodel chromatin (84). Interestingly, knockout of the histone acetyltransferase CREB Binding Protein (CBP) in the hypothalamus resulted in higher food intake and obesity (85). Thus, modification of CREB by OGT may decrease signaling through this transcription factor and influence the expression of behaviors such as learning and memory and feeding. OGT has also been studied in the modulation of epilepsy, a neurological disease whose severity is influenced by diet (86). Moreover, manipulations of OGT levels or its catalytic activity has been implicated in dopaminergic (87), hypothalamic (79, 88) and hippocampal circuits (89–91), GABAergic neurons (92), and sensory neurons (93), in ways that alter DA neuron cell viability, food intake, energy balance, and synaptic maturity, plasticity, and function (94). This opens the possibility that the alterations in gene expression and DNA methylation described above may occur via this

metabolic signaling pathway. However, a metabolomics study in flies showed that a high sugar diet reshaped not just the HBP, but also 1C metabolism and the TCA cycle (95) which could impact neural activity via other metabolite cofactors. Many studies have examined the effects of these metabolic pathways prenatally or across generations, which hints that these alterations could have long term consequences (96, 97). Taken together, evidence from flies and rodents fed high nutrient diets suggest that the disruptions in memory, sweet taste detection, and feeding behavior are associated with epigenetic processes and alterations in gene expression in both the peripheral and central nervous system.

1.4 The gustatory system links diet to feeding behavior

In a variety of model organisms and humans research suggests that the levels of salt, fat, and sugar in diets alters taste sensation (Fig. 2). For example, diets high in sodium lead to lower perceived intensity and a preference towards higher salt concentrations (22, 98, 99). Similarly, consumption of a high-fat diet has been linked to a decrease in fat sensation and higher preference for fatty foods (24, 100, 101). While studies on levels of salt and fat have conclusively determined the relationship between dietary salt and fat and taste perception, this has not been the case for the levels of dietary sugar. A study on overweight/obese individuals has shown that overweight/obese subjects perceive sweetness as less intense compared to non-obese individuals and that overweight/obese individuals are more implicitly attracted to sweetness (102). Multiple other studies have also reported lower sweet taste intensity in obese individuals compared to lean individuals (103, 104). A 2017 study reported that normal-weight humans who have had partial inhibition of their sweet taste receptors after drinking *Gymnema sylvestre* tea preferred higher concentrations of sucrose in a flavored beverage (105). This suggests that alterations in sweet taste could promote shifts in food preference and intake. More recently,

research on rodents found that animals genetically prone to obesity or fed high energy diets have decreased behavioral (104, 106) and physiological responses of the taste buds to sweet or fatty stimuli (26, 107), and changes in the number of taste buds (108), and lower expression of the sweet taste receptors (109), but these changes were not causally linked to taste function and feeding behavior. Thus, while there is accumulating evidence that taste signals are dulled in obese mammals, it is not clear whether this is a consequence of the obese state or a direct result of the dietary environment. Additionally, it is unclear whether changes in taste responses are causally linked to increased food intake and obesity. Furthermore, we know next to nothing about the molecular mechanisms through which diet composition affects taste sensation and obesity. Thus, studies in genetically tractable model organisms could help shed light on this question and define evidence-based strategies to curb the prevalence of obesity and metabolic disease, which currently affects billions of people worldwide.

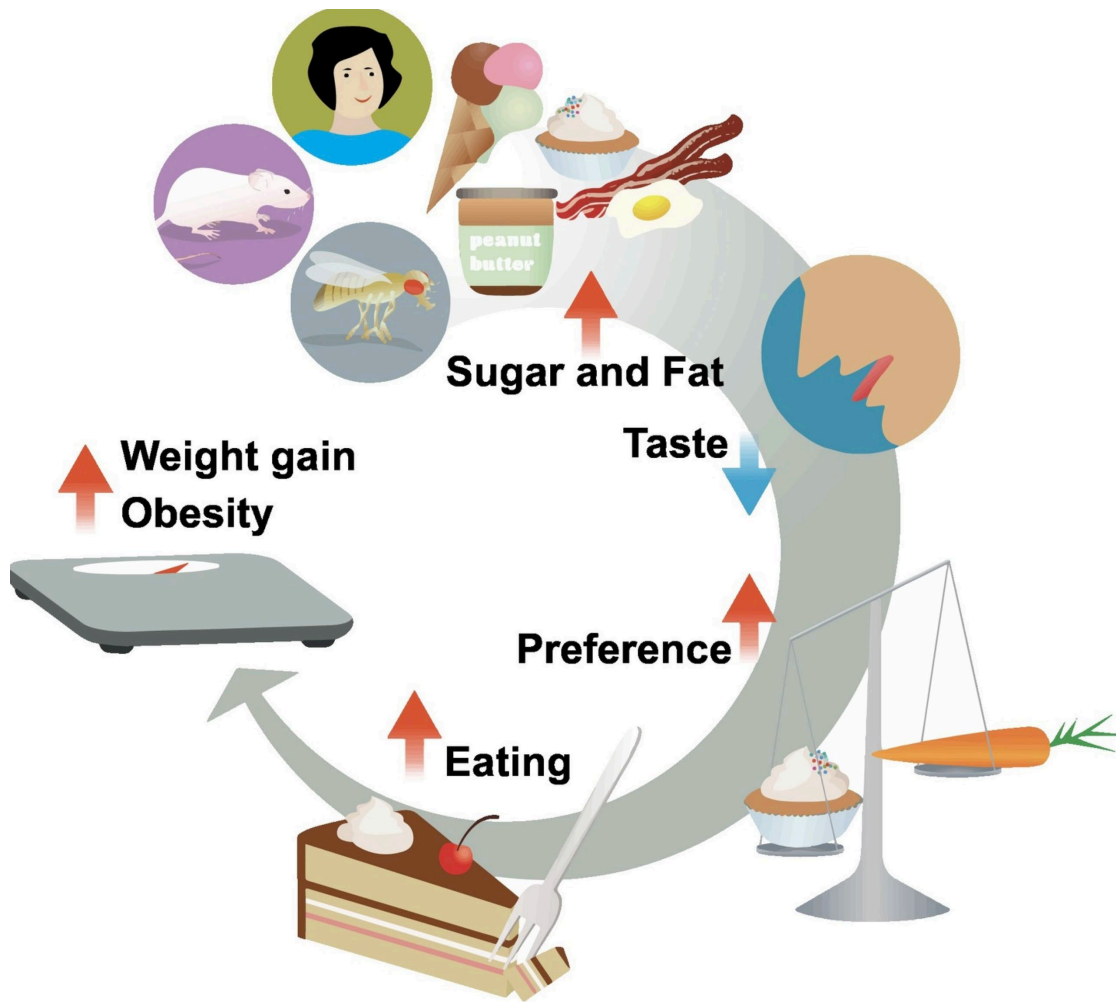


Figure 1.2 A Model for the Role of Chemosensory Plasticity in Nutrition and Metabolic Disease.

1.5 The mechanisms of diet-induced taste dysfunction

To understand the mechanisms of diet-induced taste dysfunction most studies up to date have investigated changes in the expression of genes important for taste (25, 26, 109, 110) as well as changes in the anatomy of the gustatory system. In these experiments the researchers found that the mRNA levels of *a-gustducin* and *phospholipase C-β2 (PLC-β2)* were decreased in mice fed a high-fat diet (26, 110). In humans, studies have shown that the *PLC-β2* gene has decreased mRNA levels (111). Additionally, others have reported a decrease in the mRNA levels of the *transient receptor potential M5 (TRPM5)* and the *taste 1 receptor member 2 (TAS1R2)* in the fungiform papillae of obese individuals (111), and an increase in DNA methylation at these genes from blood samples of people with high BMI. Interestingly, some studies have reported that changes in taste could be the result of changes in the number of circumvallate and fungiform papillae and in the markers of taste receptor cell (TRC) proliferation in mice fed high-fat diets (108). While other studies observed no changes in the number of taste buds and taste cell types in rats fed sucrose or mice fed high-energy diets (112). While some avenues of research are underway in rodent and human models, research on other model organisms has been limited. One study in *Drosophila melanogaster* flies found a transcription based mechanism dependent on the *peroxisome proliferator-activated receptor γ coactivator 1α (PGC1α)* (83). Collectively, these lines of evidence suggest that changes in taste by diet is most likely attributed to changes in gene expression because of the diet.

1.6 *Drosophila melanogaster* as a model for diet induced obesity

Drosophila melanogaster more commonly known as the vinegar fly, has transformed our understanding of biology and medicine. The short generation cycle, advanced genetic tools, and the remarkable conservation of disease genes and pathways have made flies an ideal model to

study in a variety of fields including cell biology, genetics, neurobiology, and aging. In the past decade *D.melanogaster* flies have been used to understand the mechanisms by which diet and obesity affects overall physiology (113). Many of these studies are conducted by manipulating the flies' standard diet by adding varying amounts of sugars (sucrose, fructose, glucose), sweeteners (sucralose), or fats (lard, coconut oil or other fats). This process can be done at any time throughout the flies' development from larvae to adults. Similar to manipulating their standard diets by adding other nutrients, pharmacological manipulations can also be done by adding compounds directly to their standard food. Importantly, the use of the GAL4/UAS system (114) to manipulate the expression of any gene in a cell specific manner with temporal control has allowed researchers to make substantial discoveries, most notably the molecular clock system which led to the 2017 Nobel Prize in Physiology or Medicine.

In recent years researchers have found that adult flies fed a high fat (10%) or high sugar (20-30%) diet for 7-14 days have higher lipid levels and altered insulin and glucose homeostasis (95, 113, 115), as well as changes in the levels of hundreds of metabolites, including amino acids, 1C metabolism, and nucleotides, organic acids, and carbon-nitrogen balance depending on the type and length of diet exposure (95, 116). These metabolic phenotypes reflect hallmarks of obesity, metabolic syndrome, and despite differences in anatomy, they contribute to defects in heart contractility and structure (117, 118) and in the filtration of the malpighian tubules; they also shorten lifespan (118, 119) and lower the resistance to other metabolic stresses (120). The similarities in metabolic and physiological outcomes is not surprising considering that they are the result of the activation of conserved nutrient-sensing pathways, such as insulin-TOR (117) hexosamine biosynthesis (118) and JAK-STAT (115).

Like mammals, flies fed high fat and high sugar diets show changes in genes involved in immune response, inflammation, metabolism, neural signaling, synaptic function, and sensory perception in the brain (119, 121, 122); although these alterations are yet to be causally linked. Differences in the levels of neurotransmitters and neuromodulators have also been observed with both high sucrose (95) and high fat diets (10-20% hydrogenated vegetable oils or lard), including a decrease in serotonin and octopamine (123), and increase in inflammatory factors homologue to TGF- β (124). As with rodents, many different behaviors have been phenotyped in response to dietary manipulations in flies, including feeding and reward, taste and olfaction, sleep, and mood, while less is known about their effects on learning and memory.

In adult flies consumption of a high fat diet (2% palmitic acid, 10% sucrose) for 7 and 14 days was associated with lower olfactory sensitivity to both appetitive and aversive odors, and differences in olfactory choice preference, presumably due to changes in the mRNA levels of olfactory receptor and olfactory binding proteins in the antenna (119). Changes in behavioral olfactory responses to some, but not most odors, as well as the head mRNA levels of genes involved in sensory perception, metabolism, and motor function, were also revealed in flies fed a 20% coconut oil diet for 7 and 14 days (125). In addition to olfactory deficits, studies have shown dietary taste plasticity in response to sugar by engaging a signaling pathway that activated the transcription factors CREB and PGC1 α (83). However, no studies to date have shown the effect of diet on taste plasticity independent of obesity, linked taste plasticity to food intake, and identified the underlying mechanisms that lead to taste plasticity.

1.7 Epigenetic reprogramming of sweet taste

In this work my aim is to utilize *D.melanogaster* flies as a model of diet induced obesity to investigate the link between high nutrient diets, food intake and taste plasticity. To do this we

used the relative simplicity of the *Drosophila* taste system, where the sweet-sensing cells that are neurons project directly to the brain, to tackle several important questions. First, do changes in taste sensation occur with diet-induced obesity? Are these changes a consequence of the altered physiology of the obese state or do they result from chronic exposure to a high nutrient diet? If changes in taste function occur, what role do they play in the etiology of obesity? Importantly I will explore the metabolic and molecular mechanisms that link diet to changes in taste plasticity.

To tackle these questions, we used a variety of behavioral and neural imaging tools to find that high dietary sugar dulls the responses of the *Drosophila melanogaster* taste neurons to sweet stimuli, causing higher food intake and weight gain. By monitoring feeding behavior at high resolution and using neuro- and optogenetic manipulations of sweet taste cell excitability, we show the dulling of sweet taste leads to overfeeding and obesity. Preventing a decrease in sweet taste sensation rescues feeding and obesity in animals exposed to the high sugar diet. Together, our results implicate deficits in sweet taste as drivers of obesity and begin to map the molecular underpinnings through which exposure to excess dietary sugar reshapes taste function and behavior (chapter 2). To discover the underlying molecular mechanism that promote taste changes we used targeted neurogenetic tools in combination with cell specific transcriptional and chromatin profiling and found that the Polycomb Repressive Complex 2.1 (PRC2.1), a chromatin-silencing complex conserved from plants to humans tunes the activity of the sweet sensory neurons and taste sensation in response to the food environment. This is through the repression of a neurodevelopmental transcriptional program that shapes the synaptic, signaling, and metabolic properties of these cells. This diet-dependent transcriptional remodeling persisted even when animals were returned to the control diet, leading to lasting changes in sweet taste behavior that depended on the constitutive activity of PRC2.1 (chapter 3). Finally, we discovered

that this deficit is caused by excess dietary sugar, not obesity, and is mediated by the increased activity of a nutrient information pathway mediated by the conserved sugar sensor OGT. OGT and PRC2.1 act together to reprogram the transcriptional properties of the sweet taste neurons in a way that alters the activity of these cells to promote food intake (chapter 4). Together, our findings suggest that diet composition activates metabolic-epigenetic mechanisms that reprogram sensory responses to food; this sensory reprogramming determines the perception of future stimuli, leading to long-lasting alterations in behavior that increase the risk for obesity and metabolic disease.

1.8 References

1. I. Platina, M. E. Milham, *Platina, on right pleasure and good health: a critical edition and translation of De honesta voluptate et valetudine* (Tempe, Ariz.: Medieval & Renaissance Texts & Studies, 1998).
2. S. Oleson, M. M. Gonzales, T. Tarumi, J. N. Davis, C. K. Cassill, H. Tanaka, A. P. Haley, Nutrient intake and cerebral metabolism in healthy middle-aged adults: Implications for cognitive aging. *Nutr. Neurosci.* **20**, 489–496 (2017).
3. M. K. Zamroziewicz, A. K. Barbey, Nutritional Cognitive Neuroscience: Innovations for Healthy Brain Aging. *Front. Neurosci.* **10**, 240 (2016).
4. CDC, Body Mass Index (BMI) (2021), (available at <https://www.cdc.gov/healthyweight/assessing/bmi/index.html>).
5. CDC, Adult obesity facts (2021), (available at <https://www.cdc.gov/obesity/data/adult.html>).
6. C. Funk, Public views about Americans’ eating habits (2016), (available at <https://www.pewresearch.org/science/2016/12/01/public-views-about-americans-eating-habits/>).
7. Scientific Report of the 2020 Dietary Guidelines Advisory Committee, “Dietary Guidelines Advisory Committee. 2020.”
8. C. E. May, M. Dus, Confection Confusion: Interplay Between Diet, Taste, and Nutrition. *Trends Endocrinol. Metab.* **32**, 95–105 (2021).
9. S. W. Ng, M. M. Slining, B. M. Popkin, Use of caloric and noncaloric sweeteners in US consumer packaged foods, 2005–2009. *J. Acad. Nutr. Diet.* **112**, 1828–34.e1–6 (2012).
10. J. P. Block, S. V. Subramanian, Moving Beyond “Food Deserts”: Reorienting United States Policies to Reduce Disparities in Diet Quality. *PLoS Med.* **12**, e1001914 (2015).
11. A. Hilmers, D. C. Hilmers, J. Dave, Neighborhood disparities in access to healthy foods and their effects on environmental justice. *Am. J. Public Health.* **102**, 1644–1654 (2012).
12. R. K. Johnson, M. Br, B. V. Howard, M. Lefevre, R. H. Lustig, F. Sacks, L. M. Steffen, J. Wylie-rosett, M. Br, F. Barbara, V. Howard, Dietary sugars intake and cardiovascular health: a scientific statement from the American Heart Association. *Circulation* 2009. *Circulation* (2009) (available at <http://citeseerx.ist.psu.edu/viewdoc/summary?doi=10.1.1.334.7440>).
13. V. S. Malik, W. C. Willett, F. B. Hu, Global obesity: trends, risk factors and policy implications. *Nat. Rev. Endocrinol.* **9**, 13–27 (2013).

14. L. Haddad, C. Hawkes, P. Webb, S. Thomas, J. Beddington, J. Waage, D. Flynn, A new global research agenda for food. *Nature*. **540** (2016), pp. 30–32.
15. B. M. Popkin, L. S. Adair, S. W. Ng, Global nutrition transition and the pandemic of obesity in developing countries. *Nutr. Rev.* **70**, 3–21 (2012).
16. N. M. Avena, P. Rada, B. G. Hoebel, Evidence for sugar addiction: behavioral and neurochemical effects of intermittent, excessive sugar intake. *Neurosci. Biobehav. Rev.* **32**, 20–39 (2008).
17. K. D. Hall, A. Ayuketah, R. Brychta, H. Cai, T. Cassimatis, K. Y. Chen, S. T. Chung, E. Costa, A. Courville, V. Darcey, L. A. Fletcher, C. G. Forde, A. M. Gharib, J. Guo, R. Howard, P. V. Joseph, S. McGehee, R. Ouwerkerk, K. Raisinger, I. Rozga, M. Stagliano, M. Walter, P. J. Walter, S. Yang, M. Zhou, Ultra-Processed Diets Cause Excess Calorie Intake and Weight Gain: An Inpatient Randomized Controlled Trial of Ad Libitum Food Intake. *Cell Metabolism*. **30** (2019), pp. 67-77.e3.
18. C. R. Freeman, A. Zehra, V. Ramirez, C. E. Wiers, N. D. Volkow, G.-J. Wang, Impact of sugar on the body, brain, and behavior. *Front. Biosci.* . **23**, 2255–2266 (2018).
19. S. Faruque, J. Tong, V. Lacmanovic, C. Agbonghae, D. Minaya, K. Czaja, The Dose Makes the Poison: Sugar and Obesity in the United States – a Review. *Polish Journal of Food and Nutrition Sciences*. **69** (2019), pp. 219–233.
20. L. T. Morenga, L. Te Morenga, S. Mallard, J. Mann, Dietary sugars and body weight: systematic review and meta-analyses of randomised controlled trials and cohort studies. *BMJ*. **346** (2012), pp. e7492–e7492.
21. P. González-Muniesa, M.-A. Martínez-González, F. B. Hu, J.-P. Després, Y. Matsuzawa, R. J. F. Loos, L. A. Moreno, G. A. Bray, J. A. Martinez, Obesity. *Nat Rev Dis Primers*. **3**, 17034 (2017).
22. M. Bertino, G. K. Beauchamp, K. Engelman, Long-term reduction in dietary sodium alters the taste of salt. *Am. J. Clin. Nutr.* **36**, 1134–1144 (1982).
23. M. Bertino, G. K. Beauchamp, K. Engelman, Increasing dietary salt alters salt taste preference. *Physiol. Behav.* **38**, 203–213 (1986).
24. J. M. Heinze, A. Costanzo, I. Baselier, A. Fritsche, S. Frank-Podlech, R. Keast, Detection thresholds for four different fatty stimuli are associated with increased dietary intake of processed high-caloric food. *Appetite*. **123**, 7–13 (2018).
25. M. S. Weiss, A. Hajnal, K. Czaja, P. M. Di Lorenzo, Taste Responses in the Nucleus of the Solitary Tract of Awake Obese Rats Are Blunted Compared With Those in Lean Rats. *Front. Integr. Neurosci.* **13**, 35 (2019).
26. A. B. Maliphol, D. J. Garth, K. F. Medler, Diet-induced obesity reduces the responsiveness of the peripheral taste receptor cells. *PLoS One*. **8**, e79403 (2013).

27. K. M. Appleton, H. Tuorila, E. J. Bertenshaw, C. de Graaf, D. J. Mela, Sweet taste exposure and the subsequent acceptance and preference for sweet taste in the diet: systematic review of the published literature. *Am. J. Clin. Nutr.* **107**, 405–419 (2018).
28. L. Chambers, K. McCrickerd, M. R. Yeomans, Optimising foods for satiety. *Trends Food Sci. Technol.* **41**, 149–160 (2015).
29. M. R. Yeomans, in *Flavor, Satiety and Food Intake* (John Wiley & Sons, Ltd, Chichester, UK, 2017), pp. 1–12.
30. C. E. May, J. Rosander, J. Gottfried, E. Dennis, M. Dus, Dietary sugar inhibits satiation by decreasing the central processing of sweet taste. *Elife.* **9** (2020), doi:10.7554/eLife.54530.
31. F. Bellisle, J. E. Blundell, in *Satiation, Satiety and the Control of Food Intake* (Elsevier, 2013), pp. 3–11.
32. C. G. Forde, N. van Kuijk, T. Thaler, C. de Graaf, N. Martin, Oral processing characteristics of solid savoury meal components, and relationship with food composition, sensory attributes and expected satiation. *Appetite.* **60**, 208–219 (2013).
33. M. Müller, S. Kersten, Nutrigenomics: goals and strategies. *Nat. Rev. Genet.* **4**, 315–322 (2003).
34. D. Haro, P. F. Marrero, J. Relat, Nutritional regulation of gene expression: Carbohydrate-, fat- and amino acid-dependent modulation of transcriptional activity. *Int. J. Mol. Sci.* **20**, 1386 (2019).
35. T. Bartke, R. Schneider, You are what you eat – How nutrition and metabolism shape the genome through epigenetics. *Molecular Metabolism* (2020), p. 100987.
36. S. A. Haws, C. M. Leech, J. M. Denu, Metabolism and the Epigenome: A Dynamic Relationship. *Trends Biochem. Sci.* (2020), doi:10.1016/j.tibs.2020.04.002.
37. R. Janke, A. E. Dodson, J. Rine, Metabolism and epigenetics. *Annu. Rev. Cell Dev. Biol.* **31**, 473–496 (2015).
38. J.-P. Etchegaray, R. Mostoslavsky, Interplay between Metabolism and Epigenetics: A Nuclear Adaptation to Environmental Changes. *Mol. Cell.* **62**, 695–711 (2016).
39. Y. Zhang, T. G. Kutateladze, Diet and the epigenome. *Nat. Commun.* **9**, 3375 (2018).
40. A. Decourcelle, D. Leprince, V. Dehennaut, Regulation of Polycomb Repression by O-GlcNAcylation: Linking Nutrition to Epigenetic Reprogramming in Embryonic Development and Cancer. *Front. Endocrinol.* **10**, 117 (2019).
41. A. Z. Kalea, K. Drosatos, J. L. Buxton, Nutriepigenetics and cardiovascular disease. *Curr. Opin. Clin. Nutr. Metab. Care.* **21**, 252 (2018).

42. C. Sapienza, J.-P. Issa, Diet, Nutrition, and Cancer Epigenetics. *Annu. Rev. Nutr.* **36**, 665–681 (2016).
43. S. Zeisel, Choline, Other Methyl-Donors and Epigenetics. *Nutrients.* **9** (2017), p. 445.
44. X. Li, G. Egervari, Y. Wang, S. L. Berger, Z. Lu, Regulation of chromatin and gene expression by metabolic enzymes and metabolites. *Nat. Rev. Mol. Cell Biol.* **19**, 563–578 (2018).
45. G. S. Ducker, J. D. Rabinowitz, One-Carbon Metabolism in Health and Disease. *Cell Metab.* **25**, 27–42 (2017).
46. S. L. Berger, The complex language of chromatin regulation during transcription. *Nature.* **447**, 407–412 (2007).
47. S. J. Mentch, M. Mehrmohamadi, L. Huang, X. Liu, D. Gupta, D. Mattocks, P. Gómez Padilla, G. Ables, M. M. Bamman, A. E. Thalacker-Mercer, S. N. Nichenametla, J. W. Locasale, Histone Methylation Dynamics and Gene Regulation Occur through the Sensing of One-Carbon Metabolism. *Cell Metab.* **22**, 861–873 (2015).
48. M. Serefidou, A. V. Venkatasubramani, A. Imhof, The impact of one carbon metabolism on histone methylation. *Front. Genet.* **10**, 764 (2019).
49. T. Q. Tran, X. H. Lowman, M. Kong, Molecular pathways: Metabolic control of histone methylation and gene expression in cancer. *Clin. Cancer Res.* **23**, 4004–4009 (2017).
50. S. Sivanand, I. Viney, K. E. Wellen, Spatiotemporal Control of Acetyl-CoA Metabolism in Chromatin Regulation. *Trends Biochem. Sci.* **43**, 61–74 (2018).
51. C. Cantó, K. J. Menzies, J. Auwerx, NAD Metabolism and the Control of Energy Homeostasis: A Balancing Act between Mitochondria and the Nucleus. *Cell Metabolism.* **22** (2015), pp. 31–53.
52. J. C. Newman, E. Verdin, B-hydroxybutyrate: A signaling metabolite. *Annu. Rev. Nutr.* **37**, 51–76 (2017).
53. X. Yang, K. Qian, Protein O-GlcNAcylation: emerging mechanisms and functions. *Nat. Rev. Mol. Cell Biol.* **18**, 452–465 (2017).
54. S. Olivier-Van Stichelen, P. Wang, M. Comly, D. C. Love, J. A. Hanover, Nutrient-driven O-linked N-acetylglucosamine (O-GlcNAc) cycling impacts neurodevelopmental timing and metabolism. *J. Biol. Chem.* **292**, 6076–6085 (2017).
55. S. Olivier-Van Stichelen, J. A. Hanover, You are what you eat: O-linked N-acetylglucosamine in disease, development and epigenetics. *Curr. Opin. Clin. Nutr. Metab. Care.* **18**, 339–345 (2015).

56. J. Y. Altarejos, M. Montminy, CREB and the CRTC co-activators: sensors for hormonal and metabolic signals. *Nat. Rev. Mol. Cell Biol.* **12**, 141–151 (2011).
57. K. Timper, J. C. Brüning, Hypothalamic circuits regulating appetite and energy homeostasis: pathways to obesity. *Dis. Model. Mech.* **10**, 679–689 (2017).
58. A. Marco, T. Kisliouk, A. Weller, N. Meiri, High fat diet induces hypermethylation of the hypothalamic Pomc promoter and obesity in post-weaning rats. *Psychoneuroendocrinology.* **38**, 2844–2853 (2013).
59. A. Marco, T. Kisliouk, T. Tabachnik, A. Weller, N. Meiri, DNA CpG methylation (5-methylcytosine) and its derivative (5-hydroxymethylcytosine) alter histone posttranslational modifications at the Pomc promoter, affecting the *Diabetes* (2016) (available at <https://diabetes.diabetesjournals.org/content/65/8/2258.abstract>).
60. C. Cifani, M. V. Micioni Di Bonaventura, M. Pucci, M. E. Giusepponi, A. Romano, A. Di Francesco, M. Maccarrone, C. D’Addario, Regulation of hypothalamic neuropeptides gene expression in diet induced obesity resistant rats: possible targets for obesity prediction? *Front. Neurosci.* **9**, 187 (2015).
61. A. Plagemann, K. Roepke, T. Harder, M. Brunn, A. Harder, M. Wittrock-Staar, T. Ziska, K. Schellong, E. Rodekamp, K. Melchior, J. W. Dudenhausen, Epigenetic malprogramming of the insulin receptor promoter due to developmental overfeeding. *J. Perinat. Med.* **38**, 393–400 (2010).
62. P. Kühnen, D. Handke, R. A. Waterland, B. J. Hennig, M. Silver, A. J. Fulford, P. Dominguez-Salas, S. E. Moore, A. M. Prentice, J. Spranger, A. Hinney, J. Hebebrand, F. L. Heppner, L. Walzer, C. Grötzinger, J. Gromoll, S. Wiegand, A. Grütters, H. Krude, Interindividual Variation in DNA Methylation at a Putative POMC Metastable Epiallele Is Associated with Obesity. *Cell Metab.* **24**, 502–509 (2016).
63. G. Deng, L. L. Morselli, V. A. Wagner, K. Balapattabi, S. A. Sapouckey, K. L. Knudtson, K. Rahmouni, H. Cui, C. D. Sigmund, A. E. Kwitek, J. L. Grobe, Single-nucleus RNA sequencing of the hypothalamic arcuate nucleus of C57BL/6J mice after prolonged diet-induced obesity. *Hypertension.* **76**, 589–597 (2020).
64. G. P. Lazzarino, M. F. Andreoli, M. F. Rossetti, C. Stoker, M. V. Tschopp, E. H. Luque, J. G. Ramos, Cafeteria diet differentially alters the expression of feeding-related genes through DNA methylation mechanisms in individual hypothalamic nuclei. *Mol. Cell. Endocrinol.* **450**, 113–125 (2017).
65. M. A. Rossi, M. L. Basiri, J. A. McHenry, O. Kosyk, J. M. Otis, H. E. van den Munkhof, J. Bryois, C. Hübel, G. Breen, W. Guo, C. M. Bulik, P. F. Sullivan, G. D. Stuber, Obesity remodels activity and transcriptional state of a lateral hypothalamic brake on feeding. *Science.* **364**, 1271–1274 (2019).
66. A. G. DiFeliceantonio, D. M. Small, Dopamine and diet-induced obesity. *Nat. Neurosci.* **22** (2019), pp. 1–2.

67. S.-J. Leigh, M. J. Morris, The role of reward circuitry and food addiction in the obesity epidemic: An update. *Biol. Psychol.* **131**, 31–42 (2018).
68. L. Décarie-Spain, C. Hryhorczuk, S. Fulton, Dopamine signalling adaptations by prolonged high-fat feeding. *Curr. Opin. Behav. Sci.* **9**, 136–143 (2016).
69. N. D. Volkow, G.-J. Wang, J. S. Fowler, D. Tomasi, F. Telang, Addiction: beyond dopamine reward circuitry. *Proc. Natl. Acad. Sci. U. S. A.* **108**, 15037–15042 (2011).
70. Z. Vucetic, J. L. Carlin, K. Totoki, T. M. Reyes, Epigenetic dysregulation of the dopamine system in diet-induced obesity. *J. Neurochem.* **120**, 891–898 (2012).
71. Z. Vucetic, J. Kimmel, T. M. Reyes, Chronic high-fat diet drives postnatal epigenetic regulation of μ -opioid receptor in the brain. *Neuropsychopharmacology.* **36**, 1199–1206 (2011).
72. O. Ramos-Lopez, J. I. Riezu-Boj, F. I. Milagro, J. A. Martinez, MENA Project, Dopamine gene methylation patterns are associated with obesity markers and carbohydrate intake. *Brain Behav.* **8**, e01017 (2018).
73. M. Bieliński, M. Jaracz, N. Lesiewska, M. Tomaszewska, M. Sikora, R. Junik, A. Kamińska, A. Tretyn, A. Borkowska, Association between COMT Val158Met and DAT1 polymorphisms and depressive symptoms in the obese population. *Neuropsychiatr. Dis. Treat.* **13**, 2221–2229 (2017).
74. E. C. Bruggeman, J. T. Garretson, R. Wu, H. Shi, B. Xue, Neuronal Dnmt1 Deficiency Attenuates Diet-Induced Obesity in Mice. *Endocrinology.* **159**, 145–162 (2018).
75. D. Kohno, S. Lee, M. J. Harper, K. W. Kim, H. Sone, T. Sasaki, T. Kitamura, G. Fan, J. K. Elmquist, Dnmt3a in Sim1 neurons is necessary for normal energy homeostasis. *J. Neurosci.* **34**, 15288–15296 (2014).
76. M. O. Dietrich, C. Antunes, G. Geliang, Z.-W. Liu, E. Borok, Y. Nie, A. W. Xu, D. O. Souza, Q. Gao, S. Diano, X.-B. Gao, T. L. Horvath, Agrp neurons mediate Sirt1's action on the melanocortin system and energy balance: roles for Sirt1 in neuronal firing and synaptic plasticity. *J. Neurosci.* **30**, 11815–11825 (2010).
77. L. Gan, J. Sun, S. Yang, X. Zhang, W. Chen, Y. Sun, X. Wu, C. Cheng, J. Yuan, A. Li, M. A. Corbett, M. P. Dixon, T. Thomas, A. K. Voss, J. Gécz, G.-Z. Wang, A. Bonni, Q. Li, J. Huang, Chromatin-Binding Protein PHF6 Regulates Activity-Dependent Transcriptional Networks to Promote Hunger Response. *Cell Rep.* **30**, 3717-3728.e6 (2020).
78. S. Hardivillé, G. W. Hart, Nutrient regulation of signaling, transcription, and cell physiology by O-GlcNAcylation. *Cell Metab.* **20**, 208–213 (2014).
79. O. Lagerlöf, J. E. Slocomb, I. Hong, Y. Aponte, S. Blackshaw, G. W. Hart, R. L. Haganir, The nutrient sensor OGT in PVN neurons regulates feeding. *Science.* **351**, 1293–1296 (2016).

80. J. E. Rexach, P. M. Clark, D. E. Mason, R. L. Neve, E. C. Peters, L. C. Hsieh-Wilson, Dynamic O-GlcNAc modification regulates CREB-mediated gene expression and memory formation. *Nat. Chem. Biol.* **8**, 253–261 (2012).
81. G. Cavaliere, G. Trinchese, E. Penna, F. Cimmino, C. Pirozzi, A. Lama, C. Annunziata, A. Catapano, G. Mattace Raso, R. Meli, M. Monda, G. Messina, C. Zammit, M. Crispino, M. P. Mollica, High-Fat Diet induces neuroinflammation and mitochondrial impairment in mice cerebral cortex and synaptic fraction. *Front. Cell. Neurosci.* **13**, 509 (2019).
82. J. Kalivarathan, K. Kalaivanan, S. P. Chandrasekaran, D. Nanda, V. Ramachandran, A. Carani Venkatraman, Apigenin modulates hippocampal CREB-BDNF signaling in high fat, high fructose diet-fed rats. *J. Funct. Foods.* **68**, 103898 (2020).
83. Q.-P. Wang, Y. Q. Lin, M.-L. Lai, Z. Su, L. J. Oyston, T. Clark, S. J. Park, T. M. Khuong, M.-T. Lau, V. Shenton, Y.-C. Shi, D. E. James, W. W. Ja, H. Herzog, S. J. Simpson, G. G. Neely, PGC1 α Controls Sucrose Taste Sensitization in *Drosophila*. *Cell Rep.* **31**, 107480 (2020).
84. A. A. Butler, R. G. Sanchez, T. J. Jarome, W. M. Webb, F. D. Lubin, O-GlcNAc and EZH2-mediated epigenetic regulation of gene expression during consolidation of fear memories. *Learn. Mem.* **26**, 373–379 (2019).
85. C. L. Moreno, L. Yang, P. A. Dacks, F. Isoda, J. M. A. van Deursen, C. V. Mobbs, Role of hypothalamic Creb-binding protein in obesity and molecular reprogramming of metabolic substrates. *PLoS One.* **11**, e0166381 (2016).
86. I. Sánchez Fernández, H. P. Goodkin, R. C. Scott, Pathophysiology of convulsive status epilepticus. *Seizure.* **68**, 16–21 (2019).
87. B. E. Lee, H. Y. Kim, H.-J. Kim, H. Jeong, B.-G. Kim, H.-E. Lee, J. Lee, H. B. Kim, S. E. Lee, Y. R. Yang, E. C. Yi, J. A. Hanover, K. Myung, P.-G. Suh, T. Kwon, J.-I. Kim, O-GlcNAcylation regulates dopamine neuron function, survival and degeneration in Parkinson disease. *Brain.* **143**, 3699–3716 (2020).
88. H.-B. Ruan, M. O. Dietrich, Z.-W. Liu, M. R. Zimmer, M.-D. Li, J. P. Singh, K. Zhang, R. Yin, J. Wu, T. L. Horvath, X. Yang, O-GlcNAc transferase enables AgRP neurons to suppress browning of white fat. *Cell.* **159**, 306–317 (2014).
89. H. Hwang, H. Rhim, Acutely elevated O-GlcNAcylation suppresses hippocampal activity by modulating both intrinsic and synaptic excitability factors. *Sci. Rep.* **9**, 7287 (2019).
90. M. K. Tallent, N. Varghis, Y. Skorobogatko, L. Hernandez-Cuebas, K. Whelan, D. J. Vocadlo, K. Vosseller, In vivo modulation of O-GlcNAc levels regulates hippocampal synaptic plasticity through interplay with phosphorylation. *J. Biol. Chem.* **284**, 174–181 (2009).
91. E. W. Taylor, K. Wang, A. R. Nelson, T. M. Bredemann, K. B. Fraser, S. M. Clinton, R. Puckett, R. B. Marchase, J. C. Chatham, L. L. McMahon, O-GlcNAcylation of AMPA

- receptor GluA2 is associated with a novel form of long-term depression at hippocampal synapses. *J. Neurosci.* **34**, 10–21 (2014).
92. A. C. Giles, M. Desbois, K. J. Opperman, R. Tavora, M. J. Maroni, B. Grill, A complex containing the O-GlcNAc transferase OGT-1 and the ubiquitin ligase EEL-1 regulates GABA neuron function. *J. Biol. Chem.* **294**, 6843–6856 (2019).
 93. C. Su, T. L. Schwarz, O-GlcNAc transferase is essential for sensory neuron survival and maintenance. *J. Neurosci.* **37**, 2125–2136 (2017).
 94. O. Lagerlöf, G. W. Hart, R. L. Huganir, O-GlcNAc transferase regulates excitatory synapse maturity. *Proc. Natl. Acad. Sci. U. S. A.* **114**, 1684–1689 (2017).
 95. D. Wilinski, J. Winzeler, W. Duren, J. L. Persons, K. J. Holme, J. Mosquera, M. Khabiri, J. M. Kinchen, P. L. Freddolino, A. Karnovsky, M. Dus, Rapid metabolic shifts occur during the transition between hunger and satiety in *Drosophila melanogaster*. *Nat. Commun.* **10**, 4052 (2019).
 96. A. Öst, A. Lempradl, E. Casas, M. Weigert, T. Tiko, M. Deniz, L. Pantano, U. Boenisch, P. M. Itskov, M. Stoeckius, M. Ruf, N. Rajewsky, G. Reuter, N. Iovino, C. Ribeiro, M. Alenius, S. Heyne, T. Vavouri, J. A. Pospisilik, Paternal diet defines offspring chromatin state and intergenerational obesity. *Cell.* **159**, 1352–1364 (2014).
 97. M. Sarangi, M. Dus, Crème de la Créature: Dietary Influences on Behavior in Animal Models. *Front. Behav. Neurosci.* **15** (2021), doi:10.3389/fnbeh.2021.746299.
 98. G. K. Beauchamp, M. Bertino, D. Burke, K. Engelman, Experimental sodium depletion and salt taste in normal human volunteers. *Am. J. Clin. Nutr.* **51**, 881–889 (1990).
 99. R. M. Pangborn, S. D. Pecore, Taste perception of sodium chloride in relation to dietary intake of salt. *Am. J. Clin. Nutr.* **35**, 510–520 (1982).
 100. D. Liu, N. Archer, K. Duesing, G. Hannan, R. Keast, Mechanism of fat taste perception: Association with diet and obesity. *Prog. Lipid Res.* **63**, 41–49 (2016).
 101. L. P. Newman, D. P. Bolhuis, S. J. Torres, R. S. J. Keast, Dietary fat restriction increases fat taste sensitivity in people with obesity. *Obesity (Silver Spring)*. **24**, 328–334 (2016).
 102. F. Sartor, L. F. Donaldson, D. A. Markland, H. Loveday, M. J. Jackson, H.-P. Kubis, Taste perception and implicit attitude toward sweet related to body mass index and soft drink supplementation. *Appetite*. **57**, 237–246 (2011).
 103. L. M. Bartoshuk, V. B. Duffy, J. E. Hayes, H. R. Moskowitz, D. J. Snyder, Psychophysics of sweet and fat perception in obesity: problems, solutions and new perspectives. *Philos. Trans. R. Soc. Lond. B Biol. Sci.* **361**, 1137–1148 (2006).
 104. H.-R. Berthoud, H. Zheng, Modulation of taste responsiveness and food preference by obesity and weight loss. *Physiol. Behav.* **107**, 527–532 (2012).

105. S. Turner, C. Diako, R. Kruger, M. Wong, W. Wood, K. Rutherford-Markwick, A. Ali, Consuming *Gymnema sylvestre* Reduces the Desire for High-Sugar Sweet Foods. *Nutrients*. **12** (2020), doi:10.3390/nu12041046.
106. M. Chevrot, A. Bernard, D. Ancel, M. Buttet, C. Martin, S. Abdoul-Azize, J.-F. Merlin, H. Poirier, I. Niot, N. A. Khan, P. Passilly-Degrace, P. Besnard, Obesity alters the gustatory perception of lipids in the mouse: plausible involvement of lingual CD36. *J. Lipid Res.* **54**, 2485–2494 (2013).
107. M. H. Ozdener, S. Subramaniam, S. Sundaresan, O. Sery, T. Hashimoto, Y. Asakawa, P. Besnard, N. A. Abumrad, N. A. Khan, CD36- and GPR120-mediated Ca²⁺ signaling in human taste bud cells mediates differential responses to fatty acids and is altered in obese mice. *Gastroenterology*. **146**, 995–1005 (2014).
108. A. Kaufman, E. Choo, A. Koh, R. Dando, Inflammation arising from obesity reduces taste bud abundance and inhibits renewal. *PLoS Biol.* **16**, e2001959 (2018).
109. K. Chen, J. Yan, Y. Suo, J. Li, Q. Wang, B. Lv, Nutritional status alters saccharin intake and sweet receptor mRNA expression in rat taste buds. *Brain Res.* **1325**, 53–62 (2010).
110. Z. C. Ahart, L. E. Martin, B. R. Kemp, D. Dutta Banik, S. G. E. Roberts, A.-M. Torregrossa, K. F. Medler, Differential effects of diet and weight on taste responses in diet-induced obese mice. *Obesity (Silver Spring)*. **28**, 284–292 (2020).
111. N. Archer, J. Shaw, M. Cochet-Broch, R. Bunch, A. Poelman, W. Barendse, K. Duesing, Obesity is associated with altered gene expression in human tastebuds. *Int. J. Obes. (Lond)*. **43**, 1475–1484 (2019).
112. L. P. McCluskey, L. He, G. Dong, R. Harris, Chronic exposure to liquid sucrose and dry sucrose diet have differential effects on peripheral taste responses in female rats. *Appetite*. **145**, 104499 (2020).
113. L. P. Musselman, R. P. Kühnlein, *Drosophila* as a model to study obesity and metabolic disease. *J. Exp. Biol.* **221** (2018), doi:10.1242/jeb.163881.
114. A. H. Brand, N. Perrimon, Targeted gene expression as a means of altering cell fates and generating dominant phenotypes. *Development*. **118**, 401–415 (1993).
115. F. Lourido, D. Quenti, D. Salgado-Canales, N. Tobar, Domeless receptor loss in fat body tissue reverts insulin resistance induced by a high-sugar diet in *Drosophila melanogaster*. *Sci. Rep.* **11**, 3263 (2021).
116. E. T. Heinrichsen, H. Zhang, J. E. Robinson, J. Ngo, S. Diop, R. Bodmer, W. J. Joiner, C. M. Metallo, G. G. Haddad, Metabolic and transcriptional response to a high-fat diet in *Drosophila melanogaster*. *Mol. Metab.* **3**, 42–54 (2014).

117. R. T. Birse, J. Choi, K. Reardon, J. Rodriguez, S. Graham, S. Diop, K. Ocorr, R. Bodmer, S. Oldham, High-fat-diet-induced obesity and heart dysfunction are regulated by the TOR pathway in *Drosophila*. *Cell Metab.* **12**, 533–544 (2010).
118. J. Na, L. P. Musselman, J. Pendse, T. J. Baranski, R. Bodmer, K. Ocorr, R. Cagan, A *Drosophila* model of high sugar diet-induced cardiomyopathy. *PLoS Genet.* **9**, e1003175 (2013).
119. Y. Jung, D. Goldman, Role of RNA modifications in brain and behavior. *Genes Brain Behav.* **17**, e12444 (2018).
120. E. T. Heinrichsen, G. G. Haddad, Role of high-fat diet in stress response of *Drosophila*. *PLoS One.* **7**, e42587 (2012).
121. W. Hemphill, O. Rivera, M. Talbert, RNA-Sequencing of *Drosophila melanogaster* head tissue on high-sugar and high-fat diets. *G3 (Bethesda).* **8**, 279–290 (2018).
122. T. Stobdan, D. Sahoo, P. Azad, I. Hartley, E. Heinrichsen, D. Zhou, G. G. Haddad, High fat diet induces sex-specific differential gene expression in *Drosophila melanogaster*. *PLoS One.* **14**, e0213474 (2019).
123. L. B. Meichtry, M. R. Poetini, M. M. M. Dahleh, S. M. Araujo, E. A. S. Musachio, V. C. Bortolotto, S. de Freitas Couto, S. Somacal, T. Emanuelli, M. C. Gayer, R. Roehrs, G. P. Guerra, M. Prigol, Addition of saturated and trans-fatty acids to the diet induces depressive and anxiety-like behaviors in *Drosophila melanogaster*. *Neuroscience.* **443**, 164–175 (2020).
124. S.-H. Hong, M. Kang, K.-S. Lee, K. Yu, High fat diet-induced TGF- β /Gbb signaling provokes insulin resistance through the tribbles expression. *Sci. Rep.* **6** (2016), doi:10.1038/srep30265.
125. O. Rivera, L. McHan, B. Konadu, S. Patel, S. Sint Jago, M. E. Talbert, A high-fat diet impacts memory and gene expression of the head in mated female *Drosophila melanogaster*. *J. Comp. Physiol. B.* **189**, 179–198 (2019).

Chapter 2 High Dietary Sugar Reshapes Sweet Taste to Promote Feeding Behavior in *Drosophila melanogaster*

This chapter has been published as:

May CE, **Vaziri A**, Lin YQ, Grushko O, Khabiri M, Wang QP, Holme KJ, Pletcher SD, Freddolino PL, Neely GG, Dus M. High Dietary Sugar Reshapes Sweet Taste to Promote Feeding Behavior in *Drosophila melanogaster*. Cell Rep. 2019 May 7;27(6):1675-1685.e7.

2.1 Abstract

The sensation of pleasurable food qualities plays a crucial role in regulating eating. Recent studies found that humans with obesity have lower taste responses to sweet stimuli, but whether these sensory changes impact food intake is unclear. To tackle this question, we studied the effects of a high sugar diet on sweet taste sensation and feeding behavior in *Drosophila melanogaster*. Fruit flies on this diet had lower behavioral and physiological responses to sweet stimuli, overconsumed food, and developed obesity. Correcting taste deficits by manipulating the excitability of the sweet gustatory neurons, prevented overeating and fat accumulation in animals exposed to the high sugar diet. By using genetically obese and lean animals, we found that excess dietary sugar, but not obesity or dietary sweetness alone, promoted taste deficits and eating via the cell-autonomous action of the sugar sensor *O-GlcNAc Transferase* in the sweet-sensing neurons. Our work demonstrates that the reshaping of sweet taste sensation by high dietary sugar is a driver of obesity and highlights the role of glucose metabolism in altering neural activity and behavior.

2.2 Introduction

Many arguments about the underlying cause in the rise of obesity point towards the increased availability of highly palatable foods. Such foods are thought to alter the activity of reward pathways at least partly via their taste properties, and this leads to overconsumption and weight gain (Small, 2009; Volkow et al., 2011). No doubt the perception of palatable food qualities such as sweetness plays a key role in eating behaviors. However, this hypothesis does not fit with a growing body of evidence that associates obesity with reduced taste perceptions (Bartoshuk et al., 2006; Berthoud and Zheng, 2012; Rodin et al., 1976). Specifically, obesity has been associated with lower sweetness intensity (Bartoshuk et al., 2006; Overberg et al., 2012; Sartor et al., 2011) and sensitivity to sweet (Proserpio et al., 2016), umami (Pepino et al., 2010), MSG (Donaldson et al., 2009), and salt (Simchen et al., 2006; Skrandies and Zschieschang, 2015). However, other studies reported no or opposite associations between BMI and taste sensitivity (Donaldson et al., 2009; Grinker, 1978; Hardikar et al., 2017; Thompson et al., 1977). Recently, research on rodents found that animals genetically prone to obesity or fed high energy diets have decreased behavioral (Berthoud and Zheng, 2012; Chevrot et al., 2013; Robinson et al., 2015) and physiological responses of the taste buds to sweet or fatty stimuli (Maliphol et al., 2013; Ozdener et al., 2014), changes in the number of taste buds (Kaufman et al., 2018) and lower expression of the sweet taste receptors (Chen et al., 2010), but these changes were not causally linked to taste function and feeding behavior. Thus, while there is accumulating evidence that taste signals are dulled in obese mammals, the picture is complex, and studies in model organisms with a simpler taste system and conserved metabolism would be greatly beneficial in probing the connection between taste function, feeding behavior, and obesity. Here we exploited the relative simplicity of the *Drosophila* taste system, where the sweet-sensing cells are neurons that project directly to the brain

to tackle a few important questions. First, do changes in taste sensation occur with diet-induced obesity? Are these a consequence of the altered physiology of the obese state or do they result from chronic exposure to a high nutrient diet? And, finally, if changes in taste function occur, what role do they play in the etiology of obesity?

Using behavioral assays and *in vivo* imaging we found that fruit flies fed a high sugar diet show a dulled sense of sweet taste, and that this occurs because of lower responses of the sweet taste neurons to sugar. This deficit is caused by excess dietary sugar, not obesity, and is mediated by the increased activity of the conserved sugar sensor *O-GlcNAc-Transferase* (OGT) (Hanover et al., 2010; Hardiville and Hart, 2014) in the sweet taste cells. By monitoring feeding behavior at high resolution and using neuro- and optogenetic manipulations of sweet taste cell excitability, we show the dulling of sweet taste leads to overfeeding and obesity. Preventing a decrease in sweet taste sensation rescues feeding and obesity in animals exposed to the high sugar diet. Together, our results implicate deficits in sweet taste as drivers of obesity and begin to map the molecular underpinnings through which exposure to excess dietary sugar reshapes taste function and behavior.

2.3 Results

A sugar diet promotes a reduction in sweet taste responses independently of obesity.

Recent reports found that humans with obesity and rodents fed highly palatable diets have a dulled sense of sweet taste (Bartoshuk et al., 2006; Berthoud and Zheng, 2012; Overberg et al., 2012; Pasquet et al., 2007; Proserpio et al., 2016; Sartor et al., 2011). However, it is unclear whether this reduction is a metabolic consequence of obesity or an effect of diet. To address this question, we fed *Drosophila melanogaster* fruit flies an established model of high

sugar diet (Musselman et al., 2011; Musselman and Kuhnlein, 2018) and assessed their taste responses to sweet stimuli (*see* STAR Methods for dietary manipulations). Fruit flies fed a 30% sucrose diet for several weeks develop obesity, metabolic syndrome, peripheral insulin resistance, and recapitulate the hallmarks of kidney and heart disease in their corresponding organs (Musselman et al., 2011; Musselman and Kuhnlein, 2018; Na et al., 2013). In contrast, short, up to 1-week exposures to the high sugar diet (SD, 1.4 calories/gram) lead to fat accumulation compared to animals on a control diet (CD, 0.58 calories/gram), (Fig. 1A and Supplementary Information Fig. S1A), but have no effect on *Drosophila insulin-like peptide (dilp)* transcript levels (Supplementary Information Fig. S2A and B). The 30% sugar concentration in the diet is similar to that found in many cookies available at grocery stores; for comparison, mango and banana contain about ~15% sucrose, while the majority of children's cereal in US grocery stores has 45-60% sugar content (Ng et al., 2012).

In *Drosophila*, taste cells are neurons that sense the environment through taste hairs located on the labellum at the tip of the proboscis, the main taste organ in the fly (Supplementary Information Fig. S3B *for a schematic of the anatomy*). Taste neurons, which express receptors for only one taste modality, send their projections to the SubEsophageal Zone (SEZ), the taste processing center in the fly brain, where taste modalities remain segregated (Harris et al., 2015; Marella et al., 2006; Scott, 2018). We examined fly taste responses using the Proboscis Extension Response (PER) assay, a behavioral measure of taste that records the magnitude of proboscis extension in response to stimulation of the taste hairs with a sweet stimulus (Shiraiwa and Carlson, 2007). Age-matched flies fed a SD showed a rapid and progressive decrease in taste responses to supra-threshold (30, 5, 1%) concentrations of sucrose with time (Fig. 1B). In flies, gustatory receptor neurons are also located in the legs and wings, and a SD also reduced

proboscis responses induced by the stimulation of the leg sensory cells (Supplementary Information Fig. S1B). The decrease in taste responses was not due to motor defects because proboscis responses to the fatty acid octanoic acid (Masek and Keene, 2013) were unchanged between flies on the two diets (Supplementary Information Fig. S1C). Furthermore, taste deficits occurred regardless of fasting time (Supplementary Information Fig. S1D), ruling out the possibility that they are a consequence of higher energy stores in flies fed a SD. Thus, flies fed a SD have lower behavioral responses to supra-threshold concentrations of sucrose. To determine if a SD diet also alters the thresholds for detection of sweetness, we counted the percent of animals able to detect the non-caloric sweetener L-glucose at different concentrations in the range of 10 to 90 mM. We used L-glucose instead of other sweet sugars to eliminate any potential post-ingestive effects on food detection, since animals with impaired taste can still detect the presence of nutritious sugars (de Araujo et al., 2008; Dus et al., 2011; Stafford et al., 2012); the taste of L-glucose is transduced through the same cellular and molecular machinery as sucrose (Dus et al., 2013; Fujita and Tanimura, 2011). Compared to flies on a CD, animals fed a SD had a taste detection curve shifted to higher concentrations of the sweetener, suggesting that their sensitivity to sweetness was also lower (Supplementary Information Fig. S1E).

To probe whether taste deficits were due to high dietary sweetness, we examined the taste responses of animals fed a sweet, non-caloric sucralose diet. However, taste responses to sucrose remained unchanged in these flies (Fig. 1C, *dark green*) and there was no fat accumulation (Supplementary Information Fig. S1F). Similarly, flies fed a calorically-dense (1.4 calories/gram as the 30% high sugar diet), but not sweet, lard-supplemented diet accumulated fat (Supplementary Information. Fig. S1G, *lime green*), but had normal taste responses (Fig. 1C), indicating that sweetness or excessive calories alone are insufficient to lower sweet taste

sensation. In contrast, only sweet *and* nutritious diets such as those supplemented with D-fructose, D-glucose, and sucrose promoted a decrease in sweet taste responses (Fig. 1D).

In mammals, the molecular mechanisms through which diet-induced obesity lowers taste sensation are unknown. To test whether there is a connection between taste deficits and obesity, we set out to genetically uncouple excess body fat from dietary sugar exposure. First, we tested the taste responses of fly mutants for the Adipose Triglyceride Lipase *brummer* (*bmm*), which is involved in the breakdown of fat (Gronke et al., 2005) (Fig. 2A). *bmm* mutants have as much body fat on a control diet as wild-type flies on a SD (Fig. 2B), but their taste responses as measured by PER were normal on a CD and reduced on a SD (Fig. 2C), suggesting that obesity alone is not sufficient to promote a reduction in sweet taste. This is consistent with our observation that a lard diet had no effect on sweet taste (Fig. 1C and Supplementary Information Fig. S1G). Next, we tested genetically lean flies to ask if a decrease in taste responses was linked to high dietary sugar, instead of obesity. *perilipin2* (*plin2*) is a gene essential for fat mobilization (Beller et al., 2010) (Fig. 2A); despite remaining lean (Fig. 2B) and maintaining normal *Drosophila insulin-like peptide* transcript levels on a SD (Supplementary Information Fig. S2A and B), *plin2* mutants experienced a comparable decrease in taste responses to that of control and *bmm* mutant flies (Fig. 2C). These results suggest that obesity is neither necessary nor sufficient for the reduction in sweet taste, and that, instead, excess dietary sugar – but not just dietary sweetness, since a sweet sucralose diet did not dull sweet taste – may alter taste directly.

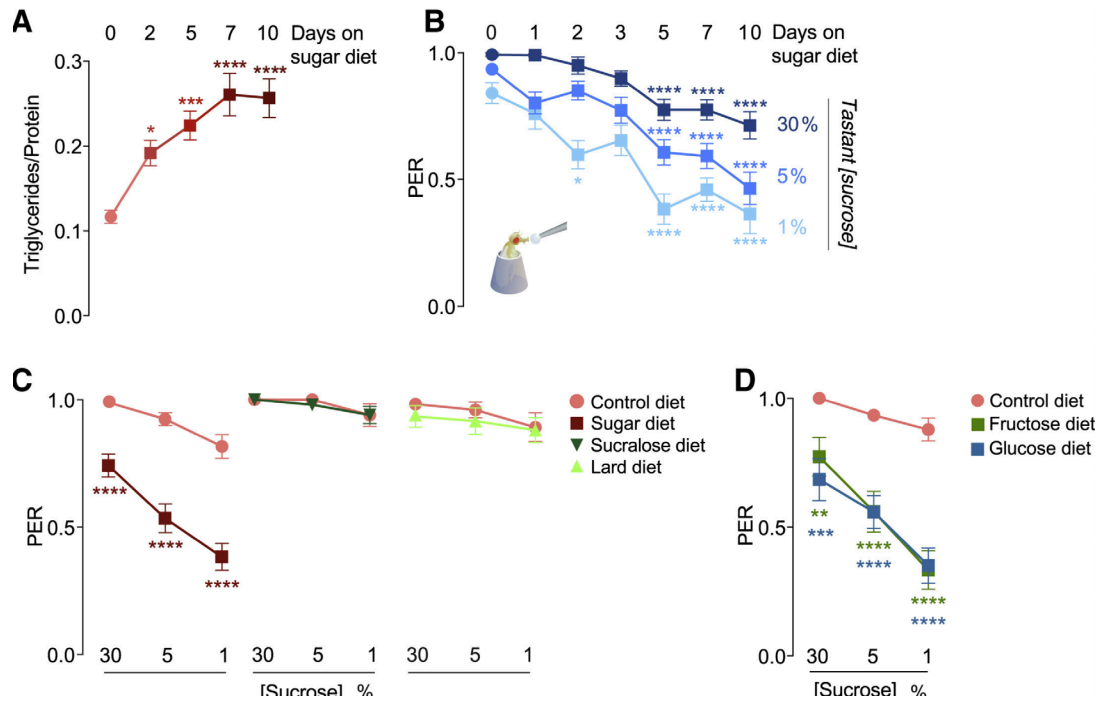


Figure 2.1 High sugar diet decreases sweet taste sensation

(A) Triglyceride levels normalized to protein in age-matched male *w1118^{CS}* flies on a control (salmon) or 30% sucrose diet (burgundy) for 2, 5, 7, or 10 days. $n = 24$, one-way ANOVA with Dunnett's test, comparisons to control diet. (B) Taste responses measured by the Proboscis Extension Response (PER) to the stimulation of the labellum with 1%, 5%, and 30% sucrose (right y axis, shades of blue) in age-matched male *w1118^{CS}* flies fed a control (circles) or 30% sugar (squares) diet over 10 days. $n = 24-61$, Kruskal-Wallis with Dunn's test, comparisons to control diet. (C) Taste responses to 1%, 5%, and 30% sucrose stimulation (x axis) of the labellum in *w1118^{CS}* flies fed a control, sucrose, lard, or sucralose diet for 7 days. $n = 22-28$, Wilcoxon matched-pairs signed rank test, comparisons to control diet response. (D) Taste responses to 1%, 5%, and 30% sucrose stimulation (x axis) of the labellum in *w1118^{CS}* flies fed diets supplemented with 30% fructose, 30% glucose, or a control diet for 7 days. $n = 24-28$, two-way ANOVA with Fisher's LSD test, comparisons to control diet for each concentration. All data shown as mean \pm SEM, **** $p < 0.0001$, *** $p < 0.001$, ** $p < 0.01$, and * $p < 0.05$ for all panels unless indicated.

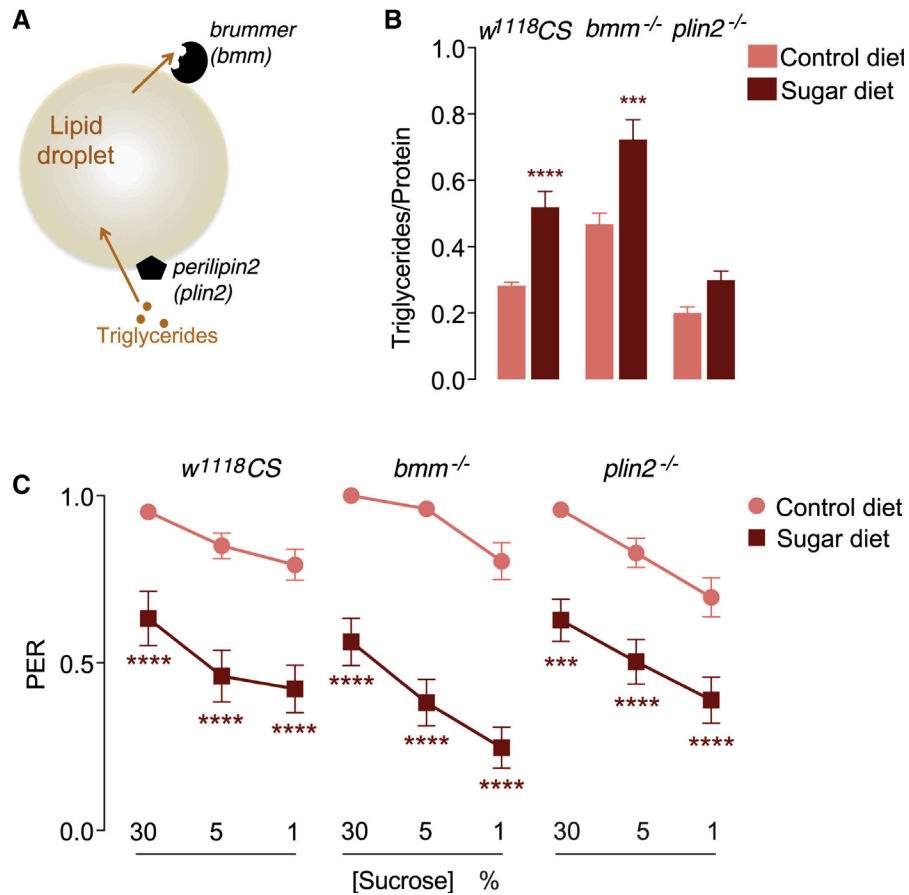


Figure 2.2 A sugar diet decreases taste sensation independently of obesity

(A) Overview of the function of the ATG-lipase *brummer* (*bmm*) and *perilipin2* (*plin2*) in lipid homeostasis. (B) Triglyceride levels normalized to protein in age-matched male *w^{1118CS}* (control), *bmm^{-/-}*, and *plin2^{-/-}* flies on control or 30% sugar diet for 7 days. $n = 8-16$, two-way ANOVA with Sidak's test, comparisons to control diet. (C) Taste responses to 1%, 5%, and 30% sucrose (x axis) of age-matched male *w^{1118CS}*, *bmm^{-/-}*, and *plin2^{-/-}* flies on control (circles) or sugar (squares) diet for 7 days. $n = 26-56$, multiple t tests, comparisons to control diet. All data shown as mean \pm SEM, **** $p < 0.0001$, *** $p < 0.001$, ** $p < 0.01$, and * $p < 0.05$ for all panels unless indicated.

A high sugar diet decreases the responses of the sweet-sensing neurons to sugar.

To better understand how a sugar diet decreases sweet taste sensation, we examined the physiology of the sweet taste neurons. Since, we observed no changes in the number of sweet taste neurons labeled by the sweet *Gustatory Receptor 5a-GAL4* transgene (Chyb et al., 2003; Fujii et al., 2015; Marella et al., 2006) driving GFP in the labellum of flies on a SD (Supplementary Information Fig. S3A), we reasoned that a high sugar diet may instead alter the response of these neurons to sugar. To test this possibility, we measured the *in vivo*, real time responses of the sweet *Gustatory receptor 64f (Gr64f)*+ (Dahanukar et al., 2007) neurons to stimulation of the labellum with 30% sucrose using the genetically encoded, presynaptic calcium sensor *GCaMP6s-Brp-mCherry* (Kiragasi et al., 2017) (Fig. 3A). Presynaptic responses to 30% sucrose stimulation of the proboscis were identical after 1-day exposure to the SD but decreased gradually with longer exposures (Fig. 3B and C), which matched the magnitude and progression of sweet taste deficits as measured by PER (Fig. 1B). In addition, we also found that animals had fewer sugar-induced action potentials after both short- and long-term exposure to the SD (Supplementary Information Fig. S3B and C). Thus, exposure to high dietary sugar decreases the responsiveness of the taste neurons to sugar; while we measured both changes in presynaptic calcium responses and action potentials, defects in synaptic activity more faithfully track the decrease in PER.

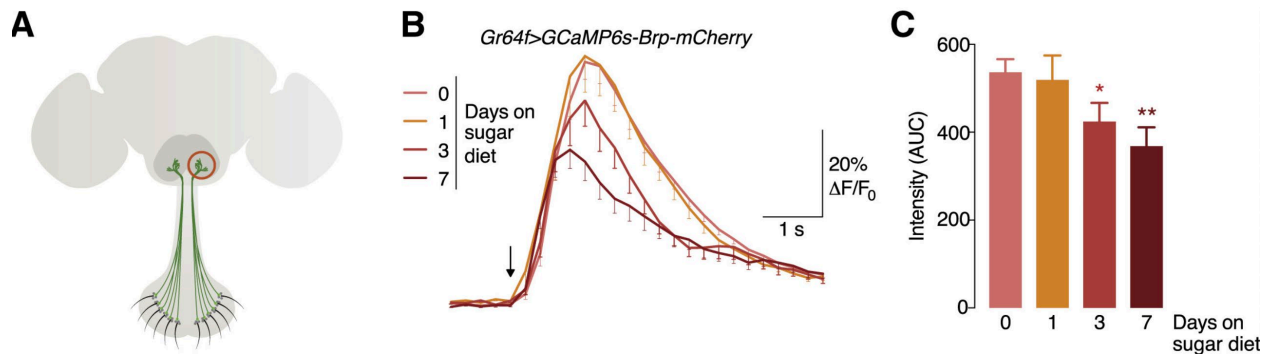


Figure 2.3 A sugar diet decreases synaptic responses to a sugar stimulus in the sweet taste neurons

(A) The cell bodies of chemosensory neurons are in the labellum with dendrites protruding into the taste hair (sensillum, black) and the axons (red circle) terminating in the subesophageal zone (SEZ, darker gray) of the brain. Sweet taste cells are in green. (B and C) Average $\Delta F/F_0$ calcium response traces (B) and their area under the curve (C) in the synaptic terminals of *Gr64f>GCaMP6s-Bruchpilot-mCherry* flies fed a control diet (day 0) or a sugar diet for 1, 3, and 7 days, before and after (arrow) stimulation of the proboscis with 30% sucrose. $n = 26$ brains, Kruskal-Wallis with uncorrected Dunn's, comparisons to control diet (day 0). All data shown as mean \pm SEM, **** $p < 0.0001$, *** $p < 0.001$, ** $p < 0.01$, and * $p < 0.05$ for all panels unless indicated.

A sugar diet promotes feeding by increasing the size and duration of meals.

To analyze the effects of changes in sweet taste function on feeding behavior, we first examined the effects of excess dietary sugar on feeding behavior using modifications to the Fly-to-Liquid-food-Interaction Counter (FLIC) (Ro et al., 2014), an assay that measures feeding behaviors by detecting electronic signals, “licks”, when the fly proboscis touches the food. By attaching food reservoirs to the FLIC apparatus, we were able to record the feeding patterns of individual flies continuously and at a high temporal resolution (5 Hz) for days without disturbance or fasting. Because 30% sucrose was viscous, we conducted the experiments with 20% sucrose, which also promotes obesity and taste deficits (Supplementary Information Fig. S4A and B). Control *w¹¹¹⁸CS* flies fed a 5% sucrose control diet while on the FLIC showed a stable number of licks per day (Fig. 4A, *salmon*). In contrast, flies fed a sweeter diet of 20% sucrose, showed a progressive increase in licks over time; by days 3-5 these flies licked more per day than those fed 5% sucrose (Fig. 4A, *burgundy*). Flies fed a CD or SD in standard fly food vials for 10 days and placed on the FLIC for a single day also showed an increase in licks on 20% sucrose (Supplementary Information Fig. S4C). To better characterize the temporal dynamics and investigate the effect of diet on meal patterns, we binned licks in 30’ intervals over many days for individual flies (Fig. 4B) and as a group average (Fig. 4C). We found that flies, like mammals, eat in discrete patterns, here termed “meals”, that closely follow circadian activity (Fig. 4B and C). Flies on 20% sucrose still consumed only two meals per day, but the peaks became higher and wider with more time on the diet (Fig. 4C). Furthermore, while the onset of each morning (AM) and evening (PM) meal was similar to that of flies on 5% sucrose, the offset changed with more days on diet, suggesting that meals became longer while flies are eating 20% sucrose (Fig. 4C). To quantify meal duration, we measured the time of meal start and end for

AM and PM meals for each fly (Fig. 4D). The duration of the AM and PM meals of flies on 5% sucrose remained the same over 7 days (Fig. 4E). In contrast, that of flies eating 20% sucrose became longer with more days on diet. By day 7 the meal duration of flies eating 20% sucrose was twice as long as that of flies eating 5% sucrose (Fig. 4E). We next quantified the size of each meal by calculating the area under each AM and PM meal peaks (Fig. 4D, *gray*). Like with duration, the size of each AM and PM meals increased with more days on a 20% diet, while it stayed unchanged in flies eating 5% sucrose (Fig. 4F). Overall, we observed a strong relationship between meal size and duration (Fig. 4E and F), indicating that longer meals may contribute to increased meal size. Together, our high-resolution analysis of meal patterns suggests that a high sugar diet alters feeding by extending the duration and size of each meal, rather than by increasing the number of meals per day, which points to potential changes in satiety rather than hunger.

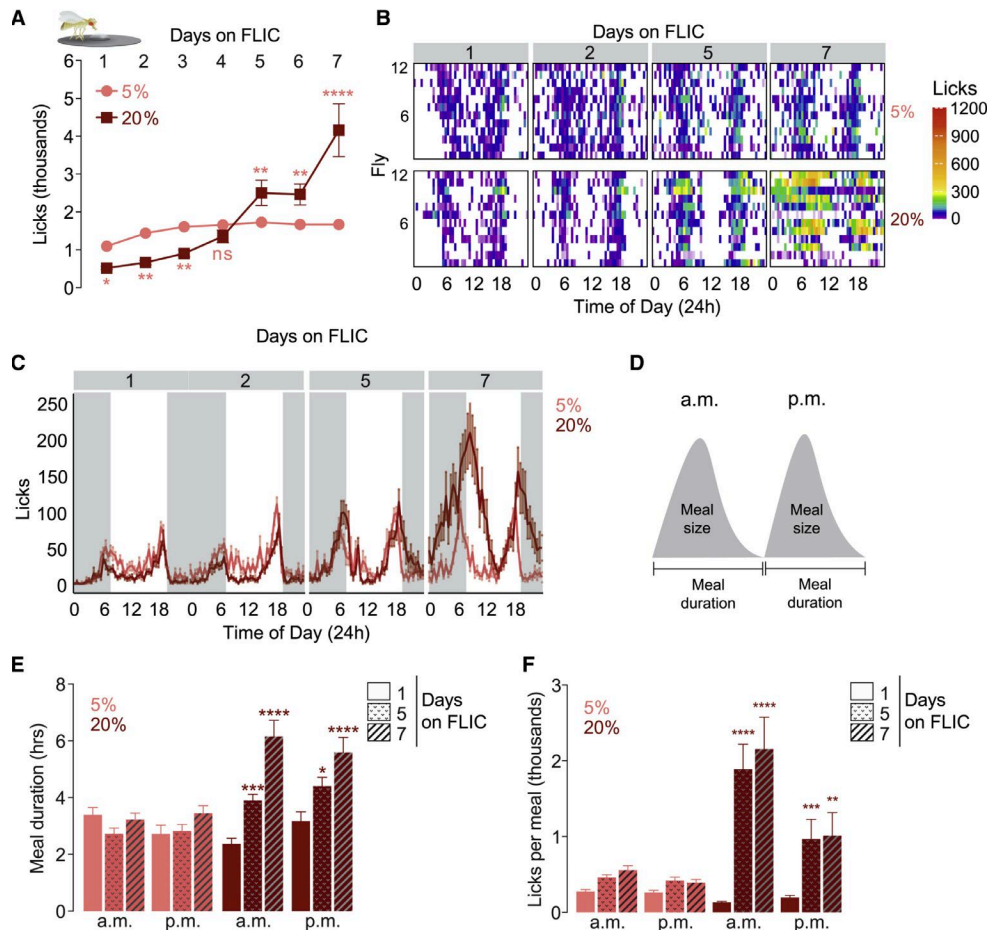


Figure 2.4 Flies fed a high sugar diet show increased feeding behavior, meal size, and duration

(A) Average licks per day of age-matched *w1118^{CS}* male flies feeding continuously on 5% (salmon) or 20% (burgundy) sucrose on the FLIC. $n = 26-72$, two-way ANOVA with Fisher's LSD, compared to same-day 5% sucrose licks. (B) Heatmap of the licks binned by 30 minutes of individual flies (left y axis) feeding continuously on 5% or 20% sucrose on the FLIC at days 1, 2, 5, and 7. The x axis represents time in 24 h, time 0 indicates midnight (Zeitgeber time 17 [ZT17]). (C) Meal patterns quantified as average licks binned by 30 min for flies feeding on 5% or 20% sucrose on selected days 1, 2, 5, or 7 (from A). The x axis is as in (B). (D) Schematic for how meal duration and size were determined for morning (a.m.) and evening (p.m.) meals. (E and F) The meal (E) duration (h) and (F) size in licks of the morning (a.m.) and evening (p.m.) meals of flies feeding on 5% or 20% sucrose on day 1 (solid bars), day 5 (spotted bars), and day 7 (hatched bars). $n = 23-65$, two-way ANOVA with Fisher's LSD, comparisons to same-diet day-1 meal-time duration or size. All data shown as mean \pm SEM, **** $p < 0.0001$, *** $p < 0.001$, ** $p < 0.01$, and * $p < 0.05$ for all panels unless indicated.

To investigate if these alterations in feeding behavior are a consequence of diet-induced obesity (Fig. 1A and B) or possibly a result of high dietary sugar, we tested the feeding patterns of genetically-obese *brummer* (*bmm*) and genetically-lean *perilipin2* (*plin2*) mutant flies (Gronke et al., 2005; Ro et al., 2014). *bmm* mutants, despite being as obese as control flies on a SD (Fig. 2B), showed similar patterns of feeding behavior with diets as control flies (Fig. 5A, C, E and Supplementary Information Fig. S5A-C for controls). Therefore, obesity in the absence of high dietary sugar has no effect on meal size and duration. In contrast, 20% sucrose leads to an increase in meal size and duration even in the absence of obesity in the *plin2* mutant flies (Fig. 5B, D, F and Supplementary Information Fig. S5A-C for controls). These data suggest that obesity alone does not drive the observed changes in feeding patterns and open the possibility that, instead, these are a direct consequence of dietary sugar and linked to changes in sweet taste sensation.

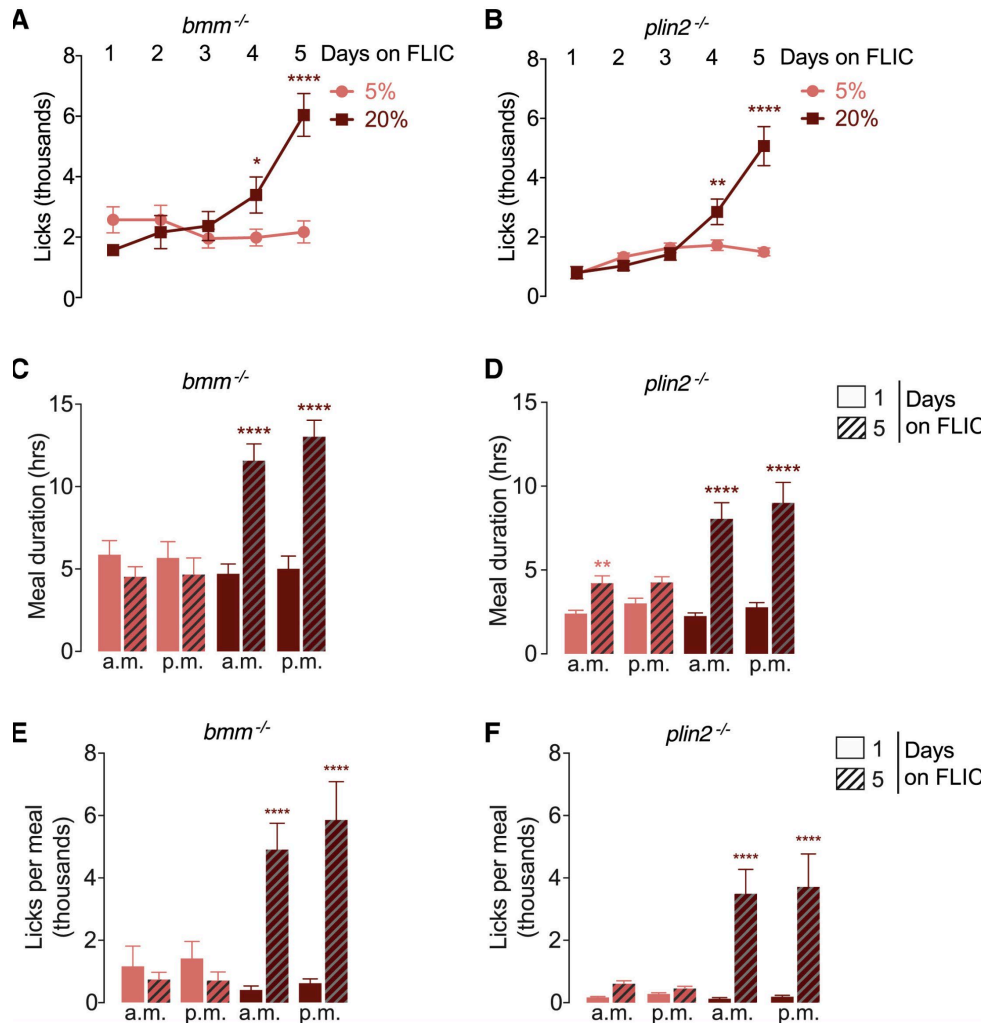


Figure 2.5 Sugar diet promotes increased feeding behaviors independently of fat accumulation

(A and B) Average licks per day of age-matched male (A) *bmm*^{-/-} and (B) *plin2*^{-/-} mutant flies feeding on either 5% or 20% sucrose food on the FLIC. n = 15–36, two-way ANOVA with Fisher’s LSD, comparisons to same-day 5% sucrose licks. (C and D) The meal duration (h) for the morning (a.m.) and evening (p.m.) meals of (C) *bmm*^{-/-} and (D) *plin2*^{-/-} mutant flies feeding on 5% or 20% sucrose on day 1 (solid bars) and day 5 (hatched bars). n = 16–33 and n = 18–30, two-way ANOVA with Fisher’s LSD, comparisons to same-diet day-1 meal-time duration. (E and F) The size as licks per meal for the morning (a.m.) and evening (p.m.) meals of (E) *bmm*^{-/-} and (F) *plin2*^{-/-} mutant flies feeding on 5% or 20% sucrose on day 1 (solid bars) and day 5 (hatched bars). n = 11–29 and n = 16–30, two-way ANOVA with Fisher’s LSD, comparisons to same-diet day-1 meal size. All data shown as mean ± SEM, ****p < 0.0001, ***p < 0.001, **p < 0.01, and *p < 0.05 for all panels unless indicated.

A deficit in sweet taste sensation promotes feeding behavior.

Consumption of a high sugar diet promotes a decrease in the responses of sweet taste neurons to sugar and an increase in feeding. Are these phenomena linked and does a dulling of sweet taste sensation contribute to overfeeding? If diet-dependent deficits in sweet taste drive higher feeding behavior, then preventing animals from experiencing these should rescue overeating and obesity. To test this possibility, we expressed the bacterial voltage-gated sodium channel *NaChBac* – which is used to activate neurons in *Drosophila* (Nitabach et al., 2006)– exclusively in the sweet taste neurons using *Gr64f*-GAL4 (Fujii et al., 2015) and assayed taste responses and feeding behavior. The taste responses of *Gr64f*>*NaChBac* flies were identical to those of genetic controls on a CD (Fig. 6A). However, while control animals experienced a decrease in sweet taste when fed the SD, *Gr64f*>*NaChBac* flies retained the same taste responses to sucrose on both a CD and SD (Fig. 6A, 20% and 30% sucrose stimuli). Since, expression of *UAS-NachBac* in the *Gr64f*⁺ neurons corrected taste deficits so that *Gr64f*>*NaChBac* animals do not experience a sugar diet-dependent decrease in taste function, we next measured their feeding patterns. *Gr64f*>*NaChBac* flies fed 20% sucrose showed little to no increase in feeding interactions compared to controls (Fig. 6B). In addition, while the meals of control flies became longer, those of *Gr64f*>*NaChBac* animals stayed the same (Fig. 6C). Consistent with these data, *Gr64f*>*NaChBac* flies also remained lean on 20% sucrose, while control flies accumulated fat (Fig. 6D and Supplementary Fig. S5D for adult-specific *NaChBac* expression). Thus, preventing animals from experiencing a diet-dependent decrease in sweet taste sensation rescued feeding behavior and obesity.

To further test the hypothesis that a decrease in the activity of the sweet taste neurons drives overfeeding, we used optogenetics to acutely activate the *Gr64f*⁺ neurons by expressing

the light-activated channel *csChrimson* (Klapoetke et al., 2014). To ensure that the sweet taste neurons were activated only during feeding, we developed a closed-loop system so that the animals received light stimulation only upon eating. Feeding-initiated light stimulation of the sweet taste neurons in *Gr64f>csChrimson* animals fed retinal prevented overconsumption compared to *Gr64f>csChrimson* flies without retinal treatment (Fig. 6E) or *csChrimson* flies without the *GALA* (Supplementary Fig. S5E). Thus, acute, feeding-dependent, activation of the sweet-tasting cells prevented overeating. Together, these experiments argue that a sugar-diet-dependent decrease in sweet taste function increases feeding behavior and promotes obesity.

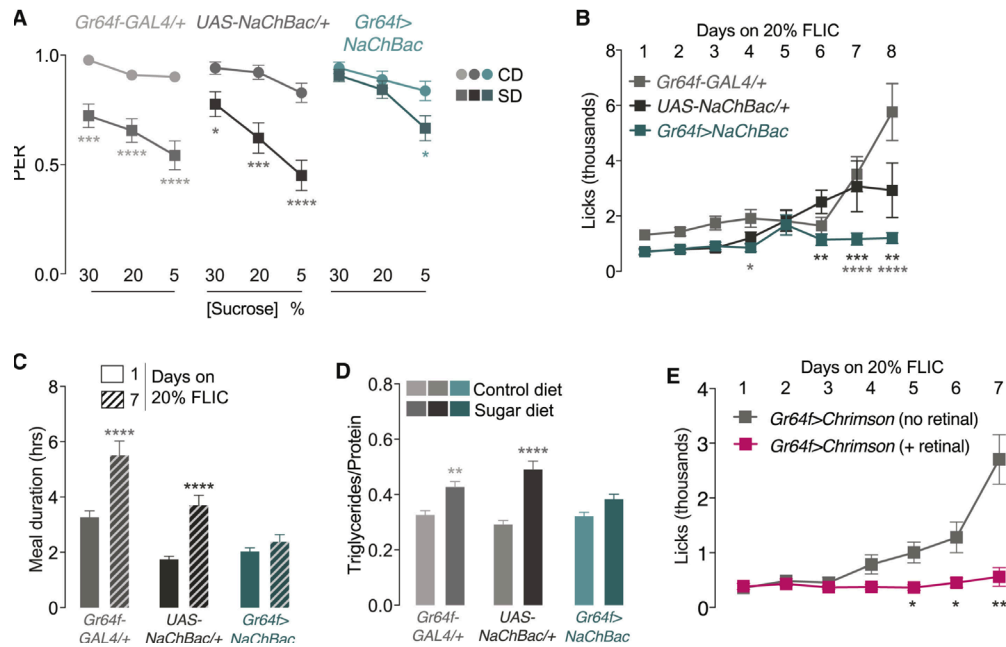


Figure 2.6 Restoring sweet taste sensation and optogenetic activation of the *Gr64f*⁺ neurons protects animals from diet-induced obesity

(A) Taste responses to 5%, 20%, and 30% sucrose stimulation (x axis) of the labellum in *Gr64f*[>]*NaChBac* (teal) and parental transgenic controls flies (gray, crossed to *w1118*^{CS}) fed a control (CD, circles) or sugar (SD, squares) diet for 7 days. $n = 35-54$, multiple t tests, comparisons to control diet. (B) Representative average licks per day of *Gr64f*[>]*NaChBac* (teal) and parental transgenic controls (gray) flies feeding continuously on 20% sucrose on the FLIC. $n = 10-17$, two-way ANOVA with uncorrected Fisher's LSD, comparisons to each control genotype per day. (C) Quantification of the average meal duration (both a.m. and p.m.) of *Gr64f*[>]*NaChBac* (teal) and parental transgenic controls (gray, crossed to *w1118*^{CS}) flies feeding on 20% sucrose on day 1 (solid bars) and day 7 (hatched bars) on the FLIC. $n = 56-90$, two-way ANOVA with uncorrected Fisher's LSD, comparisons to day-1 duration. (D) Triglyceride levels normalized to protein in *Gr64f*[>]*NaChBac* (teal) and parental transgenic controls (gray, crossed to *w1118*^{CS}) flies after feeding on a control (lighter-colored bars) or sugar (darker-colored bars) diet for 7 days. $n = 15-16$, two-way ANOVA with Sidak's test, comparisons to control diet per each genotype. (E) Average licks per day of *Gr64f*[>]*csChrimson* flies feeding on 20% sucrose with (fuchsia) or without (gray) all-trans-retinal pretreatment during closed loop, feeding-initiated 60-Hz red light pulse stimulation. $n = 6-9$, multiple t test with Holm-Sidak correction, comparisons per day to no-retinal condition. All data shown as mean \pm SEM, **** $p < 0.0001$, *** $p < 0.001$, ** $p < 0.01$, and * $p < 0.05$ for all panels unless indicated.

The sugar sensor OGT mediates the effects of sugar on sweet taste sensation.

We next probed how dietary sugar alters sweet taste sensation. Our observations that a diet supplemented with the non-caloric sweetener sucralose or a non-sweet, high-fat diet did not lower sweet taste sensation (Fig. 1C), while diets supplemented with 30% sucrose, D-fructose, or D-glucose decreased sweet taste responses, suggest that glucose metabolism plays a role in reducing sweet taste sensation (Fig. 1D). The Hexosamine Biosynthesis Pathway (HBP) is a conserved nutrient sensing signaling pathway that mediates the deleterious effects of dietary sugar on cell physiology and has been implicated in most diseases caused by high-nutrient diets, such as diabetes, kidney, heart, and liver diseases (Hanover et al., 2010; Hardiville and Hart, 2014). The levels of the metabolic end product of HBP, UDP-GlcNAc, are increased by high nutrient diets; a single enzyme, *O-GlcNAc Transferase (OGT)*, also known as *super sex combs* in *Drosophila*, adds the O-linked N-Acetylglucosamine (O-GlcNAc) moiety from UDP-GlcNAc onto the serine and threonine residues of proteins to modify their activity, competing with protein phosphorylation (Hanover et al., 2010; Hardiville and Hart, 2014) (*see Supplementary Information Fig. S6A for schematic of the HBP*). Recent data suggests that OGT may also play a role in the brain: OGT activity is high in neurons and regulates metabolism and synaptic maturation (Lagerlof et al., 2017; Lagerlof et al., 2016; Ruan et al., 2014). In fly heads, the levels of the first committed HBP metabolite glucosamine-6-phosphate were increased with a SD (Fig. S6B). To test if OGT mediates the molecular effects of a SD on sweet taste, we used a previously characterized OGT RNA interference (RNAi) transgene (Radermacher et al., 2014) to knock it down in the *Gr64f*⁺ neurons (50% knock down efficiency, Supplementary Information Fig. S6C). *Gr64f*[>]*OGT* knockdown (KD) animals had normal PER on a CD (Supplementary Information Fig. S6D), but this manipulation rescued sweet taste responses on a SD compared to

controls (Fig. 7A and Supplementary Information Fig. S6E for a second independent *OGT RNAi* transgene).

Since correcting a decrease in sweet taste sensation by expression of *NaChBac* and activating the sweet taste cells with *csChrimson* prevented increased feeding and obesity (Fig. 6), we asked if *OGT* KD could also restore feeding behavior. Indeed, KD of *OGT* in the *Gr64f+* cells prevented feeding on 20% sucrose (Fig. 7B); consistent with its effect on feeding, *Gr64f+>OGT* KD animals remained lean compared to genetic control flies (Fig. 7C). Thus, decreasing *OGT* activity solely in the sweet taste neurons blocked the effects of sugar diet on taste responses, feeding behavior, and obesity.

OGT integrates cell physiology and nutrient environment by altering transcriptional and signaling pathways (Hanover et al., 2010; Hardiville and Hart, 2014). To identify the cellular processes through which excess dietary sugar decreases sweet taste function, we measured changes in RNA abundance in the labella of flies fed a CD and SD for 7 days and with *OGT* KD (Supplementary Table 1 and Supplementary Fig. S7). Since knockdown of *OGT* in the sweet-sensing cells restores taste function and prevents overfeeding and obesity on a high sugar diet, we reasoned that the genes altered on a sugar diet *and* important for taste function would show an opposite expression trend when *OGT* is knocked down (i.e., up in SD/down in *OGT* knockdown; down in SD/up in *OGT* knockdown). To carry out this analysis, we first selected only the set of genes showing significant changes in labellar expression between CD and SD ($q < 0.2$), and then conditioning on membership in that set, calculated FDR-corrected p -values for the significance of changes in transcript level for the same genes between the *OGT* KD animals and their corresponding *GAL4* control. Genes showing significant expression changes in both RNAseq experiments were classified based on the signs of the observed log₂-fold changes. Using

this approach, we found about ~150 genes changed by diet and “reverted” in *Gr64f*>*OGT* KD (Fig. 7D). We used iPAGE, a pathway discovery program (Goodarzi et al., 2009) to identify GO terms showing significant mutual information with the expression status of genes as being in either one of the two oppositely-regulated categories (up/down or “reverting,” Fig. 7E). GO terms altered by a SD and reversed by *OGT* KD were enriched in processes involved in neural function (Regulation of membrane potential, Phototransduction, Neurotransmitter transporter activity) and metabolism (Glutaminase activity, Chitin catabolic process, Carbonate dehydratase activity). Combining these results on gene expression with the targeted behavioral experiments above, we propose a model where excess dietary sugar, through the cell-autonomous action of *OGT*, leads to a decrease in the responses of the sweet taste cells to sugar, which lowers sweet taste sensation (Fig. 7F). This weakening of sweet taste alters feeding patterns to promote obesity, providing a mechanism for how excess dietary sugar functions as a driver of obesity.

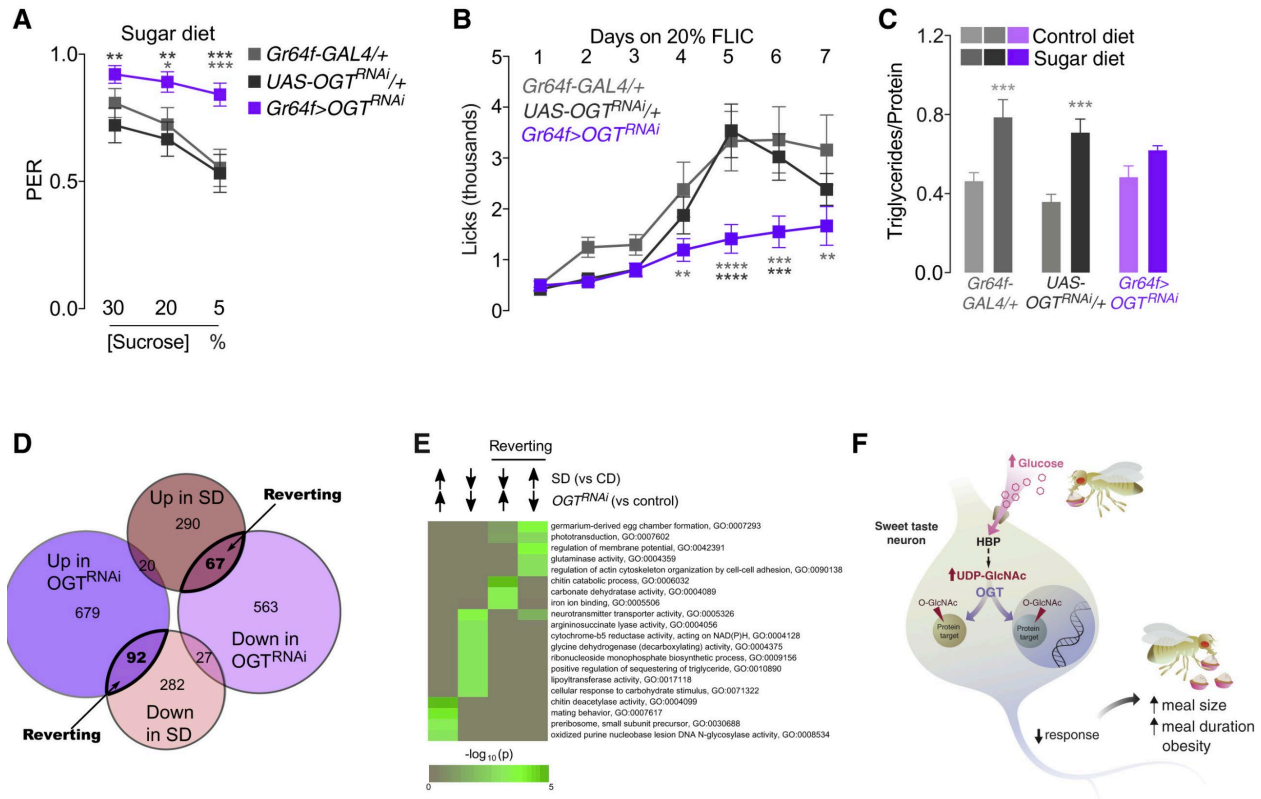


Figure 2.7 OGT mediates the effects of sugar diet on sweet taste, feeding behavior, and obesity

(A) Taste responses to 5%, 20%, or 30% sucrose stimulation (x axis) of the labellum in *Gr64f > OGT^{RNAi}* (purple) and parental transgenic control (gray, crossed to *w¹¹¹⁸^{CS}*) flies fed a sugar diet for 7 days. n = 36–60, multiple t tests, comparisons to genetic controls. (B) Average licks per day of *Gr64f > OGT^{RNAi}* (purple) and parental transgenic control (gray, crossed to *w¹¹¹⁸^{CS}*) flies fed on 20% sucrose. n = 11–44, two-way ANOVA with Fisher’s LSD, comparisons to control genotypes. (C) Triglyceride levels normalized to protein in *Gr64f > OGT^{RNAi}* (purple) and parental transgenic control (gray, crossed to *w¹¹¹⁸^{CS}*) flies on control (lighter shades) or sugar (darker shades) diet for 7 days. n = 8, two-way ANOVA with Sidak’s test, comparisons to CD. (D) Overlap of genes showing differential expression in SD versus CD labella, compared with those showing significant changes with OGT knockdown compared to GAL4/+ control alone. Genes with opposite expression (see text for explanation of analysis) are marked as “reverting.” (E) The iPAGE-based identification of pathways enriched in the set of genes from (D) showing opposing transcription changes in flies fed a SD with or without OGT knockdown. Coloration shows hypergeometric p values from iPAGE. (F) Model of physiological and metabolic changes in sweet taste neurons in flies fed a high sugar diet. HBP, hexosamine biosynthesis pathway; OGT, O-GlcNAc transferase. All data shown as mean ± SEM, ****p < 0.0001, ***p < 0.001, **p < 0.01, and *p < 0.05 for all panels unless indicated.

2.4 Discussion

Obesity has been linked to the high availability of affordable, tasty foods that contain sugar as a food additive (Small, 2009; Volkow et al., 2011). The increased eating in the presence of these palatable foods seems to be an evolutionarily conserved behavior from flies, to rodents and humans (Avena et al., 2008; Small, 2009). How these foods promote eating is still an open question with obvious public health implications. Changes in taste sensation with dietary sugar or obesity have been examined in humans, but no consensus has been reached on their role in feeding behavior and obesity (Bartoshuk et al., 2006; Berthoud and Zheng, 2012; Grinker, 1978; Hardikar et al., 2017; Overberg et al., 2012; Pasquet et al., 2007; Proserpio et al., 2016; Sartor et al., 2011; Thompson et al., 1977). Studies in rodent models found changes in behavior and physiology consistent with a decrease in taste function with diet-induced obesity, but did not draw a causal connection between the two (Chevrot et al., 2013; Kaufman et al., 2018; Maliphol et al., 2013; Ozdener et al., 2014; Robinson et al., 2015). Here we show in fruit flies that excess dietary sugar, independently of obesity, causes a decrease in sweet taste function because of lower responses of the taste cells to sugar stimuli – similar to what was observed in the isolated taste buds of mice fed a high-fat diet (Maliphol et al., 2013). This dulling, in turn, promotes eating and obesity by increasing the duration and size of meals. Correcting taste deficits by activating the sweet-sensing cells so that the animals do not experience a lowering of their sweet taste world prevented overeating and obesity, drawing a causal link between diet-induced changes in taste function and obesity.

Diet composition is well known to change sensory perceptions (Hill, 2004). For example, high dietary sodium alters the intensity for salt perception in humans (Bertino et al., 1982; Huggins et al., 1992) and rodents (Contreras and Frank, 1979; Hill et al., 1986) and this

promotes higher sodium intake (Bertino et al., 1982; Huggins et al., 1992). Exposure to savory or bitter foods in development or adulthood also alters taste preference across species, from humans (Mennella and Trabulsi, 2012), to mouse (Ackroff et al., 2012), to invertebrates like *Manduca* and *Drosophila* (Glendinning et al., 2001; Zhang et al., 2013). Here we show that, as with high dietary sodium, in flies excess dietary sugar decreases sweet taste sensation and promotes overconsumption. How this occurs remains an open question, and raises the intriguing possibility that the dulling of sweet taste may contribute to changes in the central reward processing of food observed in humans with obesity (Kroemer and Small, 2016).

An exciting finding from our work is the role of glucose metabolism in altering neural activity and behavior. While our experiments do not exclude the possibility that peripheral insulin resistance may also play a role in taste changes, they do highlight the role of the enzyme *OGT* as a potential modulator of sweet taste neuron function. *OGT* activity was recently reported to modulate synapse maturation and behavior (Lagerlof et al., 2017; Lagerlof et al., 2016; Ruan et al., 2014). There are a few examples where metabolic sensors have been implicated in the modulation of neural activity, such as TOR and eEF2 (Davis, 2013), raising the interesting question of whether *OGT* may also function in a similar manner in the taste neurons. While the exact molecular mechanisms by which *OGT* mediates the effects of excess dietary sugar on sweet taste neuron physiology remain to be understood, our analysis indicates that *OGT* alters the expression of genes involved in neural function and metabolism. Given the conservation of *OGT* function from flies to humans, and the role of *OGT* in the etiology of obesity and diabetes (Hanover et al., 2010; Hardiville and Hart, 2014), our findings raise the exciting possibility that increased *OGT* activity may act to dull taste function in response to excess dietary sugar in

mammals. Finally, our work also brings to light the broader question of how diet may impact brain physiology and behavior through its action on metabolic pathways and their byproducts.

Together, the identification of the neural and molecular underpinnings of diet-induced alterations in taste promises an avenue of investigation that is broadly relevant to understanding the etiology of obesity in humans. Based on our work and available human and rodent studies, the development of public health or therapeutic solutions that seek to correct dietary sweetness and the weakening of taste sensation may help curb the spread of obesity and reduce the risk of chronic disease.

2.5 Method Details

Drosophila melanogaster

Flies were grown and maintained on cornmeal food (Bloomington Food B recipe) at 25°C and 45-55% humidity under a 12:12 hour light-dark cycle (ZT0 at 7 AM) for all experiments. We collected male flies under CO₂ anesthesia at day 1-3 after eclosion. After collection, flies were aged for an additional 1-2 days before starting experiments, except in the case of lines carrying RNAi constructs, which were allowed to age with parental controls for an additional 5-6 days to promote expression of the RNAi transgene and knockdown of the target gene. For dietary manipulations, age-matched male flies were placed on either Bloomington Food B or Bloomington Food B supplemented with different sugars (See Dietary manipulations in Method Details) in groups of 30-35 flies. In experiments where flies were fasted (e.g., PER), all flies were food-deprived for 18-24 h. For optogenetic manipulations, flies were maintained on Bloomington cornmeal food supplemented with 200 μM all-*trans*-retinal for 6 days in the dark. For all manipulations, flies were changed to new food vials every other day. The GAL4-UAS

system was used to express the transgenes of interest in specific neuron subtypes. For each GAL4/UAS cross, transgenic controls were made by crossing the *w^{1118CS}* (gift from A. Simon) to GAL4 or UAS flies, sex-matched to those used in the GAL4/UAS cross.. GAL4 was expressed in sweet taste neurons by using the *Gr64f* (gift from H. Amrein) or *Gr5a* (gift from K. Scott) promoters. For neuron visualization and cell counting, we used *UAS-nls-GFP* (Bloomington #4775). *UAS-GCaMP6s-Brp-mCherry* (Bloomington #77131) was used for visualization of calcium transients in axon terminals. We used *UAS-NaChBac* (gift from M. Nitabach) and *UAS-csChrimson* (Bloomington #55135) to increase the excitability of sweet taste neurons. Two RNAi lines (RNAi-1 from C. Lehner; RNAi-2 from Bloomington, #50909) were used to knock down expression of *O-GlcNAc transferase (OGT)* in the sweet taste neurons. To uncouple taste deficits from fat accumulation, we compared mutants for *perilipin2* (RKF610) and *brummer* (SGF529) (both gifts from R. Kühnlein) to *w^{1118CS}* flies.

Dietary manipulations

For each diet, the following compounds were mixed into standard cornmeal food (Bloomington Food B recipe) (0.58 calories per gram) by melting, mixing, and pouring new vials as in (Musselman et al., 2011; Na et al., 2013).

Sugar diet²⁰ = 20% Domino granulated sugar w/v (1.15 calories per gram)

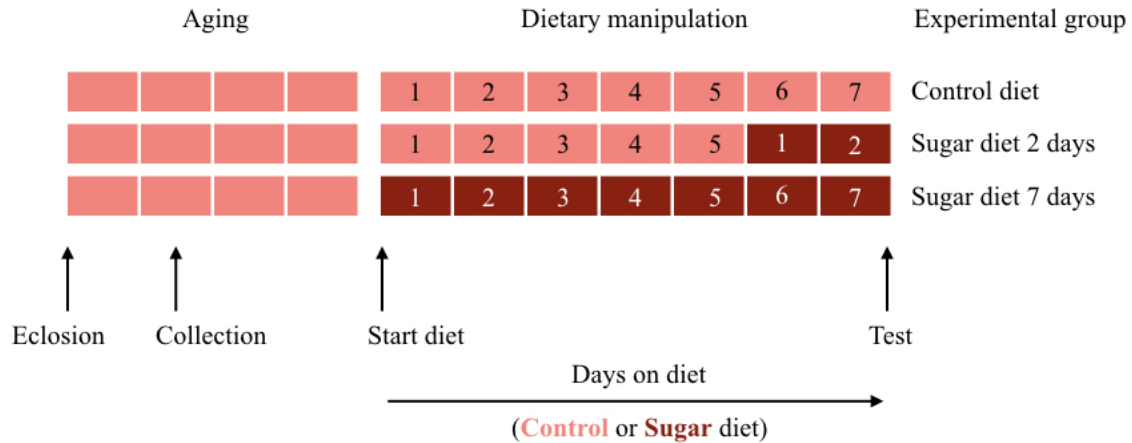
Sugar diet / Sugar diet³⁰ = 30% Domino granulated sugar w/v (1.41 calories per gram)

Lard = 10% lard w/v (1.42 calories per gram)

Sucralose = 0.02% sucralose w/v (this is the concentration found in diet soda and (Dus et al., 2011)).

FLIC diets were made with 5, 20, or 30% w/v D-sucrose (Fisher Scientific) dissolved in milliQ-filtered deionized water with 4 mg/L MgCl₂ (Sigma-Aldrich).

Age-matching of flies on the different diets occurred as in the schematic below:



Triacylglyceride (TAG) Assay

We assayed total TAGs normalized to total protein in whole flies (described in (Tennesen et al., 2014)). Following dietary manipulation, male flies were CO₂-anesthetized and flash frozen. Two flies per biological replicate were homogenized in lysis buffer (140 mM NaCl, 50 mM Tris-HCl pH 7.4, 0.1% Triton-X) containing protease inhibitor (Thermo Scientific) and centrifuged, and the supernatants were frozen at -20°C. For total protein, supernatant and standards were reacted with protein reagent (Thermo Scientific Pierce™ BCA Protein Assay) for 30 min at 37°C and the absorbance of 562 nm measured by a Tecan Plate Reader Infinite 200. For TAGs, supernatant and standards were reacted with TAG reagent (Stanbio Triglycerides LiquiColor Test) for 5 min at 37°C, and the absorbance of 500 nm measured by the Tecan Plate Reader.

Nile Red Staining

We stained abdominal fat body in male flies following dietary manipulation as described in (Tennessen et al., 2014). Nile red stain stock was 10% in DMSO, and the mounting solution diluted stock 1:1000 in 1xPBS with 30% glycerol. Fly abdomens were dissected in 1xPBS by removing intestines and other internal organs, then separating the abdomen and transecting it along the ventral side to expose the subcuticular fat body. This was flattened and transferred to the Nile red mounting solution on slides with coverslips for confocal imaging 30 minutes later. Images were acquired on an Olympus FV1200 with a 543-nm laser.

Proboscis Extension Response

On the seventh day of dietary manipulation, vials of 35-40 flies were fasted between ZT8 and ZT10 (ZT0 is 7 AM) in a vial with a Kimwipe dampened with 2 mL of milliQ-filtered deionized (milliQ DI) water. 18-24 hours later, proboscis extension response (PER) testing was performed as in (Shiraiwa and Carlson, 2007). Flies were anesthetized on ice then placed in the narrow end of a P200 pipette tip. The tip was cut such that the fly could be gently pushed (with the round end of a melted glass capillary tube) to the end of the tip until the fly head showed through, with the legs still trapped within the tip. Once the fly was awake, it was presented with milliQ water on the labellum and allowed to drink. Water and all tastants were delivered manually via a small solution-soaked Kimwipe piece held in a clean pair of forceps. Sucrose solutions were dissolved in milliQ water and presented in order of descending concentration. Each concentration presentation consisted of three successive touches to the proboscis, and the response to each touch was scored. The touches were brief to ensure the fly did not drink any of the sucrose solution. After the three touches of a sucrose solution, the fly was again allowed to drink water,

before progressing to the next concentration presentation. Groups of 7-10 flies were tested simultaneously.

Fly-to-Liquid-food Interaction Counter (FLIC)

We used the FLIC, described previously in Ro *et al.* 2014, to measure fly-to-food interactions as an estimate of feeding behavior over many days without fasting or interruption. The FLIC consists of a *Drosophila* Feeding Monitor (DFM) which communicates fly-to-food interactions to computer software called FLICMonitor via a Master Control Unit (MCU). For FLIC experiments, flies were CO₂-anesthetized and males were collected 1-3 days after eclosion. They were then allowed to recover on Bloomington Food B for at least one day before starting the FLIC. For a single experiment, all fly ages were within 3 days of each other. To load flies onto the FLIC, we briefly ice-anesthetized them and rapidly aspirated individual flies into arenas with a single food well. Each DFM has 12 food wells in two rows of six, and each row of six wells is supplied by a single food reservoir (cell culture flasks, Biofil). Once all flies for an experiment were loaded into the FLIC, we began the recording of their food interactions. A fly-to-food interaction on the FLIC occurs when the fly stands on the capacitance pad surrounding the food well and contacts the food with its proboscis, as during feeding, or with its leg, as during tasting. The liquid food is a solution of sucrose (5% for normal diet and 20% for high sugar diet) and 4 mg/L MgCl₂ in milliQ water, and so can carry electrical current. The fly's connection of the food to the capacitance pad with its body closes a circuit and changes the voltage readout for that well. The signal intensity is sufficient to distinguish tasting from food-intake-related contacts, a.k.a. "licks". Signal threshold for licks was set to 40 units above calculated baseline, while tasting occurred between 10 and 40. The MCU samples the voltage from all wells every 200 ms. Long-

term FLIC was run in an incubator with a 12-hour light cycle (ZT0 is 7 AM), at 25°C and 35-50% humidity. (Humidity greater than 60% can affect the baseline signal of the wells.) To correct sugar concentrations as water was lost to evaporation over many days, we added a small volume of fresh milliQ water daily to each reservoir.

Optogenetic Stimulation for FLIC (optoFLIC)

We developed a closed-loop optoFLIC setup to time a pulsed light stimulation to a fly-to-food interaction in order to augment sweet taste neuron activity in a behaviorally relevant way. This apparatus was a collaboration between the Dus and Pletcher labs. Stimulation programs were written by SP and modified by CEM and KH, and can be found on Github. The FLIC lids were customized to allow placement of one high-intensity LED (627nm SinkPAD-II, Luxeon) on the ceiling of each of the twelve single-well chambers. Modified “optolids” were constructed from black polyoxymethylene (e.g., Delrin), which prohibited the leakage of light among chambers. To control LED illumination, each modified lid was connected to its corresponding DFM through the existing expansion port. LEDs were individually controlled cooperatively by each DFM and the FLIC Master Control Unit (MCU) using custom firmware. Customization details, including firmware updates and electrical specifications, are available from the authors upon request.

OptoFLIC is technically similar to FLIC, but for a few exceptions: Unlike FLIC, optoFLIC requires a stimulation program for the MCU to deliver to the optolids. For our data, the light pulse frequency (0 or 60 Hz) and duration of pulsing (100 ms) were chosen based on our sensillar electrophysiology data and optimized to have no influence on feeding on control diet of

5% sucrose. OptoFLIC has a range of parameters associated with near instantaneous LED illumination in response to the behavior of the animal. These parameters include: signal activation threshold to control illumination in response to the intensity of a feeding event; Illumination frequency and pulse width to control the intensity of neuronal stimulation or inhibition; and duration of illumination following the termination of feeding to maintain stimulation after the behavior has ended. For all experiments, signal threshold was set to 10; pulse width was set to 8 ms; duration of illumination was set to 100 ms. Also, the delay from onset of feeding signal to onset of light stimulus was set to 0 ms; however, because the response rate of the system was tuned to ensure feeding signals were distinct from background, the realtime delay in light onset was 200 ms after the initial feeding signal. Flies were maintained in the dark and fed on Bloomington cornmeal food supplemented with 200 μ m all-*trans*-retinal for 6 days prior to experiments for the proper functioning of Chrimson. At the time of the optoFLIC experiments, the MCU had been upgraded to perform all the data collection independent of a computer and the FLICMonitor software.

Taste Sensitivity Assay

Following dietary manipulation for 7 days, male flies were fasted for 22 hours (ZT9 until ZT7 next day) and then placed for 30 minutes on 1% agar containing non-caloric L-glucose (CarboSynth) at the concentrations indicated and colored with 0.5% blue dye (McCormick Culinary). Flies were kept at 25°C for the entirety of the experiment.

Sensillar Electrophysiology

Electrophysiological recordings were made at labellar sensilla of flies fed sugar or control diet for 1 or 7 days, following a protocol similar to those described previously (Hiroi *et al.*, 2002; Wang *et al.*, 2016). Briefly, three to five L-type labellar bristles were recorded on each fly. The recording electrode (tip diameter, 12–15 μm) was filled with designed experimental tastants. Each chosen L-type bristle was stimulated by different concentrations of sucrose (in text) in 30mM tricholine citrate (TCC, Sigma-Aldrich, as electrolyte). To avoid adaptation, each labellar taste sensilla was stimulated up to 4 seconds and allowed to recover for >2 minutes before applying another stimulus. Signals were acquired using an AxonClamp 900A amplifier and digitized with a 1400A D-A converter and AxoScope 10 software (Molecular Devices) at sampling rate of 10 kHz, filtered at 3 kHz. Electric signals were further amplified and filtered by a second amplifier (CyberAmp 320, Axon Instrument, Inc., USA, with gain X 100, Lowpass filter 1600 Hz).

Metabolomics

Glucosamine-6-phosphate measurements were performed by Metabolon, Inc., using Ultrahigh Performance Liquid Chromatography-Tandem Mass Spectroscopy. The measurements were conducted on samples of 100 heads from age-matched male flies fed a control or high-sugar diet for 7 days. On the seventh day they were food-deprived for 24h, then refed 400 mM D-glucose (“fed”) or 1% agar (“fasted”) for 1 hour. Animals were then flash-frozen in liquid nitrogen, and their heads collected with a sieve.

Calcium Imaging

The brains of awake, behaving male flies expressing *GCaMP6s-Brp-mCherry* (Kiragasi et al., 2017) in the *Gr64f*⁺ neurons were prepared for imaging similarly to the preparation of (LeDue et al., 2016), following 18-24 hours food deprivation. Briefly, each fly was fixed to a custom-printed plastic slide with paraffin wax. The fly's distal leg segments were removed to prevent tarsal interference with labellar stimulation and response. The proboscis was wax-fixed in an extended position prevent retraction, minimizing brain movement during imaging and aiding in accuracy of stimulus delivery. Each fly was tested with milliQ water before stimulating with 30% sucrose dissolved in milliQ water. To image the SEZ, the well surrounding the head was filled with sugarless artificial hemolymph solution (recipe in mM: 108 NaCl, 8.2 MgCl₂, 4 NaHCO₃, 1 NaH₂PO₄, 2 CaCl₂, 5 KCl, 5 HEPES, pH 7.4) and the dorsal cuticle between the eyes was removed by microdissection. Stimulus (a piece of Kimwipe soaked in tastant and held in a clean pair of forceps) delivery to the proboscis was manual and timed to coincide with the 100th recording sample of each time series. Imaging was done with an upright confocal microscope (Olympus, FluoView 1200 BX61WI) with a 20x water-immersion objective and laser excitation at 488 and 543 nm. Images were recorded at 4 Hz (512 x 512 pixels). The plane of interest was kept to the most ventral neuropil regions innervated by the *Gr64f*⁺ neurons.

RNA Extraction

The proboscis of 20 *Gr5a-GAL4/UAS-OGT^{RNAi}* flies were dissected into Trizol (Ambion) and homogenized with plastic pestles and 4-5 biological replicates collected over two days. RNA was extracted by acid phenol chloroform (Ambion), and precipitated by isopropanol with Glycoblue Coprecipitant (Invitrogen). RNA pellet was washed as needed with 75% ethanol. RNA was eluted in nuclease free water and treated by DNase I, following manufacturer's instructions

(Turbo DNA-free DNA removal kit, Ambion). *Gr5a-GAL4* was used instead of *Gr64f-GAL4* because the *Gr64f* transgene is a 10kb fragment that includes the coding regions for the *Gr64a-e* genes, which increases the RNA abundance of these gustatory receptors and interferes with quantification of possible changes in the abundance of these transcripts. For *Gr5a-GAL4/UAS-OGT^{RNAi}* experiment flies were first tested according to their taste responses to 20, 10 and 5% sucrose using the proboscis extension response: *Gr5a-GAL4/UAS-OGT^{RNAi}* flies with PER <0.5 and *Gr5a-GAL4/+* flies with PER >0.5 were selected. For the SD and CD libraries, 200 probosces were dissected in 1xPBS and homogenized in Trizol (Ambion). RNA was extracted by chloroform followed by RNA clean up using RNeasy MinElute Clean Up Kit (Qiagen), and on column DNA digestion by DNase I (Qiagen). The concentration and integrity of RNA was validated using the Agilent Bio-analyzer system and Qubit RNA High Sensitivity Assay (Invitrogen). All steps were carried out in RNase free conditions, and RNA was stored at -80C until library preparation.

RNA-seq library preparation

Sequencing libraries were generated using the Ovation RNA-Seq System for Model Organisms (Nugen, 0350-32) for CD vs SD experiments, and Ovation SoLo RNA-Seq System for *Drosophila* (Nugen, 0502-96) for *Gr5a-GAL4>UAS-OGT-RNAi* SD experiments. All reactions included integrated HL-dsDNase treatment (ArcticZymes, Cat. #70800-201). All libraries were sequenced on the Illumina NextSeq platform (paired read, High-output kit v2 75 cycles) using 38x37 bp paired end reads.

Proboscis Immunofluorescence

Probosces from *Gr5a>nls-GFP* flies were dissected in 1xPBS and fixed in 4% PFA, mounted in FocusClear (CelExplorer) on coverslips, and the cell bodies imaged using a FV1200 Olympus confocal with a 40x objective.

Quantitative RT-PCR

RNA was extracted from 10 heads per group with 4-5 biological replicates in the OGT experiment (Supplementary Fig. 7) and from 10 heads per group with 3 biological replicates in the *dilp2* and *dilp5* experiment (Supplementary Fig. 2). Complementary DNA was synthesized by Superscript III (Invitrogen) reverse transcriptase, and iScript Reverse Transcription Supermix for RT-qPCR (Bio-Rad Laboratories) with the addition of Ribolock RNase inhibitor (Thermo Fisher Scientific). qPCR reactions were carried out using Power SYBR Green PCR master mix (Applied Biosystems) based on manufacturer's instructions. Primers were added at a 2.5uM concentration. All reactions were run on a 96-well plate on the StepOnePlus Real-Time PCR System (Applied Biosystems) and quantifications were made relative to the reference gene *Ribosomal protein 49 (Rp49)*. The following primers were used:

Rp49 Forward ATGCTAAGCTGTCGCACAAA

Rp49 Reverse ACTTCTTGAATCCGGTGGGC

OGT Forward CGTCCGCGGCCCATATATTA

OGT Reverse CCAACTCGAGTAAACCGACTGA

Dilp2 Forward TCAATCCCCTGCAGTTTGTC

Dilp2 Reverse TTGAGTACACCCCAAGATA

2.6 Statistical Analysis

Triacylglyceride (TAG) Assay

Data as presented are averages of the triglyceride:protein concentration ratio for each biological replicate per genotype and dietary manipulation. Each experiment had 8 biological replicates per group, and each experiment was replicated at least once. Figure panels and statistical tests were made in GraphPad Prism.

Nile Red Staining

Quantification of droplet surface area was performed using Imaris (Bitplane). Figure panels and statistical tests were made in GraphPad Prism.

Proboscis Extension Response

The fly's response to a sugar stimulus was scored as follows: a full extension given a score of 1, a partial extension a score of 0.5, and no extension a score of 0. Each fly's average response to a sucrose concentration was used to create the mean response per genotype for that concentration.

Flies that neither kicked their legs nor responded to water or any of the sucrose solutions were removed from analysis as they had likely been killed or compromised in the course of the prep. Figure panels and statistical tests were made in GraphPad Prism.

FLIC and optoFLIC

All analysis and visualization code for the FLIC is in R, and can be found on Github. Raw data collected by FLICMonitor was analyzed in RStudio to calculate a moving baseline and to count

licks. Once licks were calculated, we used RStudio code to sum the number of licks in 30-minute bins. With this, we could calculate total daily licks or produce heatmaps of fly-to-food interaction intensity per 30-minute bin. We also calculated meal duration by finding feeding maxima for each fly, then acquiring the times of the last 30-minute bin with zero or minimal licks before each maximum and the first 30-minute bin with zero or minimal licks after each maximum. Duration was then calculated as $[(meal\ end) - (meal\ start)]$ per meal per fly. Meal size was calculated from meal duration as the number of licks occurring between meal start and meal end. Per meal per day, these were averaged for genotype and concentration of sucrose in FLIC food. Figure panels and statistical tests were made in GraphPad Prism or in RStudio.

Taste Sensitivity Assay

Flies were scored for ingestion of the blue food by visual inspection of their abdomens. Figure panels and statistical tests were made in GraphPad Prism.

Sensillar Electrophysiology

Data were analyzed using the Clampfit 10 software (Molecular Devices). Spikes between 0 and 2 s after initiation of stimuli were counted as firing frequency evoked by the tastant. The mean value of spikes was calculated on 3-5 bristles recorded on each fly as one statistical sample. Figure panels and statistical tests were made in GraphPad Prism.

Metabolomics

Raw data was extracted, peak-identified and QC processed using Metabolon's hardware and software. Compounds were identified by comparison to library entries of purified standards or

recurrent unknown entities. Metabolon maintains a library based on authenticated standards that contains the retention time/index (RI), mass to charge ratio (m/z), and chromatographic data (including MS/MS spectral data) on all molecules present in the library. Furthermore, biochemical identifications are based on three criteria: retention index within a narrow RI window of the proposed identification, accurate mass match to the library +/- 10 ppm, and the MS/MS forward and reverse scores between the experimental data and authentic standards. The MS/MS scores are based on a comparison of the ions present in the experimental spectrum to the ions present in the library spectrum. Metabolite peaks were quantified using area-under-the-curve and their amounts normalized by the total protein present in each sample. Figure panels and statistical tests were made in GraphPad Prism.

Calcium Imaging

Areas of interest were drawn around the two neuropil regions apparent in the images taken. Data analysis was done in Microsoft Excel by calculating $\Delta F/F_0$ for each channel, subtracting the mCherry signal (red) from the GCaMP6s signal (green) to correct for movement, and then calculating the area under the curve after sugar stimulation. Figure panels and statistical tests were made in GraphPad Prism.

Analysis of high throughput RNA sequencing

Because we observed high rates of likely PCR duplicates among the reads for most samples, the raw reads were de-duplicated using ParDRe (Gonzalez-Dominguez and Schmidt, 2016), allowing one mismatch and using an 18 bp prefix. Testing on internal controls using the ERCC spike-in mix showed that de-duplication improved the correlation of transcript abundances with

known relative values (data not shown). Surviving reads that had any recognizable fragment of the Nugen sequencing adapter were removed using cutadapt 1.8.1 (Martin. 2011) and low quality ends were removed using Trimmomatic 0.22 (Bolger *et al.*, 2014) to remove all terminal bases with quality scores below three, and then requiring that for surviving bases, their average quality score over a 4 bp window was at least 15. Reads with fewer than 20 surviving bases were subsequently dropped. Preprocessed reads were aligned to the *Drosophila melanogaster* Flybase release 6.08 transcriptome, augmented with Gal4 and EGFP transcript sequences, using kallisto 0.43.0 (Bray *et al.*, 2016) with a k-mer size of 21 and 200 bootstrap replicates. We used sleuth (Pimentel *et al.*, 2017) for further postprocessing of the RNA-seq data; in particular, all significance tests for differential expression on RNA-seq data use p-values or q-values (as noted) from sleuth for a Wald test on the coefficient distinguishing the groups in question. While we initially obtained three biological replicates for each of the CD and SD cases, we noted that one replicate from each condition was a substantial outlier from all other points (across both conditions) based on the Jensen-Shannon divergence between samples; we excluded that outlier pair from all described analysis. Similar pruning was applied to other sample sets. The final numbers of biological replicates for analyzed sequencing data are given in Supplementary Table 1. For the pathway analysis in Supplementary Figure S7, we used iPAGE (Goodarzi *et al.*, 2009) to find gene ontology (GO) terms showing significant mutual information with the profile of fitted gene-level effect sizes from sleuth. Note that due to the several tests incorporated into the iPAGE pipeline (many of which are not shown), the overall false discovery rate of the procedure on expression profiles has been empirically been shown to be less than 0.05 (Goodarzi *et al.*, 2009). To classify genes for the Venn diagram in Fig. 7D, we first selected only the set of genes showing significant changes in expression between CD and SD ($q < 0.1$), and then conditioning

on membership in that set, calculated FDR-corrected p-values for the significance of changes in transcript level for the same genes between the *Gr5a-GAL4/UAS-OGT RNAi* flies and the corresponding *Gr5a-GAL4/+* controls, (using a threshold of an FDR-corrected p value < 0.2). Genes showing significant expression changes in both experiments were classified based on the signs of the observed log fold changes. For the pathway analysis shown in Fig. 7E, we used iPAGE (Goodarzi et al., 2009) to identify GO terms showing significant mutual information with the status of genes as being in any of the oppositely-regulated categories of Fig. 7D, or among the set of all other genes (a ‘background’ set that is not shown). iPAGE calculations used GO term annotations from the dmel_r6.08 Flybase release. Data was uploaded to GEO as submission # GSE113159.

qPCR analysis

Primer efficiency was calculated by serial dilution of primers and only primers with efficiencies greater than 90% were selected. Relative fold changes in transcript abundance was determined with the Livak method using the Ribosomal protein 49 (Rp49) transcript as a housekeeping control.

Statistics

Statistical tests, sample size, and *p* or *q* values are listed in each figure legend. Data were evaluated for normality and appropriate statistical tests applied if data were not normally distributed. All data are shown as Mean \pm SEM, **** $p < 0.0001$, *** $p < 0.001$, ** $p < 0.01$, * $p < 0.05$ for all figures unless otherwise indicated.

2.7 Data and Software Availability

Firmware for FLIC and optoFLIC is available upon request of the authors. Software for FLIC and optoFLIC data analysis and visualization in RStudio for this paper can be found on Github (<https://github.com/chrismayumich/May-et-al-FLIC-Analysis/branches>).

RNA sequencing data sets are available at the Gene Expression Omnibus under Accession #GSE113159.

2.8 Supplemental Figures

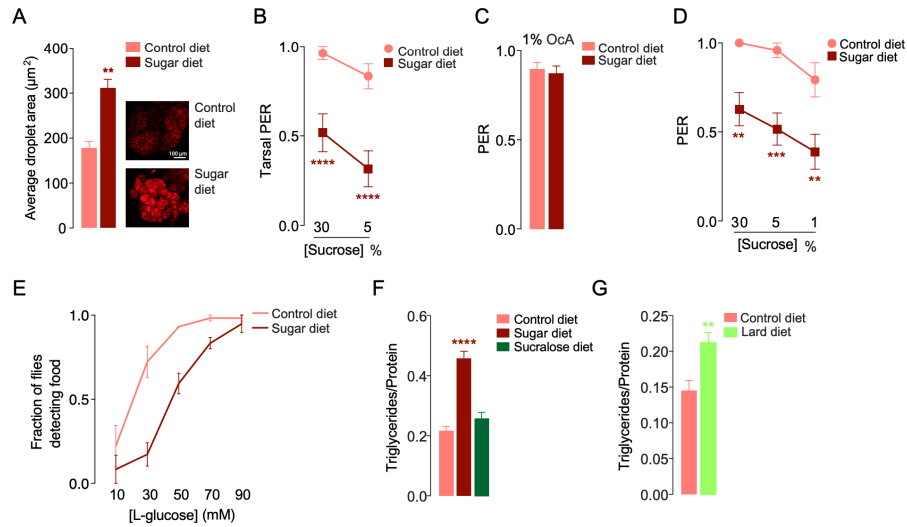


Figure 2.8 Changes in sweet taste sensation and obesity with different diets. Related to Figure 1

All data shown as Mean \pm SEM, **** $p < 0.0001$, *** $p < 0.001$, ** $p < 0.01$, * $p < 0.05$ for all panels unless indicated.

A) Quantification of lipid droplet size in the adipose tissue of *w1118^{CS}* flies fed a control or sugar diet for 7 days. $n = 1939-4007$ droplets in the visceral fat of 3 animals per dietary condition, Wilcoxon signed rank test, comparison to control diet. (Right, Nile Red staining of the fat body on a control or 7-day sugar diet fly, scale bar = 100 μm .) **B)** Measurement of taste responses by PER to 30 or 5 % sucrose (x axis) stimulation to the tarsi in age-matched male *w1118^C* flies fed a control (circles) or sugar (squares) diet for 7 days. $n = 19-27$, two-way ANOVA with Fisher's LSD test, comparisons to control diet per concentration. **C)** Taste responses to stimulation of the proboscis with 1% octanoic acid in *w1118^{CS}* flies fed a control or sugar diet for 7 days. $n = 43-48$, no significance, Mann-Whitney test, comparison to control diet. **D)** Taste responses to proboscis stimulation with sucrose in *w1118^{CS}* flies fed a control or sugar diet for 7 days and fasted for 32-34 hours. $n = 16-21$, two-way ANOVA with Fisher's LSD test, comparisons to control diet per concentration. **E)** Fraction of flies feeding on different L-glucose concentrations (x axis) following 22 hours fasting. $n = 50$ flies, two-way ANOVA for diet effect. **F)** Triglyceride levels normalized to protein in *w1118^C* flies fed a control diet or diets supplemented with 0.02% sucralose or 30% sucrose for 7 days. $n = 16$, one-way ANOVA with Fisher's LSD test, comparisons to control diet. **G)** Triglyceride levels normalized to protein in flies fed a control or 10% lard diet for 7 days. $n = 10$, unpaired t test, comparison to control diet.

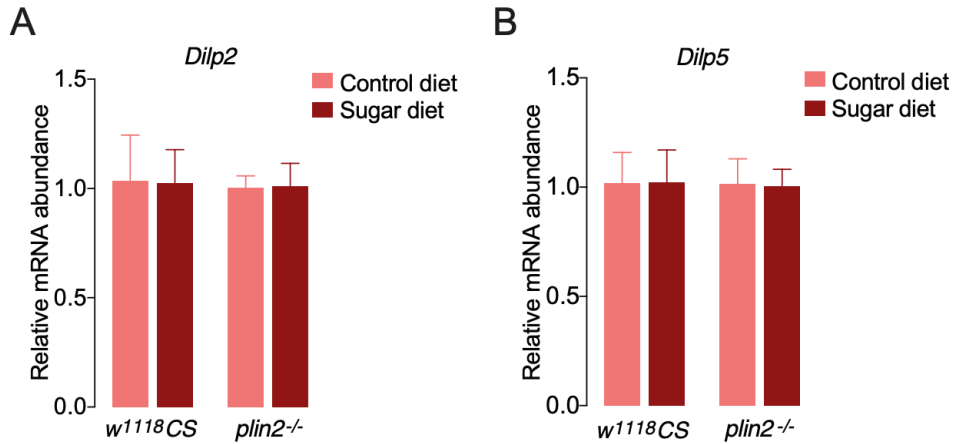


Figure 2.9 The mRNA levels of *Drosophila* insulin-like peptides *Dilp2* and *Dilp5* are unchanged in control and *plin2* mutant flies on a sugar diet. Related to Figure 2.

All data shown as Mean \pm SEM, **** $p < 0.0001$, *** $p < 0.001$, ** $p < 0.01$, * $p < 0.05$ for all panels unless indicated.

A-B) Changes in the relative mRNA abundance of A) *Dilp2* and B) *Dilp5* transcripts measured by qPCR in *w1118^C* or *plin2* mutant flies fed a control (salmon) or sugar (burgundy) diet for 7 days. $n=3$, two-way ANOVA with Sidak's test, comparisons to control diet.

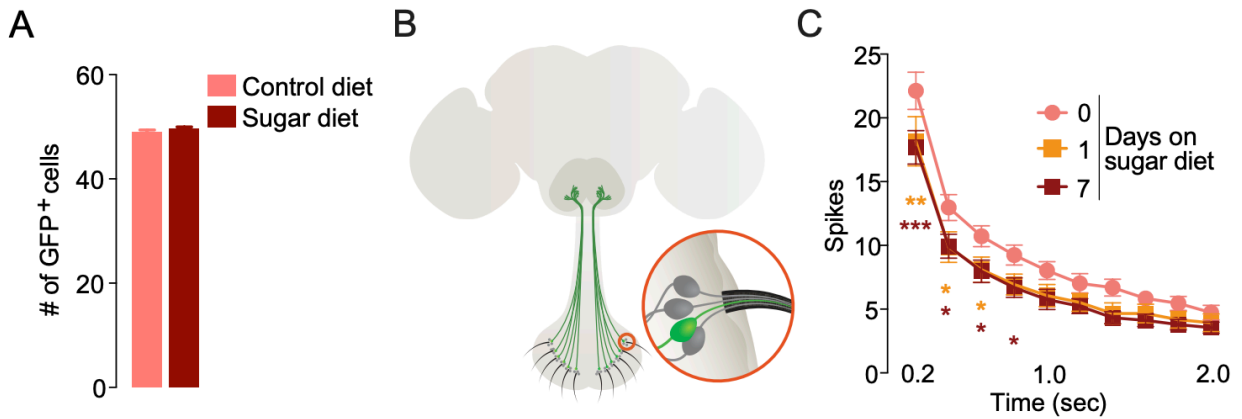


Figure 2.10 A sugar diet has no effect on the number of sweet taste cells in the proboscis. Related to Figure 3.

All data shown as Mean \pm SEM, **** $p < 0.0001$, *** $p < 0.001$, ** $p < 0.01$, * $p < 0.05$ for all panels unless indicated.

A) Quantification of the number of GFP-labeled cells in the labella of *Gr5a>nls-GFP* flies fed a control or sugar diet for 10 days. $n=17-19$ probosces, no significance, unpaired t test, comparison to control diet. **B)** The cell bodies of chemosensory neurons are in the labellum with dendrites protruding into the taste hair (sensillum, black) and the axons terminating in the SubEsophageal Zone (SEZ, dark grey) of the brain. Sweet taste cells are in green. **C)** Quantification of average spike frequency per 200 ms from electrophysiological recordings of the labellar taste sensilla stimulated with 25-mM sugar, in age-matched *w1118^C* flies fed a control or sugar diet for 1 or 7 days. $n=10$, two-way ANOVA with uncorrected Fisher's LSD, comparisons to control diet per day.

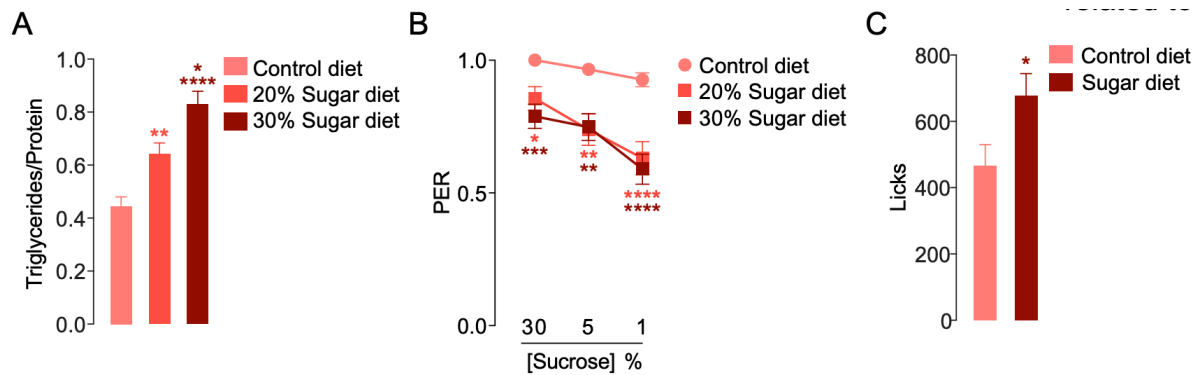


Figure 2.11 A 20% sucrose diet leads to a diminished sweet taste responses and obesity. Related to Figure 4.

All data shown as Mean \pm SEM, **** $p < 0.0001$, *** $p < 0.001$, ** $p < 0.01$, * $p < 0.05$ for all panels unless indicated.

A) Triglyceride levels normalized to protein in *w1118^C* flies fed a control, 20% or 30% sucrose diet for 7 days. $n=8$, one-way ANOVA with Tukey's test, comparisons to control and 20% sucrose diet. **B)** Taste responses to 30, 5, and 1% sucrose stimulation (x axis) of the labellum in *w1118CS* flies fed control, 20% or 30% sucrose diet for 7 days. $n=42-52$, two-way ANOVA with Fisher's LSD test, comparisons to control and 30% sucrose diet. **C)** The feeding behaviors of *w1118^C* flies fed for 10 days a control or sucrose diet on standard fly vials and assayed for a single day on the FLIC on 20% sucrose. $n=24-32$, one-way ANOVA with Fisher's LSD test, comparisons to control diet.

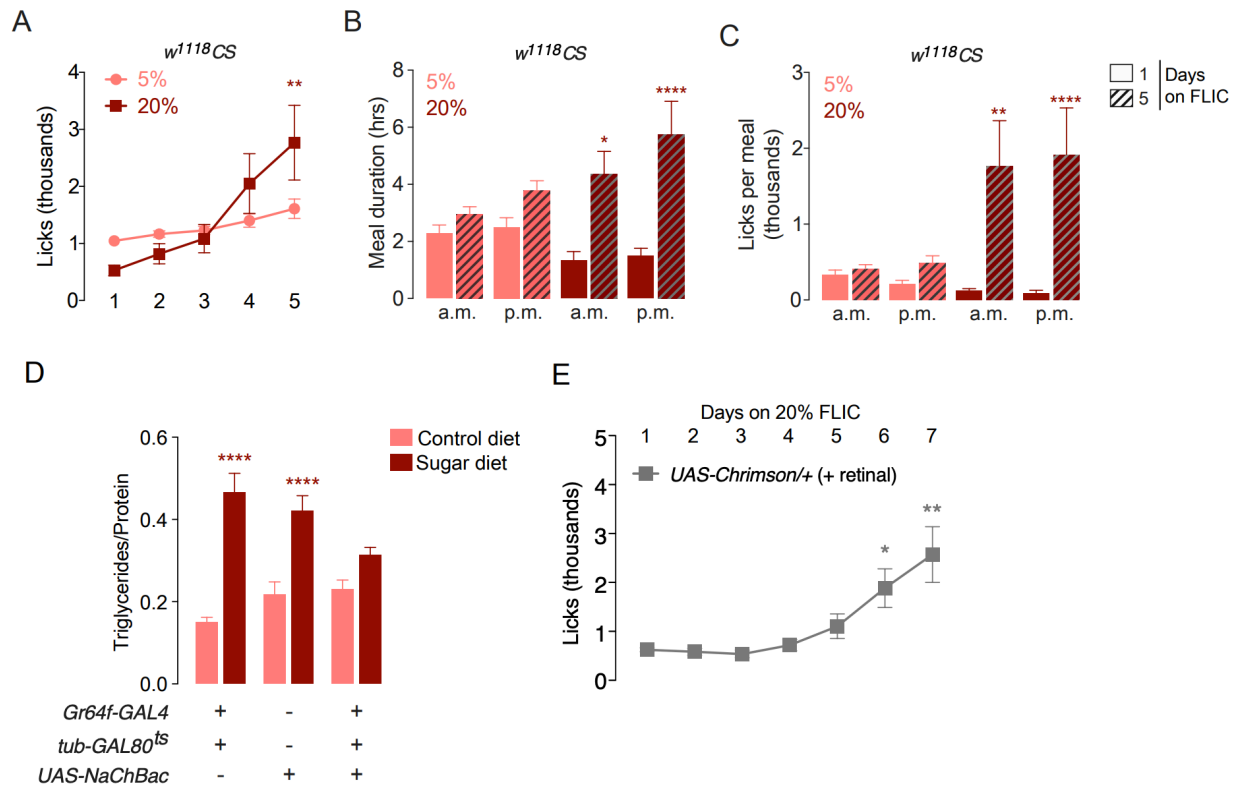


Figure 2.12 Control flies for *bmm*, *plin2* mutant, *NaChBac* and *csChrimson* FLIC experiments. Related to Figures 5 and 6.

All data shown as Mean \pm SEM, **** $p < 0.0001$, *** $p < 0.001$, ** $p < 0.01$, * $p < 0.05$ for all panels unless indicated.

A) Average daily licks of *w¹¹¹⁸C* flies fed 5% and 20% sucrose on the FLIC. $n=18-30$, two-way ANOVA with uncorrected Fisher's LSD, comparisons to 5% sucrose licks each day. **B-C)** Quantification of meal **B)** duration in hours (hrs) and **C)** size of the morning (a.m.) and evening (p.m.) meals of flies feeding on 5 or 20% sucrose on day 1 (solid bars) and day 5 (hatched bars) on the FLIC. $n=17-30$ and $n=18-30$, two-way ANOVA with Fisher's LSD, comparisons to same-diet day 1 meal. **D)** Triglyceride levels normalized to protein in *Gr64f*>*NaChBac*, tubulin-GAL80^{ts} and parental transgenic control flies (crossed to *w¹¹¹⁸C*) fed a control or sugar diet for 7 days. $n=15-16$, two-way ANOVA with Sidak's test, comparisons to control diet per genotype. **E)** Average licks of adult *UAS-Chrimson/+* flies (treated with 200 μ M all-trans-retinal), on 20% sucrose FLIC, without red light stimulation. $n=12$, one-way ANOVA with Kruskal-Wallis test, comparisons to Day 1.

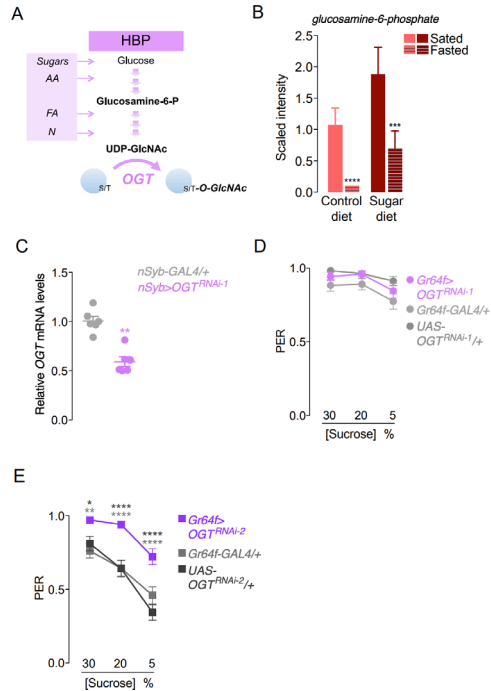


Figure 2.13 The HBP mediates changes in sweet taste sensation. Related to Figure 7.

All data shown as Mean \pm SEM, **** $p < 0.0001$, *** $p < 0.001$, ** $p < 0.01$, * $p < 0.05$ for all panels unless indicated.

A) Overview of the Hexosamine Biosynthesis Pathway (HBP): sugars, amino acids (AA), fatty acids (FA), and nucleotide (N) metabolism feed into the HBP. Addition of the N-acetylglucosamine moiety (O-GlcNAc) O-linked to the serine (S) and threonine (T) residues of proteins is catalyzed by the enzyme OGT. B) The levels of the HBP metabolite glucosamine-6-phosphate in the heads of sated (solid bars) or 24-hour fasted (striped bars) *w1118^C* flies fed a control or sugar diet for 7 days. $n=4-5$, Diet main effect, **** $p=0.001$, *** $p=0.0289$, two-way ANOVA, comparisons to control diet. C) Fold change of OGT mRNA levels in the heads of flies with and without pan-neuronal OGT knockdown (lavender and grey, respectively) measured by qPCR. $n=6$, Mann-Whitney test, compared to GAL4 transgenic control (crossed to *w1118^C*). D) Taste responses to 5, 20, or 30% sucrose stimulation (x axis) of the proboscis in *Gr64f>OGT RNAi-1* (purple) and parental transgenic control (grey, crossed to *w1118^C*) flies fed a control diet. $n=36-60$, multiple t tests, comparisons to genetic controls. E) Taste responses to 30, 20, 5 % sucrose stimulation (x axis) of the labellum in *Gr64f>OGT RNAi-2* (purple) and parental transgenic control (grey, crossed to *w1118^C*) flies fed a sugar diet for 7 days. $n=51-58$, two-way ANOVA with Fisher's LSD test, comparisons to transgenic controls per tastant.

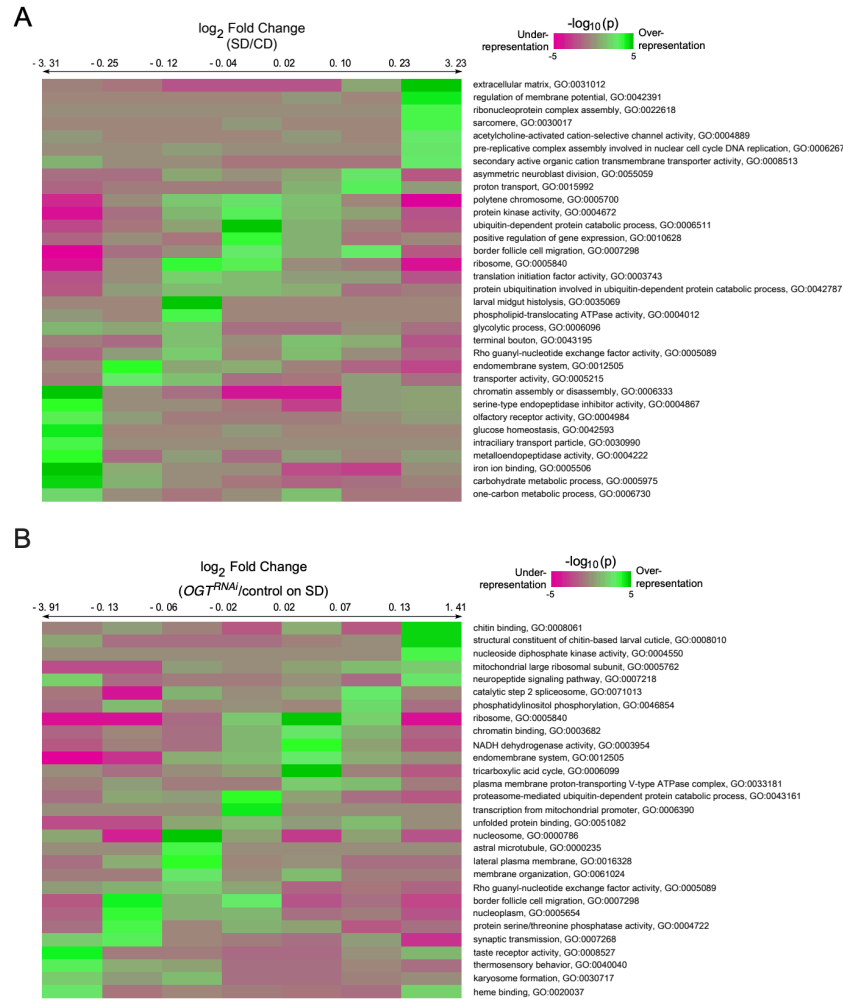


Figure 2.14 . iPAGE profile of differential gene expression changes in the labella of flies fed a sugar diet with or without OGT knockdown. Related to Figure 7.

A-B) iPAGE-based identification of GO pathways enriched in genes showing log₂ fold changes in the labella of A) w1118CS flies fed a SD for 7 days and B) *Gr5a>OGTRNAi-1* and *Gr5a-GAL4/+* flies, compared to those in the whole transcriptome. Coloration shows hypergeometric p values from iPAGE. The numbers on the horizontal arrow indicate the magnitude of log₂ fold changes in each of the 7 bins. In each bin, genes within a GO term may be over or under-represented compared to the transcriptome background.

2.9 References

1. Ackroff, K., Weintraub, R., and Sclafani, A. (2012). MSG intake and preference in mice are influenced by prior testing experience. *Physiol Behav* *107*, 207-217.
2. Avena, N.M., Rada, P., and Hoebel, B.G. (2008). Evidence for sugar addiction: behavioral and neurochemical effects of intermittent, excessive sugar intake. *Neurosci Biobehav Rev* *32*, 20-39.
3. Bartoshuk, L.M., Duffy, V.B., Hayes, J.E., Moskowitz, H.R., and Snyder, D.J. (2006). Psychophysics of sweet and fat perception in obesity: problems, solutions and new perspectives. *Philos Trans R Soc Lond B Biol Sci* *361*, 1137-1148.
4. Beller, M., Bulankina, A.V., Hsiao, H.H., Urlaub, H., Jackle, H., and Kuhnlein, R.P. (2010). PERILIPIN-dependent control of lipid droplet structure and fat storage in *Drosophila*. *Cell Metab* *12*, 521-532.
5. Berthoud, H.R., and Zheng, H. (2012). Modulation of taste responsiveness and food preference by obesity and weight loss. *Physiol Behav* *107*, 527-532.
6. Bertino, M., Beauchamp, G.K., and Engelman, K. (1982). Long-term reduction in dietary sodium alters the taste of salt. *Am J Clin Nutr* *36*, 1134-1144.
7. Bray, N.L., Pimentel, H., Melsted, P., and Pachter, L. (2016). Near-optimal probabilistic RNA-seq quantification. *Nat Biotechnol* *34*, 525-527.
8. Chen, K., Yan, J., Suo, Y., Li, J., Wang, Q., and Lv, B. (2010). Nutritional status alters saccharin intake and sweet receptor mRNA expression in rat taste buds. *Brain Res* *1325*, 53-62.
9. Chevrot, M., Bernard, A., Ancel, D., Buttet, M., Martin, C., Abdoul-Azize, S., Merlin, J.F., Poirier, H., Niot, I., Khan, N.A., et al. (2013). Obesity alters the gustatory perception

- of lipids in the mouse: plausible involvement of lingual CD36. *J Lipid Res* 54, 2485-2494.
10. Chyb, S., Dahanukar, A., Wickens, A., and Carlson, J.R. (2003). *Drosophila* Gr5a encodes a taste receptor tuned to trehalose. *Proc Natl Acad Sci U S A* 100 *Suppl 2*, 14526-14530.
 11. Contreras, R.J., and Frank, M. (1979). Sodium deprivation alters neural responses to gustatory stimuli. *J Gen Physiol* 73, 569-594.
 12. Dahanukar, A., Lei, Y.T., Kwon, J.Y., and Carlson, J.R. (2007). Two Gr genes underlie sugar reception in *Drosophila*. *Neuron* 56, 503-516.
 13. Davis, G.W. (2013). Homeostatic signaling and the stabilization of neural function. *Neuron* 80, 718-728.
 14. de Araujo, I.E., Oliveira-Maia, A.J., Sotnikova, T.D., Gainetdinov, R.R., Caron, M.G., Nicolelis, M.A., and Simon, S.A. (2008). Food reward in the absence of taste receptor signaling. *Neuron* 57, 930-941.
 15. Donaldson, L.F., Bennett, L., Baic, S., and Melichar, J.K. (2009). Taste and weight: is there a link? *Am J Clin Nutr* 90, 800S-803S.
 16. Dus, M., Ai, M., and Suh, G.S. (2013). Taste-independent nutrient selection is mediated by a brain-specific Na⁺ /solute co-transporter in *Drosophila*. *Nat Neurosci* 16, 526-528.
 17. Dus, M., Min, S., Keene, A.C., Lee, G.Y., and Suh, G.S. (2011). Taste-independent detection of the caloric content of sugar in *Drosophila*. *Proc Natl Acad Sci U S A* 108, 11644-11649.

18. Fujii, S., Yavuz, A., Slone, J., Jagge, C., Song, X., and Amrein, H. (2015). *Drosophila* sugar receptors in sweet taste perception, olfaction, and internal nutrient sensing. *Curr Biol* *25*, 621-627.
19. Fujita, M., and Tanimura, T. (2011). *Drosophila* evaluates and learns the nutritional value of sugars. *Curr Biol* *21*, 751-755.
20. Glendinning, J.I., Domdom, S., and Long, E. (2001). Selective adaptation to noxious foods by a herbivorous insect. *J Exp Biol* *204*, 3355-3367.
21. Goodarzi, H., Elemento, O., and Tavazoie, S. (2009). Revealing global regulatory perturbations across human cancers. *Mol Cell* *36*, 900-911.
22. Grinker, J. (1978). Obesity and sweet taste. *Am J Clin Nutr* *31*, 1078-1087.
23. Gronke, S., Mildner, A., Fellert, S., Tennagels, N., Petry, S., Muller, G., Jackle, H., and Kuhnlein, R.P. (2005). Brummer lipase is an evolutionary conserved fat storage regulator in *Drosophila*. *Cell Metab* *1*, 323-330.
24. Hanover, J.A., Krause, M.W., and Love, D.C. (2010). The hexosamine signaling pathway: O-GlcNAc cycling in feast or famine. *Biochim Biophys Acta* *1800*, 80-95.
25. Hardikar, S., Hochenberger, R., Villringer, A., and Ohla, K. (2017). Higher sensitivity to sweet and salty taste in obese compared to lean individuals. *Appetite* *111*, 158-165.
26. Hardiville, S., and Hart, G.W. (2014). Nutrient regulation of signaling, transcription, and cell physiology by O-GlcNAcylation. *Cell Metab* *20*, 208-213.
27. Harris, D.T., Kallman, B.R., Mullaney, B.C., and Scott, K. (2015). Representations of Taste Modality in the *Drosophila* Brain. *Neuron* *86*, 1449-1460.
28. Hill, D.L. (2004). Neural plasticity in the gustatory system. *Nutr Rev* *62*, S208-217; discussion S224-241.

29. Hill, D.L., Mistretta, C.M., and Bradley, R.M. (1986). Effects of dietary NaCl deprivation during early development on behavioral and neurophysiological taste responses. *Behav Neurosci* *100*, 390-398.
30. Hiroi, M., Marion-Poll, F., and Tanimura, T. (2002). Differentiated response to sugars among labellar chemosensilla in *Drosophila*. *Zoolog Sci* *19*, 1009-1018.
31. Huggins, R.L., Di Nicolantonio, R., and Morgan, T.O. (1992). Preferred salt levels and salt taste acuity in human subjects after ingestion of untasted salt. *Appetite* *18*, 111-119.
32. Kaufman, A., Choo, E., Koh, A., and Dando, R. (2018). Inflammation arising from obesity reduces taste bud abundance and inhibits renewal. *PLoS Biol* *16*, e2001959.
33. Kiragasi, B., Wondolowski, J., Li, Y., and Dickman, D.K. (2017). A Presynaptic Glutamate Receptor Subunit Confers Robustness to Neurotransmission and Homeostatic Potentiation. *Cell Rep* *19*, 2694-2706.
34. Klapoetke, N.C., Murata, Y., Kim, S.S., Pulver, S.R., Birdsey-Benson, A., Cho, Y.K., Morimoto, T.K., Chuong, A.S., Carpenter, E.J., Tian, Z., et al. (2014). Independent optical excitation of distinct neural populations. *Nat Methods* *11*, 338-346.
35. Kroemer, N.B., and Small, D.M. (2016). Fuel not fun: Reinterpreting attenuated brain responses to reward in obesity. *Physiol Behav* *162*, 37-45.
36. Lagerlof, O., Hart, G.W., and Haganir, R.L. (2017). O-GlcNAc transferase regulates excitatory synapse maturity. *Proc Natl Acad Sci U S A* *114*, 1684-1689.
37. Lagerlof, O., Slocomb, J.E., Hong, I., Aponte, Y., Blackshaw, S., Hart, G.W., and Haganir, R.L. (2016). The nutrient sensor OGT in PVN neurons regulates feeding. *Science* *351*, 1293-1296.

38. LeDue, E.E., Mann, K., Koch, E., Chu, B., Dakin, R., and Gordon, M.D. (2016). Starvation-Induced Depotentiation of Bitter Taste in *Drosophila*. *Curr Biol* 26, 2854-2861.
39. Maliphol, A.B., Garth, D.J., and Medler, K.F. (2013). Diet-induced obesity reduces the responsiveness of the peripheral taste receptor cells. *PLoS One* 8, e79403.
40. Marella, S., Fischler, W., Kong, P., Asgarian, S., Rueckert, E., and Scott, K. (2006). Imaging taste responses in the fly brain reveals a functional map of taste category and behavior. *Neuron* 49, 285-295.
41. Masek, P., and Keene, A.C. (2013). *Drosophila* fatty acid taste signals through the PLC pathway in sugar-sensing neurons. *PLoS genetics* 9, e1003710.
42. Mennella, J.A., and Trabulsi, J.C. (2012). Complementary foods and flavor experiences: setting the foundation. *Ann Nutr Metab* 60 *Suppl* 2, 40-50.
43. Musselman, L.P., Fink, J.L., Narzinski, K., Ramachandran, P.V., Hathiramani, S.S., Cagan, R.L., and Baranski, T.J. (2011). A high-sugar diet produces obesity and insulin resistance in wild-type *Drosophila*. *Disease models & mechanisms* 4, 842-849.
44. Musselman, L.P., and Kuhnlein, R.P. (2018). *Drosophila* as a model to study obesity and metabolic disease. *J Exp Biol* 221.
45. Na, J., Musselman, L.P., Pendse, J., Baranski, T.J., Bodmer, R., Ocorr, K., and Cagan, R. (2013). A *Drosophila* model of high sugar diet-induced cardiomyopathy. *PLoS genetics* 9, e1003175.
46. Ng, S.W., Slining, M.M., and Popkin, B.M. (2012). Use of caloric and noncaloric sweeteners in US consumer packaged foods, 2005-2009. *J Acad Nutr Diet* 112, 1828-1834 e1821-1826.

47. Nitabach, M.N., Wu, Y., Sheeba, V., Lemon, W.C., Strumbos, J., Zelensky, P.K., White, B.H., and Holmes, T.C. (2006). Electrical hyperexcitation of lateral ventral pacemaker neurons desynchronizes downstream circadian oscillators in the fly circadian circuit and induces multiple behavioral periods. *J Neurosci* *26*, 479-489.
48. Overberg, J., Hummel, T., Krude, H., and Wiegand, S. (2012). Differences in taste sensitivity between obese and non-obese children and adolescents. *Arch Dis Child* *97*, 1048-1052.
49. Ozdener, M.H., Subramaniam, S., Sundaresan, S., Sery, O., Hashimoto, T., Asakawa, Y., Besnard, P., Abumrad, N.A., and Khan, N.A. (2014). CD36- and GPR120-mediated Ca(2)(+) signaling in human taste bud cells mediates differential responses to fatty acids and is altered in obese mice. *Gastroenterology* *146*, 995-1005.
50. Pasquet, P., Frelut, M.L., Simmen, B., Hladik, C.M., and Monneuse, M.O. (2007). Taste perception in massively obese and in non-obese adolescents. *Int J Pediatr Obes* *2*, 242-248.
51. Pepino, M.Y., Finkbeiner, S., Beauchamp, G.K., and Mennella, J.A. (2010). Obese women have lower monosodium glutamate taste sensitivity and prefer higher concentrations than do normal-weight women. *Obesity (Silver Spring)* *18*, 959-965.
52. Pimentel, H., Bray, N.L., Puente, S., Melsted, P., and Pachter, L. (2017). Differential analysis of RNA-seq incorporating quantification uncertainty. *Nat Methods* *14*, 687-690.
53. Proserpio, C., Laureati, M., Bertoli, S., Battezzati, A., and Pagliarini, E. (2016). Determinants of Obesity in Italian Adults: The Role of Taste Sensitivity, Food Liking, and Food Neophobia. *Chem Senses* *41*, 169-176.

54. Radermacher, P.T., Myachina, F., Bosshardt, F., Pandey, R., Mariappa, D., Muller, H.A., and Lehner, C.F. (2014). O-GlcNAc reports ambient temperature and confers heat resistance on ectotherm development. *Proc Natl Acad Sci U S A* *111*, 5592-5597.
55. Ro, J., Harvanek, Z.M., and Pletcher, S.D. (2014). FLIC: high-throughput, continuous analysis of feeding behaviors in *Drosophila*. *PLoS One* *9*, e101107.
56. Robinson, M.J., Burghardt, P.R., Patterson, C.M., Nobile, C.W., Akil, H., Watson, S.J., Berridge, K.C., and Ferrario, C.R. (2015). Individual Differences in Cue-Induced Motivation and Striatal Systems in Rats Susceptible to Diet-Induced Obesity. *Neuropsychopharmacology* *40*, 2113-2123.
57. Rodin, J., Moskowitz, H.R., and Bray, G.A. (1976). Relationship between obesity, weight loss, and taste responsiveness. *Physiol Behav* *17*, 591-597.
58. Ruan, H.B., Dietrich, M.O., Liu, Z.W., Zimmer, M.R., Li, M.D., Singh, J.P., Zhang, K., Yin, R., Wu, J., Horvath, T.L., et al. (2014). O-GlcNAc transferase enables AgRP neurons to suppress browning of white fat. *Cell* *159*, 306-317.
59. Sartor, F., Donaldson, L.F., Markland, D.A., Loveday, H., Jackson, M.J., and Kubis, H.P. (2011). Taste perception and implicit attitude toward sweet related to body mass index and soft drink supplementation. *Appetite* *57*, 237-246.
60. Scott, K. (2018). Gustatory Processing in *Drosophila melanogaster*. *Annu Rev Entomol* *63*, 15-30.
61. Shiraiwa, T., and Carlson, J.R. (2007). Proboscis extension response (PER) assay in *Drosophila*. *J Vis Exp*, 193.

62. Simchen, U., Koebnick, C., Hoyer, S., Issanchou, S., and Zunft, H.J. (2006). Odour and taste sensitivity is associated with body weight and extent of misreporting of body weight. *Eur J Clin Nutr* *60*, 698-705.
63. Skrandies, W., and Zschieschang, R. (2015). Olfactory and gustatory functions and its relation to body weight. *Physiol Behav* *142*, 1-4.
64. Small, D.M. (2009). Individual differences in the neurophysiology of reward and the obesity epidemic. *Int J Obes (Lond)* *33 Suppl 2*, S44-48.
65. Stafford, J.W., Lynd, K.M., Jung, A.Y., and Gordon, M.D. (2012). Integration of taste and calorie sensing in *Drosophila*. *J Neurosci* *32*, 14767-14774.
66. Tennessen, J.M., Barry, W.E., Cox, J., and Thummel, C.S. (2014). Methods for studying metabolism in *Drosophila*. *Methods* *68*, 105-115.
67. Thompson, D.A., Moskowitz, H.R., and Campbell, R.G. (1977). Taste and olfaction in human obesity. *Physiol Behav* *19*, 335-337.
68. Volkow, N.D., Wang, G.J., and Baler, R.D. (2011). Reward, dopamine and the control of food intake: implications for obesity. *Trends Cogn Sci* *15*, 37-46.
69. Wang, Q.P., Lin, Y.Q., Zhang, L., Wilson, Y.A., Oyston, L.J., Cotterell, J., Qi, Y., Khuong, T.M., Bakhshi, N., Planchenault, Y., et al. (2016). Sucralose Promotes Food Intake through NPY and a Neuronal Fasting Response. *Cell Metab* *24*, 75-90.
70. Zhang, Y.V., Raghuwanshi, R.P., Shen, W.L., and Montell, C. (2013). Food experience-induced taste desensitization modulated by the *Drosophila* TRPL channel. *Nat Neurosci* *16*, 1468-1476.

Chapter 3 Persistent Epigenetic Reprogramming of Sweet Taste by Diet

This chapter has been published as:

Vaziri A, Khabiri M, Genaw BT, May CE, Freddolino PL, Dus M. Persistent epigenetic reprogramming of sweet taste by diet. *Sci Adv.* 2020 Nov 11;6(46):eabc8492.

3.1 Abstract

Diets rich in sugar, salt, and fat alter taste perception and food preference, contributing to obesity and metabolic disorders, but the molecular mechanisms through which this occurs are unknown.

Here we show that in response to a high sugar diet, the epigenetic regulator Polycomb

Repressive Complex 2.1 (PRC2.1) persistently reprograms the sensory neurons of *D.*

melanogaster flies to reduce sweet sensation and promote obesity. In animals fed high sugar, the

binding of PRC2.1 to the chromatin of the sweet gustatory neurons is redistributed to repress a developmental transcriptional network that modulates the responsiveness of these cells to sweet

stimuli, reducing sweet sensation. Importantly, half of these transcriptional changes persist

despite returning the animals to a control diet, causing a permanent decrease in sweet taste. Our

results uncover a new epigenetic mechanism that, in response to the dietary environment,

regulates neural plasticity and feeding behavior to promote obesity.

3.2 Introduction

Diets high in processed foods promote higher calorie intake and weight gain, increasing the risk for chronic and metabolic diseases (1). How these foods cause overconsumption, however, is still unclear. Processed foods are high in salt, and fat, which we are genetically programmed to like because of their high caloric-density (2). Interestingly, evidence is emerging that the levels of salt, sugar, and fat in diets can alter taste sensation in humans (3–5), raising the question of whether these sensory changes may influence food intake, obesity, and metabolic disease (6, 7). This idea is supported by a number of recent animal studies which found changes in taste, neural responses, and food preferences in rodents fed high nutrient diets (8–13). However, due to the complexity of the mammalian taste system and the lack of genetic tools, we know next to nothing about the molecular mechanisms through which diet composition affects taste sensation and obesity. Thus, studies in genetically tractable model organisms could help shed light on this question and define evidence-based strategies to curb the prevalence of obesity and metabolic disease, which currently affects billions of people worldwide.

We recently found that high dietary sugar dulls the responses of the *D. melanogaster* taste neurons to sweet stimuli, causing higher food intake and weight gain, arguing that the effects of diet on taste are conserved (14, 15). In this manuscript we exploited the exquisite genetics tools of the fly and the relative simplicity of its sensory system to uncover the mechanisms through which high levels of dietary sugar reshape the sensory neurons to promote weight gain and obesity. We report that the Polycomb Repressive Complex 2.1 (PRC2.1), a chromatin silencing complex conserved from plants to humans (16), tunes the activity of the sweet sensory neurons and taste sensation in response to the food environment by repressing a transcriptional program that shapes the synaptic, signaling, and metabolic properties of these

cells. Interestingly, this diet-dependent transcriptional remodeling persisted even when animals were returned to the control diet, leading to lasting changes in sweet taste behavior that depended on the constitutive activity of PRC2.1. Together our findings suggest that diet composition activates epigenetic mechanisms that reprogram sensory responses to food; this sensory reprogramming determines the perception of future stimuli, leading to long-lasting alterations in behavior that increase the risk for obesity and metabolic disease.

3.3 Results

PRC2.1 modulates sweet taste in response to the dietary environment

Drosophila melanogaster flies fed high dietary sugar experience lower sweet taste sensation as a result of the decreased responsiveness of the sweet sensory neurons to sugar stimuli (14, 15). Given the importance of sensory cues to control eating, and recent data that diet also impacts taste in mammals (8–12), we set out to identify the molecular mechanisms through which dietary experience shapes sensory responses. We previously reported that sweet taste deficits develop within 2–3 days upon exposure to the high sugar diet, depended on the concentration of sugar in the diet, but were independent of fat accumulation and weight gain (14). We thus reasoned that gene regulatory mechanisms may be involved in modulating the responses of the sensory neurons to diet composition. To test this hypothesis, we conducted a screen for gene regulatory and epigenetic factors necessary for the sweet taste defects caused by a high sugar diet. To do this, we fed control (*w¹¹¹⁸^{CS}*) and mutant flies a control diet (CD, ~5% sucrose) or a diet supplemented with 30% sucrose (sugar diet, SD) for 7 days and then tested their taste responses to sweetness using the Proboscis Extension Response (17). This behavioral assay measures taste perception by quantifying the amount of proboscis extension (0= no

extension, 0.5=partial extension, 1= full extension) when the fly labellum – where the dendrites and cell bodies of the taste neurons are located (Fig. 1A) – is stimulated with three different concentrations of sucrose (30%, 10%, 5%); when used in this way, PER generates a taste curve where flies respond more intensely to higher sugar stimuli (Fig. 1B, gray circles). Flies fed a sugar diet show a marked decrease in PER to sucrose compared to control diet flies (Fig. 1B, gray squares); however, mutants for the core Polycomb Repressive Complex 2 (PRC2) – which includes the histone 3 lysine 27 (H3K27) methyltransferase *Enhancer of Zeste (E(z))*, and the obligate accessory factors *Suppressor of zeste 12, (Su(z)12)* and *extra sex combs, (esc)* (Fig. 1B) – had largely the same proboscis extension response (PER) on a control and sugar diet (Fig. 1B, right, red shades). Of note, the PER of *Su(z)12* mutant flies on a CD was lower than control animals, likely because of the additional roles this gene plays in heterochromatin formation (18). To confirm the role of PRC2 in sweet taste deficits, we supplemented the control and sugar diet with EED226, a PRC2 inhibitor (herein referred to as EEDi) that destabilizes the core complex by binding to the tri-methyl H3K27 (H3K27me3) binding pocket of EED (the homologue of *esc* in *M. musculus*) (19). While animals fed a sugar diet plus vehicle (10% DMSO) experienced lower PER, those fed a SD+EEDi retained normal sweet taste responses in a dose dependent manner (Fig. 1C), consistent with results from the PRC2 mutants. Thus, mutations and inhibition of PRC2 prevents the blunting of sweet taste that occurs in the high sugar food environment.

In flies PRC2 forms two main complexes, PRC2.1 and PRC2.2, which contain distinct accessory factors that influence the targeting of the core complex to the chromatin (18). Mutations in the *Polycomb-like (Pcl)* gene, the accessory factor to PRC2.1, phenocopied PRC2 mutants and prevented sweet taste deficits in flies fed a sugar diet (Fig. 1D). In contrast, flies with deficits in the PRC2.2-members *Jumonji*, *AT rich interactive domain 2 (Jarid2)* and *jing*

still showed a blunting of sweet taste responses in flies fed a sugar diet (Fig. S1A). Interestingly, members of the Polycomb Repressive Complex 1 (PRC1) and the recruiter complex PhoRC were also not required for the taste changes in responses to a sugar diet (Fig. S1B-D). Thus, the PRC2.1 complex is necessary for the sensory changes that occur in the high sugar environment.

We next asked if PRC2.1 is required specifically in the sweet sensory neurons to decrease their responses to sweet stimuli on the sugar diet. To do this, we used the GAL4/UAS system to knock down *Pcl* in neurons that express the sweet taste receptor gene *Gustatory receptor 5a* with the *Gr5a-GAL4*, which labels ~60 cells in the proboscis of adult flies (20); we selected *Pcl* to narrow the effect to the PRC2.1 complex. Incidentally, *Gr5a+* cells also respond to fatty acids (21), but this modality was not affected by the high sugar diet (14). Knockdown of *Pcl* in *Gr5a+* neurons using two independent RNAi transgenes (50% knockdown efficiency, Fig. S2A) prevented sweet taste deficits in animals fed a sugar diet (Fig. 1E, and Fig. S2B). *Pcl* knockdown, however, had no effect on sweet taste on a control diet (Fig. S2C), in accordance with the observation that *E(z)* and *Pcl* mutants have normal sweet taste on a control diet (Fig. 1B, C, D) and suggesting that these phenotypes are uncovered only by the high sugar food environment.

Since *Pcl* is thought to target the PRC2 core complex to chromatin (18), we hypothesized that its overexpression may be sufficient to induce sweet taste deficits even in the absence of a high sugar food environment. Indeed, overexpression of *Pcl* specifically in the *Gr5a+* neurons lead to sweet taste deficits in flies fed a control diet compared to transgenic controls (Fig. 1F). The effects of *Pcl* overexpression were abolished by treatment with the PRC2 inhibitor EEDi (Fig. 1G), arguing that *Pcl* overexpression causes sweet taste deficits entirely through the action of PRC2, and not through some yet unidentified mechanism. Importantly, *Pcl* overexpression

had no effect on the number of *Gr5a*⁺ neurons in the proboscis (Fig. S2D), and so the taste deficits cannot be attributed to a decrease in the number of cells. To exclude the possibility that the effects of manipulating *Pcl* on sweet taste were developmental, we used the temperature sensitive *tubulin-GAL80^{ts}* transgene to limit expression of *UAS-Pcl* and *Pcl^{RNAi}* only to adult flies. Switching the flies to the non-permissive temperature and the respective diet 4 days post eclosion, resulted in the same effects on sweet taste as using the *Gr5a-GAL4* alone (Fig. S2E). Together, these experiments establish that the PRC2.1 complex is required cell-autonomously in the *Gr5a*⁺ neurons to mediate the effects of a high sugar diet on sweet taste.

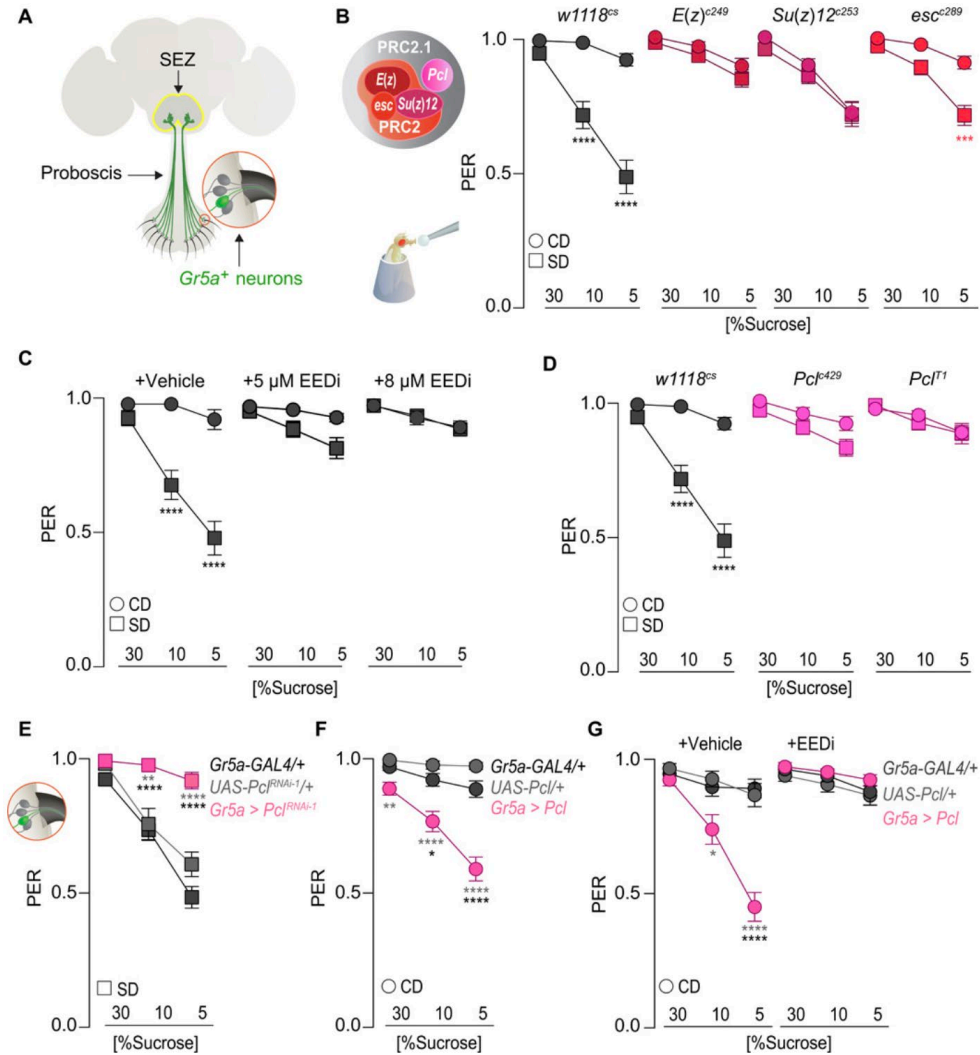


Figure 3.1 PRC2.1 modulates sweet taste in response to diet

(A) Schematic of sweet sensory neurons. **(B)** The PRC2 complex: *E(z)*, *Su(z)12*, *esc*, and the accessory protein *Pcl*.

(B to G) Taste responses (y axis) to stimulation of the labellum with 30, 10, and 5% sucrose (x axis) of age-matched male **(B)** *w1118^{cs}*, *E(z)^{c249/+}*, *Su(z)12^{c253/+}*, and *esc^{c289/+}* flies on a control or sugar diet. n = 34 to 68. *w1118^{cs}* on a CD compared to *E(z)^{c249/+}* (ns), *Su(z)12^{c253/+}* (****), and *esc^{c289/+}* (ns). **(C)** *w1118^{cs}* flies on a control or sugar diet with vehicle (10% DMSO) or 5 and 8 μ M EEDi. n = 32 to 43. **(D)** *w1118^{cs}*, *Pcl^{c429/+}*, and *Pcl^{T1/+}* flies on a control or sugar diet. n = 36 to 82. **(E)** *Gr5a > Pcl^{RNAi-1}* and transgenic controls. n = 42 to 63. **(F)** *Gr5a > Pcl* and transgenic controls on a control diet. n = 36 to 61. **(G)** *Gr5a > Pcl* flies on a control diet with vehicle (10% DMSO) or 8 μ M EEDi. n = 30 to 35. In all panels, flies were on a control (circle) or sugar (square) diet for 7 days. Data are shown as means \pm SEM. ****P < 0.0001, ***P < 0.001, **P < 0.01, and *P < 0.05.

***Pcl* mutant animals have the same sensory responses to sucrose, regardless of diet**

Flies on a high sugar diet have lower sweet taste because the neural responses of the taste neurons to sweet stimuli are decreased (14, 15). Since *Pcl* mutants have identical sweet taste sensation on a control and sugar diet (Fig. 1), we hypothesized that the responses of the sensory neurons to sucrose stimulation should also be similar. To test this, we expressed the genetically encoded presynaptic calcium indicator *UAS-GCaMP6s-Brp-mCherry* (22) in the sweet sensing neurons and measured their *in vivo* responses to stimulation of the proboscis with 30% sucrose in control and *Pcl* mutant animal brains (Fig. 2A-D). As we previously showed, the responses to sucrose stimulation were lower in control flies fed a high sugar diet (Fig. 2A, B and Fig. S2F); however, in *Pcl* mutants the magnitude of calcium responses to sucrose was nearly identical between animals fed a control diet and sugar diet (Fig. 2C, D and Fig. S2G), matching the behavioral data (Fig. 1); importantly, this rescue was not due to an increase in the number of sweet taste cells (Fig. 2E). Despite the fact that *Pcl* mutant or *Pcl* knockdown animals had identical PER to control flies on a control diet (Fig. 1 and Fig. S2), the calcium responses to sucrose in the taste neurons were lower in the mutants.

We previously showed that restoration of sweet taste neuron activity in flies fed high dietary sugar protected them from diet-induced obesity (14, 15), here defined by an increase in fat mass over protein levels. Since *Pcl* mutants abolished the deficits in neural and behavioral responses to sweetness in animals fed a high sugar diet, we anticipated that they should also prevent a diet-dependent increase in triglycerides. Indeed, sugar-diet flies with knockdown of *Pcl* in the *Gr5a*⁺ neurons showed the same triglyceride levels as animals on a control diet (Fig. 2F), while these were increased in control flies fed a sugar diet (Fig. 2F). Importantly, there was no difference in the levels of triglycerides between control and *Pcl* knockdown flies fed a control

diet (Fig. 2F). Of note, mutants in the PRC2.1 complex were also protected from diet-induced obesity (Fig. S2H). Together, these data suggest that, in response to the food environment, *Pcl* modulates the responsiveness of the sweet gustatory neurons to promote diet-induced obesity. The differences between PER and calcium responses to sucrose in *Pcl* mutant and control animals also suggest that the relative activity of the sensory neurons in response to diet, rather than their absolute activity, likely plays a role in taste sensation and diet-induced obesity.

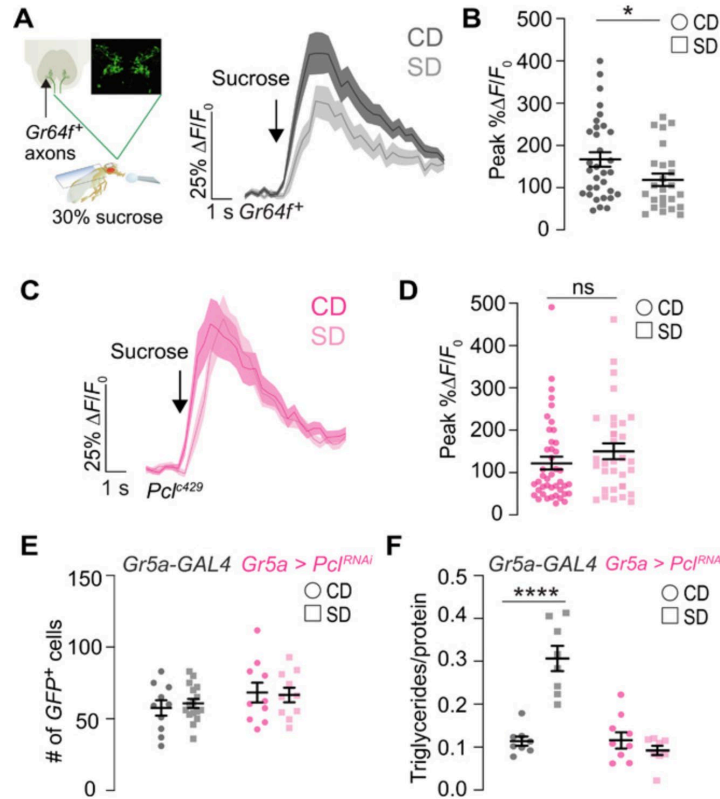


Figure 3.2 *Pcl* mutant animals have the same neural responses to sucrose, regardless of diet

(A) Setup for in vivo calcium imaging: The proboscis is stimulated with 30% sucrose while recording from the SEZ containing the presynaptic terminals of the sweet taste neurons here (labeled with synaptotagmin::GFP). (A and C) Average $\% \Delta F/F_0$ calcium traces to stimulation of the proboscis (arrow) in age-matched male *Gr64f > GCaMP6s-Bruchpilot-mCherry* (A) and *Gr64f > GCaMP6s-Bruchpilot-mCherry; Pcl^{c429}* flies (C). (B and D) peak $\% \Delta F/F_0$ responses on a control or sugar diet for flies in (A) and (C), respectively. $n = 28$ to 46 , Mann-Whitney test, comparisons within genotypes. (E) Quantification of green fluorescent protein (GFP)-labeled cells in *Gr64f; CD8-GFP* flies crossed to *w¹¹¹⁸^{cs}* or *Gr64f; CD8-GFP > Pcl^{RNAi}* on a control or sugar diet. $n = 5$ to 16 , Kruskal-Wallis Dunn's multiple comparisons, comparison to control diet of each genotype, no significance. (F) Triglyceride levels normalized to protein in *Gr5a > Pcl^{RNAi}* and transgenic control flies fed a control or sugar diet. $n = 8$, two-way analysis of variance (ANOVA) with Sidak's multiple comparisons test, comparisons to control diet within genotype. For all panels flies were on a control (circle) or sugar (square) diet for 7 days. All data are shown as means \pm SEM, **** $P < 0.0001$ and * $P < 0.05$ for all panels.

***Pcl* chromatin occupancy is redistributed in the high sugar environment**

Our experiments show that PRC2.1 plays a critical role in the neural activity, behavior, and the metabolic state of animals exposed to the high sugar food environment. To identify the molecular mechanisms underlying these phenotypes, we measured the chromatin occupancy of *Pcl* in the ~60 *Gr5a*⁺ neurons using Targeted DNA Adenine Methyltransferase Identification (TaDa) (Fig. 3A) (23). To do this we generated *Dam::Pcl* (*UAS-LT3-Dam::Pcl*) transgenic flies and compared them to *Dam*-only flies (*UAS-LT3-Dam*) to control for non-specific methylation by the freely diffusing *Dam* protein (24) (Fig. 3A) and to obtain a measure of chromatin accessibility *in vivo* (CATaDa) (25). To specifically profile *Pcl* binding to chromatin in the sweet sensory neurons and limit the induction of *Dam*, we expressed the *Dam::Pcl* and *Dam* transgenes in combination with *Gr5a-GAL4;tubulin-GAL80^{ts}*. To induce the expression of each UAS transgene we shifted the flies to the permissive temperature (28°C) for 20 hours after they had been exposed to a control or sugar diet for 3 days (Fig. 3A). We selected this time point because we previously showed that sweet taste defects developed within 3 days of exposure to the sugar diet (14).

Most of the variation in the biological replicates of *Dam::Pcl* normalized to *Dam* alone (see Methods) was due to diet (Fig. S3A), consistent with high Pearson correlations within each dietary condition (Fig. S3B). Further, the chromatin accessibility profile of *Dam* at the *Gr5a* sweet taste receptor gene promoter was high, while at the *Gr66a* bitter taste receptor promoter – which is only expressed in bitter cells, closely located near the sweet cells – was low (Fig. 3B), suggesting that the transgenes were appropriately targeted to the sweet taste neurons and that the limited induction controlled for background DNA methylation.

We first analyzed *Pcl* chromatin occupancy in the *Gr5a+* neurons of flies on a control diet by comparing our data to a previous study that annotated five major chromatin types in *D. melanogaster* using a similar technique (DNA Adenine Methyltransferase Identification, Dam-ID) (26). *Pcl* targets were enriched in Polycomb chromatin (blue), compared to other chromatin types (green and black = repressive; red and yellow = active) (Fig. 3C); for example, *Pcl* occupancy was high and *Dam* accessibility low at two known Polycomb blue chromatin clusters, (Fig. S3E), while the opposite was true for regions in other chromatin types (Fig. S3F, red and yellow chromatin) (26). We next asked whether *Pcl* was enriched at Polycomb Response Elements (PREs), cis-regulatory sequences to which Polycomb Group Proteins bind in *D. melanogaster* (27). Using a recently developed tool that predicts PRE regions genome-wide (28), we found that *Pcl* was present in these regions (Fig. 3D, gray line), with an enrichment for intergenic (3.2-fold enriched, $p < 0.001$, Monte Carlo permutation test) and enhancer PREs (2.9-fold enriched, $p < 0.001$, Monte Carlo permutation test).

To determine changes in *Pcl* occupancy with diet, we compared *Pcl* chromatin binding between flies fed a control and sugar diet. While ~70% of the overall *Pcl* and CATaDa peaks were shared between the control and sugar diet (Fig. S3C, D), we found more *Pcl* at PREs on a sugar compared to a control diet (Fig. 3D, purple line). Interestingly, chromatin accessibility at both *Pcl* peaks (Fig. 3E) and PREs (Fig. 3F) was decreased in the sugar diet condition. Our analysis also showed that differentially bound *Pcl* peaks had a 3.3-fold enrichment of overlap for enhancer-type PREs ($p < 0.001$, Monte Carlo permutation test). Further examination of the differentially bound genes, revealed a redistribution in *Pcl* occupancy (Fig. S3G), with a similar number of genes with higher (group 1) and lower (group 2) *Pcl* binding on a sugar diet compared to the control diet (Fig. 3G). To determine the biological pathways and function of the *Pcl*-

targets, we used iPAGE (29). This pathway enrichment analysis revealed that most of the genes differentially bound by *Pcl* were transcription factors that targeted promoters and enhancers. Notably, transcription factors implicated in Axon Target Recognition and Nervous System Development showed an enrichment in *Pcl* binding on a sugar diet, while those involved in Gene Ontology (GO) terms such as Proboscis Development and Feeding Behavior had both an increase and decrease in *Pcl* occupancy on a sugar diet (Fig. 3H, for full iPAGE GO term analysis see Fig. S4). While the large majority of genes differentially bound by *Pcl* were in the gene regulation category (80%), the pathway enrichment analysis also uncovered a few metabolism GO terms (Fig. 3H and Fig. S4). In summary, we found that in the high sugar environment, the chromatin occupancy of PRC2.1 in the *Gr5a*⁺ neurons was redistributed at loci that encode for transcription factors involved in neuronal processes and development. This redistribution could result in changes in the expression of these transcription factors and their targets, and in turn, affect the responsiveness of the sensory neurons and sweet taste sensation.

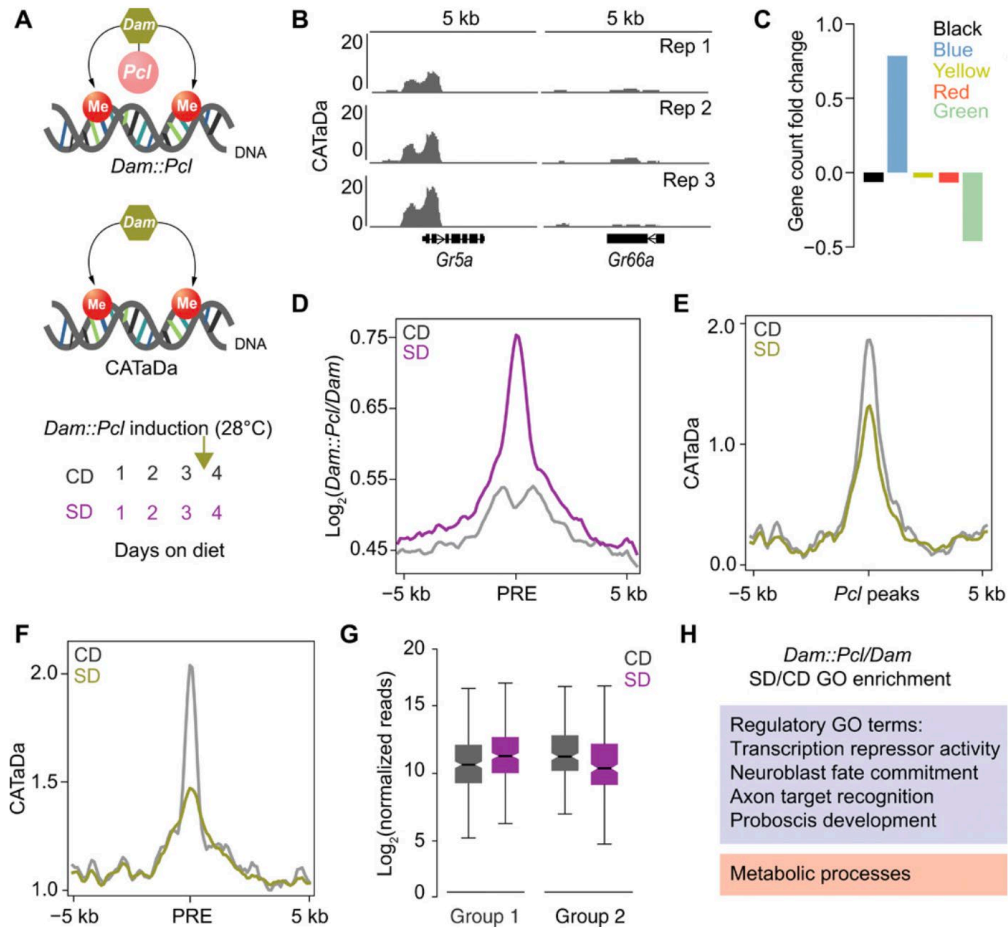


Figure 3.3 *Pcl* chromatin occupancy is redistributed in the high sugar environment.

(A) Targeted Dam-ID (TaDa) of *Dam::Pcl* and Dam (CATaDa) and induction paradigm. Age-matched *Gr5a;tubulin-GAL80^{ts} > UAS-LT3-Dam::Pcl* and *Gr5a;tubulin-GAL80^{ts} > UAS-LT3-Dam* flies were placed on a control or sugar diet for 3 days at 20° to 21°C and then switched to 28°C between days 3 and 4 to induce Dam. (B) CATaDa from control diet flies at the sweet gustatory receptor *Gr5a* and the bitter gustatory receptor *Gr66a*. (C) Proportion of genes allocated to the five chromatin states according to their transcription start site, normalized to the expected proportion across the whole genome. (D) Mean $\log_2(Dam::Pcl/Dam)$ centered at PREs on a control and sugar diet. (E and F) Mean CATaDa centered at (E) *Pcl* peaks and (F) PREs on a control and sugar diet. (G) The median and variance of $\log_2(Dam::Pcl/Dam)$ reads for genes differentially bound on a control and sugar diet. Genes are grouped into higher (group 1) or lower (group 2) *Pcl* binding on a sugar diet. (H) GO terms associated with differentially bound genes identified by iPAGE; boxes represent GO category, regulatory (lavender) and metabolism (orange) (for the full iPAGE, see fig. S4). For all panels, peaks are a false discovery rate (FDR) of <0.01.

PRC2.1 sculpts the transcriptional responses of the *Gr5a*⁺ neurons in response to diet

To test the hypothesis that redistribution of PRC2.1 chromatin occupancy alters the physiology of the sensory neurons by changing gene expression, we used Translating mRNA Affinity Purification (TRAP) (30) to isolate mRNAs associated with the ribosomes of the *Gr5a*⁺ cells. (Fig. 4A). To capture the dynamics of this process, we collected samples from age-matched *Gr5a*[>]*Rpl3-3XFLAG* flies fed a sugar diet for 3 and 7 days (Fig. S5A). We first verified that this technique selected for mRNAs in the *Gr5a*⁺ neurons by quantifying the normalized read counts (*Gr5a*⁺/input) for genes expressed only in the *Gr5a*⁺ cells, such as the sweet taste receptor genes *Gr5a*, *Gr64f*, and *Gr64a*, and the fatty acids taste receptor *Ir56D* (31, 32). Indeed, these transcripts were enriched in the *Gr5a*⁺ fraction compared to the input (Fig. S5B), while the opposite was true for the bitter receptor genes *Gr66a* and *Gr32a*, which are expressed in the bitter sensing neurons in the taste sensilla, but not in *Gr5a*⁺ cells (33) (Fig. S5B).

We observed a robust negative skew in gene expression in the *Gr5a*⁺ neurons of flies fed a sugar diet for 3 (SD3, mint; compared to the control diet) and 7 days (SD7, teal; compared to the control diet) (Fig. 4B, C, -0.8 and -1.7 skew, refer to methods for details of how skewness was calculated), consistent with the idea that a repressive gene regulatory mechanism is at play. Overall, we found ~800 differentially expressed genes at each time point (DEG, each compared to control diet, Wald test, $q < 0.1$, Supplementary File 1), while ~190 changed at both time points (Fig. 4D, Venn diagram, Wald test, $q < 0.1$); of these ~68% and 87% showed negative log₂ fold changes (l₂fc) respectively (Fig. 4B-C, SD3 and SD7). GO term analysis using iPAGE (29) revealed that these genes were part of biological pathways involved in 3 broad categories: neural function/signaling, metabolism, and gene regulation (Fig. S6 and Fig. S7). GO terms for neuron-specific processes, such as Dendritic Membrane, Sensory Perception of Chemical Stimulus, and

Presynaptic/Vesicle Transport, were enriched at both timepoints (Fig. S6 and Fig. S7), suggesting that PRC2.1 may alter the physiology of the sensory neurons through these pathways in response to a high sugar environment. Flies fed a sugar diet for 7 days showed additional changes in GO terms, specifically those linked to neurodevelopmental processes, such as Asymmetric Neuroblast Division and Neuron Projection Morphogenesis (Fig. S7), which may explain the worsening of sweet taste sensation at this time point (14). We also observed changes in “regulatory” GO terms such as Transcription Factor and Corepressor, consistent with the redistribution of *Pcl* chromatin occupancy in response to a high sugar diet that we had observed in the TaDa experiments (Fig. 3). Finally, GO terms associated with metabolic changes were also higher in flies fed a sugar diet for 7 days (Fig. S7), in line with the findings that longer consumption of the high sugar diet leads to higher fat accumulation (14). Together this analysis shows that consumption of a high sugar diet altered neural, regulatory, and metabolic genes in the *Gr5a*⁺ cells. Of note, the mRNA levels of the sweet taste receptors genes, *Gr5a*, *Gr64a-f*, and *Gr61a* were not changed at either time point.

To determine the role of PRC2.1 in these changes, we performed the transcriptional profiling experiments in the *Gr5a*⁺ neurons of *Pcl*^{c429} mutant animals fed a control diet and sugar diet for 7 days (CD and SD7) (Fig. S5C). Strikingly, the *Pcl* mutation abolished the negative skew (Fig. S5D, Supplementary File 1) and largely nullified the effects of the high sugar diet environment on differential gene expression. Specifically, of the genes repressed by a sugar diet (Fig. 4D, heatmap) 32% now had a positive log₂ fold change (Wald test, $q < 0.1$) and 76% were unchanged ($q < 0.1$, practical equivalence test using a null hypothesis of a change of at least 1.5-fold; see Methods for details) between *Pcl* mutants fed a control and sugar diet. This effect was reflected in the GO analysis where terms changed by a high sugar diet in wild-type

animals, such as Dendritic Membrane, Sensory Perception of Chemical Stimuli, Synapse, and Carbohydrate Metabolic Process, showed opposite trends in log₂ fold changes in *Pcl* mutants (Fig. S8). Thus, *Pcl* mutations abolished nearly all the gene expression changes induced by a high sugar diet consistent with their effects on behavior (PER, Fig.1), neural function (*in vivo* calcium imaging, Fig. 2), and metabolism (triglycerides, Fig. 2). Together, these findings support the hypothesis that PRC2.1 tunes sweet taste sensation to the food environment by influencing the expression of genes involved in different aspects of sensory neuron physiology.

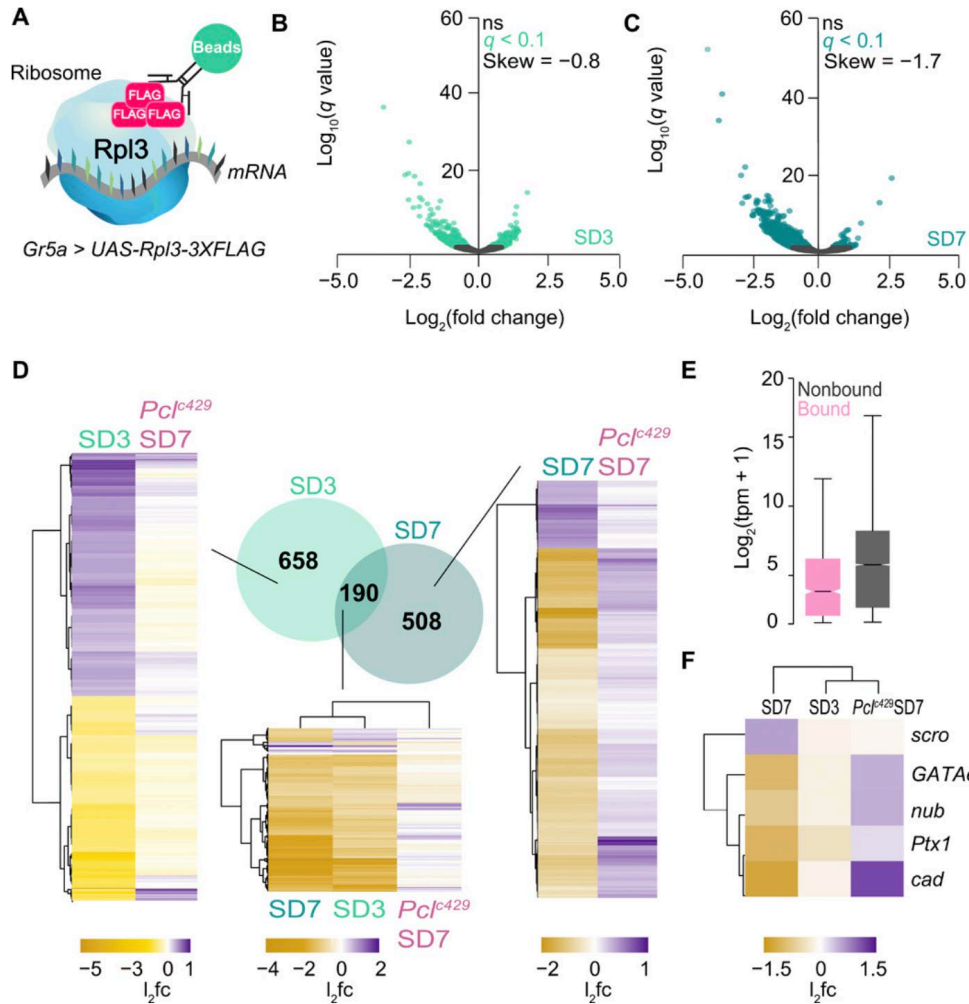


Figure 3.4 PRC2.1 sculpts the transcriptional responses of the *Gr5a*+neurons in response to diet.

(A) TRAP to profile changes in the *Gr5a*+ neurons. (B and C) Volcano plots representing differential expression in the *Gr5a*+ neurons of age-matched male *Gr5a* > *UAS-Rpl3-3XFLAG* flies on SD3 (mint) and SD7 (teal). $n = 2$ to 3 replicates per condition. Nonsignificant genes are in black, and genes with $q < 0.1$ (Wald test) are in mint or teal for SD3 and SD7, respectively. (D) Venn diagram of DEGs at SD3, SD7, and the overlap between SD3 and SD7 (Wald test, $q < 0.1$). Heatmaps show l_2fc for DEGs under each condition in Venn diagram (left columns in heatmap, SD3, SD7, and SD3 + SD7) and *Pclc429* mutant flies (right column in heatmap, *Pclc429* SD7). (E) Read counts from TRAP for *Pcl* bound (pink) and not bound genes (gray) on a control diet. Box plots represent median and variance, two-tailed t test, $P = 3.196 \times 10^{-6}$. (F) l_2fc for scarecrow (*scro*), Paired-like homeobox domain 1 (*Ptx1*), caudal (*cad*), *GATAe*, and nubbin (*nub*) in SD7, SD3 flies, and *Pclc429*SD7 mutant flies. For all panels, comparisons are to control diet, and l_2fc ranges from purple (high) to gold (low).

PRC2.1 represses a transcriptional program required for sweet taste sensation

Our transcriptomics analysis shows that a high sugar diet environment repressed gene expression in the sweet sensory neurons, and that *Pcl* mutations almost entirely abolished this effect. This, together with the finding that, on a sugar diet, *Pcl* binding primarily changed at the enhancers of transcription factor genes (Fig. 3), suggests that *Pcl* redistribution may affect the expression of transcription factors that control genes responsible for the overall responsiveness of these sensory neurons to sweetness. This idea is supported by the observation that *Pcl*-bound genes have lower expression levels than those not bound by it in the *Gr5a+* neurons (Fig. 4E), with many genes showing high binding and low expression ($\log_2\text{tpm} < 2$, dark purple), while others having higher mRNA read counts ($\log_2\text{tpm} > 5$, light purple) (Fig. S5E). To test this hypothesis, we looked for transcription factors that were directly and differentially bound by *Pcl* in the TaDa analysis and that showed changes in gene expression on a sugar diet in the TRAP experiments (Fig. S5F). This analysis revealed 5 genes: four transcriptional activators and one repressor. The four activators— *GATAe* (Zn finger), *nubbin/pdm* (*nub*, POU homeobox), *Ptx1* (paired-domain homeobox), and *caudal* (*cad*, hox-like homeobox)— had higher *Pcl* binding (Fig. 5A) and lower mRNA levels on a sugar diet (Fig. 4F). In contrast, the repressor *scarecrow* (*scro*, NK-like homeobox) had lower *Pcl* binding (Fig. 5A) and higher mRNAs levels on a sugar diet (Fig. 4F). Importantly, mutations in *Pcl* reversed the effects of a high sugar diet on the expression of these 5 genes, suggesting that the occupancy of *Pcl* to chromatin modulates their mRNA levels (Fig. 4F). Interestingly, we also noticed that *cad*, *Ptx1*, *GATAe*, and *nub* were enriched in the *Gr5a+* neurons compared to the input, while *scro* was depleted in these cells (Fig. S9A). To test the effects of these five transcription factors on sweet taste, we manipulated their expression to mimic the direction of change on a high sugar diet. Knockdown of *cad*, *Ptx1*,

GATAe, or *nub*, and overexpression of *scro* (Fig. S9B, C) in the *Gr5a+* neurons of flies fed a control diet led to a decrease in sweet taste sensation (Fig. 5B) comparable to that experienced by animals on a sugar diet (Fig. 1B). These lines of evidence show that *cad*, *Ptx1*, *GATAe*, and *nub* are direct targets of PRC2.1 and necessary for sweet taste, while overexpression of *scro* is sufficient to decrease it. However, overexpression of each activator alone and knockdown of *scro* was not sufficient to rescue sweet taste in flies fed a sugar diet (Fig. S9D).

Given that the 4 activators are required for sweet taste sensation, we reasoned that they may control the expression of genes important for the proper function of the *Gr5a+* neurons and normal sweet taste. To identify candidate target genes, we tiled the entire *D. melanogaster* genome using the motifs for each of these 5 transcription factors, converted the hits for each transcription factor to z-scores, and determined candidate regulatory targets based on estimates of the z-score threshold for binding in each case (Fig. S9E; see Methods for details). We then flagged as “targets” the set of genes that had a putative binding site (exceeding our transcription factors-specific z-score cutoff) within a 2 kb region upstream of the annotated ORF start (Fig. S9F-J), and examined their expression pattern in the *Gr5a+* neurons of flies on a control and sugar diet. This analysis revealed 658 genes that were collectively regulated by these five transcription factors and also changed by a high sugar diet in the *Gr5a+* cells (Supplementary File 1). Targets of the transcriptional activators Cad, Ptx1, GATAe and Nub— which *Pcl* repressed on a sugar diet— showed negative log₂ fold changes on a sugar diet (Fig. 5C, SD7, teal) that reverted in the *Pcl* mutants (Fig. 5C, pink). Conversely, targets of the transcriptional repressor Scro – which was released from *Pcl* binding and had higher mRNA levels on a sugar diet – showed negative log₂ fold changes on a sugar diet (Fig. 5C, SD7, teal) that reverted in *Pcl* mutants (Fig. 5C, pink). Strikingly, the 658 putative targets of these 5 transcription factors

accounted for nearly all the genes changed by a high sugar diet as measured by TRAP (Fig. 4), suggesting that by directly modulating the expression of these 5 regulators—*Ptx1*, *cad*, *GATAe*, *nub*, and *scro*—and their targets, PRC2.1 influences the responsiveness of the *Gr5a+* neurons to sweet stimuli and the animal's taste sensation.

We next asked whether these targets may be cooperatively regulated by these 5 transcription factors. Indeed, we observed a significant overlap among the regulons of all of the 4 transcriptional activators (Fisher's exact test, FDR-corrected $p < 0.000001$) with the exception of *Ptx1-nub* (Fig. 5D), suggesting that, together, the 4 transcription factors suppressed by PRC2.1 in the high sugar diet environment, may cooperate to direct the expression of a common set of target genes. We also found evidence for *scro* binding sites in the genes targeted by the 4 activators (Fisher's exact test, $q < 0.000001$). This is interesting, because binding of Scro to these gene targets could ensure a more direct and robust way to repress them, compared to PRC2.1 only silencing their activators (*cad*, *Ptx1*, *GATAe* and *nub*). Of note, this double repression mechanism, the first via Pcl and the second via Scro, could explain the large negative skew in gene expression on a high sugar diet we observed in the TRAP data. Transcription factors that share common targets are often part of feed-forward loops, where they regulate one another and themselves to ensure stability of gene expression. Indeed, we found that *GATAe* had predicted binding sites in the promoters of all four regulators considered here (*cad*, *scro*, *Ptx1*, *nub*), in addition to binding its own promoter in a auto-regulatory loop (Fig. 5E). Furthermore, our predictions show that Cad also could target itself, Ptx1 could target *nub*, and that Scro may regulate both *cad* and *GATAe*, forming a negative feedback loop with the latter (Fig. 5E, Supplementary File 1). Thus, the 5 transcription factors differentially bound by PRC2.1 on a high sugar diet likely form a hub that regulates the physiology of the *Gr5a+* neurons.

To probe which aspects of physiology were changed, we used pathway enrichment analysis on the regulons for each transcription factor. GATAe targets, which comprise a large number of the genes targeted by the 4 other transcription factors, were enriched for GO terms involved in Synaptic Assembly and Growth, Terminal Bouton, Neural Projection Morphogenesis, and Protein Kinase Regulation (summarized in Fig. 5E, and Supplementary File 1). In contrast, Ptx1 targets were enriched in GO terms implicated in Cyclic AMP Signaling, Detection of Chemical Stimuli, and Morphogenesis (summarized in Fig. 5E, and Supplementary File 1), Cad targets showed enrichments in GO terms Adenylate Cyclase Activity, Sensory Perception, and Neuropeptide Signaling (summarized in Fig. 5E, and Supplementary File 1), and Nub targets in Calcium Signaling and Nucleosome (summarized in Fig. 5E, and Supplementary File 1). The targets of the repressor Scro showed enrichment in both neural and metabolic GO terms such as Olfactory Behavior and Carbohydrate Metabolic Process (summarized in Fig. 5E, and Supplementary File 1). Thus, we predict that these transcriptional regulators may contribute to different aspects of the physiology of the *Gr5a*⁺ cells.

To test the possibility that these targets form a functional network, we used STRING, a database of known and predicted physical and functional protein-protein interactions (34). We found a significant number of interactions above the expected number (protein-protein interaction enrichment of $p < 1.0e-16$, Supplementary File 2) suggesting that the targets may be part of a functional and biologically connected network in the *Gr5a*⁺ neurons. We used a subset of the targets with GO terms in neural processes to build a smaller network to identify target genes that may play a direct role in sweet taste sensation. This network showed strong interactions between genes involved in synaptic organization and signal transduction and their connection with the upstream regulators (Fig. S10A). We chose two genes at the edges of the

network, which are less likely to have redundant functions, the *Adenylyl Cyclase X D (ACXD)* gene (35) and the *Activity Regulated Cytoskeleton Associated Protein 1 (Arc1)* (36). Knockdown and mutations of *Arc1* or *ACXD* in the *Gr5a+* cells of flies on a control diet led to a significant decrease in sweet taste responses compared to the transgenic controls (Fig. S10B-D). Together, these lines of evidence suggest that PRC2.1 mediates the effects of a high sugar diet on sweet taste by directly controlling the expression of a transcriptional program important for sweet taste.

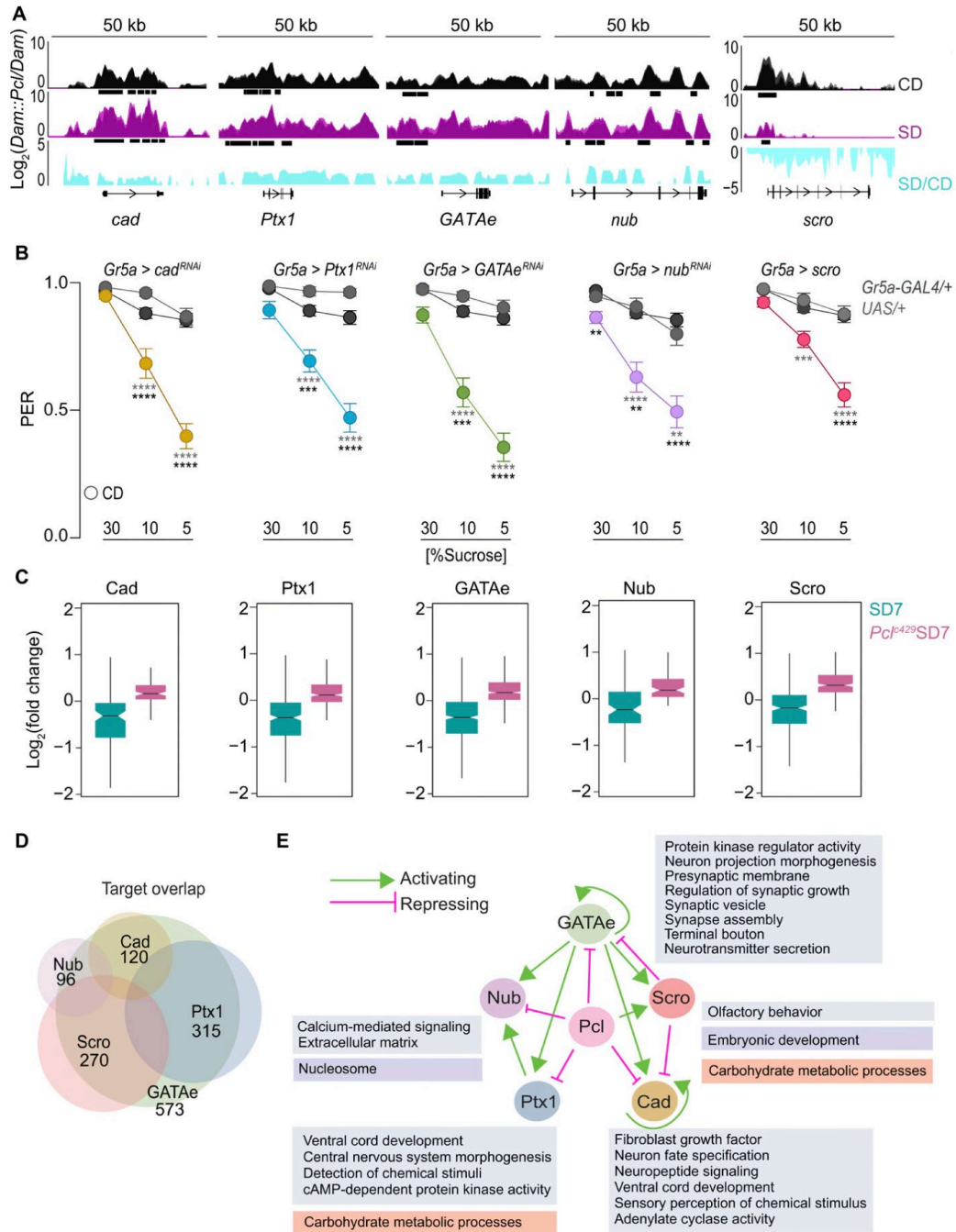


Figure 3.5 PRC2.1 represses a transcriptional program required for sweet taste.

(A) $\text{Log}_2(\text{Dam}::\text{Pcl}/\text{Dam})$ on a control and sugar diet within a 50-kb window at *cad*, *Ptx1*, *GATAe*, *nub*, and *scro*. Replicates are superimposed. Turquoise traces are SD/CD fold changes. Peaks are black boxes ($q < 0.01$), genes are in dense format to include all isoforms. (B) Taste responses (y axis) to stimulation of the labellum with 30, 10, and 5% sucrose (x axis) in age-matched males of *Gr5a > cad^{RNAi}*, *Gr5a > Ptx1^{RNAi}*, *Gr5a > GATAe^{RNAi}*, *Gr5a > nub^{RNAi}*, *Gr5a > scro*, and transgenic control flies on a control diet for 7 days. $n = 30$ to 54 . All data shown as means \pm SEM. *** $P < 0.0001$, *** $P < 0.001$, and ** $P < 0.01$. (C) l2fcs for candidate gene targets of Cad, Ptx1, GATAe, Nub, and Scro (see Materials and Methods and fig. S9) at SD7 and *Pcl⁴²⁹* mutants at SD7. (D) Venn diagram of the overlap of the candidate gene targets of Cad, Ptx1, GATAe, Nub, and Scro. (E) Transcriptional loop between Cad, Ptx1, GATAe, Nub, and Scro mediated by Pcl. GO terms associated with each regulator and identified by iPAGE. Boxes represent GO category, metabolism (orange), regulatory (lavender), and neural/signal (blue) (for full iPAGE see file S1). cAMP, cyclic adenosine 3',5'-monophosphate.

The persistent phenotypic memory of the food environment is dependent on PRC2.1

The cellular fates created by Polycomb Group proteins are inherited as memories across cell divisions to ensure phenotypic stability even in the absence of the triggering stimuli (37, 38). We therefore asked if the neural and behavioral state created by PRC2.1 in the high sugar diet environment was maintained when flies were moved to the control diet for different durations (7, 10, 15, and 20 days) after eating a sugar diet for 7 days (SD>CD) (Fig. 6A, B and Fig. S10E). We found that animals switched to the control diet still had a dulled sweet taste, similar to that of age-matched flies fed a sugar diet for 7 days (Fig. 6B, SD7>CD7 compared to CD7>SD7, top panel). However, their triglyceride levels were similar to those of control diet flies (Fig. S10F), suggesting that while fat storage was reversible when flies were switched to the “healthy” control diet, sweet taste deficits persisted for up to 20 days (Fig. S10E). Interestingly, we also found that persistence required exposure to the high sugar diet for at least 5 days (Fig. S10G).

To understand how this phenotype compares to that of the control diet flies at the molecular level, we conducted TRAP of the *Gr5a+* neurons of flies in the SD7>CD7 and CD7>CD7 conditions. mRNAs from flies on a SD7>CD7 showed a strong negative skew in overall log₂ fold changes compared to the control diet group (Fig. 6C, -2.06), reminiscent of the skew we observed in flies fed a sugar diet (Fig. 4C). Furthermore, we observed that 47% (310/658) of genes in the transcriptional network repressed by PRC2.1 on a sugar diet were still decreased in SD7>CD7 flies (Fig. 6D). Interestingly, the SD7>CD7 animals clustered with the sugar diet 7 (SD7) group compared to sugar diet 3 (SD3) and *Pcl* mutants fed a sugar diet (Fig. 6D). Thus, half of the transcriptional state established by dietary sugar via PRC2.1 persisted when the dietary environment was changed.

To test the hypothesis that PRC2.1 plays an active role in the maintenance of this transcriptional state in the absence of the sugar diet, we inhibited PRC2 activity during the “recovery” diet using an EEDi inhibitor (SD7>CD7+EEDi). Remarkably, these animals showed a restoration of wild-type sweet taste (Fig. 6B, green diamonds, bottom panel) compared to flies fed the recovery diet without EEDi supplementation (Fig. 6B, SD7>CD7, top panel). Similarly, knockdown of *Pcl* only during the recovery period using the temperature sensing *tubulin-GAL80^{ts}*, also rescued sweet taste deficits (Fig. S10H). Together, these data indicate that the sensory neurons retain a transcriptional and phenotypic memory of the sugar diet environment that leads to long lasting behavioral deficits, and that PRC2.1 is actively and constitutively required for the persistence of this state.

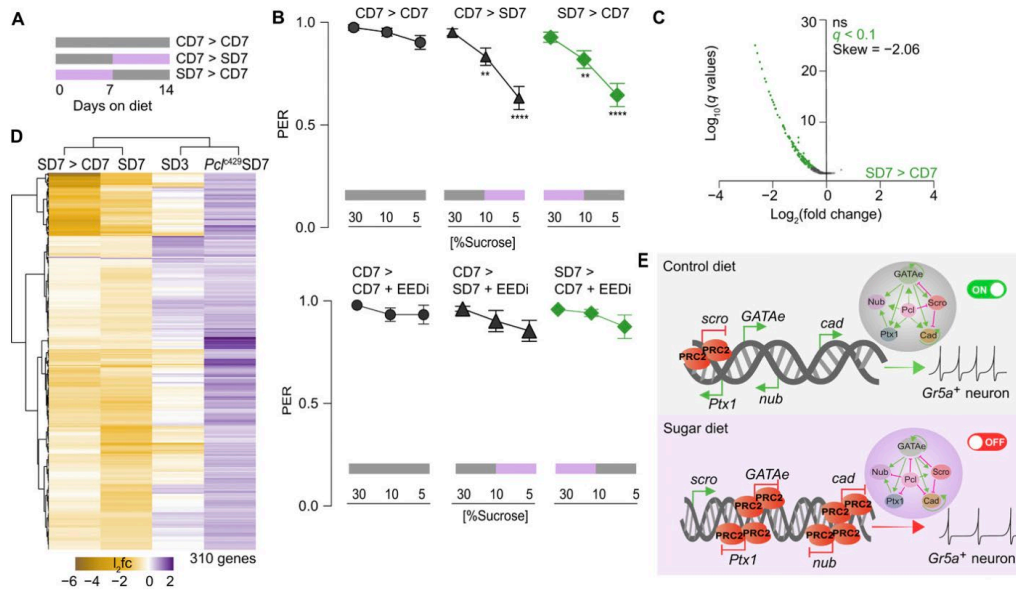


Figure 3.6 The persistent phenotypic memory of the food environment is dependent on PRC2.1.

(A) Control (CD7), sugar (SD7) diet, and > represents dietary switch. **(B)** Taste responses (y axis) to stimulation of the labellum with 30, 10, and 5% sucrose (x axis) of age-matched male w^{1118cs} flies on a control (CD7 > CD7), control to sugar (CD7 > SD7), and sugar to control (SD7 > CD7) diet without (top; n = 57 to 64) or with EEDi (bottom; n = 34 to 46); comparisons between CD7 > CD7 and CD7 > CD7 + EEDi (ns), CD7 > SD7 and CD7 > SD7 + EEDi (****), and SD7 > CD7 and SD7 > CD7 + EEDi (****). Data are shown as means ± SEM. ****P < 0.0001 and **P < 0.01. **(C)** Differential expression in the Gr5a⁺ neurons of age-matched male *Gr5a* > *UAS-Rpl3-3XFLAG* flies on a sugar to control (SD7 > CD7) diet compared to control diet (CD7 > CD7), q < 0.1 (green), ns is nonsignificant, n = 2 replicates per condition. **(D)** Heatmap of DEGs from Fig. 5C that change in the SD7 > CD7 (48%) compared to SD3, SD7, and *Pcl⁴²⁹SD7*. l2fc ranges from purple (high) to gold (low). **(E)** Model of molecular changes in the Gr5a⁺ neurons on a control and sugar diet, showing the redistribution of PRC2.1, and the effects on the regulators and neural responses to sweetness.

3.4 Discussion

In this study we set out to understand how dietary experience alters the gustatory system to promote food intake and weight gain. Specifically, we took advantage of the simple sensory system of *D. melanogaster* and its exquisite genetic and neural tools to identify the molecular mechanisms through which diet composition changes neural physiology and behavior. We previously found that high dietary sugar decreased the responsiveness of the sensory neurons to sugar stimuli, leading to a dulled sense of sweet taste, independently of fat accumulation (14). Here we show that the decrease in sweet taste sensation that flies experience after chronic exposure to a high sugar diet is caused by the cell-autonomous action of the Polycomb Repressive Complex 2.1 in the sweet gustatory neurons. Mutations and pharmacological inhibition of PRC2.1 blocked the effects of the food environment on neural activity, behavior, and obesity. While we do not exclude the possibility that PRC1 and PhoRC may also be involved, we found that mutations or knockdown in these complexes had no effect on taste. To this point, we observed that in *Pcl* mutants, even if the neural responses to sucrose were identical in control and sugar diet fed flies, they were of lower magnitude than those of control flies, suggesting that PRC2.1 may modulate plasticity bidirectionally in response to the nutrient environment. This also suggests that, within limits, it is the relative, rather than the absolute output of the sensory neurons, that is important for taste sensation and diet-induced obesity.

In the high sugar food environment, PRC2.1 chromatin occupancy was redistributed, leading to the repression of transcription factors, neural, signaling, and metabolic genes that decreased the responsiveness of the *Gr5a*⁺ neurons and the fly's sensory experience of sweetness. However, we discovered that PRC2.1 did not directly bind to neuronal genes in these cells and that, instead, it targeted transcription factors involved in processes such as sensory

neuron development, synaptic function, and axon targeting. Specifically, *Pcl* binding was increased at the loci of transcription factors *cad*, *GATAe*, *nub/pdm*, *Ptx1* and decreased at the *scro* locus on a high sugar diet, and lead to corresponding changes in the mRNA levels of these genes (Fig. 6E, model). Our computational analysis revealed that in the *Gr5a+* cells these 5 transcriptional factors regulate a network of ~658 candidate target genes implicated in synaptic function, signal transduction, and metabolism. Changes in the levels of the 5 transcription factors on a high sugar diet, resulted in the overall repression of their target genes, providing a possible explanation for the alterations in the responsiveness of the *Gr5a+* cells we observed. Interestingly, we predicted several positive and negative regulatory loops among the 5 transcriptional regulators, suggesting that they could form a regulatory hub that is responsive to changes in the dietary environment. Knockdown of the four activators and a few of their targets, as well as overexpression of *scro* (Fig. 5B and Fig. S10B-D), resulted in a decrease in sweet taste on a control diet. However, overexpression of *cad*, *Ptx1*, and *nub* alone, as well as knockdown of *scro*, did not rescue taste deficiencies in animals fed a high sugar diet. Since there is 1) overlap in the predicted targets between the repressor *scro* and each of the 4 activators, as well as 2) overlap among the targets of the 4 activators, one possibility is that, as long as *scro* levels are higher because of the sugar diet, the repressive drive is so strong that overcoming it requires collaborative binding among the activators. Together, these findings suggest that this transcriptional hub and the gene battery it controls, is necessary for sweet taste and reshaped by high dietary sugar.

How do these transcription factors and their targets modulate the physiology of these gustatory neurons? Several of these transcription factors (*Ptx1*, *scro*, and *nub/pdm*) control the proper branching, synaptic connectivity, and activity of sensory neurons (39–45), while others

(*cad*, *nub/pdm*) play a role in neuroblast development (46); PRC2 also functions as a competence factor in neural proliferation, differentiation, and sensory neurons (39, 46, 47). We propose that the transcriptional network of ~658 genes controlled by this transcriptional hub may define the intrinsic properties of the sweet sensing neurons. Interestingly, we observed that the 4 activators that are repressed by *Pcl* in the high sugar condition are enriched in the *Gr5a*⁺ cells on a control diet, while *scro* is depleted. Further, many of the target genes are involved in signaling, synaptic function, and cell adhesion, including the kinase *haspin*, the adenylate cyclase *ACXD*, *syt-alpha*, *Arc1*, and the tetraspanin, *jonan*, and innexin proteins among others. These genes were part of a highly interconnected network, which could affect the sweet gustatory neurons at both the functional and connectivity levels. Since we did not observe a change in the expression of the sweet taste receptors, or the misexpression of other taste receptors, our data are not consistent with a complete “loss” of identity of the *Gr5a*⁺ neurons with a high sugar diet. Instead, we hypothesize that PRC2.1 tunes these sensory neurons to the dietary environment by altering a transcriptional network that controls the intrinsic properties of the *Gr5a*⁺ cells, particularly those involved in signal transduction, connectivity, synaptic function, and metabolism. Studies that test the effects of this network on the connectivity, morphology, and signal transduction of the sweet sensory neurons will shed light on how exactly the transcriptional remodeling caused by PRC2.1 we discovered here impacts the physiology of *Gr5a*⁺ cells.

While our experiments show that PRC2.1 chromatin occupancy shifts with the dietary environment, we did not define the signaling mechanisms through which this change in binding occurs. Thus, the question of how exactly PRC2.1 binding is altered in response to the food environment remains open. Recent studies suggest that the activity of Polycomb Group proteins is directly and indirectly linked to cellular metabolism, including kinase signaling cascades,

GlcNAcylation, and the availability of cofactors for histone modifications (48, 49). Interestingly, our previous work showed that the Hexosamine Biosynthesis Pathway enzyme *O-GlcNAc Transferase (OGT)* acts in the *Gr5a*⁺ neurons to mediate the effects of high dietary sugar on sweet taste (14); whether the interaction between OGT and PRC2 is what promotes the repressive activity of the latter in these sensory neurons is a question worth investigating. Of note, the dysregulation of Polycomb-associated chromatin has been found in mice and humans with diet-induced obesity (50, 51), suggesting that the mechanisms we discovered here could also underlie the chemosensory alterations reported in mammals (8–12).

More broadly our work opens up the exciting possibility that PRC2 may modulate neural plasticity in response to environmental conditions. Despite its central role in development and maintenance of neural identity, studies have not directly linked PRC2.1 to neural plasticity. However, in other post-mitotic cells such as muscle, Polycomb Group Proteins are known to reshape transcriptional programs according to environmental stressors, such as oxidative stress, injury, temperature, and light (48, 49). Our findings advance the conceptual understanding of the role of Polycomb Group Proteins in the nervous system and suggest that they could also modulate “neural states” and metaplasticity in response to environment stimuli. Using neuroepigenetic mechanisms like those employed by Polycomb Group Proteins to tune neural states to external conditions could provide several advantages compared to the medley of other cellular, receptor, or synaptic plasticity based mechanisms. Specifically, it would allow cells to 1) orchestrate a coordinated response, 2) create a memory of the environment, and 3) buffer small fluctuations until a substantial challenge is perceived. It is particularly fascinating to think about the molecular mechanisms through which these neural states may be established. The need of neurons to constantly maintain their identity may mean that environmental signals like the

extent of sensory stimulation could alter the expression of developmental gene batteries and affect neural physiology (52). Indeed, it has been speculated that some forms of plasticity may re-engage developmental programs that specify the intrinsic properties of neurons (53). Here we observed that the regulators of the transcriptional network we uncovered function in sensory neuron development and are enriched in the *Gr5a+* cells. Thus, it could be a hallmark of neuroepigenetic plasticity to exploit developmental programs, linking the known role of PRC2 in establishing cell fates with this newly discovered function in modulating cell states.

Incidentally, reengaging developmental programs could be the reason why some environments and experiences leave a memory that leads to the persistent expression of the phenotype beyond the presence of the triggering stimulus, as these could target neural connectivity and set synaptic weight thresholds. Here we found that the changes in taste sensation and half of the sugar diet neural state set by PRC2.1 remained even after animals were moved back to the control diet for up to 20 days. A limitation of our study is that due to the small number of *Gr5a+* neurons and their anatomically inaccessible location, we were not able to measure the identity of the molecular memory in these cells alone. However, we saw that the phenotypic memory of the high sugar food environment was dependent on the constitutive action of PRC2.1. Thus, based on other studies showing that the H3K27 methyl mark acts as a molecular memory during development (37, 38) we speculate that this is likely to be the memory signal in the *Gr5a+* cells too. Stable maintenance of the memory requires active recruitment of PRC2 (38); while we did not measure *Pcl* occupancy and chromatin accessibility at PREs in the recovery diet with and without the inhibitor, our findings that PRC1.2 is actively required for the maintenance of the taste phenotype and that 47% of its indirect targets are still repressed, indicates that PRC2.1 may be stably recruited to the transcription factors loci. Perhaps conditions

that lead to metabolic remodeling such as prolonged fasting, could reset its binding. Finally, we do not know if the diet-induced chemosensory plasticity observed in humans and rodents is persistent or reversible. Unlike in *D. melanogaster*, mammalian taste cells are not post-mitotic neurons, and so they regenerate every few weeks. Thus, the persistence of chemosensory plasticity in mammals, if it exists, may involve different mechanisms in the taste cells, such as a decrease in their renewal (8). However, a decrease in the responses of the Chorda Tympani to sweetness has been observed in rats fed a 30% sucrose diet (12), and thus our findings may be applicable to the sensory nerves.

In conclusion, we show that PRC2.1 mediates the effects of high dietary sugar on sweet taste by establishing persistent alterations in the taste neurons that remain as a phenotypic and transcriptional memory of the previous food environment. We speculate that this memory may lock animals into patterns of feeding behavior that become maladaptive and promote obesity. Thus, dietary experience, in ways not unlike trauma, can induce lasting molecular alterations that restrict the behavioral plasticity of animals and impact disease risk. Since the content of sugar in processed foods is similar to that we fed flies and the function of Polycomb Group Proteins is conserved from plants to humans (16), our work is broadly relevant to understanding the effects of processed food on the mammalian taste system and its impact on food intake and a whole range of diet-related conditions and diseases that affect billions of people around the globe.

3.5 Materials and Methods

Fly Husbandry

All flies were grown and maintained on cornmeal food (Bloomington Food B recipe) at 25°C and 45%–55% humidity under a 12:12 hour light-dark cycle (ZT0 at 9 AM). Male flies were collected under CO₂ anesthesia 1-3 days after eclosion and maintained in a vial that housed 35-40 flies. Flies were acclimated to their new vial environment for an additional 2 days. For all experiments, flies were changed to fresh food vials every other day.

For all dietary manipulations, the following compounds were mixed into standard cornmeal food (Bloomington Food B recipe) (0.58 calories per gram) by melting, mixing, and pouring new vials as in (54) and (55). For the 30% sugar diet (1.41 calories per gram) Domino granulated sugar w/v was added. For the EED226 inhibitor diet (AxonMedchem), EED226 was solubilized in 10% DMSO and added to control or 30% sugar diet at a total concentration of 5 or 8 uM.

For genetic manipulations the GAL4/UAS system was used to express transgenes of interest in *Gustatory receptor 5a Gr5a-GAL4*. For each GAL4/UAS cross, transgenic controls were made by crossing the *w1118^{CS}* (gift from A. Simon, CS and *w1118* lines from the Benzer lab) to GAL4 or UAS flies, sex-matched to those used in the GAL4/UAS cross. PRC2 mutants were not in a *w1118^{CS}* background but were crossed to this line for all experiments shown here. The fly lines used for this paper are listed in Supplementary File 1.

Proboscis Extension Response:

Male flies were food deprived for 18-24 hours in a vial with a Kimwipe dampened with 2 mL of milliQ-filtered deionized (milliQ DI) water. Proboscis extension response (PER) was carried out

as described in (17). Extension responses were scored manually and when possible, blind observers were used.

Proboscis Immunofluorescence:

Probosces were dissected in 1xPBS and fixed in 4% PFA, mounted in FocusClear (CelExplorer) on coverslips. Cell bodies were imaged using a FV1200 Olympus confocal with a 20x objective. Cells were counted using Imaris Image analysis software.

Triglyceride Measurements:

Total triglycerides normalized to total protein were measured as described in (14). Briefly, two flies per biological replicate were homogenized in lysis buffer (140 mM NaCl, 50 mM Tris-HCl pH 7.4, 0.1% Triton-X) containing protease inhibitor cocktail (Thermo Scientific). Lysate extract was used to determine protein and triglyceride concentrations using Pierce BCA assay (Thermo Scientific, abs 562 nm) and Triglycerides LiquiColor test (Stanbio, abs 500 nm), respectively.

Calcium Imaging:

Male flies expressing *GCaMP6s-Brp-mCherry* (22) in the sweet sensing neurons were food deprived for 18-24 hours. Flies were imaged as in (14): briefly, animals were fixed to a custom-printed plastic slide with paraffin wax and the proboscis waxed to an extended position. Distal leg segments were removed to prevent tarsal interference with labellar stimulation. To image the SEZ, a sugarless artificial hemolymph solution filled the well surrounding the head.

Subsequently, the dorsal cuticle between the eyes was removed by microdissection to expose the brain. Each fly proboscis was tested with milliQ water before stimulating with 30% sucrose

dissolved in milliQ water. Stimulus (a piece of Kimwipe soaked in tastant and held with forceps) delivery to the proboscis was manual and timed to coincide with the 100th recording sample of each time series. Imaging was carried out using an upright confocal microscope (Olympus, FluoView 1200 BX61WI), a 20x water-immersion objective and laser excitation at 488 and 543 nm. Recordings were made at 4 Hz (512 x 512 pixels). Plane of interest was kept to the most ventral neuropil regions innervated by the sweet sensing neurons. Percent $\Delta F/F_0$ was calculated for regions of interest (ROIs) enclosing the *Gr64f*⁺ neuropil regions in the SEZ, one per hemisphere. To calculate $\% \Delta F/F_0$ the ROI intensity during the 10 frames preceding stimulus delivery was averaged to create the baseline intensity value F_0 . The baseline value was then subtracted from the ROI intensity value in each frame (F), and the result (ΔF) was then divided by the baseline and multiplied by 100 to produce $\% \Delta F/F_0$. The red channel $\% \Delta F/F_0$ was subtracted from the green channel $\% \Delta F/F_0$ for each frame to correct for movement. For all flies, there were no detectable taste responses in the red channel. Peak $\% \Delta F/F_0$ for each fly was determined by selecting the highest $\% \Delta F/F_0$ response after stimulation.

RNA Extraction and Quantitative RT-PCR:

For all RNA extractions used for qPCR, heads from 10-20 flies were dissected into Trizol (Ambion) and homogenized with plastic pestles. RNA was extracted by phenol chloroform (Ambion), and precipitated by isopropanol with Glycobluie Coprecipitant (Invitrogen). RNA pellet was washed as needed with 75% ethanol and subsequently eluted in nuclease free water and treated with DNase I, according to manufacturer's instructions (Turbo DNA-free DNA removal kit, Ambion). All steps were carried out in RNase free conditions, and RNA was stored at -80C until further processing.

Complementary DNA was synthesized by Superscript III (Invitrogen) reverse transcriptase with the addition of Ribolock RNase inhibitor (Thermo Fisher Scientific). qPCR reactions were carried out using Power SYBR Green PCR master mix (Applied Biosystems) based on manufacturer's instructions. Primers were added at a 2.5 μ M concentration. All reactions were run on a 96-well plate on the StepOnePlus Real-Time PCR System (Applied Biosystems) and quantifications were made relative to the reference gene Ribosomal protein 49 (Rp49). Primer sequences are listed in Supplementary File 1 and were tested for efficiency prior to the qPCR experiment. Relative fold changes in transcript abundance were determined with the Livak method using the Ribosomal protein 49 (Rp49) transcript as a housekeeping control.

Affinity purification of ribosome associated mRNA (TRAP):

300 heads (10,000 *Gr5a*⁺ cells) per biological replicate were collected using pre-chilled sieves in liquid nitrogen on dry ice. Frozen heads were then lysed as previously described (30). From the lysate total RNA was extracted by TRIzol LS Reagent (ThermoFisher scientific, 10296010) as input. The remainder of the lysate was incubated with Dynabeads protein G (ThermoFisher scientific, 10004D) to preclear samples for 2 hours and subsequently incubated with Dynabeads protein G coated with an anti-Flag antibody (Sigma, F1804). The lysate-beads mixture was incubated at 4°C with rotation for 2 hours, then. RNA was extracted from ribosomes bound to the beads by TRIzol Reagent (30).

Targeted DNA Adenine Methyltransferase Identification (TaDa):

For the *UAS-LT3-Dam::Pcl* construct, the coding region of the *Pcl* gene was amplified from the *pCRE-NDAM-Myc-DO69-Pcl* (gift from Bas Van Steensel, The Netherlands Cancer Institute)

with primers listed in Supplementary File 1 and assembled into the *UAS-LT3-DAM* plasmid (gift from Andrea Brand, University of Cambridge) using the NEBuilder® HiFi DNA Assembly kit based on manufacturer's instructions (NEB). Transgenic animals were validated by RT-PCR for correct insert. These lines were crossed to *Gr5a-GAL4;tubulin-GAL80^{ts}*. All animals were raised and maintained at 20 °C. Expression of *Dam::Pcl* and *Dam* were induced at 28 °C for 18-20 hours. For all experiments 300 heads of males and female flies were collected per replicate on dry ice by sieving. DNA was extracted from frozen heads following kit instructions (Invitrogen). For identification of methylated regions purified DNA was digested by DpnI followed by PCR purification of digested sequences. TaDa adaptors were ligated by T4 DNA ligase (NEB). Adapter ligated DNA was PCR amplified according to protocol (23), and subsequently purified. Purified DNA was digested with DpnII followed by sonication to yield fragments averaging 200-300bp. TaDa adaptors were removed from sonicated DNA by digestion. Sonicated DNA is used for library preparation (23).

Library Preparation for TRAP and TaDa:

RNA sequencing libraries were generated using the Ovation SoLo RNA-Seq System for *Drosophila* (Nugen, 0502-96). All reactions included integrated HL-dsDNase treatment (ArcticZymes, Cat. #70800-201). DNA sequencing libraries were generated using the Takara ThruPlex kit (cat #022818) using 3ng input and 10 cycles of PCR. All libraries were sequenced on the Illumina NextSeq platform (High-output kit v2 75 cycles) at the University of Michigan core facility.

High Throughput RNA-seq Analysis

Fastq files were assessed for quality using FastQC (56). Reads with a quality score below 30 were discarded. Sequencing reads were aligned by STAR (57) to dm6 genome downloaded from Ensemble, and gene counts were obtained by HTseq (58). Count files were used as input to call differential RNA abundance by DESeq2 (59). To determine the efficiency of the TRAP experiment pairwise comparisons were made between the *Gr5a+* specific IP fraction and the input, where the numerator is the IP and the denominator is the Input. For comparisons between dietary conditions, *deseq2* was only applied to the *Gr5a+* specific IP condition. All pairwise comparisons were made to the control diet of the corresponding genotypes, such that sugar diet three days and sugar diet seven days were compared to the age matched control diet group. In *Pcl* mutant experiments, the pairwise comparison was made between sugar diet and control diet within the age-matched *Pcl^{c429}* genotype group. A cutoff of $qval < 0.1$ was used to call differentially expressed genes. Skew in \log_2 fold changes was measured using the R package *Skewness* (e1071). The skew determination is based on the l_2fc for all genes detected, not just those that are significantly differentially expressed. Skewness is calculated from the second and third central moments of the observed distribution of \log_2 fold changes, using the formula $Skewness = m_3 / (m_2)^{3/2}$. Where $m_r = \sum_i (x_i - \mu)^r / n$, with r an integer, i indexing the data observations (genes in this case), and n the total number of observations (genes). In general, a negative skewness in a unimodal distribution indicates the presence of a long negative tail, whereas a positive skewness indicates a long positive tail. RNAseq data visualization was carried out in R studio using *ggplot2* and the following packages, *heatmap* (60), *Vennuler* (61), and *EnhancedVolcano* (62). To cluster columns and rows in *heatmap* "Ward.D" clustering was used.

High Throughput TaDa and CATaDa Analysis

Fastq files were assessed for quality using FastQC (56). Reads with a quality score below 30 were discarded. The damidseq_pipeline was used to align, extend, and generate log₂ ratio files (*Dam::Pcl/Dam*) in GATC resolution as described previously (63). In short, the pipeline uses Bowtie2 (64) to align reads to dm61-all-chromosomes of the dm6 genome downloaded from Ensemble, followed by read extension to 300 bp (or to the closest GATC, whichever is first). Bam output is used to generate the ratio file in bedgraph format. Bedgraph files were converted to bigwig and visualized in the UCSD genome browser. Correlation coefficients and PCA plot between biological replicates were computed by multibigwigSummary and plotCorrelation in deepTools (65). Fold Change traces for SD/CD of log₂(*Dam::Pcl/Dam*) were generated by calculating the mean coverage profile of all replicates for each condition and subsequently calculating fold change between the sugar diet and control diet condition with deepTools bigwigCompare (65). Peaks were identified from log₂(*Dam::Pcl/Dam*) ratio files using find_peaks (FDR<0.01) (63). To do this, the binding intensity thresholds are identified from the dataset, the dataset is then shuffled randomly, and the frequency of consecutive regions (i.e. GATC fragments or bins) with a score greater than the threshold is calculated. The FDR is the observed / expected for a number of consecutive fragments above a given threshold. Association of genes to peaks was made using the peaks2genes script (63) and dm6 genome annotations. Overlapping intervals or nearby intervals were merged into a single interval using MergeBED in Bedtools (66). Intervals common in all replicate peak files were identified by Multiple Intersect in Bedtools (66). DiffBind was used to determine differentially bound sites on peak files based on differences in read intensities (67). All differentially bound sites are presented in Supplementary File 1. For CATaDa experiments, all analyses were performed similar to those of

TaDa with the exceptions that 1) *Dam* only profiles were not normalized as ratios but shown as non-normalized binding profiles, 2) *Dam* only coverage plots were generated by converting bam files to bigwig files normalized to 1x dm6 genome, and 3) peaks were called using MACS2 call peaks on alignment files without building the shifting model with an of FDR<0.05 (68). To determine the proportion of genes that fit within the various chromatin domain subtypes, we first matched *Dam::Pcl/Dam* targets to coordinates identified by (26) and then determined their gene count in each chromatin subtype (observed) compared to the whole genome (expected). All chromatin tracks are visualized with the UCSD genome browser.

iPAGE Analysis

All Gene Ontology (GO) term enrichment analysis was performed using the iPAGE package (29), using gene-GO term associations extracted from the Flybase dmel 6.08 2015_05 release (69). For analysis of TRAP data, iPAGE was run in continuous mode, with log₂ fold changes divided into seven equally populated bins. For analysis of TaDa and TF regulatory targets, iPAGE was run in discrete mode, using the groups specified for each calculation. For all discrete calculations, independence filtering was deactivated due to the less informative available signal. All other iPAGE settings were left at their default values. All shown GO terms pass the significance tests for overall information described in (29); in addition, for each term, individual bins showing especially strong contributions (*p*-value such that a Benjamini-Hochberg FDR (70) calculated across that row, yields $q < 0.05$) are highlighted with a strong black box.

PREdictor

Identification of predicted PRE sites was performed exactly as described in (28), using the dm6 genome. As suggested in (28), we use a threshold confidence score of 0.8 to identify the PREs used in the present analysis. A complete list of predicted PREs, with accompanying confidence scores, is shown in Supplementary File 1. Enrichments of overlap between different PRE classes and *Pcl* occupancy locations were calculated by comparing the observed overlap frequency with the overlaps for 1,000 random shuffling of the binding/differential binding peak locations (calculated using bedtools 2.17.0 (66)).

Calculation of regulatory targets of transcription factors

To identify likely targets of each transcription factor of interest, we drew upon the transcription factor binding site calculations described in (28), in which the motif of each transcription factor was scanned along every base pair of the *D. melanogaster* dm6 genome using FIMO (71), and the base pair-wise binding results converted to robust z-scores. For each TF, we then considered its regulon to consist of all genes with at least one binding site with z-score above a TF-specific threshold within 2 kb upstream of the beginning of the gene. We identified TF-specific thresholds by manual inspection of a plot of the average expression changes between conditions vs. threshold, aiming to identify a point of maximum information content relative to noise (see Supplemental Figure 9 for the plots used to identify TF-specific z-score thresholds). Once the set of targets (regulon) for each factor was identified, we tested for significant enrichment or depletion of overlaps between the regulons using Fisher's exact test, reporting Benjamini-Hochberg false discovery rates (FDRs) (70). All calculated odds ratios were positive, indicating enriched overlaps between the regulons.

STRING network analysis

To develop a functional network between the candidate neural targets of Cad, Ptx1, Nub, GATAe and Scro, we uploaded genes categorized into neural/signaling GO terms based on DAVID functional annotations (72) to the STRING database (34), which includes both predicted physical and functional protein-protein interactions (34). Genes were clustered by their reported protein-protein interactions and corresponding confidence scores (34) and plotted in Cytoscape (v3.7.1). In this network edges do not represent direct protein-protein interaction but rather represent a functional interaction. For network file see Supplementary File 2.

3.6 Data Analysis and Statistics

Statistical tests, sample size, and p or q values are listed in each figure legend. For all PER experiments Kruskal-Wallis Dunn's multiple comparisons was used. Comparisons are either to control diets within genotypes or transgenic controls within dietary conditions. Data were evaluated for normality and appropriate statistical tests applied if data were not normally distributed, all the tests, biological samples, and the p and q values are listed in the figure legends and specific analysis under each methods session. Because the inferential value of a failure to reject the null hypothesis in frequentist statistical approaches is limited, for all RNA-seq expression datasets, we coupled our standard differential expression with a test for whether each gene could be flagged as 'significantly not different'. Defining a region of practical equivalence (ROPE) as a change of no more than 1.5-fold in either direction, we tested the null hypothesis of at least a 1.5-fold change for each gene, using the gene-wise estimates of the standard error in \log_2 fold change (reported by Deseq2) and the assumption that the actual \log_2 fold changes are normally distributed. Rejection of the null hypothesis in this test is taken as positive evidence

that the gene's expression is not changed substantially between the conditions of interest. Python code for the practical equivalence test can be found on Github as `calc_sig_unchanged.py`. All data in the figures are shown as Mean \pm SEM, **** $p < 0.0001$, *** $p < 0.001$, ** $p < 0.01$, * $p < 0.05$ unless otherwise indicated. Statistical analysis and tests are listed in every legend unless otherwise noted in the text.

Data availability: All data needed to evaluate the conclusions of the paper are present in the paper and/or the Supplementary Materials, additional resources and data are available upon request. All high throughput sequencing data files can be found on Gene Expression Omnibus GSE146245.

3.7 Supplemental Figures

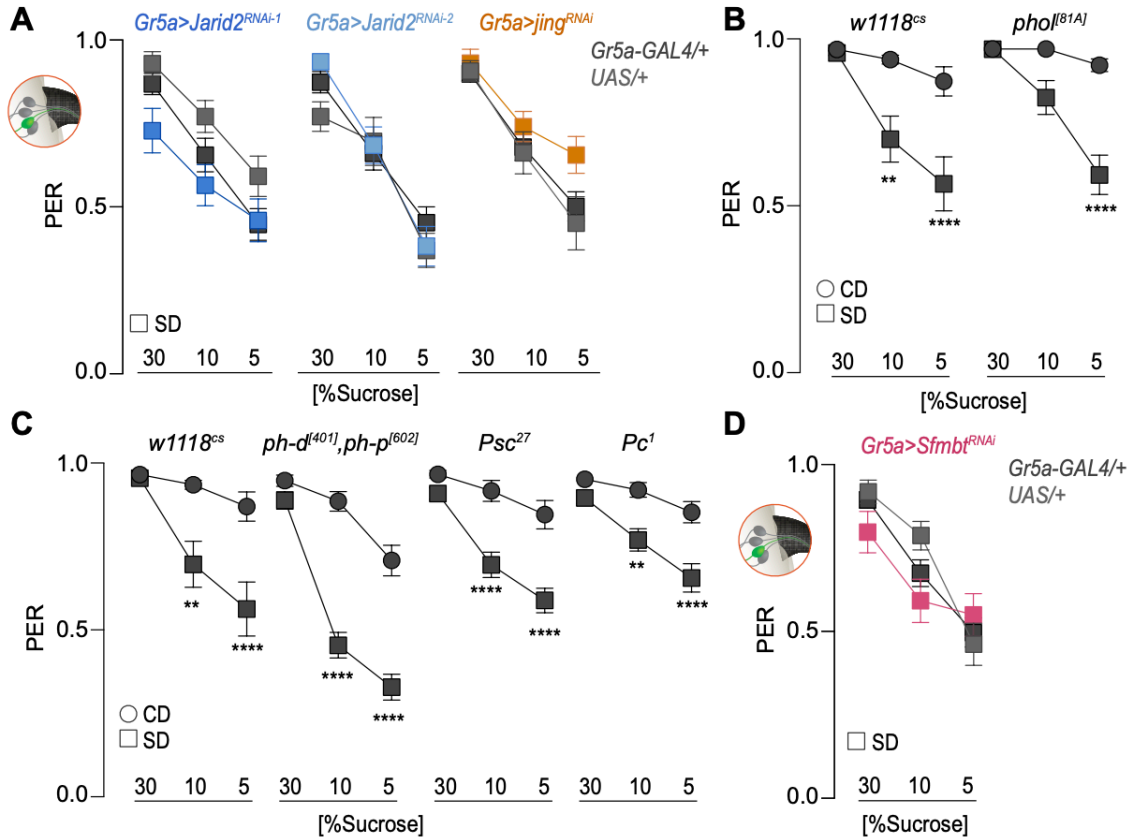


Figure 3.7 The PRC1 and PhoRC complex are not required for sugar diet mediated sweet taste defects

(A-D) Taste responses (y axis) to stimulation of the labellum with 30%, 10% and 5% sucrose (x axis) of age-matched males of (A) *Gr5a>Jarid2RNAi-1* (dark blue), *Gr5a>Jarid2RNAi-2* (light blue), and *Gr5a>jingRNAi* (orange) and parental transgenic control (gray, crossed to *w1118^{cs}*) flies on a sugar diet for 7 days. n = 25- 34, Kruskal-Wallis Dunn's multiple comparisons, comparisons to transgenic controls; (B) *w1118^{cs}*, and *phol^[81A]/+* flies on a control (circle) or sugar (square) diet for 7 days. n = 32-34, Kruskal-Wallis Dunn's multiple comparisons, comparisons to control diet within each genotype group; (C) *w1118^{cs}*, *ph-d^[401]/+*, *ph-p^[602]/+*, *Psc²⁷/+*, and *Pc¹/+* flies on a control (circle) or sugar (square) diet for 7 days. n = 30-42, Kruskal-Wallis Dunn's multiple comparisons, comparisons to control diet within each genotype group; (D) *Gr5a>SfmbtRNAi* (dark pink) and parental transgenic control (gray, crossed to *w1118^{cs}*) flies on a sugar diet for 7 days. n = 26-46, Kruskal-Wallis Dunn's multiple comparisons, comparisons to transgenic controls. All data shown as mean \pm SEM, ****p < 0.0001, ***p < 0.001, **p < 0.01, and *p < 0.05 for all panels unless indicated.

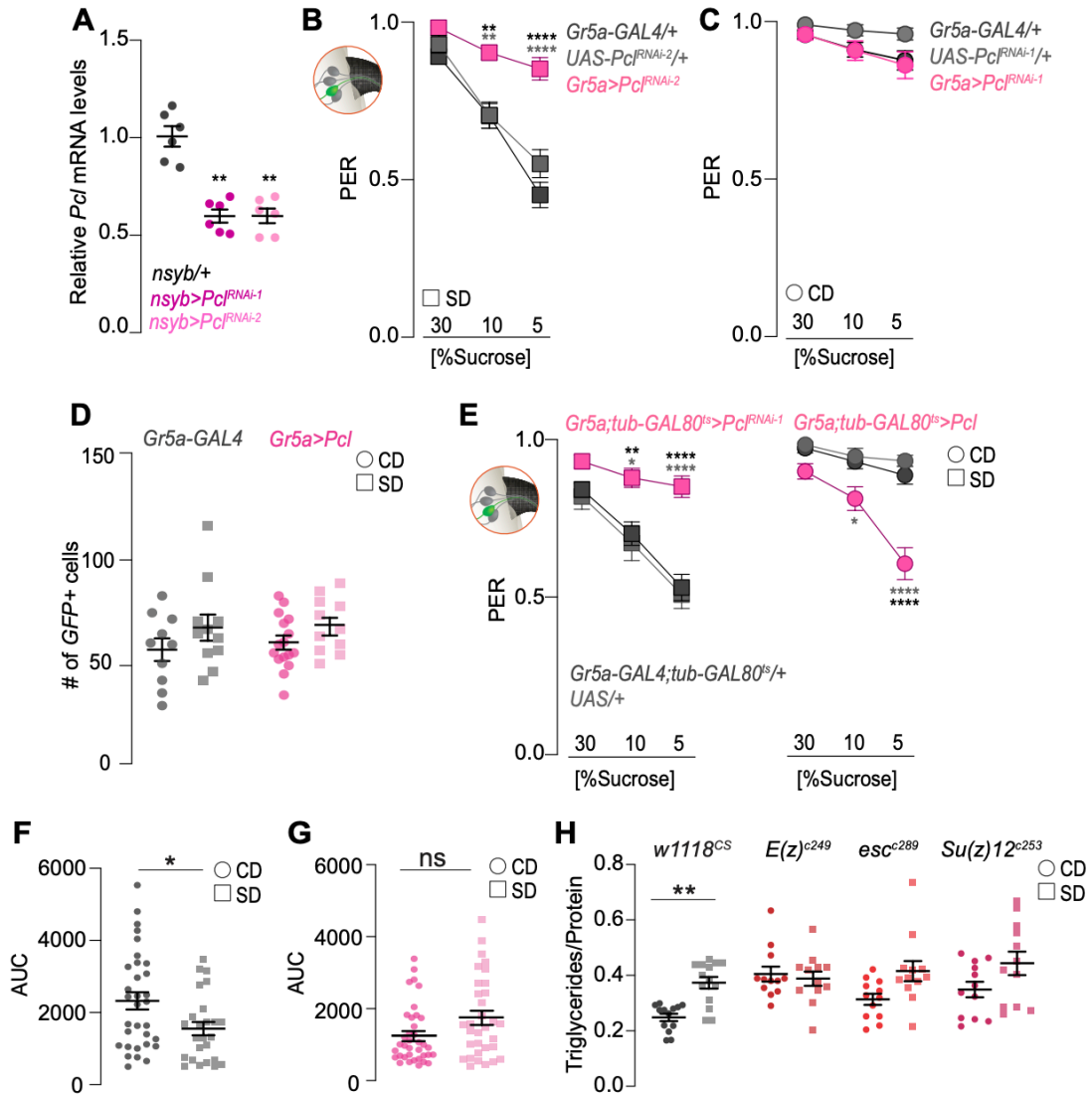


Figure 3.8 The effects of *Pcl* on sweet taste are independent of changes in cell number or development

(A) Fold change of *Pcl* mRNA levels in the heads of flies with and without pan-neuronal (*nsyb-GAL4*, gray) *Pcl* knockdown with two independent RNAi lines (plum, and pink respectively) measured by qPCR and normalized to the gene *Rp49*. n=6, Kruskal-Wallis Dunn's multiple comparisons, compared to transgenic control (crossed to *w1118^{CS}*). (B-C) Taste responses (y axis) to stimulation of the labellum with 30%, 10% and 5% sucrose (x axis) of age-matched males of (B) *Gr5a>Pcl^{RNAi-2}* and parental transgenic control (gray, crossed to *w1118^{CS}*) flies on a sugar diet for 7 days. n = 42-51, Kruskal-Wallis Dunn's multiple comparisons, comparisons to transgenic controls; (C) *Gr5a>Pcl^{RNAi-1}* and parental transgenic control (gray, crossed to *w1118^{CS}*) flies on a control diet for 7 days. n = 30-35, Kruskal-Wallis Dunn's multiple comparisons, comparisons to transgenic controls. (D) Quantification of the number

of sweet taste GFP-labeled cells in the labella of *Gr64f;CD8-GFP* flies crossed to *w1118^{cs}* (as control, gray) or *Gr64f;CD8-GFP>Pcl* (pink) on a control (circle) or sugar (square) diet for 7 days. n=5-16 probosces, no significance, Kruskal-Wallis Dunn's multiple comparisons, comparison to control diet of each genotype. **(E)** Taste responses (y axis) to stimulation of the labellum with 30%, 10% and 5% sucrose (x axis) of age-matched males of *Gr5a;tubulinGAL80ts>Pcl^{RNAi-1}*, *Gr5a;tubulin-GAL80ts>Pcl*, and parental transgenic control (gray, crossed to *w1118^{cs}*) flies on a control (circle, right) or sugar (square, left) diet for 7 days. n = 34-49, Kruskal-Wallis Dunn's multiple comparisons, comparisons to transgenic control. (F-G) Area under the curve (AUC) for averaged $\Delta F/F0$ calcium response traces to sucrose stimulation of the proboscis in age-matched male *Gr64f>GCaMP6s-Bruchpilot-mCherry* (gray) **(F)** and *Gr64f>GCaMP6s-Bruchpilot-mCherry;Pcl^{c429}* (pink) **(G)** flies fed a control (circle) or sugar (square) diet for 7 days, n = 28-46, Mann-Whitney test. **(H)** Triglyceride levels normalized to protein in age-matched male *w1118^{cs}*, *E(z)^{c249}*, *esc^{c289}*, and *Su(z)12^{c253}* fed a control (circle) or sugar (square) diet for 7 days. n=12-14, Kruskal-Wallis Dunn's multiple comparisons, comparisons to control diet of each genotype. All data shown as mean \pm SEM, ****p < 0.0001, ***p < 0.001, **p < 0.01, and *p < 0.05 for all panels unless indicated.

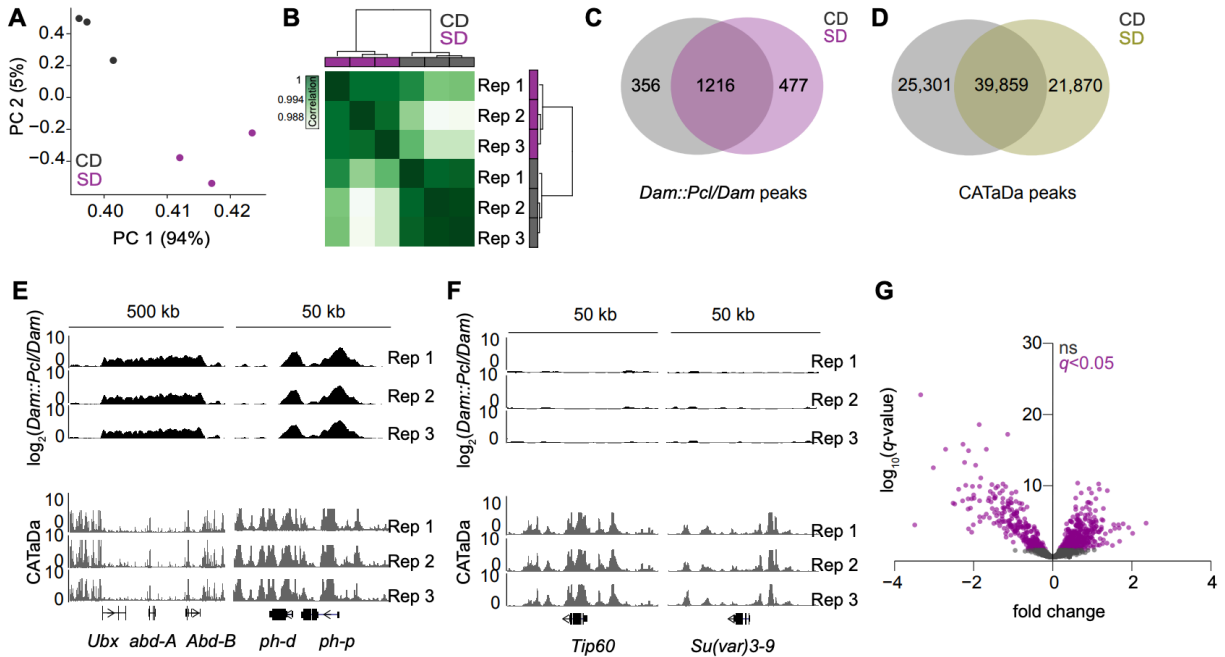


Figure 3.9 Chromatin occupancy and accessibility analysis of *Pcl* in the *Gr5a+* neurons.

(A) Principal component analysis of normalized $\log_2(Dam::Pcl/Dam)$ flies on a control (CD, gray) or sugar (SD, purple) diet. (B) The three biological replicates of $\log_2(Dam::Pcl/Dam)$ on a control (CD, gray) or sugar (SD, purple) diet are shown, with high Pearson correlation coefficients within each dietary condition, and low correlation coefficients between dietary conditions. Scale shows degree of correlation. (C-D) Left panel: overlap of $\log_2(Dam::Pcl/Dam)$ chromatin binding peaks between a control (gray) and sugar (purple) diet (find_peaks, $q < 0.01$). Right panel: overlap of CATaDa chromatin peaks between a control (gray) and sugar (yellow) diet (MACS2, $q < 0.05$). (E-F) $\log_2(Dam::Pcl/Dam)$ chromatin binding tracks at Ultrabithorax (*Ubx*), abdominal A (*abd-A*), Abdominal B (*Abd-B*), polyhomeotic distal (*ph-d*) and polyhomeotic proximal (*ph-p*) (Top panel, E), and Tat interactive protein 60 (*Tip60*) and Suppressor of variegation 3-9 (*Su(var)3-9*) (Top panel, F). Bottom panel: CATaDa chromatin coverage (chromatin accessibility) of the three biological replicates at the loci mentioned above. (G) Volcano plot showing the differential chromatin binding of *Dam::Pcl* on a sugar diet compared to a control diet, (Wald test, $q < 0.05$, purple), non-significant peaks are shown in black (ns).

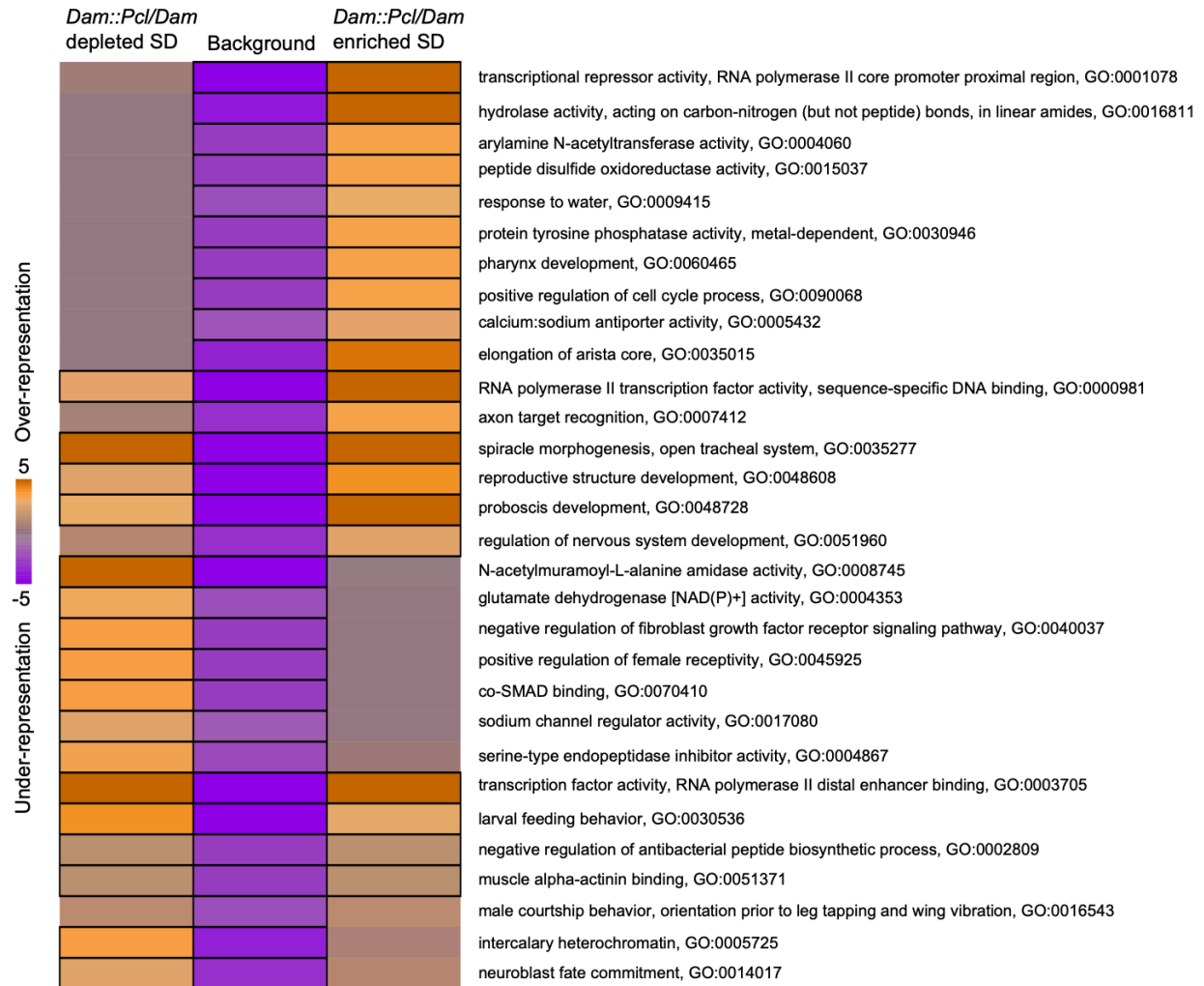


Figure 3.10 Pathway enrichment analysis of *Pcl* chromatin targets in the *Gr5a*+ neurons

iPAGE identification of pathways depleted (left) or enriched (right) compared to background gene list (middle) from the differentially bound chromatin peaks by *Dam::Pcl* flies on a sugar diet compared to a control diet. Scale represents over-representation (orange) or under-representation (purple) of genes within a specific bin for the corresponding GO term. Black outlined boxes represent $q < 0.05$.

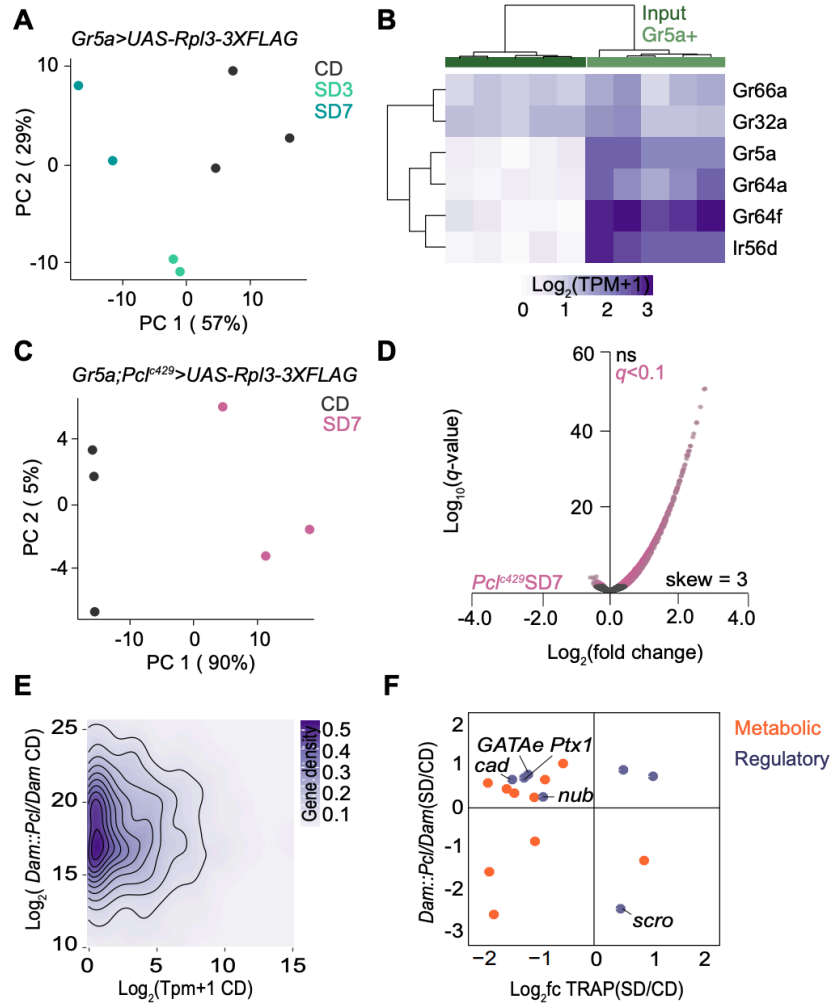


Figure 3.11 PRC2.1 mediates the transcriptional responses of the *Gr5a*+ neurons to diet.

(A) Principal component analysis of age-matched male *Gr5a>UAS-Rpl3-3XFLAG* flies on a control diet (CD, gray), sugar diet for three days (SD3, mint), and sugar diet for seven days (SD7, teal). (B) Normalized read counts for Gustatory receptor *Gr66a*, and Gustatory receptor *Gr32a* (both bitter), Gustatory receptor *Gr64f*, Gustatory receptor *Gr5a*, and Gustatory receptor *Gr64a* (all sweet) and the Ionotropic receptor 56d (fatty acid) from the input fraction (dark green box) and *Gr5a+* fraction (light green box). Both samples also include the dietary conditions (not specified in figure), hues of purple from light to dark represent low to high expression. (C) Principal component analysis of age-matched male *Gr5a;Pcl⁴²⁹>UAS-Rpl3-3XFLAG* flies on a control diet (CD, gray) and sugar diet for seven days (SD7, pink). (D) Volcano plot with changes in gene expression in the *Gr5a+* neurons of age matched male *Gr5a;Pcl⁴²⁹>UAS-Rpl3-3XFLAG* flies on a SD for 7 days (*Pcl⁴²⁹SD7*, pink) compared to the control diet condition in the same genotype (Wald test, $q < 0.1$, $n = 3$ replicates per condition (~10,000 *Gr5a+* cells per replicate).

(E) Normalized reads from TRAP for genes (x-axis) bound by *Pcl* and normalized to $\log_2(Dam::Pcl/Dam)$ reads at these genes (y-axis) on a control diet. Scale represents gene density (light to dark purple). **(F)** Fold change of *Dam::Pcl* chromatin binding for genes differentially bound on sugar diet compared to control diet (y-axis) ($q < 0.05$) and their respective differentially expressed \log_2 fold changes on a sugar diet compared to control diet (x-axis) ($q < 0.1$). Genes are shown as circles and colored based on GO term category, metabolism (orange) and regulatory (lavender).

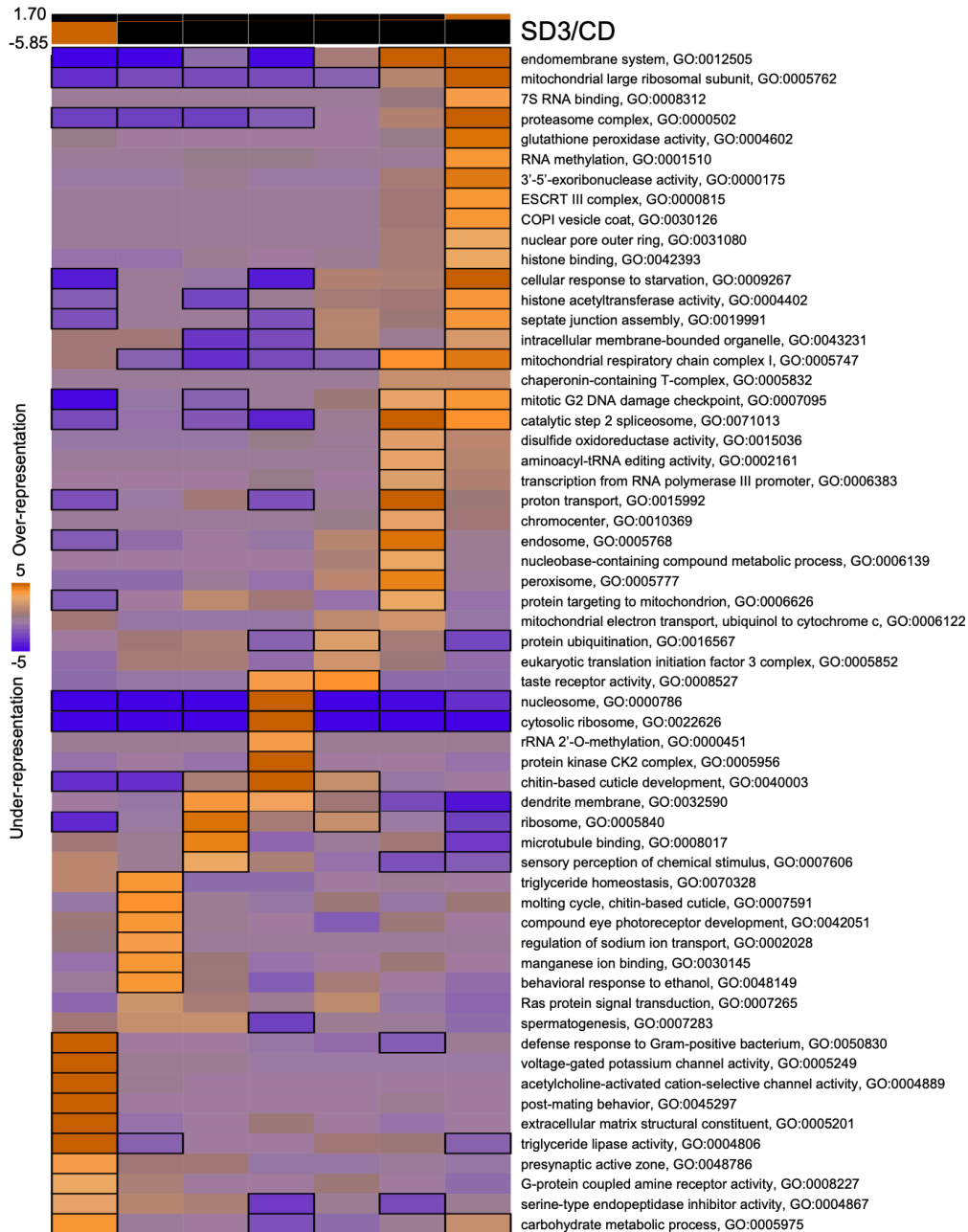


Figure 3.12 Pathway enrichment analysis of the *Gr5a*⁺ neurons in flies fed a sugar diet for 3 days.

iPAGE identification of pathways enriched in age-matched male *Gr5a*>*UAS-Rp13-3XFLAG* flies on a sugar diet for three days compared to a control diet. Bins (top) show the range of log₂ fold changes for genes within their corresponding GO terms. Scale represents over-representation (orange) or under-representation (purple) of genes within a specific bin for the corresponding GO term. Black outlined boxes represent $q < 0.05$.



Figure 3.13 . Pathway enrichment analysis of the *Gr5a*+ neurons in flies fed a high sugar diet for 7 days.

iPAGE identification of pathways enriched in age-matched male *Gr5a*>*UAS-Rp13-3XFLAG* flies on a sugar diet for seven days compared to a control diet. Bins (top) show the range of log₂ fold changes for genes within their corresponding GO terms. Scale represents over-representation (orange) or under-representation (purple) of genes within a specific bin for the corresponding GO term. Black outlined boxes represent $q < 0.05$.

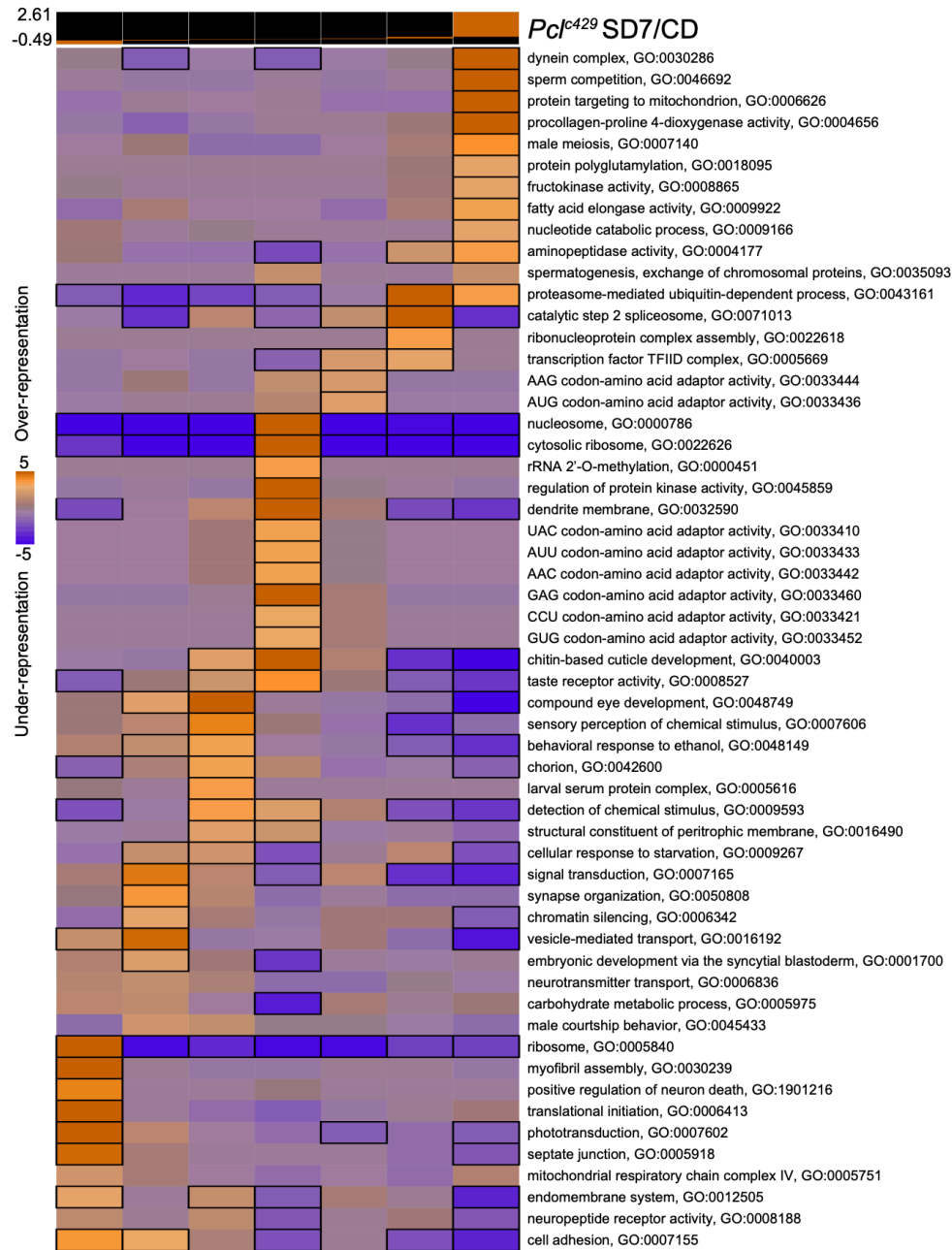


Figure 3.14 Pathway enrichment analysis of the *Gr5a*⁺ neurons in *Pcl^{c429}* mutant flies fed a high sugar diet for 7 days.

iPAGE identification of pathways enriched in age-matched male *Gr5a*;*Pcl^{c429}*>*UAS-Rpl3-3XFLAG* flies on a sugar diet for seven days compared to a control diet. Bins (top) show the range of log₂ fold changes for genes within their corresponding GO terms. Scale represents over-representation (orange) or underrepresentation (purple) of genes within a specific bin for the corresponding GO term. Black outlined boxes represent $q < 0.05$.

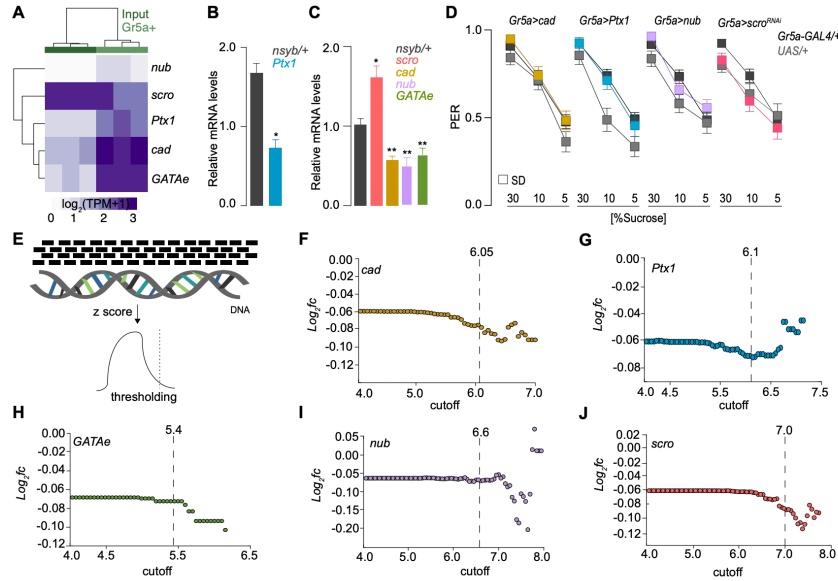


Figure 3.15 Identification of a transcriptional program mediated by PRC2.1 on a sugar diet.

(A) Normalized read counts for *scro*, *cad*, *nub*, *GATAe*, and *Ptx1* in the input fraction (dark green box) and the *Gr5a*+ fraction (light green box) from *Gr5a>UAS-Rpl3-3XFLAG* age-matched male flies on a control diet; hues of purple from light to dark show low to high expression. (B-C) Fold change of *Ptx1* (blue), *cad* (gold), *GATAe* (green), *nub* (lavender) and *scro* (coral) mRNA levels in the heads of flies with and without pan-neuronal (*nsyb*-*GAL4*) knockdown (*Ptx1*, *cad*, *GATAe*, and *nub*) or overexpression (*scro*) measured by qPCR and normalized to the gene *Rp49*. $n=3-5$, Kruskal-Wallis Dunn's multiple comparisons, compared to transgenic control (crossed to *w1118^{cs}*). (D) Taste responses (y axis) to stimulation of the labellum with 30%, 10% and 5% sucrose (x axis) of age-matched males of *Gr5a>cad* (gold), *Gr5a>Ptx1* (blue), *Gr5a>nub* (lavender), *Gr5a>scro^{RNAi}* (coral), and parental transgenic control (gray, crossed to *w1118^{cs}*) flies on a sugar diet for 7 days. $n = 31-51$, Kruskal-Wallis Dunn's multiple comparisons, comparisons to transgenic controls. (E) Schematic of how the targets of the 5 transcription factors in Figure 5 were identified: the DNA binding motifs for each transcription factor were scanned along every base pair of the *D. melanogaster* genome using FIMO, and the basepair-wise binding results converted to robust z-scores. (F-J) Threshold scores used to identify the regulons of each transcription factor. Y-axis represents the averaged log₂ fold change of the predicted targets based on the cutoff score, respectively.

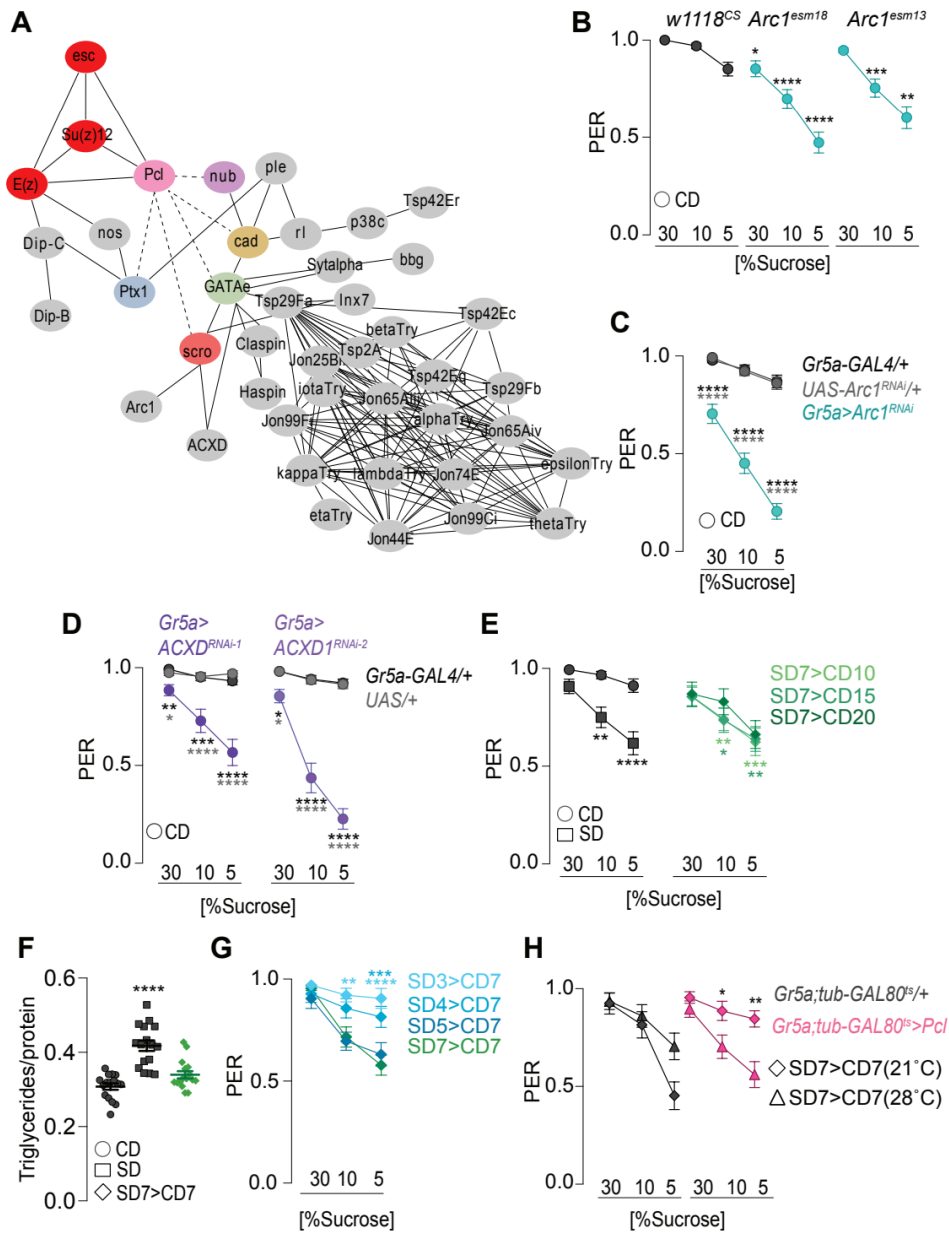


Figure 3.16 . PRC2.1 modulates the synaptic and neural properties of the *Gr5a+* neurons.

(A) Network created with STRING featuring PRC2.1, *cad*, *Ptx1*, *GATAe*, *nub*, *scro*, and their predicted targets from Figure 5C that are classified into the GO category neural/signaling. Nodes represent genes. Edges are functional protein-protein interactions, not direct interactions. Dashed edges are identified in this study. (B-E) Taste responses (y axis) to stimulation of the labellum with 30%, 10% and 5% sucrose (x axis) of age-matched males of (B) *w1118^{CS}*, *Arc1^{esm18}*, and *Arc1^{esm13}* flies on a control diet for 7 days. n = 38-45, Kruskal-Wallis Dunn's multiple comparisons, comparisons to transgenic controls; (C) *Gr5a>Arc1^{RNAi}* (turquoise), and parental transgenic control (gray, crossed to

w1118^{cs} flies on a control diet for 7 days. n = 28-47, Kruskal-Wallis Dunn's multiple comparisons, comparison to control diet; **(D)** *Gr5a>ACXD^{RNAi-1}* (dark purple) and *Gr5a>ACXD^{RNAi-2}* (light purple), and parental transgenic controls (gray, crossed to *w1118^{cs}*) flies on a control diet for 7 days. n = 28-47, Kruskal-Wallis Dunn's multiple comparisons, comparison to control diet; **(E)** *w1118^{cs}* fed a sugar diet for 7 days (SD7) and moved to the recovery diet (CD) for 10 (CD10, light green), 15 (CD15, medium green) and 20 (CD20, dark green) days. n = 21-32, Kruskal-Wallis Dunn's multiple comparisons, comparisons to control diet (circles, left panel). **(F)** Triglyceride levels normalized to protein in *w1118^{cs}* flies fed a control (circle) or sugar (square) diet for 14 days, and flies fed a SD7>CD7 reversal diet. n=16, two-way ANOVA with Sidak's multiple comparisons test, comparisons to control diet of each genotype. (G-H) Taste responses (y axis) to stimulation of the labellum with 30%, 10% and 5% sucrose (x axis) of age-matched males of **(G)** *w1118^{cs}* fed a sugar diet for 3 (SD3, light blue), 4 (SD4, medium blue), 5 (SD5, dark blue), and 7 days (SD7, green) and moved to the recovery diet for 7 days (CD7). n = 21-24, Kruskal-Wallis Dunn's multiple comparisons, comparisons to SD7>CD7 (green, diamonds); **(H)** *Gr5a;tubulin-GAL80ts>Pcl^{RNAi}* (pink), and parental transgenic control (gray, crossed to *w1118^{cs}*) flies on SD7>CD7 at 21H (diamonds), and SD7>CD7 at 28H during the recovery diet (triangles). n= 23-25, Kruskal-Wallis Dunn's multiple comparisons, comparisons within genotype to temperature controls (21H). All data are shown as mean \pm SEM, ****p < 0.0001, ***p < 0.001, **p < 0.01, and *p < 0.05 for all panels unless indicated.

3.8 References

1. K. D. Hall, A. Ayuketah, R. Brychta, H. Cai, T. Cassimatis, K. Y. Chen, S. T. Chung, E. Costa, A. Courville, V. Darcey, L. A. Fletcher, C. G. Forde, A. M. Gharib, J. Guo, R. Howard, P. V. Joseph, S. McGehee, R. Ouwerkerk, K. Raising, I. Rozga, M. Stagliano, M. Walter, P. J. Walter, S. Yang, M. Zhou, Ultra-Processed Diets Cause Excess Calorie Intake and Weight Gain: An Inpatient Randomized Controlled Trial of Ad Libitum Food Intake. *Cell Metabolism*. **30** (2019), pp. 67–77.e3.
2. G. K. Beauchamp, P. Jiang, Comparative biology of taste: Insights into mechanism and function. *Flavour*. **4**, 9 (2015).
3. M. Bertino, G. K. Beauchamp, K. Engelman, Long-term reduction in dietary sodium alters the taste of salt. *Am. J. Clin. Nutr.* **36**, 1134–1144 (1982).
4. J. E. Stewart, R. S. J. Keast, Recent fat intake modulates fat taste sensitivity in lean and overweight subjects. *Int. J. Obes.* **36**, 834–842 (2012).
5. P. M. Wise, L. Nattress, L. J. Flammer, G. K. Beauchamp, Reduced dietary intake of simple sugars alters perceived sweet taste intensity but not perceived pleasantness. *Am. J. Clin. Nutr.* **103**, 50–60 (2016).
6. D. Liu, N. Archer, K. Duesing, G. Hannan, R. Keast, Mechanism of fat taste perception: Association with diet and obesity. *Prog. Lipid Res.* **63**, 41–49 (2016).
7. A. Wittekind, K. Higgins, L. McGale, C. Schwartz, N. S. Stamataki, G. K. Beauchamp, A. Bonnema, P. Dussort, S. Gibson, C. de Graaf, J. C. G. Halford, C. F. M. Marsaux, R. D. Mattes, J. McLaughlin, D. J. Mela, S. Nicklaus, P. J. Rogers, I. A. Macdonald, A workshop

- on “Dietary Sweetness—Is It an Issue?” *Int. J. Obes.* **42**, 934 (2018).
8. A. Kaufman, E. Choo, A. Koh, R. Dando, Inflammation arising from obesity reduces taste bud abundance and inhibits renewal. *PLoS Biol.* **16**, e2001959 (2018).
 9. M. S. Weiss, A. Hajnal, K. Czaja, P. M. Di Lorenzo, Taste Responses in the Nucleus of the Solitary Tract of Awake Obese Rats Are Blunted Compared With Those in Lean Rats. *Front. Integr. Neurosci.* **13**, 35 (2019).
 10. A. B. Maliphol, D. J. Garth, K. F. Medler, Diet-induced obesity reduces the responsiveness of the peripheral taste receptor cells. *PLoS One.* **8**, e79403 (2013).
 11. Z. C. Ahart, L. E. Martin, B. R. Kemp, D. D. Banik, S. G. E. Roberts, A. M. Torregrossa, K. Medler, Differential effects of diet and weight on taste responses in diet-induced obese mice. *bioRxiv* (2019), p. 564211.
 12. L. P. McCluskey, L. He, G. Dong, R. Harris, Chronic exposure to liquid sucrose and dry sucrose diet have differential effects on peripheral taste responses in female rats. *Appetite.* **145**, 104499 (2020).
 13. F. Sartor, L. F. Donaldson, D. A. Markland, H. Loveday, M. J. Jackson, H.-P. Kubis, Taste perception and implicit attitude toward sweet related to body mass index and soft drink supplementation. *Appetite.* **57**, 237–246 (2011).
 14. C. E. May, A. Vaziri, Y. Q. Lin, O. Grushko, M. Khabiri, Q.-P. Wang, K. J. Holme, S. D. Pletcher, P. L. Freddolino, G. G. Neely, M. Dus, High Dietary Sugar Reshapes Sweet Taste to Promote Feeding Behavior in *Drosophila melanogaster*. *Cell Rep.* **27**, 1675–1685.e7 (2019).

15. C. E. May, J. Rosander, J. Gottfried, E. Dennis, M. Dus, Dietary sugar inhibits satiation by decreasing the central processing of sweet taste. *Elife*. **9** (2020), doi:10.7554/eLife.54530.
16. B. Schuettengruber, H.-M. Bourbon, L. Di Croce, G. Cavalli, Genome Regulation by Polycomb and Trithorax: 70 Years and Counting. *Cell*. **171**, 34–57 (2017).
17. T. Shiraiwa, J. R. Carlson, Proboscis extension response (PER) assay in *Drosophila*. *J. Vis. Exp.*, 193 (2007).
18. A. Laugesen, J. W. Højfeldt, K. Helin, Molecular Mechanisms Directing PRC2 Recruitment and H3K27 Methylation. *Mol. Cell*. **74**, 8–18 (2019).
19. W. Qi, K. Zhao, J. Gu, Y. Huang, Y. Wang, H. Zhang, M. Zhang, J. Zhang, Z. Yu, L. Li, L. Teng, S. Chuai, C. Zhang, M. Zhao, H. Chan, Z. Chen, D. Fang, Q. Fei, L. Feng, L. Feng, Y. Gao, H. Ge, X. Ge, G. Li, A. Lingel, Y. Lin, Y. Liu, F. Luo, M. Shi, L. Wang, Z. Wang, Y. Yu, J. Zeng, C. Zeng, L. Zhang, Q. Zhang, S. Zhou, C. Oyang, P. Atadja, E. Li, An allosteric PRC2 inhibitor targeting the H3K27me3 binding pocket of EED. *Nat. Chem. Biol.* **13**, 381–388 (2017).
20. S. Chyb, A. Dahanukar, A. Wickens, J. R. Carlson, *Drosophila* Gr5a encodes a taste receptor tuned to trehalose. *Proc. Natl. Acad. Sci. U. S. A.* **100 Suppl 2**, 14526–14530 (2003).
21. P. Masek, A. C. Keene, *Drosophila* fatty acid taste signals through the PLC pathway in sugar-sensing neurons. *PLoS Genet.* **9**, e1003710 (2013).
22. B. Kiragasi, J. Wondolowski, Y. Li, D. K. Dickman, A Presynaptic Glutamate Receptor Subunit Confers Robustness to Neurotransmission and Homeostatic Potentiation. *Cell Rep.*

- 19**, 2694–2706 (2017).
23. O. J. Marshall, T. D. Southall, S. W. Cheetham, A. H. Brand, Cell-type-specific profiling of protein–DNA interactions without cell isolation using targeted DamID with next-generation sequencing. *Nat. Protoc.* **11**, 1586–1598 (2016).
 24. B. van Steensel, S. Henikoff, Identification of in vivo DNA targets of chromatin proteins using tethered dam methyltransferase. *Nat. Biotechnol.* **18**, 424–428 (2000).
 25. G. N. Aughey, A. E. Gomez, J. Thomson, H. Yin, T. D. Southhall, CATaDa reveals global remodelling of chromatin accessibility during stem cell differentiation in vivo. *eLife*, 7 (2018).
 26. G. J. Filion, J. G. van Bemmelen, U. Braunschweig, W. Talhout, J. Kind, L. D. Ward, W. Brugman, I. J. de Castro, R. M. Kerkhoven, H. J. Bussemaker, B. van Steensel, Systematic protein location mapping reveals five principal chromatin types in Drosophila cells. *Cell.* **143**, 212–224 (2010).
 27. J. Müller, J. A. Kassis, Polycomb response elements and targeting of Polycomb group proteins in Drosophila. *Curr. Opin. Genet. Dev.* **16**, 476–484 (2006).
 28. M. Khabiri, P. L. Freddolino, Genome-wide Prediction of Potential Polycomb Response Elements and their Functions. *bioRxiv* (2019), p. 516500.
 29. H. Goodarzi, O. Elemento, S. Tavazoie, Revealing global regulatory perturbations across human cancers. *Mol. Cell.* **36**, 900–911 (2009).
 30. X. Chen, D. Dickman, Development of a tissue-specific ribosome profiling approach in

- Drosophila* enables genome-wide evaluation of translational adaptations. *PLoS Genet.* **13**, e1007117 (2017).
31. J. M. Tauber, E. B. Brown, Y. Li, M. E. Yurgel, P. Masek, A. C. Keene, A subset of sweet-sensing neurons identified by IR56d are necessary and sufficient for fatty acid taste. *PLoS Genet.* **13**, e1007059 (2017).
 32. J.-E. Ahn, Y. Chen, H. Amrein, Molecular basis of fatty acid taste in *Drosophila*. *Elife.* **6** (2017), doi:10.7554/eLife.30115.
 33. K. Scott, Gustatory Processing in *Drosophila melanogaster*. *Annu. Rev. Entomol.* **63**, 15–30 (2018).
 34. D. Szklarczyk, A. L. Gable, D. Lyon, A. Junge, S. Wyder, J. Huerta-Cepas, M. Simonovic, N. T. Doncheva, J. H. Morris, P. Bork, L. J. Jensen, C. von Mering, STRING v11: protein–protein association networks with increased coverage, supporting functional discovery in genome-wide experimental datasets. *Nucleic Acids Res.* **47**, D607–D613 (2019).
 35. K. Ueno, Y. Kidokoro, Adenylyl cyclase encoded by AC78C participates in sugar perception in *Drosophila melanogaster*. *Eur. J. Neurosci.* **28**, 1956–1966 (2008).
 36. J. Ashley, B. Cordy, D. Lucia, L. G. Fradkin, V. Budnik, T. Thomson, Retrovirus-like Gag Protein Arc1 Binds RNA and Traffics across Synaptic Boutons. *Cell.* **172**, 262–274.e11 (2018).
 37. R. T. Coleman, G. Struhl, Causal role for inheritance of H3K27me3 in maintaining the OFF state of a *Drosophila* HOX gene. *Science.* **356** (2017), doi:10.1126/science.aai8236.

38. F. Laprell, K. Finkl, J. Müller, Propagation of Polycomb-repressed chromatin requires sequence-specific recruitment to DNA. *Science*. **356**, 85–88 (2017).
39. J. Z. Parrish, K. Emoto, L. Y. Jan, Y. N. Jan, Polycomb genes interact with the tumor suppressor genes hippo and warts in the maintenance of *Drosophila* sensory neuron dendrites. *Genes Dev*. **21**, 956–972 (2007).
40. J. Z. Parrish, M. D. Kim, L. Y. Jan, Y. N. Jan, Genome-wide analyses identify transcription factors required for proper morphogenesis of *Drosophila* sensory neuron dendrites. *Genes Dev*. **20**, 820–835 (2006).
41. E. P. R. Iyer, S. C. Iyer, L. Sullivan, D. Wang, R. Meduri, L. L. Graybeal, D. N. Cox, Functional Genomic Analyses of Two Morphologically Distinct Classes of *Drosophila* Sensory Neurons: Post-Mitotic Roles of Transcription Factors in Dendritic Patterning. *PLoS ONE*. **8** (2013), p. e72434.
42. G. Vorbrüggen, R. Constien, O. Zilian, E. A. Wimmer, G. Dowe, H. Taubert, M. Noll, H. Jäckle, Embryonic expression and characterization of a Ptx1 homolog in *Drosophila*. *Mech. Dev*. **68**, 139–147 (1997).
43. S. Zaffran, G. Das, M. Frasch, The NK-2 homeobox gene scarecrow (*scro*) is expressed in pharynx, ventral nerve cord and brain of *Drosophila* embryos. *Mech. Dev*. **94**, 237–241 (2000).
44. M. M. Corty, J. Tam, W. B. Grueber, Dendritic diversification through transcription factor-mediated suppression of alternative morphologies. *Development*. **143**, 1351–1362 (2016).
45. C. J. Neumann, S. M. Cohen, Boundary formation in *Drosophila* wing: Notch activity

- attenuated by the POU protein Nubbin. *Science*. **281**, 409–413 (1998).
46. C. Q. Doe, Temporal Patterning in the Drosophila CNS. *Annu. Rev. Cell Dev. Biol.* **33**, 219–240 (2017).
 47. S. Bahrapour, C. Jonsson, S. Thor, Brain expansion promoted by polycomb-mediated anterior enhancement of a neural stem cell proliferation program. *PLoS Biol.* **17**, e3000163 (2019).
 48. F. Marasca, B. Bodega, V. Orlando, How Polycomb-Mediated Cell Memory Deals With a Changing Environment: Variations in PcG complexes and proteins assortment convey plasticity to epigenetic regulation as a response to environment. *Bioessays*. **40**, e1700137 (2018).
 49. A. Kolybaba, A.-K. Classen, Sensing cellular states—signaling to chromatin pathways targeting Polycomb and Trithorax group function. *Cell Tissue Res.* **356**, 477–493 (2014).
 50. A. Öst, A. Lempradl, E. Casas, M. Weigert, T. Tiko, M. Deniz, L. Pantano, U. Boenisch, P. M. Itskov, M. Stoeckius, M. Ruf, N. Rajewsky, G. Reuter, N. Iovino, C. Ribeiro, M. Alenius, S. Heyne, T. Vavouri, J. A. Pospisilik, Paternal diet defines offspring chromatin state and intergenerational obesity. *Cell*. **159**, 1352–1364 (2014).
 51. T. T.-H. Lu, S. Heyne, E. Dror, E. Casas, L. Leonhardt, T. Boenke, C.-H. Yang, Sagar, L. Arrigoni, K. Dalgaard, R. Teperino, L. Enders, M. Selvaraj, M. Ruf, S. J. Raja, H. Xie, U. Boenisch, S. H. Orkin, F. C. Lynn, B. G. Hoffman, D. Grün, T. Vavouri, A. M. Lempradl, J. A. Pospisilik, The Polycomb-Dependent Epigenome Controls β Cell Dysfunction, Dedifferentiation, and Diabetes. *Cell Metab.* **27**, 1294–1308.e7 (2018).

52. E. S. Deneris, O. Hobert, Maintenance of postmitotic neuronal cell identity. *Nat. Neurosci.* **17**, 899–907 (2014).
53. J. Z. Parrish, C. C. Kim, L. Tang, S. Bergquist, T. Wang, J. L. Derisi, L. Y. Jan, Y. N. Jan, G. W. Davis, Krüppel mediates the selective rebalancing of ion channel expression. *Neuron.* **82**, 537–544 (2014).
54. L. P. Musselman, R. P. Kühnlein, *Drosophila* as a model to study obesity and metabolic disease. *J. Exp. Biol.* **221** (2018), doi:10.1242/jeb.163881.
55. J. Na, L. P. Musselman, J. Pendse, T. J. Baranski, R. Bodmer, K. Ocorr, R. Cagan, A *Drosophila* Model of High Sugar Diet-Induced Cardiomyopathy. *PLoS Genetics.* **9** (2013), p. e1003175.
56. S. Andrews, Others, FastQC: a quality control tool for high throughput sequence data (2010).
57. A. Dobin, C. A. Davis, F. Schlesinger, J. Drenkow, C. Zaleski, S. Jha, P. Batut, M. Chaisson, T. R. Gingeras, STAR: ultrafast universal RNA-seq aligner. *Bioinformatics.* **29**, 15–21 (2013).
58. S. Anders, P. T. Pyl, W. Huber, HTSeq--a Python framework to work with high-throughput sequencing data. *Bioinformatics.* **31**, 166–169 (2015).
59. M. I. Love, W. Huber, S. Anders, Moderated estimation of fold change and dispersion for RNA-seq data with DESeq2. *Genome Biol.* **15**, 550 (2014).
60. R. Kolde, Pheatmap: pretty heatmaps. *R package version* (2012) (available at

https://scholar.google.ca/scholar?cluster=14492249782051319874,4384187057944727023,16059388166350612695,16769163128501098493,5741623497242498138&hl=en&as_sdt=0,5&scioldt=0,5).

61. L. Wilkinson, Exact and approximate area-proportional circular Venn and Euler diagrams. *IEEE Trans. Vis. Comput. Graph.* **18**, 321–331 (2012).
62. K. Blighe, EnhancedVolcano: Publication-ready volcano plots with enhanced colouring and labeling. R package version 1.2. 0 (2019).
63. O. J. Marshall, A. H. Brand, damidseq_pipeline: an automated pipeline for processing DamID sequencing datasets. *Bioinformatics.* **31**, 3371–3373 (2015).
64. B. Langmead, S. L. Salzberg, Fast gapped-read alignment with Bowtie 2. *Nat. Methods.* **9**, 357–359 (2012).
65. F. Ramírez, D. P. Ryan, B. Grüning, V. Bhardwaj, F. Kilpert, A. S. Richter, S. Heyne, F. Dündar, T. Manke, deepTools2: a next generation web server for deep-sequencing data analysis. *Nucleic Acids Res.* **44**, W160–5 (2016).
66. A. R. Quinlan, I. M. Hall, BEDTools: a flexible suite of utilities for comparing genomic features. *Bioinformatics.* **26**, 841–842 (2010).
67. R. Stark, G. Brown, Others, DiffBind: differential binding analysis of ChIP-Seq peak data. *R package version.* **100**, 4–3 (2011).
68. J. Feng, T. Liu, B. Qin, Y. Zhang, X. S. Liu, Identifying ChIP-seq enrichment using MACS. *Nat. Protoc.* **7**, 1728–1740 (2012).

69. J. Thurmond, J. L. Goodman, V. B. Strelets, H. Attrill, L. S. Gramates, S. J. Marygold, B. B. Matthews, G. Millburn, G. Antonazzo, V. Trovisco, T. C. Kaufman, B. R. Calvi, FlyBase Consortium, FlyBase 2.0: the next generation. *Nucleic Acids Res.* **47**, D759–D765 (2019).
70. Y. Benjamini, Y. Hochberg, Controlling the False Discovery Rate: A Practical and Powerful Approach to Multiple Testing. *J. R. Stat. Soc. Series B Stat. Methodol.* **57**, 289–300 (1995).
71. C. E. Grant, T. L. Bailey, W. S. Noble, FIMO: scanning for occurrences of a given motif. *Bioinformatics.* **27**, 1017–1018 (2011).
72. D. W. Huang, B. T. Sherman, R. A. Lempicki, Systematic and integrative analysis of large gene lists using DAVID Bioinformatics Resources. *Nature Protoc.* 2009; 4 (1): 44--57 (2008).

Chapter 4 A Nutrient Information Pathway Links Diet to Taste


4.1 Abstract

Diet composition affects the gustatory system in ways that alter taste perception, food intake, weight gain, and metabolic disease. Specifically, in *Drosophila melanogaster* flies, consumption of high dietary sugar reshapes the transcriptional properties of the sweet sensing cells to decrease sweet taste and promote obesity. Here, we show that in response to diet the transcriptional properties of the sweet sensing cells are specified through the interactions of the metabolic enzyme O-GlcNAc Transferase (OGT) and the Polycomb Repressive Complex 2.1 (PRC2.1). In the sweet sensing cells of animals fed high dietary sugar, OGT is required for the redistribution of PRC2.1 to the chromatin of the sweet gustatory neurons that reprograms the transcriptional properties of these cells. A subset of these sites is co-bound by OGT and PRC2.1. At these sites OGT is necessary for PRC2.1 mediated gene repression. Together, OGT and PRC2.1 repress a neurodevelopmental transcriptional hub that modulates the responsiveness of these cells to sweet stimuli and reduce sweet taste. Our findings reveal a nutrient information pathway that in response to diet, relays the nutrient information from the environment to epigenetic mechanisms that regulate neural plasticity and feeding behavior to promote metabolic disease.

4.2 Introduction

In the past decades, diet composition has been affected by the worldwide availability of energy-dense and highly processed foods. Consumption of high energy diets rich in salt, fat, and sugar impacts taste perception to influence food choice and promote food intake, leading to increased risks of obesity and metabolic disease (Bartoshuk et al., 2006; Bertino et al., 1982; May et al., 2019; May and Dus, 2021; Sartor et al., 2011; Stewart and Keast, 2012; Wise et al., 2016). More recent evidence suggests that changes in taste in response to high nutrient diets are associated with alterations in gene expression and epigenetic mechanisms (Vaziri et al., 2020; Wang et al., 2020), raising the question of how nutrient information is integrated into epigenetic and gene expression changes that alter taste and feeding behavior. This idea is supported by a number of recent studies that uncovered the role of diets in influencing metabolic-epigenetic mechanisms that underlie behaviors such as feeding and learning and memory (Bartke and Schneider, 2020; Haws et al., 2020; Janke et al., 2015; Vaziri and Dus, 2021). However, because of the complexity of the mammalian taste system and lack of targeted genetic tools, causal connections between nutrients, behavior, and epigenetics have yet to be established. Because of this, we know very little about how the nutrient environment regulates gene expression to alter taste perception. Therefore, research in genetically tractable model organisms could help shed light on this question and define evidence-based strategies to curb the prevalence of obesity and metabolic disease, which currently affects billions of people worldwide.

We previously found that a diet high in sugar lowers the responsiveness of the *Drosophila melanogaster* sweet sensory neurons to sweetness and lowers sweet taste perception. This decrease in sweet taste causes higher food intake and weight gain by impairing sensory-enhanced satiation processes (May et al., 2020, 2019). In *Drosophila*, nutrient-dependent decrease in sweet

taste perception is the result of the chromatin redistribution of the Polycomb Repressive Complex 2.1 (PRC2.1) that leads to persistent changes in the neural and metabolic properties of the sweet sensory  neurons (Vaziri et al., 2020). Here we utilize the relative simplicity of the fly's sensory system and advanced genetic tools to dissect the mechanisms by which the PRC2.1 complex detects the changes in the nutrient environment as a result of the high sugar diet to reprogram the sensory properties of the sweet taste neurons and promote weight gain, obesity, and metabolic disease. We report that the chromatin redistribution and transcriptional reprogramming of PRC2.1 in the high nutrient environment is dependent on the catalytic activity of the conserved metabolic enzyme O-GlcNAc Transferase (OGT). OGT is a single enzyme that links the nutrient environment to cellular physiology through the integration of multiple metabolic pathways into the Hexosamine Biosynthesis Pathway (HBP) (Hanover et al., 2010; Hardivillé and Hart, 2014). In the high nutrient environment, OGT specifies a nutrient information pathway by defining the chromatin occupancy of PRC2.1 to a subset of genes that form a neurodevelopmental transcriptional hub that sets the neural, synaptic, and metabolic properties of the sweet sensory neurons. This nutrient information pathway allows the sensory neurons to detect a chronic change in the nutrient environment in order to recalibrate their responses. Together, our findings suggest that metabolic-epigenetic mechanisms activated by diet lead to disruptions in feeding behavior increasing the risk for obesity and metabolic disease.

4.3 Results

OGT modulates sweet taste in response to diet

Drosophila melanogaster flies experience sweet taste deficits when fed high dietary sugar. This deficit is caused by lower responses from the sweet sensory neurons when stimulated

with sugar (May et al., 2019; Vaziri et al., 2020). Decreased responsiveness of the sweet sensory neurons is established by the persistent phenotypic and molecular reprogramming of these neurons by the epigenetic regulator PRC2.1 (Vaziri et al., 2020). On a sugar diet the PRC2.1 complex alters the neural, metabolic, and transcriptional properties of the sweet sensing neurons by altering a developmental transcriptional hub important for sweet sensing. Because sweet taste plays an important role in regulating eating behavior in both invertebrates and mammalian models and recent data that suggest diet affects a variety of behaviors through the nutrient regulation of epigenetic processes (Dus and Sarangi, n.d.; Vaziri and Dus, 2021), we set out to determine the metabolic link between diet and epigenetic reprogramming by PRC2.1 that promotes sweet taste disruption. We previously reported that the levels of the first committed HBP metabolite glucosamine-6-phosphate are increased in flies fed high sugar diets (May et al., 2019; Wilinski et al., 2019). Additionally, the effects of high dietary sugar on sweet taste and food intake can be rescued by the downregulation of the metabolic enzyme OGT (also known as super sex combs in *Drosophila*) (May et al. 2019). OGT adds the O-GlcNAc moiety from UDP-GlcNAc to the serine and threonine residues of proteins to modify their activity (Hanover et al., 2010; Hardivillé and Hart, 2014; Wells et al., 2001). Furthermore, many of OGT's downstream targets are epigenetic modifiers and transcriptional regulators such as TET proteins, Polycomb Group Proteins, and transcription factors such as the cyclic AMP response-element binding protein (CREB) (Altarejos and Montminy, 2011; Butler et al., 2019; Chu et al., 2014; Decourcelle et al., 2019; Olivier-Van Stichelen et al., 2017; Olivier-Van Stichelen and Hanover, 2015; Yang and Qian, 2017). We thus hypothesized that sweet taste defects in the high sugar diet environment are dependent on OGT. To test this hypothesis, we first knocked down *OGT* by RNAi specifically in the sweet taste neurons expressing the *Gustatory receptor 5a* gene with the

Gr5a-GAL4 transgene in flies fed high sugar diets. To test the flies' taste responses we stimulated the labellum (where the dendrites and cell bodies the taste neurons are located) (Figure 1A, left) with low (5%), medium (10%), and high (30%) concentrations of sucrose using the proboscis extension response (PER). PER is a behavioral measure of taste determined by the amount of proboscis extension (0 = no extension, 0.5 = partial extension, and 1 = full extension) (Figure 1A, right). While the transgenic control flies on a sugar diet showed a marked decrease in PER to sucrose, the *OGT^{RNAi}* flies showed wild-type responses (Figure 1B) comparable to our previous experiments using the *Gustatory receptor Gr64f* transgene (May et al., 2019). Because OGT regulates its targets through post-translational modifications (Hanover et al., 2010), we reasoned that its overexpression may be sufficient to induce taste defects in the absence of the sugar diet environment. Overexpression of *OGT* specifically in the *Gr5a+* neurons led to sweet taste deficits in flies fed a control diet compared to the transgenic controls (Figure 1C). To account for the possible developmental effects of *Gr5a>OGT* on sweet taste we used the temperature-sensitive *tubulin-GAL80ts* transgene to limit the expression of *Gr5a;tubulin-GAL80ts>OGT* to adult flies. Moving the flies to the nonpermissive temperature and the respective diet 4 days after eclosion resulted in the same effects on sweet taste as using the *Gr5a-GAL4* alone (Figure S1A). Thus *OGT* is required for the sensory changes that occur in the high sugar diet environment.

To validate the role of *OGT* in sugar diet mediated sweet taste defects using pharmacology, we supplemented the control and sugar diet with OSMI-1, a small molecule inhibitor of OGT. While animals on a sugar diet supplemented with vehicle (10% dimethyl sulfoxide (DMSO)) had dulled sweet taste, the animals fed a sugar diet supplemented with OSMI-1 retained their normal sweet taste responses in a dose-dependent manner (Figure S1C).

Given that the C-terminus catalytic domain of OGT is required for optimal substrate modification and OGT activity (Kreppel et al., 1997; Lubas and Hanover, 2000) (Figure 1A), we tested the responses of flies that harbor 2 independent mutations *OGT^{H567}* and *OGT^{K872}* in OGT's catalytic domain that led to a 50-60% reduction in OGT catalytic activity (Mariappa et al., 2015). Flies that were heterozygous for this mutation and fed a control diet showed PER responses similar to *w¹¹¹⁸^{CS}* flies on a control diet (Figure 1D, circle), suggesting that these mutations did not disrupt baseline OGT activity. However, flies that were heterozygous for this mutation on a sugar diet showed a decrease in PER comparable to *w¹¹¹⁸^{CS}* control animals on a sugar diet (Figure 1D, square), suggesting that the catalytic domain of OGT is necessary for diet dependent sweet taste deficits. Together, these findings establish that *OGT* is required cell-autonomously in the *Gr5a*+ neurons to mediate the effects of a high sugar diet on sweet taste.

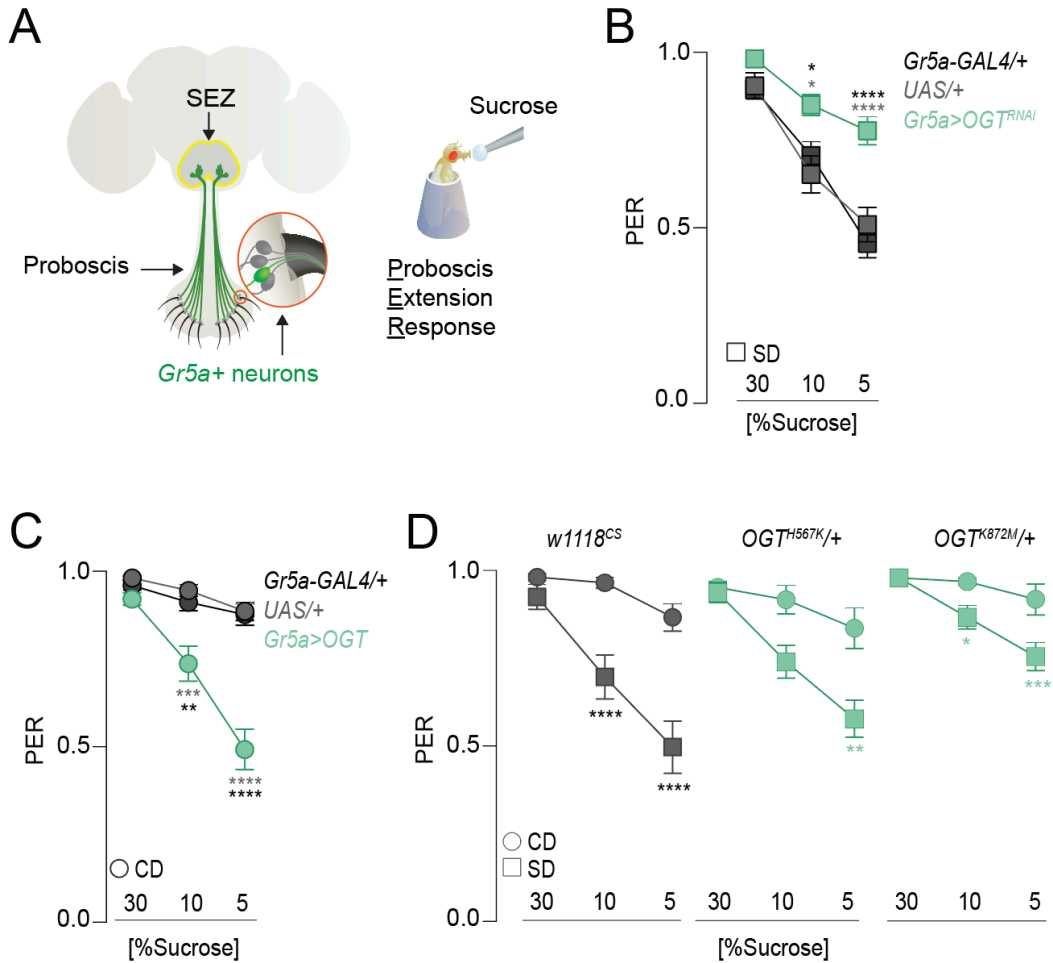


Figure 4.1 OGT modulates sweet taste in response to diet

(A) Schematic of sweet taste neurons in *Drosophila melanogaster* (right). Schematic of Proboscis Extension Response (PER). (B-D) Taste responses (y axis) to stimulation of the labellum with 30, 10, and 5% sucrose (x axis) of age-matched male (B) *Gr5a>OGT^{RNAi}* (green) and transgenic controls (shades of gray) on a sugar diet, n= 51-63, Kruskal-Wallis Dunn's multiple comparisons, comparisons to transgenic controls. (C) *Gr5a>OGT* (green) and transgenic controls (shades of gray) on a control diet, n= 36-48, Kruskal-Wallis Dunn's multiple comparisons, comparisons to transgenic controls. (D) *w1118^{CS}*, *OGT^{H567K/+}*, *OGT^{K872M/+}* flies on a control and sugar diet, n= 29-33, Kruskal-Wallis Dunn's multiple comparisons, comparisons to the control diet of the same genotype. In all panels, flies were on a control (circle) or sugar (square) diet for 7 days. Data are shown as means \pm SEM. ****P < 0.0001, ***P < 0.001, **P < 0.01, and *P < 0.05.

OGT and PRC2.1 together modulate sweet taste in response to diet

OGT and the PRC2.1 complex are both required for dulled sweet taste responses on a high sugar diet (Figure 1) (May et al., 2019; Vaziri et al., 2020). A number of studies suggest that OGT interacts with numerous members of the Polycomb Group Proteins (PcG) and plays a role in PcG repression (Chu et al., 2014; Decourcelle et al., 2019; Gambetta et al., 2009; Gambetta and Müller, 2014; Maury et al., 2015). Moreover, because of the unique role that OGT plays in integrating multiple metabolic pathways (carbohydrates, amino-acids, fatty acids, and nucleotides metabolisms) it is considered a nutritional sensor that can relay the effects of diet, obesity, and other metabolic states to cellular physiology (Baldini et al., 2016; Guinez et al., 2011; Olivier-Van Stichelen et al., 2012). To this end, we hypothesized that OGT mediates the effects of high nutrient diets on sweet taste through the actions of the PRC2.1 complex (Figure 2A). To test this hypothesis, we first generated transgenic flies that overexpress *OGT* specifically in the *Gr5a*⁺ cells and harbor mutations in the PRC2.1 member Polycomb like (*Pcl*) (Figure 2A, purple arrow). We found that *Gr5a*>*OGT*;*Pcl*^{c429} flies had taste responses similar to the transgenic control on a control diet and the *Pcl*^{c429} background control on a sugar diet (Figure 2B). However, background control *Gr5a*>*OGT* flies showed a marked decrease in PER comparable to the transgenic control on a sugar diet (Figure 2B). Because overexpression of *OGT* in the presence of *Pcl* mutations prevents a decrease in sweet taste, these results suggest that *OGT* mediated taste defects are *Pcl* dependent. To test whether the effects of OGT can be expanded to the PRC2 complex as a whole, we tested the sweet taste responses of *Gr5a*>*OGT* flies on a control diet supplemented with the PRC2 inhibitor EEDi (Figure 2A). While *Gr5a*>*OGT* animals fed a control diet supplemented with vehicle (10% DMSO) showed a marked decrease in sweet taste compared to the transgenic controls (Figure 2C, left), *Gr5a*>*OGT*

animals fed a control diet supplemented with EEDi had high responses similar to the transgenic controls (Figure 2C, right). Collectively, these experiments place *OGT* and *PRC2.1* in the same genetic pathway and indicate that the effects of high nutrient environments on sweet taste is through the actions of *OGT* and *PRC2.1*.

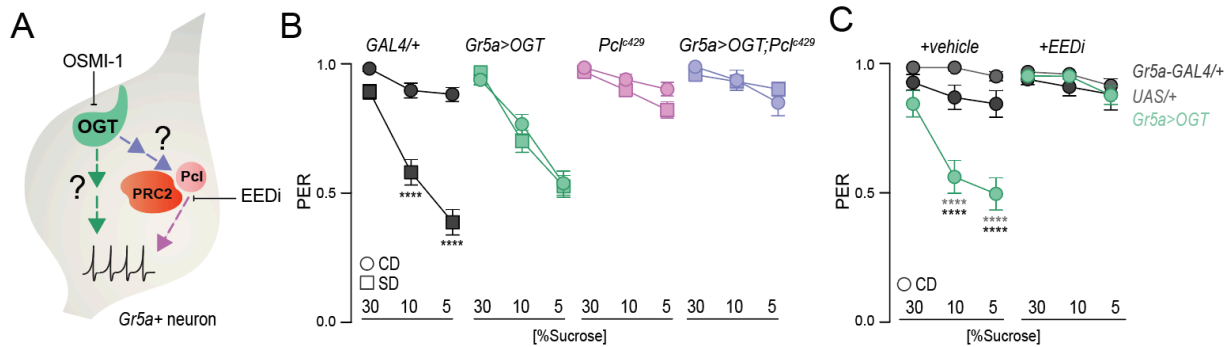


Figure 4.2 OGT modulates sweet taste through the PRC2.1 complex

(A) Model of OGT-PRC2.1 interactions in response to a sugar diet. (B-C) Taste responses (y axis) to stimulation of the labellum with 30, 10, and 5% sucrose (x axis) of age-matched male (B) *Gr5a>OGT;Pcl^{c429}* (purple), *Gr5a>OGT* (green), *Pcl^{c429}/+* (pink), and the transgenic control (gray) on a control and sugar diet, n= 20-37, Kruskal-Wallis Dunn's multiple comparisons, comparisons to the control diet of each genotype. (C) *Gr5a>OGT* (green) and transgenic controls (shades of gray) on a control diet supplemented with vehicle (10% DMSO) or control diet supplemented with 8 μ M EEDi, n=20-22, Kruskal-Wallis Dunn's multiple comparisons, comparisons to transgenic controls. In all panels, flies were on a control (circle) or sugar (square) diet for 7 days. Data are shown as means \pm SEM. ****P < 0.0001, ***P < 0.001, **P < 0.01, and *P < 0.05.

The diet dependent chromatin redistribution of *Pcl* is dependent on *OGT*

Our previous work shows that in the high sugar environment, the chromatin occupancy of PRC2.1 in the *Gr5a+* neurons was redistributed at loci that encode for transcription factors involved in neuronal processes and development resulting in lowered sweet taste (Vaziri et al., 2020). To test the hypothesis that diet mediated *Pcl* chromatin redistribution is dependent on *OGT* we performed targeted DNA adenine methyltransferase identification (Dam-ID or TaDa) for *Pcl* in the *Gr5a+* sensory neurons (Figure 3A) (Marshall et al., 2016; van Steensel and Henikoff, 2000). *Dam::Pcl* or *Dam* only flies were fed either a control (CD+OSMI-1) or sugar diet (SD+OSMI) supplemented with the OGT inhibitor OSMI-1 (Figure 3A). We first confirmed that overexpression of *Pcl* in the *Gr5a+* cells of CD+OSMI-1 flies prevented a decrease in sweet taste compared to transgenic controls and vehicle fed animals (Figure S2A). Comparison of the *Dam::Pcl* signal normalized to *Dam* alone ($\log_2(Dam::Pcl/Dam)$) showed that while the CD+OSMI-1 and SD+OSMI-1 groups clustered based on diet, the variability between dietary conditions was less than 2% (Figure S2B). Peak analysis of *Pcl* peaks revealed an 85% overlap between the CD+OSMI-1 and SD+OSMI-1 peaks (Figure S2C). To identify how OSMI-1 affects *Pcl* peaks, we compared the total number of peaks and the identity of the peaks in *Dam::Pcl* animals with (*Pcl*+OSMI-1) or without (*Pcl*) OSMI-1. Overall, we found that the total number of peaks were the same (~1800). Of these, 80% were shared between *Pcl*+OSMI-1 and *Pcl* (Figure 3B). We noticed that 20% of *Pcl* peaks were not present in the *Pcl*+OSMI-1. These peaks were mostly associated with regulatory Gene Ontology (GO) terms. Interestingly, we also observed 304 new peaks in the *Pcl*+OSMI-1 condition (Figure 3B). These peaks were also associated with regulatory GO terms. These results suggest that supplementation of OSMI-1 to the diet of

animals does not affect the overall peak number or peak identity, thus differences caused by OSMI-1 could be attributed to the amount of *Pcl* binding.

To address the hypothesis that *OGT* affects the redistribution of *Pcl* at its targets, we compared the amount of *Pcl* binding at genes that showed an increase in *Pcl* on a SD (group 1) to genes with decreased *Pcl* on a SD (group 2). While *Dam::Pcl* flies fed a CD and SD without OSMI-1 showed an increase in *Pcl* binding at group 1 genes and decrease in *Pcl* binding at group 2 genes (Figure 3C, left), *Dam::Pcl* flies with OSMI-1 did not show any changes at these two groups of regions (Figure 3C, right), suggesting that OSMI-1 prevents *Pcl* redistribution. We previously reported that in the sugar diet environment *Pcl* binding increased at Polycomb Response Elements (PREs) cis-regulatory sequences to which PcG proteins bind in *D. melanogaster* (Vaziri et al., 2020). To ask whether OSMI-1 affects *Pcl* binding at PREs we compared *Pcl* occupancy at PREs in flies on a CD+OSMI-1 and SD+OSMI-1 and found that the increase in *Pcl* at PREs was completely abolished (Figure 3D). In the high sugar diet environment, chromatin accessibility is decreased at *Pcl* peaks (Figure 3E, left). Interestingly, this decrease in chromatin accessibility is prevented in the SD+OSMI-1 animals (Figure 3E, right). Together, we find that in the high sugar environment *Pcl* chromatin redistribution and accessibility is dependent on *OGT*. This *OGT* chromatin dependency could in turn specify the targeting of *Pcl* to a subset of genes that impact the neural properties of the sensory neurons.

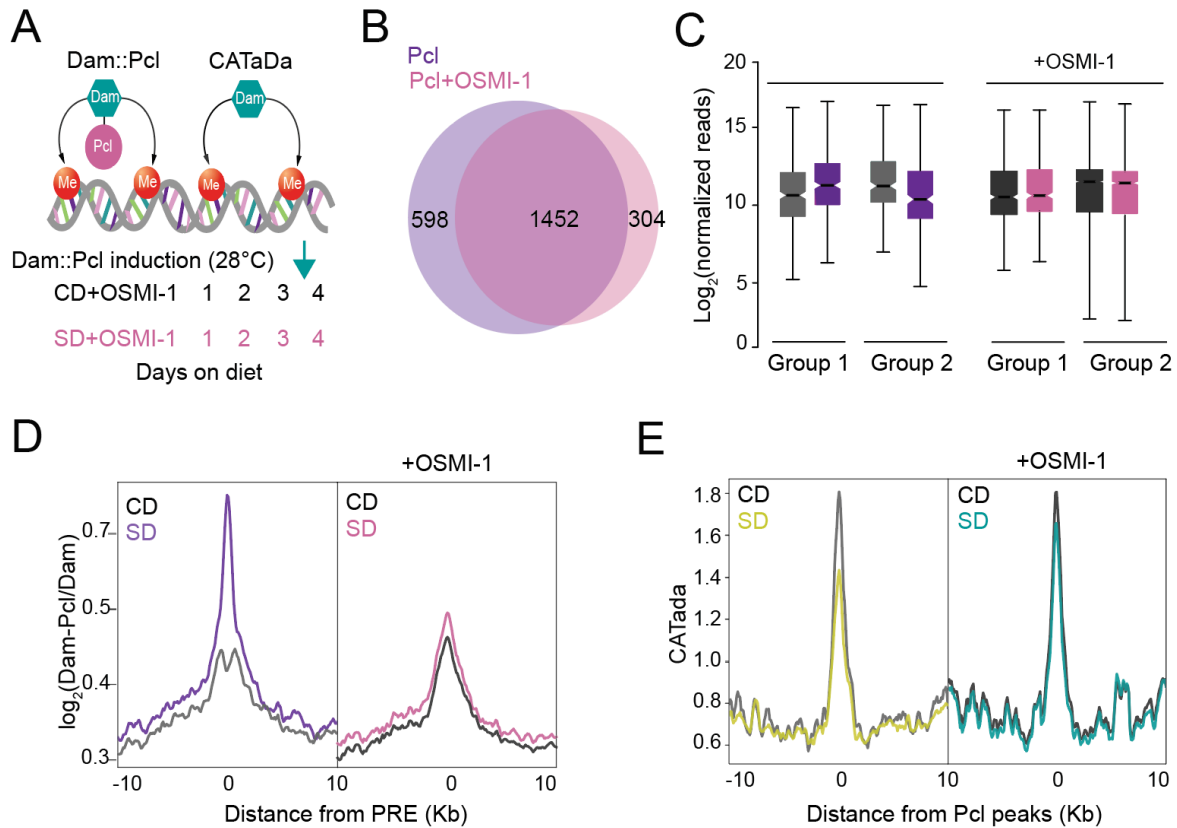


Figure 4.3 The diet dependent chromatin redistribution of *Pcl* is dependent on OGT

(A) Schematic of Targeted Dam-ID (TaDa) of *Dam::Pcl* and *Dam* (CATaDa) and the induction paradigm when OSMI-1 is added to the control and sugar diets. (B) Overlap of $\log_2(Dam::Pcl/Dam)$ chromatin binding peaks with (pink) and without (purple) OSMI-1 (find_peaks, $q < 0.01$). (C) The median and variance of $\log_2(Dam::Pcl/Dam)$ reads with (pink) and without (purple) OSMI-1 for genes bound on a control and sugar diet. Genes are grouped into higher (group 1) or lower (group 2) *Pcl* binding on a sugar diet. (D) Average $\log_2(Dam::Pcl/Dam)$ signal on a control and sugar diet supplemented with (right) or without (left) OSMI-1 centered at PREs. (E) Average CATaDa signal on a control and sugar diet supplemented with (teal) or without (yellow) OSMI-1 centered at *Pcl* peaks.

OGT specifies the chromatin targeting of *Pcl* in response to diet

Our findings suggest that OGT regulates PRC2.1 chromatin distribution in response to high sugar diets leading to a decrease in sweet taste. Because of evidence that points to the presence of OGT in a stable complex with a number of chromatin proteins such as PRC2 (Gao et al., 2018; Vella et al., 2013), we hypothesized that *OGT* is present at *Pcl* binding sites. To test this hypothesis, we first measured the chromatin occupancy of *OGT* in the *Gr5a*⁺ neurons using TaDa (Figure 4A) (Marshall et al., 2016; van Steensel and Henikoff, 2000). To do this, we generated *Dam::OGT (UAS-LT3-Dam::OGT)* transgenic flies which were compared to the *Dam* flies (*UAS-LT3-Dam*) to control for background methylation levels by the freely diffusing *Dam* protein. The control *Dam* transgenic flies are also used as a measure of chromatin accessibility *in vivo* (CATaDa) (Figure 4A) (Aughey et al., 2018). Normalized *Dam::OGT* replicates clustered together by diet (Figure S3A) and the chromatin accessibility profile of *Dam* at the *Gr5a* sweet taste receptor gene promoter was high, while at the bitter taste receptor promoters—which is only expressed in bitter cells, closely located near the sweet cells—was low (Figure S3B), suggesting that the transgenes were appropriately targeted to the sweet taste neurons. Identification of *Dam::OGT* peaks revealed that *OGT* binding was enriched for the active chromatin types (yellow), compared to other chromatin types (green and black = repressive; blue = Polycomb) (Figure S3C). Peak analysis of *OGT* revealed approximately 2000 intervals for each dietary condition (Figure S3D). About 70% of these intervals were shared between the two dietary conditions (Figure S3D, find_peaks FDR <0.01). Peak annotations revealed that 50% of *OGT* binding was at introns, 20% at promoter-TSS sites, and the remaining intervals were characterized as transcription termination sites (TTR), UTRs, intergenic regions, and exons (Figure 4B). Analysis of *OGT* binding across these introns showed an equal distribution of *OGT*

peaks at known splice sites. Whereas comparison of *OGT* binding at a 10 Kb region around all fly promoter-TSS sites showed an enrichment for TSS.

To test the relationship between *OGT* and *Pcl* occupancy we asked whether *Pcl* peaks overlap with *OGT* peaks. By intersecting the two datasets we identified ~200 shared intervals between *Pcl* and *OGT* (Figure 4C). We then compared *Pcl* occupancy at *OGT* peaks between the two dietary conditions. We found that at *OGT* peaks the occupancy of *Pcl* increased in the sugar diet environment compared to control diet (Figure 4D). However, this increase in *Pcl* at *OGT* peaks did not lead to a substantial change in chromatin accessibility (Figure S3E). Since of the ~2000 *OGT* peaks only 10% are occupied by *Pcl* (Figure 4C) we divided all *OGT* peaks into peaks that were specific to *OGT* only and peaks that were shared with *Pcl* (Figure S3F). Comparison of CATaDa signal at peaks shared between *OGT* and *Pcl* between the high sugar and control diet revealed a substantial decrease in chromatin accessibility (Figure 4E). These results suggest that *Pcl* binding overlaps with *OGT* at a subset of *OGT* target genes. In the high sugar diet environment, *Pcl* binding at this subset is increased and chromatin accessibility decreased.

Our results show that *Pcl* redistribution in the high sugar diet environment is prevented in animals fed the *OGT* inhibitor OSMI-1 (Figure 3). We therefore asked how inhibition of *OGT* affects *Pcl* binding at *OGT* peaks. We found that the increase in *Pcl* occupancy at *OGT* peaks is not rescued by OSMI-1 (Figure S3G). However, chromatin accessibility at *OGT* peaks in the high sugar diet environment is reverted to control diet levels (Figure 4F and S4H). To determine the biological pathways and function of all *OGT* targets we performed pathway enrichment analysis by iPAGE (Goodarzi et al., 2009). Comparison of *OGT* control diet and sugar diet peaks revealed an enrichment of GO terms related to neural activity (blue) and regulation (purple) such

as dendrite morphogenesis, neuron projection membrane, synaptic target attraction, as well as metabolic (red) GO terms like triglyceride metabolic process (Figure 3G and for full iPAGE GO term analysis see Figure S4). We further identified the pathways specific to *OGT* only and found an enrichment of metabolic (red) GO terms like triglyceride metabolic process, glutamate catabolic processes, and cellular zinc ion homeostasis (Figure 4F, and for full iPAGE GO term analysis see Figure S5). We also found GO terms for signal transduction, nervous system development, and axon guidance (Figure 4F, and for full iPAGE GO term analysis see Figure S5). Pathways that were specific to peaks shared between *OGT* and *Pcl* were regulatory GO terms like sequence-specific DNA binding. In summary, we discovered that a subset of *OGT* peaks that are involved in neural signaling and regulation are shared with *Pcl*. In the high sugar environment, this subset of regions have increased *Pcl* binding and decreased chromatin accessibility. This decrease in chromatin accessibility is dependent on *OGT*. This could mean that *OGT* facilitates the repressive activity of *Pcl* at these genes and tunes the sweet sensory neurons' responses to diet.

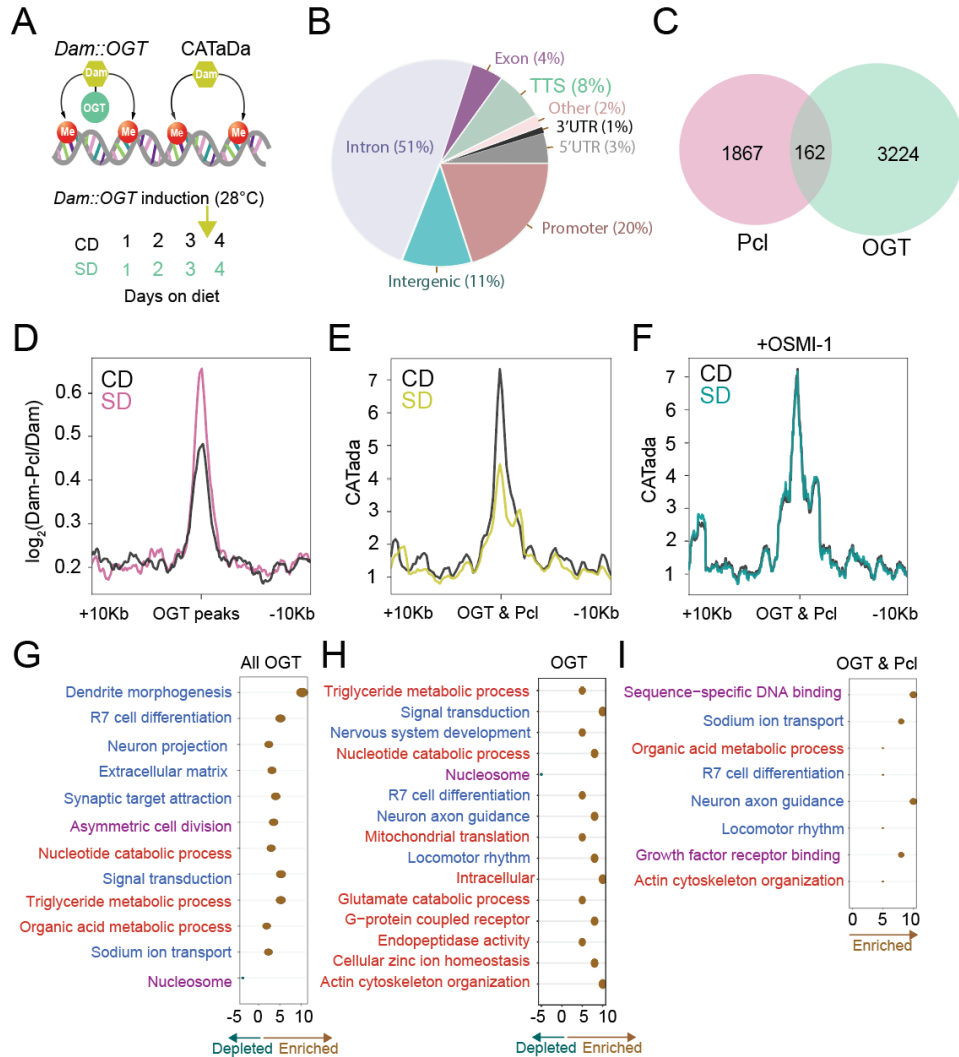


Figure 4.4 OGT specifies the chromatin targeting of *Pcl* in response to diet

(A) Schematic of Targeted Dam-ID (TaDa) of *Dam::OGT* and *Dam* (CATaDa) and the induction paradigm. Age-matched *Gr5a;tubulin-GAL80ts > UAS-LT3-Dam::OGT* and *Gr5a;tubulin-GAL80ts > UAS-LT3-Dam* flies were placed on a control or sugar diet for 3 days at 20° to 21°C and then switched to 28°C between days 3 and 4 to induce *Dam*. (B) Annotation of *OGT* chromatin occupied regions using HOMER (see Methods). (C) Overlap of $\log_2(Dam::Pcl/Dam)$ (pink) and $\log_2(Dam::OGT/Dam)$ (green) chromatin binding peaks (find_peaks, $q < 0.01$). (D) Average $\log_2(Dam::Pcl/Dam)$ signal on a control and sugar diet centered at *OGT* peaks. (E-F) Average CATaDa signal on a control and sugar diet centered at *OGT* peaks that overlap with *Pcl* peaks without (E) and with (F) OSMI-1. (G-H) iPAGE summary plots. Text in blue represents neural GO terms, red represents metabolic GO terms, and purple represents regulatory GO terms.

OGT and Pcl control a transcriptional program required for sweet taste

To test the possibility that OGT is required for the gene expression changes that lead to altered sensory neuron physiology, we isolated mRNAs associated with the ribosomes of the *Gr5a*⁺ cells using Translating mRNA Affinity Purification (TRAP) (Chen and Dickman, 2017) in flies fed a control or sugar diet that is supplemented with the OGT inhibitor OSMI-1 (Figure 5A, left). Principal component analysis revealed that most of the variation between samples was due to diet (Figure S6A). To verify the selection of mRNAs specific to the *Gr5a*⁺ cells, we calculated enrichment using log₂ fold changes (l2fc) obtained by comparing the *Gr5a*⁺ fraction to the input (*Gr5a*/Input) for the sweet taste receptor genes (*Gr5a*, *Gr64f*, and *Gr64a*) and the fatty acids taste receptor *Ir56D*. These genes were enriched in the *Gr5a*⁺ fraction compared to the input (Figure S6B), while the opposite was true for the bitter receptor genes *Gr66a* and *Gr32a*, which are expressed in the bitter sensing neurons in the taste sensilla, but not in *Gr5a*⁺ cells (Figure S6B). Flies fed a sugar diet for as little as 3 days show a robust negative skew in gene expression dependent on *Pcl* (Vaziri et al., 2020). We thus asked how inhibition of OGT by OSMI-1 affects the sugar diet dependent skew in negative l2fc. Analysis of all the differentially expressed genes (DEGs) showed a lack of skew in gene expression (Figure 5A, right) pointing to a role for OGT in the establishment of the *Pcl* dependent negative skew. To dissect the role of *OGT* and *Pcl* together in the establishment of this transcriptional state, we first identified the DEGs specific to the sugar diet environment (~700) (Vaziri et al., 2020). We then asked from these ~700 genes what are the genes that are reverted ($q < 0.1$, Wald test) or unchanged (practical equivalence test using a null hypothesis of a change of at least 1.5-fold and $q < 0.05$) in the SD+OSMI-1 and *Pcl*ΔSD group. We found that while all the differentially expressed genes in flies on a sugar diet for 7 days (SD7) either revert or are unchanged in the *Pcl*ΔSD group (Figure

5B), only 52% of SD7 DEGs were reverted or unchanged in the SD+OSMI-1 group (Figure 5B). Gene overlap analysis of these groups revealed that 367 genes in the SD7 group were shared between SD+OSMI-1, and *Pcl*ΔSD (Figure 5D, see Methods). The remaining 333 SD7 genes were only shared with the *Pcl*ΔSD group and not SD+OSMI-1. To determine the role of these genes we performed iPAGE (Goodarzi et al., 2009). Pathway analysis on the 367 genes that were changed by SD7 and reverted by *Pcl* mutations or OGT inhibition revealed pathways broadly implicated in metabolism, regulation of gene expression, and neural activity (Figure 5B, bottom). The genes changed by SD7 that were dependent on *Pcl* but not *OGT* were enriched in similar GO term categories with an increase in the number of GO terms related to neural processes (Figure 5B, top). Together, these findings suggest that *OGT* together with *Pcl* tunes the responses of the sweet taste cells by regulating the expression of a subset of genes involved in different aspects of neural physiology and metabolism. Interestingly, the expression of another subset of genes is regulated by *Pcl* alone that is also involved in other aspects of neural physiology and metabolism.

To differentiate the targets of *OGT* and *Pcl* together from the targets of *Pcl* and *OGT* alone, we first compared these differentially expressed genes to *OGT* and *Pcl* peaks (Figure 4). We found that 5/367 genes that are co-regulated by *OGT* and *Pcl* are directly bound by *OGT* and *Pcl*. These five genes were transcription factors but only the genes *Ptx1* (*paired-domain homeobox*), *caudal* (*cad*; *hox-like homeobox*), and *scarecrow* (*scro*; *natural killer-like homeobox*) showed diet-dependent changes in *OGT* and *Pcl* binding (Figure 5C, top, and in Vaziri et al. 2020). Of the genes that were only regulated by *Pcl* we found that 5/333 were directly bound by *Pcl* and only *GATAe* (Zn finger), and *nubbin/pdm* (*nub*; POU homeobox) showed a diet dependent change in *Pcl* binding (Vaziri et al. 2020). We previously reported that

these five TFs *cad*, *Ptx1*, *GATAe*, *nub*, and *scro* were differentially bound by PRC2.1 leading to their differential expression in the sugar diet environment. These TFs formed a transcriptional regulatory hub that regulated a common set of targets that affected the physiology of the *Gr5a+* neurons (Vaziri et al., 2020). Since the remaining genes are not directly targeted by *OGT* or *Pcl* we hypothesized that their expression is affected through these five TFs. Previously, we used a candidate gene approach to identify the targets of these TFs (Vaziri et al., 2020). Since only *cad*, *Ptx1*, and *scro* are targeted by *OGT* and *Pcl* in the sugar diet environment we looked at the expression of their targets at SD7, *Pcl*ΔSD, and SD+OSMI-1, these targets which collectively made up 210/367 for *cad* and *Ptx1* and 146/367 for *scro* showed negative 12fc on a sugar diet (Figure 5C, teal) that reverted in the *Pcl* mutants, and the SD+OSMI-1 group (Figure 5C, pink and green, respectively). Collectively, these genes regulate the aspects of neural physiology related to detection of chemical stimulus, sensory perception of chemical stimulus and carbohydrate metabolic processes. In summary, our results suggest that nutrient information from the environment is translated to *Gr5a+* neuron function through the targeting of *OGT* and *Pcl* to *cad*, *Ptx1*, and *scro* that define a subset of genes that control different aspects of neural physiology and metabolism. Furthermore, *Pcl* alone also controls the expression of another battery of genes regulated by *GATAe* and *nub* which mediate the synaptic properties of the *Gr5a+* cells independent of *OGT*.

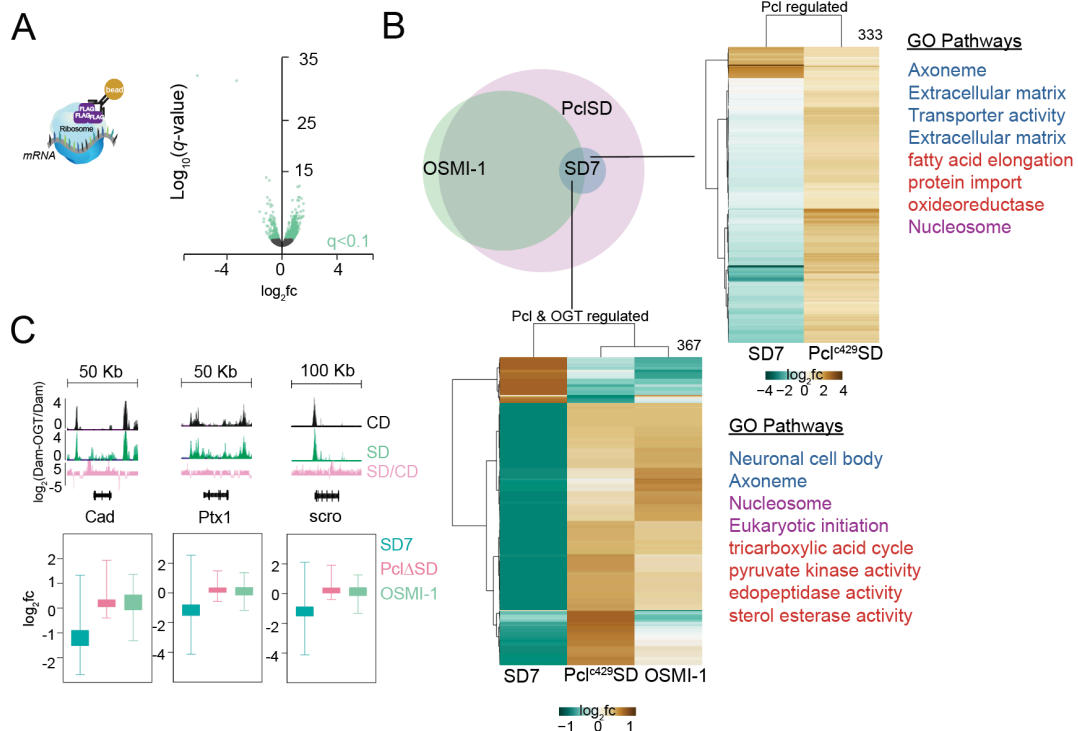


Figure 4.5 OGT and Pcl control a transcriptional program required for sweet taste

(A) Schematic of Flag tagged ribosomes expressed in the *Gr5a*+ cells and isolated by immunoprecipitation (left). Volcano plot representing differential expression in the *Gr5a*+ neurons of age-matched male *Gr5a > UAS-Rpl3-3XFLAG* flies on a sugar diet for 7 days supplemented with OSMI-1. $n = 3$ replicates per condition. Nonsignificant genes are in black, and genes with $q < 0.1$ (Wald test) are in green. (B) Gene overlap analysis (left) between SD7 (teal), *Pcl* Δ SD (pink) and SD+OSMI+1 (green) and heatmaps showing the log₂ fold change of the genes within its gene overlap group. GO terms are located next to the corresponding heatmap, and text in blue represents neural GO terms, red represents metabolic GO terms, and purple represents regulatory GO terms. (C) Log₂(Dam::OGT/Dam) on a control and sugar diet within a 50 kb window at *cad* and *Ptx1*, and a 100 kb window at *scro*. Replicates are superimposed. Pink traces are SD/CD fold changes (top). Log₂ fold changes for candidate gene targets of *Cad*, *Ptx1*, and *scro* at SD7 (teal), *Pcl*⁴²⁹SD (pink) mutants at SD7 (green), and OSMI-1 fed flies at SD7.

4.4 Discussion

Here, we set out to understand how nutrient information from the dietary environment is integrated into epigenetic mechanisms that change the gustatory system in a way that promotes food intake and weight gain. Specifically, we identified a nutrient information pathway that specifies the effects of high dietary sugar on the physiology of the sweet sensing cells. In our previous work, we found that a high sugar environment leads to a decrease in the responsiveness of the sweet sensory neurons to sugar (May et al., 2019). This lowered response decreased sweet taste perception and increased food intake. Furthermore, we found that a decrease in sweet taste is caused by the cell-autonomous action of the PRC2.1 complex in the sweet taste neurons (Vaziri et al. 2020). In the high sugar environment, PRC2.1 chromatin occupancy is redistributed at the loci of five transcription factors. These five transcription factors formed a regulatory hub that regulated the expression of a battery of genes responsible for tuning the metabolic and neural properties of the sweet taste cells in response to diet (Vaziri et al. 2020). In this work, we find the metabolic enzyme OGT is also necessary for diet dependent taste defects and that its catalytic domain exerts these effects. Mutations in the catalytic domain of OGT prevented a rescue of sweet taste defects in the sugar diet environment. These mutants when tested as heterozygotes exhibit a 45-50% reduction in activity comparable to the RNAi knockdown levels. Additionally, these effects are entirely dependent on the PRC2.1 complex. Mutations and pharmacological inhibition of the PRC2.1 complex prevented OGT induced sweet taste defects. While our results cannot place the PRC2.1 complex directly downstream of OGT, they do suggest that these two factors are exerting their effects on sweet taste through the same genetic pathway. OGT modifies the activity of its targets through O-glcNAcylation of S/T residues (Hanover et al. 2010; Hardivillé and Hart 2014; Wells et al. 2001), however we cannot say

whether OGT is directly modifying Pcl or other members of PRC2.1 that have previously been shown to be O-glcNAcylated in other organisms (Chu et al. 2014; Gambetta and Müller 2014; Dehennaut et al. 2014).

In the high sugar diet environment, the chromatin occupancy of the PRC2.1 complex is redistributed in the sweet sensing cells in a way that increases its binding to PRE regions and decreases chromatin accessibility (Vaziri et al. 2020). Here, we found that this redistribution is completely prevented when OGT is pharmacologically inhibited. Inhibition of OGT did not alter the overall number and identity of PRC2.1 targets but altered its distribution. Because OGT mRNA levels are unchanged in the *Gr5a*⁺ cells in response to diet, we explored the possibility that the targeting of OGT to the chromatin influences the chromatin occupancy of PRC2.1. Our OGT Dam-ID experiments revealed that OGT is at the chromatin of the *Gr5a*⁺ cells with a preference for introns (51%) and promoter-TSS regions (20%). OGT's relative distribution at these genomic features in the sweet sensing neurons are like what others had reported in embryonic stem cells (Vella et al. 2013). In the *Gr5a*⁺ cells about 200 chromatin regions are co-occupied by OGT and Pcl. At these regions, Pcl binding is increased, and chromatin accessibility is decreased in an OGT dependent manner in the high sugar diet environment. These lines of evidence provide support for the hypothesis that the activity of PRC2.1 in the sweet sensing cells in response to diet is dependent on OGT.

The transcriptional properties of the sweet taste cells are largely altered in the high nutrient environment and mutations in the PRC2.1 complex rescues these effects as well as sweet taste (Vaziri et al. 2020). Ribosomal profiling of the sweet sensory neurons of animals on a sugar diet supplemented with an OGT inhibitor also shows a partial reversal of the transcriptional changes on a sugar diet. However, while mutations in PRC2.1 reverses all the transcriptional

changes only 52% are reverted by OGT inhibition, suggesting that only a subset of the genes changed by diet are regulated by OGT. To this end, we performed a comprehensive analysis of *OGT* and *Pcl* peaks and compared them to the differentially expressed genes in the high sugar diet, *Pcl* mutants, and with OGT inhibition. This analysis allowed us to determine differential regulation of the five transcription factors we had identified in our previous work. Specifically, we found that the loci of the transcription factors *Ptx1*, *cad* and *scro* were co-occupied by *OGT* and *Pcl*, whereas the loci of the transcription factors *nub* and *GATAe* were occupied by *Pcl* alone. Consistent with an increase in *Pcl* and *OGT* occupancy at *Ptx1* and *cad* we observed a decrease in the expression of the genes that was rescued by mutations in *Pcl* and inhibition of *OGT*. *Scro* on the other hand had increased expression on the sugar diet that was rescued by *Pcl* mutations and OGT inhibition. The expression of *nub* and *GATAe* were decreased in the sugar diet environment and rescued by *Pcl* mutations but not OGT inhibition. These five transcription factors collectively regulate a battery of genes required for the synaptic, neural, and metabolic properties of the sweet taste neurons and their expression ultimately leads to decreased responses of the *Gr5a+* cells to sweet stimuli.

How do *Pcl* and *OGT* collectively tune the responses of the sweet sensory neurons to diet? Our results point towards a dual response to the high nutrient environment. Specifically, we see that *OGT* and *Pcl* are both necessary and sufficient for the effects of diet on sweet taste. However, they regulate a different battery of genes with substantial overlap, suggesting that their relationship could be to specify different sets of genes. How does *OGT* regulate the expression of this subset of genes in response to diet? With the targeted Dam-ID of *Pcl* in animals fed a high sugar diet supplemented with the OGT inhibitor, we see that the 1) increased *Pcl* binding at PREs is rescued, but 2) *Pcl* binding is not rescued at *Pcl* and *OGT* target genes while chromatin

accessibility and gene expression are. These two effects suggest variable roles for *OGT* that still implicate its catalytic function. In the case of the PREs, OGT inhibition is affecting the recruitment of *Pcl* in the sugar diet environment. This could be through the O-GlcNAcylation of histones or RNA polymerase II, which has been shown to impact transcription (Hardivillé and Hart 2014; Xu et al. 2021) or by influencing the formation of a stable PRC2 complex through O-glcNAcylation of E(z) (Chu et al. 2014). In the context of OGT and *Pcl* target genes, OGT inhibition is affecting chromatin accessibility and gene expression. This suggests that OGT plays a role in the ability of PRC2.1 to repress genes either through histone O-glcNAcylation, stabilization of PRC2, or modification and recruitment of other factors that mediate this process. This is a likely possibility since our experiments have not determined whether *OGT* and *Pcl* are directly interacting.

Overall, our results point to a moonlighting role for OGT (Xu et al. 2021) that is not directly linked to its metabolic activity. This leads to the question of how the activity of *OGT* is altered by diet? While we did not detect any changes in the mRNA levels of *OGT* in the *Gr5a+* sensory cells we cannot exclude the possibility that its protein abundance or stability is altered in the high sugar diet environment. We also cannot exclude the possibility that its activity is altered in the absence of any changes in protein levels. This is because we know that in the high sugar diet environment the levels of the first-committed metabolite in the HBP pathway are upregulated (May et al. 2019; Wilinski et al. 2019). Furthermore, an increase in glucose levels leads to a dynamic regulation of intracellular protein O-glcNAcylation (Swamy et al. 2016).

An exciting finding from our work is a possible mechanism for how metabolic signals modulate neural activity. Several studies have alluded to the role of OGT in regulating synaptic maturation and behavior (Butler et al. 2019; Lagerlöf et al. 2016). In our study we identify a

specific gene expression program that is specified by *OGT* in concert with the PRC2.1 complex. Our findings advance the conceptual understanding of the role of *OGT* in the nervous system and point to a way that nutrient information is integrated into gene expression changes and subsequent behavior. Incidentally, engagement of specific metabolic enzymes could determine the ways in which different dietary environments influence gene expression and behavior. Our findings indicate that *OGT* affects the battery of genes regulated by the transcription factors *Ptx1*, *cad*, and *scro*. These transcription factors control the synaptic connectivity and neural activity of sensory neurons as well neuroblast development. The transcription factors *GATAe* and *nub* which are regulated by *Pcl* alone also regulate other aspects of synaptic connectivity.

In conclusion, we show that both *OGT* and the PRC2.1 complex mediate the effects of high dietary sugar on sweet taste by regulating a subset of genes involved in establishing the responses of the sweet sensory neurons to sweet stimuli. By specifying the targeting and repressive activity of the PRC2.1 complex to a subset of genes *OGT* defines a nutrient information pathway in response to diet. Thus, *OGT* acts as the metabolic link between diet and gene expression. Given the conservation of *OGT* function from flies to humans, and the role of *OGT* in the etiology of obesity and diabetes our work is broadly relevant to understanding the effects of the high nutrient and obesogenic environments on food intake and a variety of related disorders that currently affects billions of people worldwide.

4.5 Methods

Fly husbandry

All flies were grown and maintained on cornmeal food (Bloomington Food B recipe) at 25°C and 45 to 55% humidity under a 12-hour light/12-hour dark cycle (Zeitgeber time 0 at 9:00 AM.). Male flies were collected under CO₂ anesthesia 1-3 days after eclosion and maintained in a vial that housed 35-40 flies. Flies were acclimated to their new vial environment for an additional 2 days. For all experiments, flies were changed to fresh food vials every other day. The GAL4/UAS system was used to express transgenes of interest using the gustatory receptor 5a *Gr5a-GAL4* transgene. For each GAL4/UAS cross, transgenic controls were made by crossing the w1118CS (gift from A. Simon, CS and w1118 lines from the Benzer laboratory) to GAL4 or UAS flies, sex-matched to those used in the GAL4/UAS cross. *Sxc* mutants were not in a w1118CS background but were crossed to this line for all experiments shown here. The fly lines used for this paper are listed in file.

For all dietary manipulations, the following compounds were mixed into standard cornmeal food (Bloomington Food B recipe) (0.58 calories/g) by melting, mixing, and pouring new vials as in (Musselman and Kühnlein, 2018) and (Na et al., 2013). For the 30% sugar diet (1.41 calories/g), Domino granulated sugar (w/v) was added. For the EEDi inhibitor diet (Axon Medchem), EEDi was prepared as in (Vaziri et al., 2020). For the OSMI-1 inhibitor diet (Sigma Aldrich), OSMI-1 was solubilized in 10% DMSO and added to the control or 30% sugar diet at a total concentration of 10 or 30 μM.

Proboscis extension response

Male flies were food-deprived for 18 to 24 hours in a vial with a Kimwipe dampened with 2 ml of Milli-Q filtered deionized water. Proboscis Extension Response was carried out as described in (Shiraiwa and Carlson, 2007). Scoring of extension responses were conducted manually, and when possible, blind observers were used.

Proboscis immunofluorescence

Probosces were dissected in 1× phosphate-buffered saline and fixed in 4% paraformaldehyde, mounted in FocusClear (CelExplorer) on coverslips. Cell bodies were imaged using an FV1200 Olympus confocal with a 20× objective. Cells were counted using Imaris Image Analysis software.

Affinity purification of ribosome-associated mRNA (TRAP)

Heads (300 per replicate, ~10,000 *Gr5a*⁺ cells) were collected using sieves chilled in liquid nitrogen and on dry ice. Frozen heads were then lysed as previously described (Chen and Dickman, 2017). From the lysate, total RNA was extracted by TRIzol LS Reagent (Thermo Fisher Scientific, 10296010) to use as input. The remainder of the lysate was incubated with Dynabeads Protein G (Thermo Fisher Scientific, 10004D) and precleared for 2 hours and subsequently incubated with Dynabeads Protein G coated with an anti-Flag antibody (Sigma-Aldrich, F1804). The lysate-beads mixture was incubated at 4°C with rotation for 2 hours, then RNA was extracted from ribosomes bound to the beads by TRIzol Reagent (Chen and Dickman, 2017).

Targeted DNA adenine methyltransferase identification (TaDa)

To generate the *UAS-LT3-Dam::Sxc* construct, the coding region of the *Sxc* gene was amplified from w1118CS animals with primers listed below and assembled into the *UAS-LT3-DAM* plasmid (gift from A. Brand, University of Cambridge) using the NEBuilder HiFi DNA Assembly kit based on the manufacturer's instructions (New England Biolabs). Transgenic animals were validated by reverse transcription PCR targeting the correct insert. The *UAS-LT3-Dam::Sxc* and the *UAS-LT3-Dam* line were crossed to *Gr5a-GAL4;tubulin-GAL80ts*. All animals were raised and maintained at 20°C. Expression of *Dam::Sxc* and *Dam* was induced at 28°C for 18 to 20 hours. For all experiments, 300 heads of males and female flies were collected per replicate on dry ice by sieving. DNA was extracted following kit instructions (Invitrogen). For identification of methylated regions, purified DNA was digested by Dpn I, followed by PCR purification of digested sequences. TaDa adaptors were ligated by T4 DNA ligase (NEB). Adapter ligated DNA was PCR-amplified and purified according to the protocol in (Marshall et al., 2016) Purified DNA was digested with Dpn II, followed by sonication to yield fragments averaging 300 base pairs. TaDa adaptors were removed from sonicated DNA by digestion followed by PCR purification and purified sonicated DNA was used for library preparation (Marshall et al., 2016).

pUAST-Sxc.Forward gatctgGCCGGCGCaATGCATGTTGAACAAACACGAATAAATATG
pUAST-Sxc.Reverse gttccttcacaaagatcctTTATACTGCTGAAATGTGGTCCGGAAG

Library preparation for TRAP and TaDa

RNA sequencing (RNA-seq) libraries were generated using the Ovation SoLo RNA-seq System for *Drosophila* (NUGEN, 0502-96). All reactions included integrated Heat-Labile Double-Strand

Specific DNase treatment (ArcticZymes, catalog no. 70800-201). DNA-sequencing libraries were generated using the Takara ThruPLEX Kit (catalog no. 022818). All libraries were sequenced on the Illumina NextSeq platform (High-output kit v2 75 cycles) at the University of Michigan core facility.

High-throughput RNA-seq analysis

Fastq files were assessed for quality using FastQC (Andrews and Others, 2010). Reads with a quality score below 30 were discarded. Sequencing reads were aligned by STAR (Dobin et al., 2013) to dmel-all-chromosomes of the dm6 genome downloaded from Ensemble, and gene counts were obtained by HTSeq (Anders et al., 2015). Count files were used as input to call differential RNA abundance by DESeq2 (Love et al., 2014). Pipeline was generated from (Wilinski et al., 2019). To determine the efficiency of the TRAP, experiment pairwise comparisons were made between the *Gr5a*⁺-specific fraction and the input, where the numerator is the immunoprecipitation (IP) and the denominator is the input. For comparisons between dietary conditions, DESeq2 was only applied to the *Gr5a*⁺-specific IP condition. SD7 and *Pcl^{c429}* genotype datasets were obtained from and described in (Vaziri et al., 2020). A cutoff of $q < 0.1$ was used to call DEGs. Skew in l2fcs was measured using the R package Skewness (e1071) and as described in (Vaziri et al., 2020). The skew determination is based on the l2fc for all genes detected, not only those that are significantly differentially expressed. In general, a negative skewness in a unimodal distribution indicates the presence of a long negative tail, whereas a positive skewness indicates a long positive tail. To identify overlap between dataset GeneOverlap was used (Shen and Sinai, 2013). RNA-seq data visualization was carried out in R studio using ggplot2 and the following packages, pheatmap (Kolde, 2012), Venneuler

(Wilkinson, 2012), and EnhancedVolcano (Blighe, 2019). To cluster columns and rows in heatmap, “Ward.D” clustering was used.

High-throughput TaDa and CATaDa analysis

Fastq files were assessed for quality using FastQC (Andrews and Others, 2010). Reads with a quality score below 30 were discarded. The damidseq_pipeline was used to align, extend, and generate log₂ ratio files in GATC resolution as described previously (Marshall and Brand, 2015). Briefly, the pipeline uses Bowtie2 (Langmead and Salzberg, 2012) to align reads to dm6-all-chromosomes of the dm6 genome downloaded from Ensemble, followed by read extension to 300 bp (or to the closest GATC, whichever is first). Bam output is used to generate the ratio file in bedgraph format. Bedgraph files were converted to bigwig and visualized in the UCSC Genome Browser. Correlation coefficients and principal components analysis plots between biological replicates were computed by multibigwigSummary and plotCorrelation in deepTools (Ramírez et al., 2016). Fold-change traces for SD/CD of $\log_2(Dam::Sxc/Dam)$ were generated by calculating the average coverage profile of all replicates for each condition and subsequently calculating fold change between the sugar diet and control diet condition with deepTools bigwigCompare (Ramírez et al., 2016). Peaks were identified from ratio files using find_peaks (FDR, <0.01) (Marshall and Brand, 2015). To do this, the binding intensity thresholds are identified from the dataset, the dataset is then shuffled randomly, and the frequency of consecutive regions (i.e., GATC fragments or bins) with a score greater than the threshold is calculated. The FDR is the observed/expected for a number of consecutive fragments above a given threshold. Association of genes to peaks was made using the peaks2genes script (Marshall and Brand, 2015) and dm6 genome annotations. Overlapping intervals or nearby intervals (Up to

50bp) were merged into a single interval using mergeBed in BEDtools (Quinlan and Hall, 2010). Intervals common in at least 2 replicate peak files were identified by Multiple Intersect in BEDtools and used to generate the consensus peaks (Quinlan and Hall, 2010). For CATaDa experiments, all analyses were performed similar to those of TaDa with the exceptions that (i) Dam only profiles were not normalized as ratios but shown as non-normalized binding profiles, and (ii) Dam only coverage plots were generated by converting bam files to bigwig files normalized to $1 \times$ dm6 genome. Metaplot analysis of binding intensities was performed by computing a matrix for specified regions (Ramírez et al., 2016). Multiple Intersect was used to identify shared intervals between multiple peak datasets (Quinlan and Hall, 2010). To determine the proportion of genes that fit within the various chromatin domain subtypes, we first matched Dam::Sxc/Dam targets to coordinates identified by (Filion et al., 2010) and then determined their gene count in each chromatin subtype (observed) compared to the whole genome (expected). All chromatin tracks are visualized with the UCSC genome browser. Peak annotations were conducted using HOMER (Heinz et al. 2010).

iPAGE analysis

All GO term enrichment analysis was performed using the iPAGE package (Goodarzi et al., 2009), using gene-GO term associations extracted from the Flybase dmel 6.08 2015_05 release. iPAGE was run in discrete mode, using the groups specified for each calculation. For all discrete calculations, independence filtering was deactivated because of the less informative available signal. All other iPAGE settings were left at their default values. All shown GO terms pass the significance tests for overall information described in (Goodarzi et al., 2009); in addition, for each term, individual bins showing especially strong contributions [P value, such that a

Benjamini-Hochberg FDR (Benjamini and Hochberg, 1995) calculated across that row, yields $q < 0.05$] are highlighted with a strong black box.

Data analysis and statistics

Statistical tests, sample size, and P or q values are listed in each figure legend. For all PER experiments, Kruskal-Wallis Dunn's multiple comparisons were used. Comparisons are either to control diets within genotypes or transgenic controls within dietary conditions. Data were evaluated for normality and appropriate statistical tests were applied if data were not normally distributed; all the tests, biological samples, and the P and q values are listed in the figure legends and specific analysis under each methods session. Because the inferential value of a failure to reject the null hypothesis in frequentist statistical approaches is limited, for all RNA-seq expression datasets, we coupled our standard differential expression with a test for whether each gene could be flagged as "significantly not different." Defining a region of practical equivalence as a change of no more than 1.5-fold in either direction, we tested the null hypothesis of at least a 1.5-fold change for each gene, using the gene-wise estimates of the SE in log₂fold change (reported by Deseq2) and the assumption that the actual l2fcs are normally distributed. Rejection of the null hypothesis in this test is taken as positive evidence that the gene's expression is not changed substantially between the conditions of interest. Python code for the practical equivalence test can be found on GitHub as `calc_sig_unchanged.py`. All data in the figures are shown as means \pm SEM, **** P < 0.0001, *** P < 0.001, ** P < 0.01, and *P < 0.05, unless otherwise indicated. Statistical analysis and tests are listed in every legend unless otherwise noted in the text.

4.6 Supplemental Figures

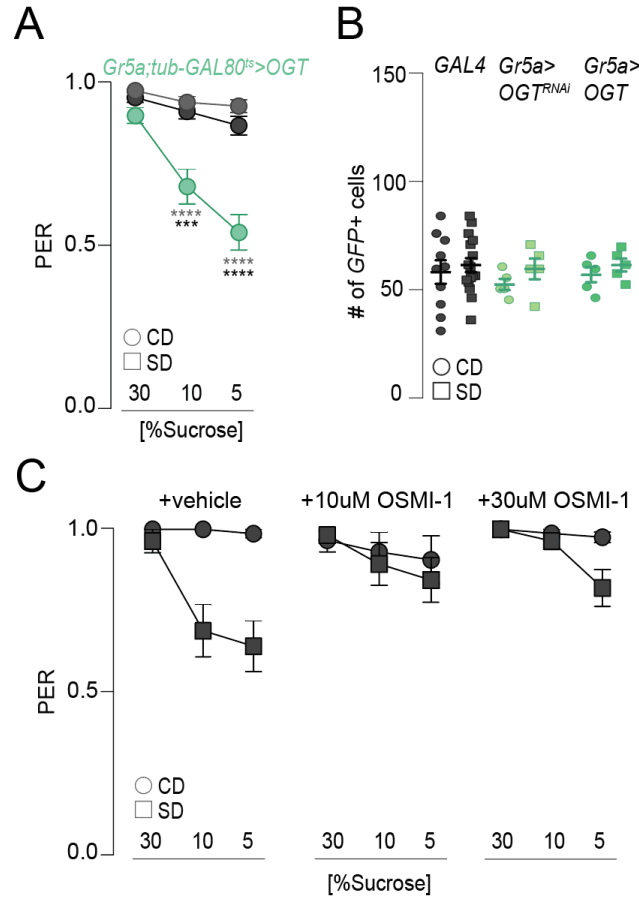


Figure 4.6 OGT modulates sweet taste in response to diet.

(A, C) Taste responses (y axis) to stimulation of the labellum with 30, 10, and 5% sucrose (x axis) of age-matched male (A) *Gr5a;tubulin-GAL80^{ts}>OGT* (green) and transgenic controls (shades of gray) on a control diet, n= 17-24. (B) Quantification of the number of sweet taste GFP-labeled cells in the labella of *Gr64f;CD8-GFP* flies crossed to *w1118^{cs}* (as control, gray), *Gr64f;CD8-GFP>OGT^{RNAi}* (light green), and *Gr64f;CD8-GFP>OGT* (dark green) on a control (circle) or sugar (square) diet for 7 days. n=5-16 probosces, no significance, Kruskal-Wallis Dunn's multiple comparisons, comparison to control diet of each genotype. (C) Taste responses (y axis) to stimulation of the labellum with 30, 10, and 5% sucrose (x axis) of age-matched male *w1118^{cs}* flies on a control or sugar diet with vehicle (10% DMSO) or 10 and 30uM OSMI-1. n = 14-17. Kruskal-Wallis Dunn's multiple comparisons, comparison to control diet of each genotype. In all panels, flies were on a control (circle) or sugar (square) diet for 7 days. Data are shown as means \pm SEM. ****P < 0.0001, ***P < 0.001, **P < 0.01, and *P < 0.05.

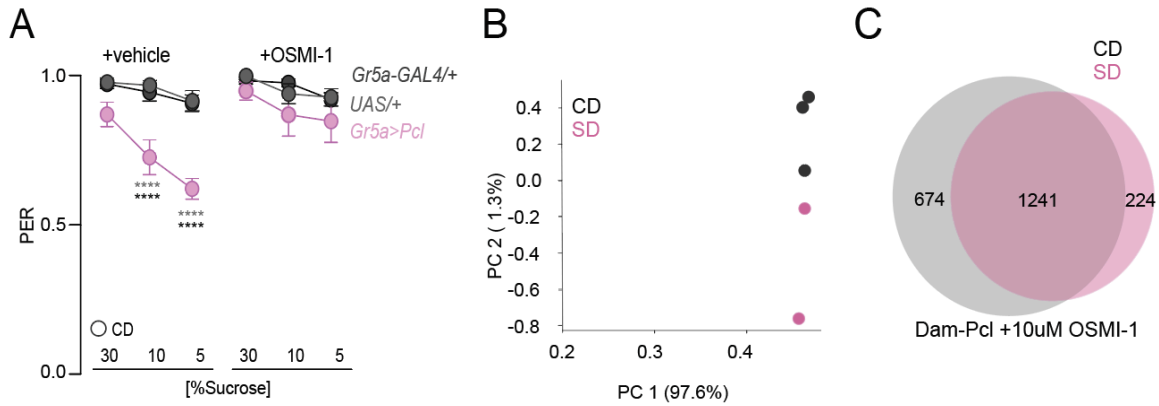


Figure 4.7 The diet mediated *Pcl* chromatin redistribution is dependent on OGT

(A) Taste responses (y axis) to stimulation of the labellum with 30, 10, and 5% sucrose (x axis) of age-matched male *Gr5a>Pcl* (pink) and transgenic controls (shades of gray) on a control diet supplemented with vehicle (10% DMSO) or control diet supplemented with 10 uM OSMI-1, n18-23, Kruskal-Wallis Dunn's multiple comparisons, comparisons to transgenic controls. (B) Principal component analysis of normalized $\log_2(Dam::Pcl/Dam)$ flies on CD+OSMI-1 (gray) or SD+OSMI-1 (pink). (C) Overlap of $\log_2(Dam::Pcl/Dam)$ chromatin binding peaks of CD+OSMI-1 (gray) and SD+OSMI-1 (pink) (find_peaks, $q < 0.01$).

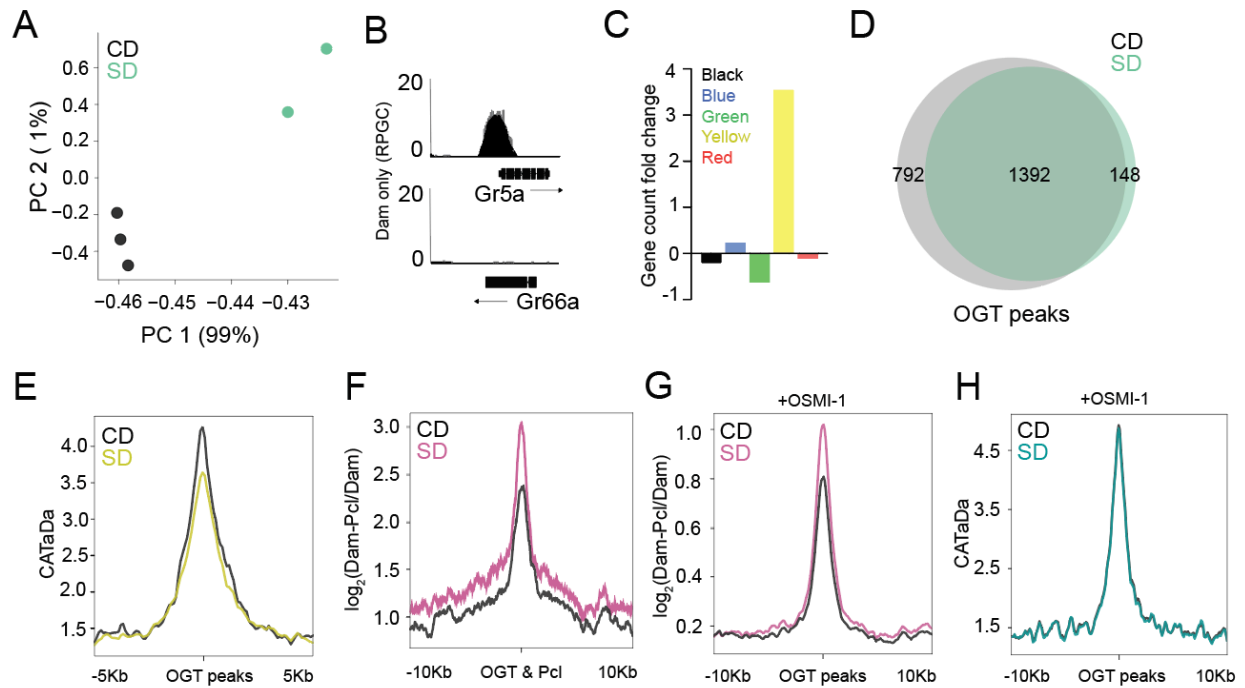


Figure 4.8 OGT specifies the chromatin targeting of *Pcl* in response to diet

(A) Principal component analysis of normalized $\log_2(Dam::OGT/Dam)$ flies on CD (gray) or SD (green). (B) CATaDa from control diet flies at the sweet gustatory receptor *Gr5a* and the bitter gustatory receptor *Gr66a*. (C) Proportion of observed Dam-OGT consensus peaks allocated to their respective chromatin domains normalized to the expected proportions across the whole genome. (D) Overlap of $\log_2(Dam::OGT/Dam)$ chromatin binding peaks of CD (gray) and SD (green) (find_peaks, $q < 0.01$). (E) Average CATaDa signal on a control and sugar diet centered at OGT peaks. (F-G) Average $\log_2(Dam::Pcl/Dam)$ signal on a control and sugar diet supplemented without (F) or with (G) OSMI-1 centered at (F) OGT and *Pcl* peak overlap and (G) OGT peaks. (H) Average CATaDa signal on a control and sugar diet centered at OGT peaks with OSMI-1.

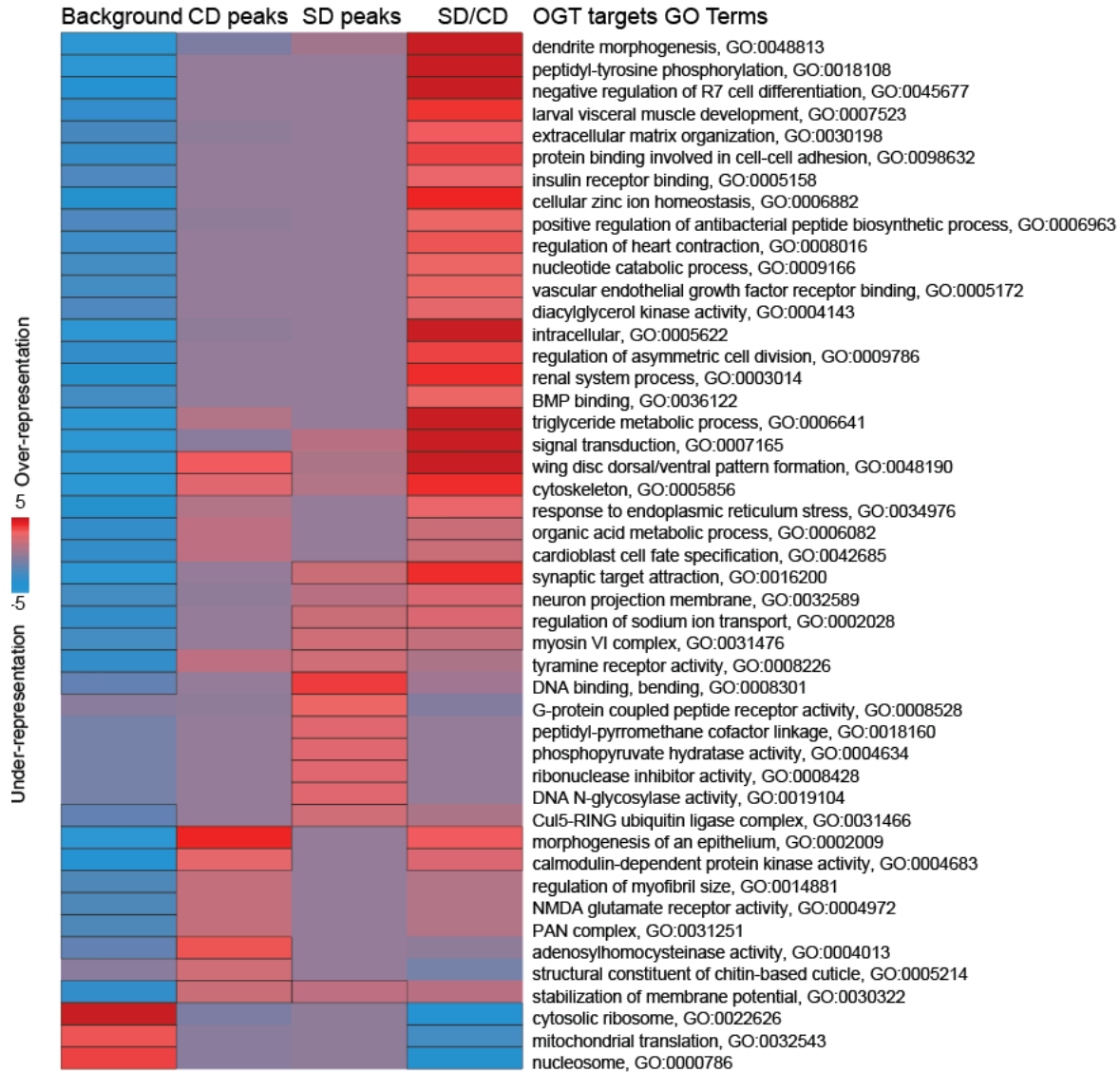


Figure 4.9 Pathway enrichment analysis on OGT chromatin targets in the *Gr5a+* neurons

iPAGE identification of pathways depleted (blue) or enriched (red) compared to background gene list from the *Dam::OGT* peaks on a control, sugar, and sugar/control diet. Scale represents over-representation (red) or under-representation (blue) of genes within a specific bin for the corresponding GO term. Black outlined boxes represent $q < 0.05$.

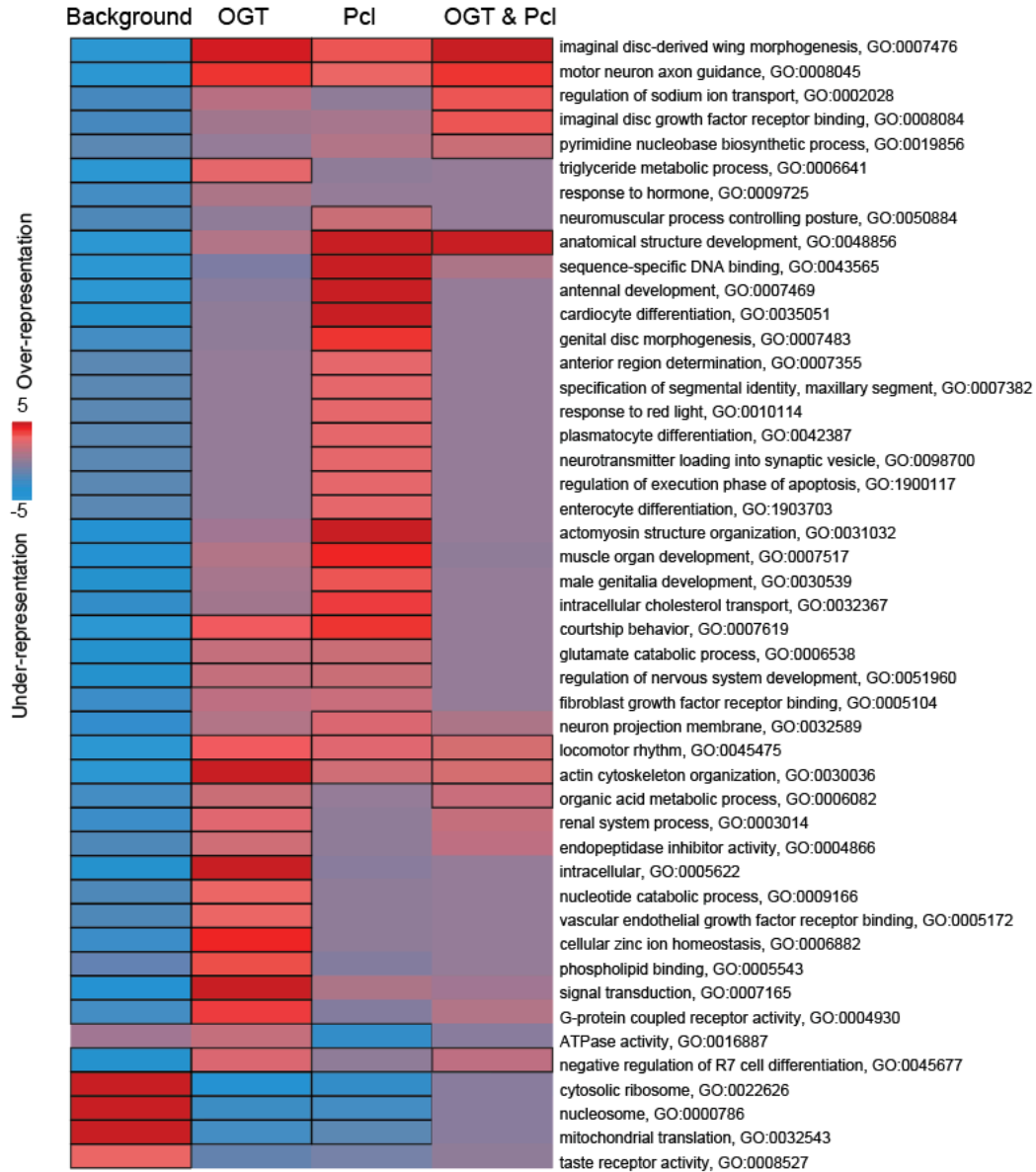


Figure 4.10 Pathway enrichment analysis on OGT and Pcl chromatin targets in the *Gr5a+* neurons

iPAGE identification of pathways depleted (blue) or enriched (red) compared to background gene list from the *Dam::OGT*, *Dam::Pcl*, and the overlap of *OGT* and *Pcl*. Scale represents over-representation (red) or under-representation (blue) of genes within a specific bin for the corresponding GO term. Black outlined boxes represent $q < 0.05$.

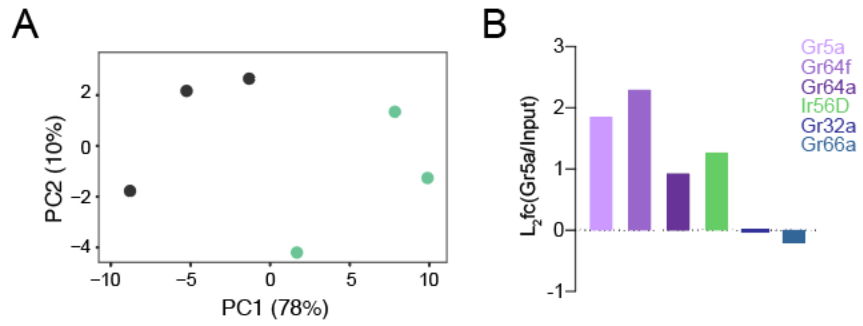


Figure 4.11 OGT and Pcl control a transcriptional program required for sweet taste

(A) Principal component analysis of normalized *Gr5a>UAS-Rp13-3xFLAG* flies on CD+OSMI-1 (gray) or SD+OSMI-1 (green). (B) $\log_2\text{fc}(Gr5a/\text{Input})$ of the genes *Gr5a*, *Gr64f*, *Gr64a*, *Ir56D*, *Gr32a*, and *Gr66a*.

4.7 References

1. Altarejos JY, Montminy M. 2011. CREB and the CRTC co-activators: sensors for hormonal and metabolic signals. *Nat Rev Mol Cell Biol* 12:141–151.
1. Anders S, Pyl PT, Huber W. 2015. HTSeq--a Python framework to work with high-throughput sequencing data. *Bioinformatics* 31:166–169.
2. Andrews S, Others. 2010. FastQC: a quality control tool for high throughput sequence data.
3. Aughey GN, Gomez AE, Thomson J, Yin H, Southhall TD. 2018. CATaDa reveals global remodelling of chromatin accessibility during stem cell differentiation in vivo. *eLife*, 7.
4. Baldini SF, Steenackers A, Olivier-Van Stichelen S, Mir A-M, Mortuaire M, Lefebvre T, Guinez C. 2016. Glucokinase expression is regulated by glucose through O-GlcNAc glycosylation. *Biochem Biophys Res Commun* 478:942–948.
5. Bartke T, Schneider R. 2020. You are what you eat – How nutrition and metabolism shape the genome through epigenetics. *Molecular Metabolism*.
doi:10.1016/j.molmet.2020.100987
6. Bartoshuk LM, Duffy VB, Hayes JE, Moskowitz HR, Snyder DJ. 2006. Psychophysics of sweet and fat perception in obesity: problems, solutions and new perspectives. *Philos Trans R Soc Lond B Biol Sci* 361:1137–1148.
7. Benjamini Y, Hochberg Y. 1995. Controlling the False Discovery Rate: A Practical and Powerful Approach to Multiple Testing. *J R Stat Soc Series B Stat Methodol* 57:289–300.

8. Bertino M, Beauchamp GK, Engelman K. 1982. Long-term reduction in dietary sodium alters the taste of salt. *Am J Clin Nutr* 36:1134–1144.
9. Blighe K. 2019. EnhancedVolcano: Publication-ready Volcano Plots With Enhanced Colouring and Labeling. R Package Version 1.20. 2019.
10. Butler AA, Sanchez RG, Jarome TJ, Webb WM, Lubin FD. 2019. O-GlcNAc and EZH2-mediated epigenetic regulation of gene expression during consolidation of fear memories. *Learn Mem* 26:373–379.
11. Chen X, Dickman D. 2017. Development of a tissue-specific ribosome profiling approach in *Drosophila* enables genome-wide evaluation of translational adaptations. *PLoS Genet* 13:e1007117.
12. Chu C-S, Lo P-W, Yeh Y-H, Hsu P-H, Peng S-H, Teng Y-C, Kang M-L, Wong C-H, Juan L-J. 2014. O-GlcNAcylation regulates EZH2 protein stability and function. *Proc Natl Acad Sci U S A* 111:1355–1360.
13. Decourcelle A, Leprince D, Dehennaut V. 2019. Regulation of Polycomb Repression by O-GlcNAcylation: Linking Nutrition to Epigenetic Reprogramming in Embryonic Development and Cancer. *Front Endocrinol* 10:117.
14. Dehennaut V, Leprince D, Lefebvre T. 2014. O-GlcNAcylation, an Epigenetic Mark. Focus on the Histone Code, TET Family Proteins, and Polycomb Group Proteins. *Front Endocrinol* 5:155.
15. Dobin A, Davis CA, Schlesinger F, Drenkow J, Zaleski C, Jha S, Batut P, Chaisson M, Gingeras TR. 2013. STAR: ultrafast universal RNA-seq aligner. *Bioinformatics* 29:15–21.

16. Dus M, Sarangi M. n.d. *Crème de la Créature: Dietary Influences on Behavior in Animal Models*. *Front Behav Neurosci* 227.
17. Fillion GJ, van Bommel JG, Braunschweig U, Talhout W, Kind J, Ward LD, Brugman W, de Castro IJ, Kerkhoven RM, Bussemaker HJ, van Steensel B. 2010. Systematic protein location mapping reveals five principal chromatin types in *Drosophila* cells. *Cell* 143:212–224.
18. Gambetta MC, Müller J. 2014. O-GlcNAcylation prevents aggregation of the Polycomb group repressor polyhomeotic. *Dev Cell* 31:629–639.
19. Gambetta MC, Oktaba K, Müller J. 2009. Essential role of the glycosyltransferase *sxc/Ogt* in polycomb repression. *Science* 325:93–96.
20. Gao J, Yang Y, Qiu R, Zhang K, Teng X, Liu R, Wang Y. 2018. Proteomic analysis of the OGT interactome: novel links to epithelial–mesenchymal transition and metastasis of cervical cancer. *Carcinogenesis* 39:1222–1234.
21. Goodarzi H, Elemento O, Tavazoie S. 2009. Revealing global regulatory perturbations across human cancers. *Mol Cell* 36:900–911.
22. Guinez C, Filhoulaud G, Rayah-Benhamed F, Marmier S, Dubuquoy C, Dentin R, Moldes M, Burnol A-F, Yang X, Lefebvre T, Girard J, Postic C. 2011. O-GlcNAcylation increases ChREBP protein content and transcriptional activity in the liver. *Diabetes* 60:1399–1413.
23. Hanover JA, Krause MW, Love DC. 2010. The hexosamine signaling pathway: O-GlcNAc cycling in feast or famine. *Biochim Biophys Acta* 1800:80–95.
24. Hardivillé S, Hart GW. 2014. Nutrient regulation of signaling, transcription, and cell physiology by O-GlcNAcylation. *Cell Metab* 20:208–213.

25. Haws SA, Leech CM, Denu JM. 2020. Metabolism and the Epigenome: A Dynamic Relationship. *Trends Biochem Sci*. doi:10.1016/j.tibs.2020.04.002
26. Heinz S, Benner C, Spann N, Bertolino E, Lin YC, Laslo P, Cheng JX, Murre C, Singh H, Glass CK. 2010. Simple combinations of lineage-determining transcription factors prime cis-regulatory elements required for macrophage and B cell identities. *Mol Cell* 38:576–589.
27. Janke R, Dodson AE, Rine J. 2015. Metabolism and epigenetics. *Annu Rev Cell Dev Biol* 31:473–496.
28. Kolde R. 2012. Pheatmap: pretty heatmaps. R package version.
29. Kreppel LK, Blomberg MA, Hart GW. 1997. Dynamic glycosylation of nuclear and cytosolic proteins. Cloning and characterization of a unique O-GlcNAc transferase with multiple tetratricopeptide repeats. *J Biol Chem* 272:9308–9315.
30. Lagerlöf O, Slocomb JE, Hong I, Aponte Y, Blackshaw S, Hart GW, Haganir RL. 2016. The nutrient sensor OGT in PVN neurons regulates feeding. *Science* 351:1293–1296.
31. Langmead B, Salzberg SL. 2012. Fast gapped-read alignment with Bowtie 2. *Nat Methods* 9:357–359.
32. Love MI, Huber W, Anders S. 2014. Moderated estimation of fold change and dispersion for RNA-seq data with DESeq2. *Genome Biol* 15:550.
33. Lubas WA, Hanover JA. 2000. Functional expression of O-linked GlcNAc transferase. Domain structure and substrate specificity. *J Biol Chem* 275:10983–10988.
34. Mariappa D, Zheng X, Schimpl M, Raimi O, Ferenbach AT, Müller H-AJ, van Aalten DMF. 2015. Dual functionality of O-GlcNAc transferase is required for *Drosophila* development. *Open Biol* 5:150234.

35. Marshall OJ, Brand AH. 2015. damidseq_pipeline: an automated pipeline for processing DamID sequencing datasets. *Bioinformatics* 31:3371–3373.
36. Marshall OJ, Southall TD, Cheetham SW, Brand AH. 2016. Cell-type-specific profiling of protein–DNA interactions without cell isolation using targeted DamID with next-generation sequencing. *Nat Protoc* 11:1586–1598.
37. Maury JJP, El Farran CA, Ng D, Loh Y-H, Bi X, Bardor M, Choo AB-H. 2015. RING1B O-GlcNAcylation regulates gene targeting of polycomb repressive complex 1 in human embryonic stem cells. *Stem Cell Res* 15:182–189.
38. May CE, Dus M. 2021. Confection Confusion: Interplay Between Diet, Taste, and Nutrition. *Trends Endocrinol Metab* 32:95–105.
39. May CE, Rosander J, Gottfried J, Dennis E, Dus M. 2020. Dietary sugar inhibits satiation by decreasing the central processing of sweet taste. *eLife*. doi:10.7554/elife.54530
40. May CE, Vaziri A, Lin YQ, Grushko O, Khabiri M, Wang Q-P, Holme KJ, Pletcher SD, Freddolino PL, Neely GG, Dus M. 2019. High Dietary Sugar Reshapes Sweet Taste to Promote Feeding Behavior in *Drosophila melanogaster*. *Cell Rep* 27:1675–1685.e7.
41. Musselman LP, Kühnlein RP. 2018. *Drosophila* as a model to study obesity and metabolic disease. *J Exp Biol* 221. doi:10.1242/jeb.163881
42. Na J, Musselman LP, Pendse J, Baranski TJ, Bodmer R, Ocorr K, Cagan R. 2013. A *Drosophila* Model of High Sugar Diet-Induced Cardiomyopathy. *PLoS Genetics*. doi:10.1371/journal.pgen.1003175
43. Olivier-Van Stichelen S, Guinez C, Mir A-M, Perez-Cervera Y, Liu C, Michalski J-C, Lefebvre T. 2012. The hexosamine biosynthetic pathway and O-GlcNAcylation drive the

- expression of β -catenin and cell proliferation. *Am J Physiol Endocrinol Metab* 302:E417–24.
44. Olivier-Van Stichelen S, Hanover JA. 2015. You are what you eat: O-linked N-acetylglucosamine in disease, development and epigenetics. *Curr Opin Clin Nutr Metab Care* 18:339–345.
45. Olivier-Van Stichelen S, Wang P, Comly M, Love DC, Hanover JA. 2017. Nutrient-driven O-linked N-acetylglucosamine (O-GlcNAc) cycling impacts neurodevelopmental timing and metabolism. *J Biol Chem* 292:6076–6085.
46. Quinlan AR, Hall IM. 2010. BEDTools: a flexible suite of utilities for comparing genomic features. *Bioinformatics* 26:841–842.
47. Ramírez F, Ryan DP, Grüning B, Bhardwaj V, Kilpert F, Richter AS, Heyne S, Dündar F, Manke T. 2016. deepTools2: a next generation web server for deep-sequencing data analysis. *Nucleic Acids Res* 44:W160–5.
48. Sartor F, Donaldson LF, Markland DA, Loveday H, Jackson MJ, Kubis H-P. 2011. Taste perception and implicit attitude toward sweet related to body mass index and soft drink supplementation. *Appetite* 57:237–246.
49. Shen L, Sinai M. 2013. GeneOverlap: Test and visualize gene overlaps. R package version 1:2013.
50. Shiraiwa T, Carlson JR. 2007. Proboscis extension response (PER) assay in *Drosophila*. *J Vis Exp* 193.
51. Stewart JE, Keast RSJ. 2012. Recent fat intake modulates fat taste sensitivity in lean and overweight subjects. *Int J Obes* 36:834–842.

52. Swamy M, Pathak S, Grzes KM, Damerow S, Sinclair LV, van Aalten DMF, Cantrell DA. 2016. Glucose and glutamine fuel protein O-GlcNAcylation to control T cell self-renewal and malignancy. *Nat Immunol* 17:712–720.
53. van Steensel B, Henikoff S. 2000. Identification of in vivo DNA targets of chromatin proteins using tethered dam methyltransferase. *Nat Biotechnol* 18:424–428.
54. Vaziri A, Dus M. 2021. Brain on food: The neuroepigenetics of nutrition. *Neurochem Int* 149:105099.
55. Vaziri A, Khabiri M, Genaw BT, May CE, Freddolino PL, Dus M. 2020. Persistent epigenetic reprogramming of sweet taste by diet. *Sci Adv* 6. doi:10.1126/sciadv.abc8492
56. Vella P, Scelfo A, Jammula S, Chiacchiera F, Williams K, Cuomo A, Roberto A, Christensen J, Bonaldi T, Helin K, Pasini D. 2013. Tet proteins connect the O-linked N-acetylglucosamine transferase Ogt to chromatin in embryonic stem cells. *Mol Cell* 49:645–656.
57. Wang Q-P, Lin YQ, Lai M-L, Su Z, Oyston LJ, Clark T, Park SJ, Khuong TM, Lau M-T, Shenton V, Shi Y-C, James DE, Ja WW, Herzog H, Simpson SJ, Neely GG. 2020. PGC1 α Controls Sucrose Taste Sensitization in *Drosophila*. *Cell Rep* 31:107480.
58. Wells L, Vosseller K, Hart GW. 2001. Glycosylation of nucleocytoplasmic proteins: signal transduction and O-GlcNAc. *Science* 291:2376–2378.
59. Wilinski D, Winzeler J, Duren W, Persons JL, Holme KJ, Mosquera J, Khabiri M, Kinchen JM, Freddolino PL, Karnovsky A, Dus M. 2019. Rapid metabolic shifts occur during the transition between hunger and satiety in *Drosophila melanogaster*. *Nat Commun* 10:4052.

60. Wilkinson L. 2012. Exact and approximate area-proportional circular Venn and Euler diagrams. *IEEE Trans Vis Comput Graph* 18:321–331.
61. Wise PM, Nattress L, Flammer LJ, Beauchamp GK. 2016. Reduced dietary intake of simple sugars alters perceived sweet taste intensity but not perceived pleasantness. *Am J Clin Nutr* 103:50–60.
62. Xu D, Shao F, Bian X, Meng Y, Liang T, Lu Z. 2021. The Evolving Landscape of Noncanonical Functions of Metabolic Enzymes in Cancer and Other Pathologies. *Cell Metab* 33:33–50.
63. Yang X, Qian K. 2017. Protein O-GlcNAcylation: emerging mechanisms and functions. *Nat Rev Mol Cell Biol* 18:452–465.

Chapter 5 Discussion

In this dissertation we set out to understand how the dietary environment alters sweet taste in a manner that promotes food intake and metabolic disease. Specifically, we set out to answer the following questions: How does the dietary environment alter sweet taste? What is the role of sweet taste in food intake? What are the molecular mechanisms that lead to changes in sweet taste? And what makes these effects persistent?

In chapter 2 we show that in fruit flies, excess dietary sugar, independent of obesity, causes a decrease in sweet taste function because of lower responses of the taste cells to sugar stimuli—similar to what was observed in the isolated taste buds of mice fed a high-fat diet (1). This dulling, in turn, promotes eating and obesity by increasing the duration and size of meals. Correcting taste deficits by activating the sweet-sensing cells so that the animals do not experience a lowering of their sweet taste would prevent overeating and obesity, drawing a causal link between diet-induced changes in taste function and obesity (11) .

In chapter 3 we found that the decrease in sweet taste sensation that flies experience after chronic exposure to a high sugar diet is caused by the cell-autonomous action of PRC2.1 in the sweet gustatory neurons. In the high sugar food environment, PRC2.1 chromatin occupancy was redistributed, leading to the repression of transcription factors, neural, signaling, and metabolic genes that decreased the responsiveness of the *Gr5a+* neurons and the fly's sensory experience of sweetness. However, we found that PRC2.1 did not directly bind to neuronal genes in these cells and that, instead, it targeted transcription factors involved in processes such as sensory neuron development, synaptic function, and axon targeting. We found that the changes in taste

sensation and half of the sugar diet neural state set by PRC2.1 remained even after animals were moved back to the control diet for up to 20 days. Leading to the establishment of a persistent state in the taste neurons that remain as a phenotypic and transcriptional memory of the previous food environment (18).

In chapter 4 we determined that the redistribution of PRC2.1 at the chromatin of the sweet sensory neurons is dependent on metabolic enzyme OGT. In the high sugar diet environment, OGT mediates the repression of a subset of genes bound by PRC2.1 that are involved in the modulation of a developmental hub essential for the responses of the sweet sensory neurons to sweet stimuli (*In prep*).

5.1 Mechanisms of diet induced obesity

Increased occurrences of metabolic disease and obesity has been linked to the availability of affordable, processed foods that contain added sugar (2, 3). Additionally, increased food intake in the presence of these foods is conserved from flies to rodents and humans (4). While the question of how these foods promote food intake is still open, changes in taste sensation has been examined as a possible mechanism (5–7). However, most these studies were unable to draw a causal connection between taste changes and food intake (1, 8–10). In the first part of our work, we identify taste changes in animals fed high dietary sugar. Our lean and obese mutant animal experiments also suggest that taste changes is a consequence of the diet and not the obese state (11). The combination of high-throughput feeding measurement with genetic and optogenetic manipulations establish that changes in taste are causally linked to feeding on a high sugar diet (11). Furthermore, when animals are fed high fat diets or high sucralose diets (non-caloric sweetener) we do not observe changes in taste. However, in these experiments, animals fed high fat diets became obese, but we did not measure any changes in other taste modalities

such as bitter. This is an interesting question as the sweet and bitter taste modalities influence each other through GABergic connections in the taste processing center of flies (12).

Flies fed high dietary sugar have increased activity of the Hexosamine Biosynthesis Pathway (HBP) measured from whole brains (11, 13). Because the metabolic OGT mediates the effects of this pathway on cellular physiology, we knocked it down in the sweet sensory cells of flies fed dietary sugar. We found that OGT depletion in the taste cells prevents sweet taste changes, food intake, and obesity (11). These findings are exciting because OGT is a known nutrient sensor (14). Suggesting that in the sweet sensory neurons OGT acts as nutrient sensor to modulate neural plasticity and activity to tune feeding behavior to the dietary environment. Currently, a number of nutrients sensors have been identified that modulate neural activity such as target of rapamycin (TOR) and eukaryotic translation elongation factor 2 (eEF2) (15). Interestingly, in our experiments we measured the levels of HBP in brains, therefore it is possible that in response to a high sugar diet OGT affects other cell types that alter behavior in a manner that is specific to the activity of that circuit. Finally, RNA sequencing (RNAseq) of the proboscis of flies on a sugar diet suggested a rapid response in RNA abundance. One caveat is that these measurements are from proboscis and not sweet taste cells only that contain high levels of muscle tissue as well as several other cell types and taste modalities. Thus, experiments targeted to the sensory neurons are required to elucidate the mechanisms by which diet alters sweet taste to promote food intake and metabolic disease.

5.2 Mechanisms of diet induced taste defects

Given the conservation between diet, sweet taste, and food intake we explored the mechanisms underlying sweet taste defects in flies. A number of studies have pointed to changes in gene expression to underly deficits in lowered sweet taste perception (1, 11, 16, 17). We

therefore explored this hypothesis using a variety of cell specific transcriptional and chromatin profiling tools. Our experiments determined that PRC2.1 mediates the effects of high dietary sugar on sweet taste by establishing persistent alterations in the taste neurons that remain as a phenotypic and transcriptional memory of the previous food environment (18). We speculate that this memory may lock animals into patterns of feeding behavior that become maladaptive and promote obesity.

Moreover, our findings define a neurodevelopmental transcriptional hub that is persistently repressed. This hub consists of transcription factors and their targets that modulate the physiology of the sweet taste neurons in a variety of ways. *Ptx1*, *scro*, and *nub/pdm* control the proper branching, synaptic connectivity, and activity of sensory neurons (19–25), while *cad* and *nub/pdm* play a role in neuroblast development (26). Based on these functions we reason that this hub may define the intrinsic properties of the sweet sensing neurons. This is because our analysis showed that these transcription factors are enriched in the *Gr5a+* cells. To our surprise we did not observe a change in the expression of the sweet taste receptors, or the misexpression of other taste receptors, or the number of taste cells. This is inconsistent with finding that show changes in the number of taste buds or changes in the expression of taste receptor genes (1, 9).

The engagement of developmental programs could be the reason why some environments and experiences leave a memory that leads to the persistent expression of the phenotype beyond the presence. Here, we found that the changes in taste sensation and half of the sugar diet transcriptional and neural state set by PRC2.1 remained even after animals were moved back to the control diet for up to 20 days. One limitation of our findings is that the number of *Gr5a+* cells is small, therefore measurements for the nature of the memory such as known epigenetic marks is difficult. But, our results show that the persistence of taste sensation is dependent on the

constitutive activity of PRC2.1. Therefore, we could speculate that the H3K27 methyl mark acts as a molecular memory during development (27, 28). While maintenance of epigenetic memory requires active recruitment of PRC2 (28); we did not directly measure this however our findings that PRC1.2 is actively required for the maintenance of the taste phenotype and that 47% of its indirect targets are still repressed indicate that PRC2.1 may be stably recruited to the transcription factors loci. Perhaps, conditions that lead to metabolic remodeling such as prolonged fasting could reset its binding. Last, we do not know whether the diet-induced chemosensory plasticity observed in humans and rodents is persistent or reversible. Unlike in *D. melanogaster*, mammalian taste cells are not postmitotic neurons, and so, they regenerate every few weeks.

A question that arises directly from our findings is how the PRC2.1 complex detects the change in the dietary environment to modulate the plasticity of the taste neurons? Because we know that OGT acts as a potential nutrient sensor in the *Gr5a+* cells in response to diet, we hypothesized that the PRC2.1 complex detects the changes in the nutrient environment through OGT. Our experiments suggest that the effects of OGT on taste are entirely dependent on the PRC2.1 complex. However, we do not test the nature of this interaction but suggest that they are in the same genetic pathway (unpublished data, refer to chapter 4). Indeed, we find that OGT is required for the redistribution of PRC2.1 at the chromatin of the sweet sensing cells in response to diet. Furthermore, we find that OGT only co-occupies a subset of the genes bound by PRC2.1, and that at this subset OGT is required for the repressive activity of PRC2.1 but not its recruitment. Interestingly, another subset of genes that modulate the responsiveness of the *Gr5a+* cells in animals fed high dietary sugar are bound by PRC2.1 but not OGT. These results reveal

that PRC2.1 activation is not entirely through OGT, but that OGT specifies a subset of the PRC2.1 bound genes.

Our ribosomal profiling experiments reveal that alterations in the expression of genes co-bound by OGT and PRC2.1 in response to diet are dependent on both OGT and PRC2.1, whereas the alterations in the expression of genes bound by PRC2.1 alone is only dependent on PRC2.1. These results suggest that in response to diet a bidirectional pathway is activated. On one hand, PRC2.1 is recruited to the genes *GATAe* and *nub*. On the other hand, PRC2.1 and OGT are recruited to *Ptx1*, *cad*, and *scro*. When analyzing all the other genes affected by OGT we did not identify any that did not go through the PRC2.1/*GATAe* and *nub* axis. This could be why OGT overexpression is sufficient to induce sweet taste defects and is dependent on PRC2.1. Incidentally, this division of labor between PRC2.1 and OGT could be attributed to the amount of time or the concentration of sugar that the animals are exposed to. Perhaps the utilization of OGT is only attributed to longer exposure times. Since our Dam-ID experiments test OGT binding after three days we cannot exclude the possibility that during shorter exposure times of less than one day OGT is not yet utilized. Furthermore, the sugar concentration used in these experiments (30%) is relatively high. Thus, it is possible that lower concentrations of sugar only activate PRC2.1 and not OGT or vice versa. In summary, we show that both OGT and the PRC2.1 complex mediate the effects of high dietary sugar on sweet taste by regulating a subset of genes involved in establishing the responses of the sweet sensory neurons to sweet stimuli. By specifying the targeting and repressive activity of the PRC2.1 complex to a subset of genes OGT defines a nutrient information pathway in response to diet. Thus, OGT acts as the metabolic link between diet and gene expression

5.3 Alterations in taste and increased food intake

An important question that arises from this dissertation is how changes in sweet taste promote food intake? In *Drosophila melanogaster*, sweet taste neurons relay taste information to a higher order brain regions that are ultimately linked to the learning center of the brain known as the Mushroom Body (MB) (29, 30). A subset of neurons that is innervated by the MB output neurons (MBON) are the fan shaped body. This region is associated with feeding behavior and is also innervated by neurons that detect changes in hunger states (31–33). In the MB, dopaminergic neurons (DANs) reinforce the formation of food associations by receiving sensory input from different taste modalities (29, 30). These circuits albeit simpler, are conserved at the genetic, wiring, and neurochemical level with mammals (34–36). Work from our lab and others have shown that diets high in fat and sugar alter dopaminergic signaling from flies to humans (37–39). Specifically, we have found that a subset of DANs that receive input from the sweet sensory neurons have lower responses to sweet stimuli (39). Our results show that this decrease in DAN activity is causally linked to lowered sweet taste because of dietary sugar (39). Furthermore, unpublished evidence from our lab suggests that this deficit is not limited to the DANs but extends to MBONs (*Pardo Garcia et al. In prep*). Thus, we hypothesize that changes in taste disrupt feeding through the downregulation of a circuit that is involved in regulating hunger and satiety states. Because this circuit modulates the interaction of the animal with food based on learned behavior it is uniquely positioned to control food intake.

5.4 Concluding remarks and future directions

Diet composition and food intake has a tremendous impact on our wellbeing. The amount of food and the composition of our diets affects body weight and the risk of developing disease, our ability to cope with it, and the quality and length of our lives. Because of this, understanding

the mechanisms by which food intake is affected by diet is essential to the enhancement of health and decreasing the impact of disease. This is most critical today given the high incidence of obesity and metabolic syndrome, which are linked to diseases such as cancer, diabetes, and neurodegeneration. While the last decade of research has uncovered many of the mechanisms that control feeding behavior, we still do not understand how these become dysregulated by diet. Specifically, we are just beginning to understand the potential interactions between metabolites and epigenetic/gene regulatory pathways and their role in brain physiology and behavior. How exactly metabolic-epigenetic signaling contributes to neural function, neurotransmitter balance, and synaptic plasticity are still unanswered questions.

Converging evidence from animal models and human studies suggests that the dietary environment influences the brain epigenome to change neural physiology and behavior in ways that promote or protect from disease. While so much remains to be defined about the molecular mechanisms through which dietary metabolites can shape the brain epigenome and alter behavior, a multidisciplinary approach that integrates tools at the intersection of neuroscience, epigenetics, and metabolism will pave the way for the next decade of research in this field (40). In particular, the development of new tools and the establishment of shared experimental approaches across model organisms will be essential to tackle the many open questions. Together, these will propel our understanding of the mechanisms that underlie the profound link between nutrition, brain health, and disease. This question has been with us for thousands of years, and it's exciting to know that soon, we may finally be able to answer it.

5.5 References

1. A. B. Maliphol, D. J. Garth, K. F. Medler, Diet-induced obesity reduces the responsiveness of the peripheral taste receptor cells. *PLoS One*. **8**, e79403 (2013).
2. C. E. May, A. Vaziri, Y. Q. Lin, O. Grushko, M. Khabiri, Q.-P. Wang, K. J. Holme, S. D. Pletcher, P. L. Freddolino, G. G. Neely, M. Dus, High Dietary Sugar Reshapes Sweet Taste to Promote Feeding Behavior in *Drosophila melanogaster*. *Cell Rep*. **27**, 1675-1685.e7 (2019).
3. A. Vaziri, M. Khabiri, B. T. Genaw, C. E. May, P. L. Freddolino, M. Dus, Persistent epigenetic reprogramming of sweet taste by diet. *Sci Adv*. **6** (2020), doi:10.1126/sciadv.abc8492.
4. D. M. Small, Individual differences in the neurophysiology of reward and the obesity epidemic. *Int. J. Obes. (Lond)*. **33 Suppl 2**, S44-8 (2009).
5. N. D. Volkow, G.-J. Wang, R. D. Baler, Reward, dopamine and the control of food intake: implications for obesity. *Trends Cogn. Sci*. **15**, 37–46 (2011).
6. N. M. Avena, P. Rada, B. G. Hoebel, Evidence for sugar addiction: behavioral and neurochemical effects of intermittent, excessive sugar intake. *Neurosci. Biobehav. Rev*. **32**, 20–39 (2008).
7. L. M. Bartoshuk, V. B. Duffy, J. E. Hayes, H. R. Moskowitz, D. J. Snyder, Psychophysics of sweet and fat perception in obesity: problems, solutions and new perspectives. *Philos. Trans. R. Soc. Lond. B Biol. Sci*. **361**, 1137–1148 (2006).
8. H.-R. Berthoud, H. Zheng, Modulation of taste responsiveness and food preference by obesity and weight loss. *Physiol. Behav*. **107**, 527–532 (2012).
9. F. Sartor, L. F. Donaldson, D. A. Markland, H. Loveday, M. J. Jackson, H.-P. Kubis, Taste perception and implicit attitude toward sweet related to body mass index and soft drink supplementation. *Appetite*. **57**, 237–246 (2011).
10. M. Chevrot, A. Bernard, D. Ancel, M. Buttet, C. Martin, S. Abdoul-Azize, J.-F. Merlin, H. Poirier, I. Niot, N. A. Khan, P. Passilly-Degrace, P. Besnard, Obesity alters the gustatory perception of lipids in the mouse: plausible involvement of lingual CD36. *J. Lipid Res*. **54**, 2485–2494 (2013).
11. A. Kaufman, E. Choo, A. Koh, R. Dando, Inflammation arising from obesity reduces taste bud abundance and inhibits renewal. *PLoS Biol*. **16**, e2001959 (2018).
12. M. H. Ozdener, S. Subramaniam, S. Sundaresan, O. Sery, T. Hashimoto, Y. Asakawa, P. Besnard, N. A. Abumrad, N. A. Khan, CD36- and GPR120-mediated Ca²⁺ signaling in human taste bud cells mediates differential responses to fatty acids and is altered in obese mice. *Gastroenterology*. **146**, 995–1005 (2014).

13. E. E. LeDue, K. Mann, E. Koch, B. Chu, R. Dakin, M. D. Gordon, Starvation-induced depotentiation of bitter taste in *Drosophila*. *Curr. Biol.* **26**, 2854–2861 (2016).
14. D. Wilinski, J. Winzeler, W. Duren, J. L. Persons, K. J. Holme, J. Mosquera, M. Khabiri, J. M. Kinchen, P. L. Freddolino, A. Karnovsky, M. Dus, Rapid metabolic shifts occur during the transition between hunger and satiety in *Drosophila melanogaster*. *Nat. Commun.* **10**, 4052 (2019).
15. S. Hardivillé, G. W. Hart, Nutrient regulation of signaling, transcription, and cell physiology by O-GlcNAcylation. *Cell Metab.* **20**, 208–213 (2014).
16. G. W. Davis, Homeostatic signaling and the stabilization of neural function. *Neuron.* **80**, 718–728 (2013).
17. C. E. May, M. Dus, Confection Confusion: Interplay Between Diet, Taste, and Nutrition. *Trends Endocrinol. Metab.* **32**, 95–105 (2021).
18. Q.-P. Wang, Y. Q. Lin, M.-L. Lai, Z. Su, L. J. Oyston, T. Clark, S. J. Park, T. M. Khuong, M.-T. Lau, V. Shenton, Y.-C. Shi, D. E. James, W. W. Ja, H. Herzog, S. J. Simpson, G. G. Neely, PGC1 α Controls Sucrose Taste Sensitization in *Drosophila*. *Cell Rep.* **31**, 107480 (2020).
19. J. Z. Parrish, K. Emoto, L. Y. Jan, Y. N. Jan, Polycomb genes interact with the tumor suppressor genes hippo and warts in the maintenance of *Drosophila* sensory neuron dendrites. *Genes Dev.* **21**, 956–972 (2007).
20. J. Z. Parrish, M. D. Kim, L. Y. Jan, Y. N. Jan, Genome-wide analyses identify transcription factors required for proper morphogenesis of *Drosophila* sensory neuron dendrites. *Genes Dev.* **20**, 820–835 (2006).
21. E. P. R. Iyer, S. C. Iyer, L. Sullivan, D. Wang, R. Meduri, L. L. Graybeal, D. N. Cox, Functional Genomic Analyses of Two Morphologically Distinct Classes of *Drosophila* Sensory Neurons: Post-Mitotic Roles of Transcription Factors in Dendritic Patterning. *PLoS ONE.* **8** (2013), p. e72434.
22. G. Vorbrüggen, R. Constien, O. Zilian, E. A. Wimmer, G. Dowe, H. Taubert, M. Noll, H. Jäckle, Embryonic expression and characterization of a Ptx1 homolog in *Drosophila*. *Mech. Dev.* **68**, 139–147 (1997).
23. S. Zaffran, G. Das, M. Frasch, The NK-2 homeobox gene scarecrow (*scro*) is expressed in pharynx, ventral nerve cord and brain of *Drosophila* embryos. *Mech. Dev.* **94**, 237–241 (2000).
24. M. M. Corty, J. Tam, W. B. Grueber, Dendritic diversification through transcription factor-mediated suppression of alternative morphologies. *Development.* **143**, 1351–1362 (2016).
25. C. J. Neumann, S. M. Cohen, Boundary formation in *Drosophila* wing: Notch activity attenuated by the POU protein Nubbin. *Science.* **281**, 409–413 (1998).

26. C. Q. Doe, Temporal Patterning in the Drosophila CNS. *Annu. Rev. Cell Dev. Biol.* **33**, 219–240 (2017).
27. F. Laprell, K. Finkl, J. Müller, Propagation of Polycomb-repressed chromatin requires sequence-specific recruitment to DNA. *Science*. **356**, 85–88 (2017).
28. R. T. Coleman, G. Struhl, Causal role for inheritance of H3K27me3 in maintaining the OFF state of a Drosophila HOX gene. *Science*. **356** (2017), doi:10.1126/science.aai8236.
29. N. Yamagata, T. Ichinose, Y. Aso, P.-Y. Plaçais, A. B. Friedrich, R. J. Sima, T. Preat, G. M. Rubin, H. Tanimoto, Distinct dopamine neurons mediate reward signals for short- and long-term memories. *Proc. Natl. Acad. Sci. U. S. A.* **112**, 578–583 (2015).
30. W. Huetteroth, E. Perisse, S. Lin, M. Klappenbach, C. Burke, S. Waddell, Sweet taste and nutrient value subdivide rewarding dopaminergic neurons in Drosophila. *Curr. Biol.* **25**, 751–758 (2015).
31. R. Cohn, I. Morante, V. Ruta, Coordinated and compartmentalized neuromodulation shapes sensory processing in Drosophila. *Cell*. **163**, 1742–1755 (2015).
32. D. Oswald, J. Felsenberg, C. B. Talbot, G. Das, E. Perisse, W. Huetteroth, S. Waddell, Activity of defined mushroom body output neurons underlies learned olfactory behavior in Drosophila. *Neuron*. **86**, 417–427 (2015).
33. Y. Aso, D. Sitaraman, T. Ichinose, K. R. Kaun, K. Vogt, G. Belliart-Guérin, P.-Y. Plaçais, A. A. Robie, N. Yamagata, C. Schnaitmann, W. J. Rowell, R. M. Johnston, T.-T. B. Ngo, N. Chen, W. Korff, M. N. Nitabach, U. Heberlein, T. Preat, K. M. Branson, H. Tanimoto, G. M. Rubin, Mushroom body output neurons encode valence and guide memory-based action selection in Drosophila. *Elife*. **3**, e04580 (2014).
34. N. J. Strausfeld, F. Hirth, Deep homology of arthropod central complex and vertebrate basal ganglia. *Science*. **340**, 157–161 (2013).
35. L. K. Scheffer, C. S. Xu, M. Januszewski, Z. Lu, S.-Y. Takemura, K. J. Hayworth, G. B. Huang, K. Shinomiya, J. Maitlin-Shepard, S. Berg, J. Clements, P. M. Hubbard, W. T. Katz, L. Umayam, T. Zhao, D. Ackerman, T. Blakely, J. Bogovic, T. Dolafi, D. Kainmueller, T. Kawase, K. A. Khairy, L. Leavitt, P. H. Li, L. Lindsey, N. Neubarth, D. J. Olbris, H. Otsuna, E. T. Trautman, M. Ito, A. S. Bates, J. Goldammer, T. Wolff, R. Svirskas, P. Schlegel, E. Neace, C. J. Knecht, C. X. Alvarado, D. A. Bailey, S. Ballinger, J. A. Borycz, B. S. Canino, N. Cheatham, M. Cook, M. Dreher, O. Duclos, B. Eubanks, K. Fairbanks, S. Finley, N. Forknall, A. Francis, G. P. Hopkins, E. M. Joyce, S. Kim, N. A. Kirk, J. Kovalyak, S. A. Lauchie, A. Lohff, C. Maldonado, E. A. Manley, S. McLin, C. Mooney, M. Ndama, O. Ogundeyi, N. Okeoma, C. Ordish, N. Padilla, C. M. Patrick, T. Paterson, E. E. Phillips, E. M. Phillips, N. Rampally, C. Ribeiro, M. K. Robertson, J. T. Rymer, S. M. Ryan, M. Sammons, A. K. Scott, A. L. Scott, A. Shinomiya, C. Smith, K. Smith, N. L. Smith, M. A. Sobeski, A. Suleiman, J. Swift, S. Takemura, I. Talebi, D. Tarnogorska, E. Tenshaw, T. Tokhi, J. J. Walsh, T. Yang, J. A. Horne, F. Li, R. Parekh, P. K. Rivlin, V. Jayaraman, M. Costa, G. S. Jefferis, K. Ito, S. Saalfeld, R. George, I. A. Meinertzhagen, G.

- M. Rubin, H. F. Hess, V. Jain, S. M. Plaza, A connectome and analysis of the adult *Drosophila* central brain. *Elife*. **9** (2020), doi:10.7554/eLife.57443.
36. R. Tomer, A. S. Denes, K. Tessmar-Raible, D. Arendt, Profiling by image registration reveals common origin of annelid mushroom bodies and vertebrate pallium. *Cell*. **142**, 800–809 (2010).
 37. K. D. Hall, A. Ayuketah, R. Brychta, H. Cai, T. Cassimatis, K. Y. Chen, S. T. Chung, E. Costa, A. Courville, V. Darcey, L. A. Fletcher, C. G. Forde, A. M. Gharib, J. Guo, R. Howard, P. V. Joseph, S. McGehee, R. Ouwerkerk, K. Raisinger, I. Rozga, M. Stagliano, M. Walter, P. J. Walter, S. Yang, M. Zhou, Ultra-processed diets cause excess calorie intake and weight gain: An inpatient randomized controlled trial of ad libitum food intake. *Cell Metab*. **32**, 690 (2020).
 38. I. E. de Araujo, M. Schatzker, D. M. Small, Rethinking food reward. *Annu. Rev. Psychol*. **71**, 139–164 (2020).
 39. C. E. May, J. Rosander, J. Gottfried, E. Dennis, M. Dus, Dietary sugar inhibits satiation by decreasing the central processing of sweet taste. *Elife*. **9** (2020), doi:10.7554/eLife.54530.
 40. T. Pizzorusso, P. Tognini, Interplay between Metabolism, Nutrition and Epigenetics in Shaping Brain DNA Methylation, Neural Function and Behavior. *Genes* . **11**, 742 (2020).